The perplexity of calcium-binding protein, spermatid-associated 1 (CABS1):

A molecule that despite its name, is present beyond the reproductive tract, with ties to stress, and possessing an anti-inflammatory domain only preserved in simians

by

Eduardo Alejandro Reyes Serratos

A thesis submitted in partial fulfillment of the requirements for the degree of

Doctor of Philosophy

Department of Medicine

University of Alberta

Abstract

A protein in rat submandibular glands (SMG) led our group to research human calcium-binding protein, spermatid associated 1 (CABS1). In a model of lung inflammation in rats where neural input was interrupted, our group observed that SMG released an anti-inflammatory factor later identified as Submandibular rat protein 1 (SMR1). Rat SMR1 was present in serum, saliva, testes, and SMG. A seven amino acid peptide near the carboxyl terminus of SMR1, TDIFEGG, was responsible for the anti-inflammatory activity. Synthetic TDIFEGG and derivates had anti-inflammatory activity in several animal models, but a human trial in mild atopic asthma showed no significant effect. SMR1 is absent in humans, but we postulated that an analogous pathway existed. Thus, our group looked for a human protein that contained a similar peptide sequence, ultimately finding CABS1, which has the seven-peptide sequence, TDIFELL, also near the carboxyl terminus.

CABS1 has been characterized previously in testes of rat, mouse, and pig. Transcript has been found in testes, uterus, and salivary glands of mammals. Previously, our group showed CABS1 protein in human (h) SMG, lungs, testes, and saliva via Western blots (WB) using a single polyclonal antibody. The data suggested that hCABS1 exists as several variants of different molecular weight. A 27 kDa band in saliva positively correlated to perceived psychosocial stress, and bands <27 kDa could be indicators of resilience to stress. Based on these data, my hypotheses were that hCABS1 is present beyond the testes, in SMG, saliva and blood, like rat SMR1, and that variants of CABS1 in saliva are biomarkers of stress.

To extend our previous findings, we analyzed WB profiles using four pAbs to hCABS1 and overexpression cell lysate controls, SMG, and saliva. We used these profiles as guidance to isolate in-gel sections that we speculated contained hCABS1 and evaluated their protein content through mass spectrometry sequencing (MS-seq). hCABS1 was detected in overexpression cell lysates via

MS-seq, yet contrary to what our WB profiles, to date we have not detected the protein in human-derived biofluids or tissue extracts.

Given the limiting amounts of pAbs available, a capillary nano-immunoassay (CNIA) was used to validate the occurrence of hCABS1 variants in saliva. With this platform, we successfully validated our previous stress-related findings, and also reported another variant of hCABS1 (60 kDa) in saliva detected by a pAb that targets TDIFELL. CNIA optimization also led to improvements in our WB protocol that encouraged reevaluation of our previous data in saliva. WB analysis using pAbs allowed us to target sites in one and two-dimensional gels for MS-seq analysis. However, efforts to confirm the presence of hCABS1 in saliva using MS-seq were unsuccessful, perhaps because of limitations in our pAbs or the amount of hCABS1. We speculated that the pAb detected hCABS1 and potentially other protein(s), and thus developed monoclonal antibodies (mAbs) targeting three domains of the protein. Using these mAbs, WB analyses of overexpression cell lysate controls, SMG, saliva and serum detected fewer bands than pAbs, but validated that hCABS1 is present beyond the testicular compartment.

We also conducted immunohistochemical (IHC) analyses of SMG with four pAbs and one mAb, showing that hCABS1 is present in the cytoplasm of duct cells of SMG. IHC of human testis, suggest that hCABS1 is present in cytoplasm of primary spermatogonia in seminiferous tubules and outside the tubules in Leydig cells. Moreover, we have begun to immunoprecipitate hCABS1 from a transient overexpression cell lysate with our mAbs, and have confirmed success using MS-seq.

We have further dissected the protein using *in silico* analyses. These studies provide evidence of disordered domains close to the carboxyl terminus of hCABS1, where its anti-inflammatory domain is located, as well as in other segments of the protein. A phylogenetic analysis showed that the peptide sequence, TDIFELL, is found exclusively in primates of the infraorder *Simiiformes*, which includes humans. Supporting our WB work, a predicted degradome analysis of hCABS1

with neutrophil elastase identified several potential cleavage sites, theoretically generating hCABS1-derived peptides. Altogether, evidence in this dissertation supports the presence of hCABS1 beyond the testes, in SMG and blood. However, evidence about hCABS1 in saliva is inconclusive and thus the link to stress remains to be clarified.

Preface

This paper-based dissertation is divided into eight chapters and three appendices. The first chapter, Introduction, provides the reader with the background to understand the rationale that has led our group to study hCABS1 in human-derived samples.

The second chapter addresses the characterization of four pAbs raised against specific domains of hCABS1. This section encompasses the gel-based separation of complex biological samples of human origin in one and two dimensions, with downstream techniques including WB and MS-seq. Representative data from immunohistochemical analyses carried out by our collaborators at the Case Western Reserve University are shown in this section too. The chapter shows the WB profiles obtained before and after modifying the methodology used in these evaluations, and how the complex profiles generated through the use of our pAbs provided us with the rationale to develop mAbs.

The third chapter of the dissertation is a published and peer-reviewed article entitled "A method to study protein biomarkers in saliva using an automated capillary nano-immunoassay platform (Wes™)". This article was published in the Journal of Immunological Methods in early 2020. This publication shows how a novel immunoprobing technique, alternate to WB, was used to validate our previous findings of saliva-derived hCABS1 under acute stress. We used pAbs H1.0 and H2.0, the first one targets CABS1 putative anti-inflammatory sequence *TDIFELL*, and the latter being the antibody we had employed in previous published WB saliva analyses.

The fourth chapter describes the characterization of mAbs targeting hCABS1 using WB of human-derived samples. Translation of the titration strategy used in capillary nano-immunoassay platform to WB, and comparison of WB banding pattern between our mAbs and controls (no primary antibody and isotype antibody) provided a better understanding of which WB bands were representative of hCABS1. This chapter also includes early work utilizing immunoprecipitation methodology, performed by Ms. Tarana A. (Riya) Mangukia, whom I had the honor to mentor.

Finally, this section shows the first immunohistochemical profile of hCABS1 in human testicular tissue, the fruit of our collaboration with Dr Lakshmi Puttagunta (University of Alberta, Edmonton, Canada).

The fifth chapter provides a brief appraisal of the collective WB banding patterns across samples and antibodies. Putatively equivalent bands detected by our pAbs and mAbs vary in molecular sizes (in kilodaltons, kDa). I speculate that the factors responsible for molecular size variation are (a) the evolution of our WB protocol over the years, (b) the use different molecular mass reference ladders, and (c) the change of the way molecular mass of WB bands were calculated.

The sixth chapter of the dissertation is a published and peer-reviewed article entitled "Structural and post-translational analysis of human calcium-binding protein, spermatid-associated 1". The article was published in the Journal of Cellular Biochemistry in mid-2020. It is the product of a collaboration with Dr Marcelo Marcet-Palacios, which used and provides *in silico* phylogenetic and sequence analyses of hCABS1 to identify an anti-inflammatory domain, possible cofactor binding sites, and hypothesizes on the intra- and extracellular roles of hCABS1.

The seventh chapter of the dissertation summarizes and provides a general discussion of the findings of the five preceding chapters. The eighth chapter proposes future approaches and directions that may further contribute to the body of knowledge and understanding of the biological function of this molecule.

Dedication

Le dedico este trabajo a mi mamá, Maya Serratos Franco, y a mi papá, Felipe Reyes Ávila, quienes siempre han apoyado mis decisiones, me han alentado a cuestionar mis límites y superarlos, y quienes constantemente me recuerdan la necesidad de ayudar a nuestras comunidades, de utilizar el conocimiento que he adquirido a lo largo de mi vida para mejorar la vida de los demás.

También quiero dedicarle esta tesis a mi hermano, Ricardo Reyes Serratos, y a mi pareja, Emilie Manny. Hablar con ellos diariamente me recuerda la importancia del amor, de la empatía, de apoyarnos, de ser solidarios, de ser humildes y de la relevancia que tiene el comunicarnos claramente.

I dedicate this work to my parents, Maya Serratos Franco and Felipe Reyes Ávila, who have always supported my decisions, encouraged me to challenge my limitations and overcome them, and who always remind me of the need to give back to our communities, to use the knowledge I have been fortunate to acquire over my life to improve the lives of others.

I also wish to dedicate this dissertation to my brother, Ricardo Reyes Serratos, and to my partner, Emilie Manny. Daily conversations with them remind me the importance of love, of empathy, of support, of togetherness, of humility, and of transparent communication.

Acknowledgements

The work shown in this dissertation is fruit of collaborations garnered through countless e-mails and rewarding conversations, of unparalleled guidance from supervisors and peers, and of backstage support from friends that have crossed my path at different points in time.

I firstly wish to acknowledge my dissertation supervisor, Dr A. Dean Befus, who has endured rivers of e-mails with constant questions and findings and who has always made time in his schedule for guiding me. As well, I wish to thank my dissertation co-supervisor Dr Marcelo Marcet-Palacios, who has been pivotal in my professional development and who has been an enthusiastic, generous, and involved mentor throughout the quest to understand hCABS1. I also would like to acknowledge the support given by the members of my supervisory committee, Dr Harissios Vliagoftis and Dr Richard Fahlman.

I wish to convey enormous gratitude to collaborators with whom I corresponded and who always went beyond the project in hand and shared glimpses of their lives and asked about my own life, they are Dr Michiko Watanabe, Dr Ibolja Cernak, and Dr Thomas Ritz.

I would like to recognize the excellent support provided by Jack Moore, facility supervisor of the Alberta Proteomics and Mass Spectrometry Facility. I also wish to acknowledge the work of Yong-Qiu Doughman, Sarah Canil and Dr Lakshmi Puttagunta, who performed immunohistochemical analyses, Tarana A. Mangukia, who arrived to our lab as a summer student, transitioned into a Honors student, and worked with tremendous effort in establishing the immunoprecipitation protocol that future students will use to capture hCABS1 from human-derived samples. I also wish to thank Dr David Rosenfield, who did the statistical analysis of our stress-related work, and Phil Hofstrand, Field Applications Scientist for ProteinSimple, who provided guidance in optimizing the capillary nano-immunoassay platform that we included in our studies.

Table of contents

List of Tables

List of Figures

List of Abbreviations

1D-e: one dimensional electrophoresis

2D-e: two dimensional electrophoresis

BALF: bronchoalveolar lavage fluid

Ca^{2+}: calcium

CABS1: calcium-binding protein, spermatid-associated 1

$CaCl_2$: calcium chloride

CLPH: casein-like phosphoprotein

CNIA: capillary nano-immunoassay

CNS: central nervous system

DTT: dithiothreitol

hCABS1: human calcium-binding protein, spermatid-associated 1

HCP: Histidine-rich Ca^{2+}-binding protein

IDP: intrinsically disordered protein

IEF: isoelectrofocusing

IP: immunoprecipitation

LH: luteinizing hormone

LPS: lipopolysaccharide

mAbs: monoclonal antibodies

MS-seq: mass spectrometry sequencing

NCL: negative control cell lysate

PA: polyacrylamide

pAbs: polyclonal antibodies

PimmS: pre-immunization serum

POI: protein of interest

PROL1: Proline-rich protein 1 (a.k.a. opiorphin prepropeptide)

PRP: Proline-rich proteins

rhCABS1 OEL: recombinant hCABS1 overexpression cell lysate

SCG: superior cervical ganglion

SDS-PAGE: sodium dodecyl sulfate-polyacrylamide gel electrophoresis

SMG: submandibular gland

SMR1: submandibular rat 1 protein

SMR3a/b: submaxillary gland androgen-regulated protein 3A/B

SNS: sympathetic nervous system

TEM: transmission electron microscopy

TSST: Trier social stress test

WB: Western blot

Chapter 1 : Introduction

Prior research of CABS1 focused on its localization and characterization in testes

In 2009, Calvel et al. published an article describing a protein in rat testis which underwent marked changes in expression levels during spermatogenesis. The group prepared cell lysates from rat spermatids and separated proteins using 2-dimensional electrophoresis (2D-e). Gel excision of a spot of interest and subsequent mass spectrometry sequencing (MS-seq) led to the identification of a protein named RSD-6 (rat sperm DNA number 6)[1]. However, successive experiments showed that this protein was phosphorylated by casein kinase-2 in a similar way to that of caseins. Therefore, this group proposed the name 'casein-like phosphoprotein' (CLPH)[1]. *In silico* gene sequence alignment showed that the *Clph* gene was found solely in placental mammals and that humans produced the equivalent protein, at that time referred to as testis development protein NYD-SP26, through the expression of a gene located in Chromosome 4, open reading frame 35[1].

To characterize this molecule in rats, Calvel et al. produced primers to the *Clph* gene, as well as a riboprobe, to track *Clph* transcript *in situ*. The group also made anti-CLPH polyclonal antibodies that were used in immunogold labelling for transmission electron microscopy (TEM), and detection of proteins in Western blot (WB).

RT-PCR analysis of diverse rat organs showed that the *Clph* gene was only expressed in the main olfactory epithelium and adult rat testis, yet protein expression assessed by WB was only found in the latter[1]. *In situ* hybridization experiments revealed that the *Clph* transcript was expressed in seminiferous tubules at sperm development stages IV through XIV[1].

Furthermore, immunogold labelling detection through TEM revealed that CLPH localized in the cytoplasm of elongated spermatids, as well as the inner membrane of mitochondria[1]. Notably in WB, migration of CLPH following 1D-e and 2D-e identified an acidic protein showing an apparent

molecular weight of 80 kDa, markedly higher than the predicted 42 kDa[1]. Similar retarded migration of proteins under denatured conditions are characteristic of acidic and intrinsically disordered proteins (IDP). In follow-up the group produced recombinant CLPH ($_r$CLPH).

Hypothesizing that the unusual shift of molecular weight was due to the high proportion of acidic residues in CLPH (23.3% aspartic and glutamic acid), Calvel et al. neutralized the negatively charged carboxyl groups of such residues and ran SDS-PAGE. The treatment showed $_r$CLPH at 44 kDa, supporting the hypothesis that delayed SDS-PAGE migration was due to a high number of acidic residues[1], a property inherent to IDPs[2,3]. Moreover, circular dichroism analysis showed that CLPH has a similar pattern to β-casein, a known IDP[1]. Additionally, *in silico* analysis of CLPH amino acid sequence predicted that the protein contains several domains that are naturally disordered[1]. Lastly, the group showed that CLPH was hypersensitive to protease digestion, indicating that CLPH does not retain a high level of compaction[1]. All these observations support the claim of CLPH being an IDP[1].

Calvel et al. also investigated the function of CLPH. *In silico* analysis indicated that rat CLPH possessed an EF-hand type calcium-binding domain that interestingly, was not present in the human, orangutan and chimpanzee homologous proteins due to point mutations[1]. On this basis, the group tested calcium binding activity *in vitro* by incubating a membrane containing $_r$CLPH with radioisotope $^{45}Ca^{2+}$. The autoradiography of this membrane produced a strong signal, evidence supporting that rat CLPH binds calcium[1].

Remarkably, also in 2009 Kawashima et al., a Japan-based group, published mice studies focusing on a protein, NYD-SP26, which had previously been reported to be highly expressed in human testis[4]. Because the group too found that the protein bound to calcium, they proposed the name <u>ca</u>lcium-<u>b</u>inding protein, <u>s</u>permatid-specific <u>1</u> (CABS1)[4]. This protein denomination was approved by the Mouse and Human Genome Organisation Gene Nomenclature Committees.

Kawashima et al. were studying spermatogonia stem cell differentiation by means of administering busulfan, an antineoplastic agent that selectively attacks dividing spermatogonia and spermatocytes without affecting the ability of testicular cells to support spermatogenesis. The group used 2D-e to resolve proteins from testicular extracts. They noticed an acidic protein whose presence decreased post-busulfan treatment, but recovered with resumption of spermatogenesis[4]. Subsequent isolation from a 2D-e gel followed by MS-seq identified the protein as CABS1[4].

Northern blot analysis on various mouse organs showed that the transcript was only present in testis and the pattern of expression of RNA, just like the protein, followed the same tendency post-busulfan treatment[4]. In contrast to Calvel et al., Kawashima et al. did not evaluate presence of transcript in the olfactory epithelium, where Calvel et al. found presence of *Cabs1* mRNA. Conversely, in agreement with Calvel et al., Kawashima et al. observed that *Cabs1* was expressed exclusively in spermatids and in the latest stages of spermatogenesis. Interestingly, gene expression preceded protein expression by three stages[4].

Because the group noted that the human homolog of *Cabs1* is located in a gene cluster containing calcium-binding phosphoproteins, they investigated whether mouse CABS1 had calcium-binding activity. To assess calcium-binding activity, the group used of Stains-all[a] in 2D-e gels, and ruthenium red using $CaCl_2$ as a control in testes-derived protein extracts transferred to PVDF membranes. Kawashima et al. performed the calcium-binding assays on protein extracts from testis and mature sperm and results showed that mouse CABS1 binds calcium[4]. Curiously, Kawashima et al. stated that mouse CABS1 does not have predicted calcium-binding domains, such as an EF-hand[4]. The group attributed the calcium-binding activity to the acidic residues within the protein[4].

---

[a] Stains-All is a dye used to detect calcium binding activity. Proteins that bind to calcium stain deep blue/violet[237].

Intriguingly, when doing 2D-e-WB without incubating with calcium they observed that CABS1 from mouse testis extract had a pI of 4.1 and a molecular mass of 66 kDa, while CABS1 from mature sperm had a pI of 5.8 and a molecular mass of 58 kDa[4]. Kawashima et al. mentioned that in theory the size of mouse CABS1 is 42 kDa, but in practice the apparent molecular weights were different depending on the source[4]. When performing WB with calcium incubation, the observed pI from both extracts was 4.1, which indicates that CABS1 binds calcium while in the testes during sperm maturation and not in the final stage, when sperm are mature[4].

Akihiro Kawashima, the first author of the mouse CABS1 article, went on to study CABS1 in porcine testis and, along with a new research group, published the findings in 2016. The group found that in porcine testis CABS1 is also expressed in the later stages of spermatogenesis[5]. Furthermore, the use of immunofluorescent staining techniques revealed that porcine CABS1 localizes in the anterior half of the head of mature sperm and is lost during the acrosome reaction, the moment when sperm fuses with an egg[5].

The group performed the same calcium-binding assays that were used to analyze mouse CABS1 and found that porcine CABS1 also binds calcium, purportedly because of a high proportion of acidic residues[5], a property that has been observed in calsequestrin[6], calmodulin[7], and calreticulin[8,9]. Such a property could also account for anomalous migration in SDS-PAGE, the same as with rat and mouse CABS1[5]. Porcine CABS1 with a theoretical molecular mass of ~43 kDa was observed at 75 and 70 kDa in testis extract, and at 70 kDa in mature sperm[5]. The authors noted that in pig, CABS1 in testes was also observed at a higher molecular weight than its counterpart in mature sperm and speculated that, just as in mouse CABS1, this shift is linked to calcium binding[5].

Independent research also published in 2016 on arsenic-induced male reproductive toxicity in rats showed that arsenic enhanced expression of 5 proteins in testis, including CABS1, and downregulated the expression of 6 proteins. This proteomic pattern was associated to germ cell

deficiency and a decrease in testosterone levels, in turn impairing spermatogenesis[10]. Finally, findings published in 2021 using *Cabs1* knockout mice identified sperm with a bent tail and disturbance in expression of cytoskeleton-related proteins[11]. Interestingly, spermatids also expressed a long, non-coding RNA of the *Cabs1* gene antisense, but knockdown of this anti-*Cabs1* did not alter sperm development, morphology or function; its significance is unknown[11]. Moreover, CABS1 deficiency was associated with subfertility of mice[11]. Supporting this observation, a study on the transcriptome of human testes[b] suggests that a decrease in expression of eight spermatogenesis-associated genes, one being CABS1, may play a role in infertility[12]. Altogether, this evidence suggests that CABS1 plays an indispensable role in optimum formation and function of sperm.

CABS1 tissue distribution and sexual dimorphism

While these articles only considered CABS1 in male mammals, expression was also identified in female mammals. In 2014, Calhoun et al. published that after exposing pregnant Rhesus macaques carrying female fetuses to bisphenol A, a broadly used industrial compound with estrogenic action, the fetal uterus had an upregulation of CABS1 mRNA[13]. The following year, Cerny et al. published findings on Angus heifers showing that CABS1 mRNA was upregulated in ampullary epithelial cells from oviducts during the follicular phase of the estrus, when compared to the luteal phase[14]. In humans, a female patient with osteosarcoma exhibited a chromosomal duplication of the locus where h*CABS1* gene is located, whether this variation in gene copy numbers is associated to tumorigenesis remains unknown[15]. What's more, Shi et al. (2016) and De la Cruz et al. (2021) showed the presence of hCABS1 mRNA in labial salivary glands of human female subjects. In these studies, CABS1 mRNA was downregulated in subjects suffering from Sjögren's syndrome when compared with healthy controls[16,17]. The presence of CABS1 mRNA in female reproductive tissue and labial salivary glands, as well as our work in salivary glands[18], may

---

[b] Samples were collected from patients diagnosed with either infertility, impaired spermatogenesis, or azoospermia

have been a determinant factor for the Human Genome Organisation Gene Nomenclature Committee to issue a name correction for CABS1 in February of 2016, from calcium-binding protein, spermatid-**specific** 1 to calcium-binding protein, spermatid-**associated** 1. In recent years, the organisation has worked to remove overly specific expression-based designations (personal communication). In 2019, a deep proteome and transcriptome analysis of human tissues reported the occurrence of CABS1 protein in testis, thyroid, colon, and pancreas[c] (see [19] – supporting information – Table EV1 – spreadsheet "B" – row 2181). However, my re-evaluation of this group's open access data found presence of CABS1 protein only in testis (data not shown). I speculate that my use of a newer version of the same quantitative proteomics software accounts for the contrasting outcome.

A quest to study neural control of the inflammatory response led us to CABS1

Our interest in human CABS1 arose from observations we published in 1990 in an article titled 'Marked anti-inflammatory effects of decentralization of the superior cervical ganglia'[20]. This led to subsequent studies that discovered CABS1 expression in salivary glands[18], presence of an anti-inflammatory peptide sequence near the carboxyl terminus of the protein[18], and association with distress[21]. Consequently, we seek to characterize CABS1 in salivary glands and determine its potential functions.

A primary research interest of the Befus lab has been to test whether interventions in the nervous system would change inflammatory responses. The group postulated that input from the sympathetic nervous system would modify pulmonary inflammatory responses in a model of anaphylaxis in rats.

The experimental design called for two rat groups, one sensitized to *Nippostrongylus brasiliensis*, and a control group that was not sensitized[20]. After 30 to 42 days, each rat group was further

---

[c] Thyroid & pancreas samples were retrieved from female patients, testis & colon samples from males

separated into four treatment subgroups: 1. sham surgery, 2. decentralization surgery, 3. removal of superior cervical ganglions (hereafter referred to as ganglionectomy), 4. no surgery[20] (see **Figure 1-1**). Notably, decentralization and ganglionectomy gave similar results, so decentralization was used as the neural intervention for most subsequent experiments[20]. Post-treatment, rats were given 7-days to recover[20]. On the 8th day, rats were either challenged with *N. brasiliensis* antigens or not[20]. Eight hours post-challenge, bronchoalveolar lavage fluid (BALF) was collected to study levels of inflammatory cells, histamine, IgG, IgM, and chemotactic activity for neutrophils (see **Figure 1-2**)[20].
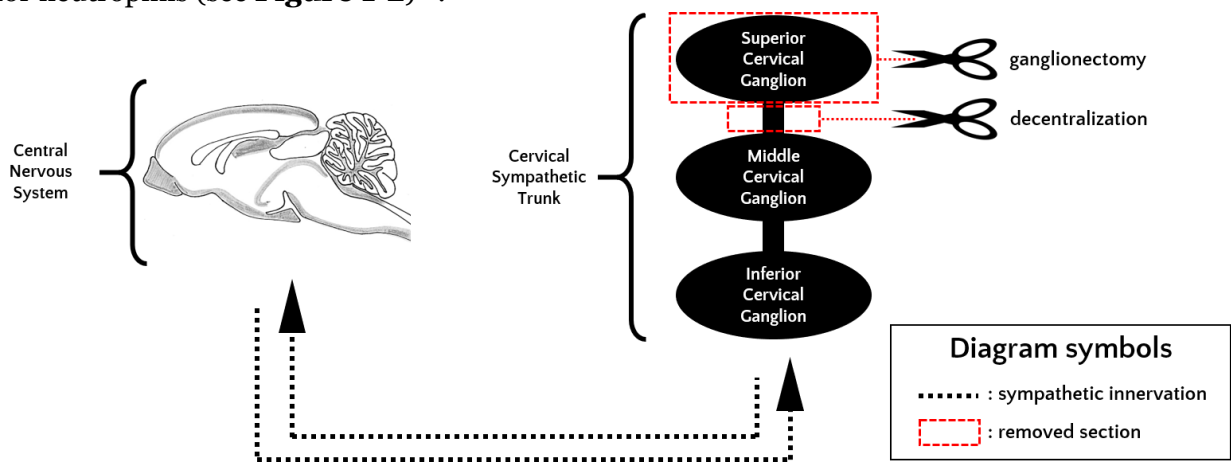
Figure 1-1. Neural interventions to test the impact of sympathetic input in rats sensitized to *N. brasiliensis*.

Top-to-bottom sympathetic innervation goes from the central nervous system, down through the spinal cord and at vertebrae C7 it enters the cervical sympathetic trunk through the inferior cervical ganglion and continues into the superior cervical ganglion (SCG) which is adjacent to vertebrae C1-C4. This ganglion, in turn, innervates several glands and organs located, mostly, in the rostral region. The group of rats subjected to decentralization had a portion of nerves between the middle and SCG removed, the group that underwent ganglionectomy had the entire SCG removed. The sham treated group was surgically manipulated in a similar way, but their cervical sympathetic trunk was left intact. A fourth group with no surgical intervention served as another control.
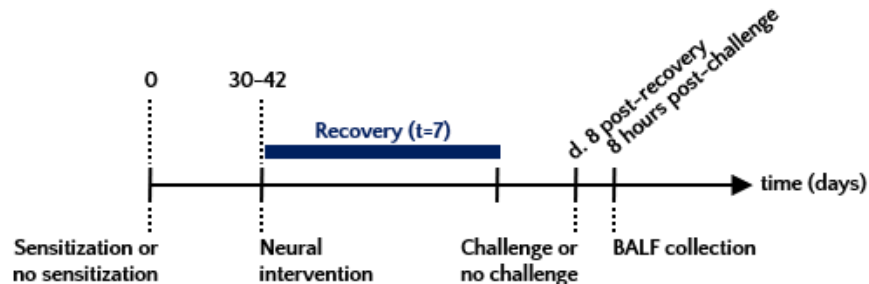
Figure 1-2. Timeline of experimental procedures to test the effect of sympathetic innervation on rat anaphylaxis.

Sensitized/non-sensitized rats were surgically treated by performing ganglionectomy, decentralization, or sham surgery. After 8 days of recovery, rat groups were challenged, or not, with *N. brasiliensis* antigen and 8 hours post-challenge BALF was collected for downstream experiments.

In rats that were sensitized to *N. brasiliensis* and challenged with parasite's antigens, BALF showed a marked increase in levels of histamine, immunoglobulins, and an influx of inflammatory cells, as well as neutrophil chemotactic activity[20]. Qualitatively, when compared to the previously described group of rats, the decentralized group had decreased histamine and leukocytes in BALF, especially neutrophils, a milder anaphylactic shock and a reduced anaphylaxis-induced mortality[20]. Overall, these data suggested that decentralization produced systemic alterations that decreased inflammatory responses to allergen challenge in sensitized rats[20].

Following these initial experiments, our lab focused on neutrophil response to insult following decentralization. At the time, neutrophils were believed to play a crucial role in the immune response to endotoxin[22]. Under normal conditions, these cells are released into the bloodstream, where they circulate for 7 to 10 h before migrating to tissues[23]. During infection, an increased number of neutrophils are produced and released into the bloodstream[23]. Commonly, these are the first to arrive at an inflammation site where, guided by chemotactic factors, they move into the affected tissue(s), phagocyte and eliminate the source of infection via proteolytic enzymes, anti-microbial substances, and reactive oxygen species (ROS)[23].

Our group used the established inflammatory model where rats were, or not (uninfected control), sensitized to *N. brasiliensis* [24]. Subsequently, a subgroup of rats was decentralized, while another rat subgroup underwent sham operation[24]. To examine neutrophils, blood was collected via either cardiac puncture or from major neck vessels[24]. Blood smears to assess differential cell counts in the different groups were made. Neutrophils were isolated for *in vitro* chemotactic assays, where cell migration was evaluated when exposing neutrophils to either N-formyl-methionyl-leucyl-phenylalanine (fMLP) or leukotriene B_4 (LTB_4)[24]. Finally, phagocytosis and oxidative metabolism of neutrophils was evaluated *in vitro* by nitroblue tetrazolium (NBT), a colourless compound that turns deep blue if the immune cells have functional NADPH oxidase, an ability needed to create reactive oxygen species[25].

Results showed that decentralization depressed neutrophil inflammatory activity[24]. fMLP- and LTB$_4$-mediated chemotaxis were dampened, as well as the ability of neutrophils to turn NBT blue; the latter in both infected and uninfected rats that underwent decentralization[24]. Once more, decentralized rats showed a decrease in neutrophil presence in BALF when compared to their unoperated and sham-operated counterparts[24]. These data indicated that the anti-inflammatory effect observed in decentralized rats was, at least in part, neutrophil mediated[24].

That same year, our lab published results on concurrent experiments to evaluate the role of the submandibular gland (SMG), an organ whose neural input comes in part from the superior cervical ganglion, on the anti-inflammatory effect. Again, decentralization and ganglionectomy had similar dampening effects on pulmonary inflammation, suggesting that the central nervous system (CNS) was involved in the anti-inflammatory effect. Notably, these experiments included a group of rats that underwent both decentralization and removal of the submandibular glands, or sialoadenectomy (see **Figure 1-3**)[26].
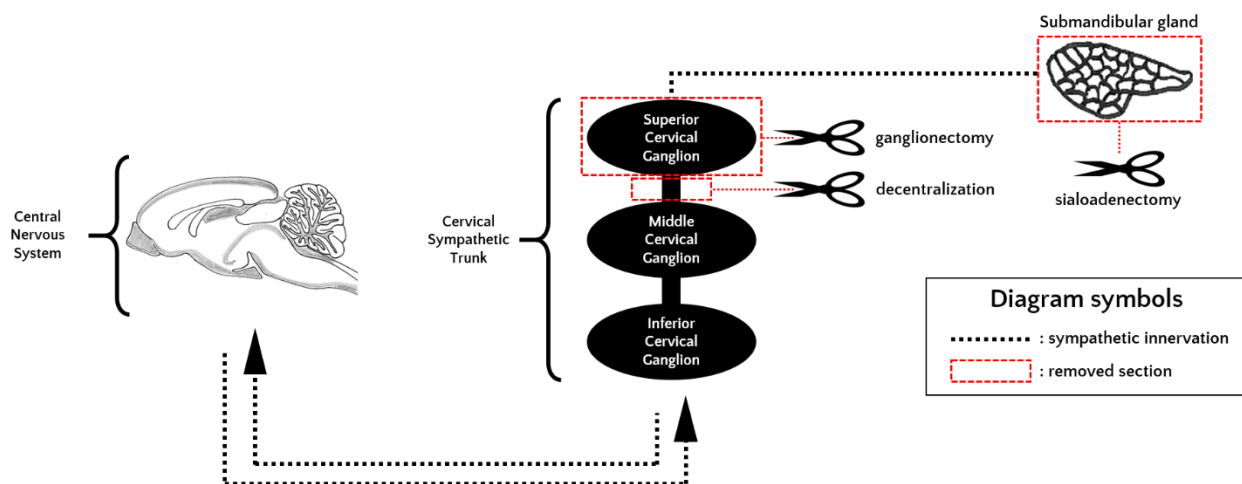
Figure 1-3. Sialoadenectomy was a surgical intervention added to our group's experiments.

Groups of rats that underwent this procedure had both submandibular glands removed. Upon recovery, further experiments were performed to assess the impact of this treatment on inflammation.

In sialoadenectomized rats, the anti-inflammatory effect was abolished and cell infiltration into the BALF comparable to sensitized and unoperated/sham operated rats was observed[26]. This

result lead to the hypothesis that SMG produced a factor(s) responsible for the anti-inflammatory effects[26]. The lab then evaluated gene expression of factors produced by SMG. Following decentralization or ganglionectomy there was an increase in nerve growth factor and epidermal growth factor mRNA in the SMG, which lead to the hypothesis that they were in part responsible for the observed anti-inflammatory activity[26].

The 1992 experiments showed that for the anti-inflammatory effect to occur, SMG needed to be present and that the sympathetic nervous system tonically inhibited synthesis and/or release of anti-inflammatory factors from the SMG that had downstream effects on neutrophils. This idea was consistent with observations from other groups that recruitment and activation of leukocytes required a functional and constant adrenergic tone and that these cells had β-adrenergic receptors that played a role in their activation and function[24,27,28].

New postulates following these observations included: 1. The SMG play a role in immunoregulation during anaphylactic and LPS-induced shock states and 2. The immunomodulatory actions of this gland can be regulated by the sympathetic nervous system. Subsequent experiments using our pulmonary inflammation model evaluated the effect of ganglionectomy and sialoadenectomy, both 1 week and just 10 minutes before (acute) exposing rats to 10 $^{mg}/_{kg}$ of endotoxin LPS[29]. In these experiments, blood from all rats was collected 5 min before and at 4 time points (15, 30, 45, 60 min) after exposure to LPS[29] (see **Figure 1-4**). Blood pressure was also recorded at these time points[29].

Before administration of endotoxin, blood pressure across all groups was between 100 – 120 mm Hg[29]. Fifteen min after exposure to LPS, all groups had a hypotensive response, a drop between 30 – 40 mm Hg[29]. Interestingly, control, sham, and acute sialoadenectomized rats showed an increase in blood pressure at 30, 45 and 60 min after insult[29], but blood pressure in ganglionectomized and sialoadenectomized rats did not recover and remained low[29] until at least 60 min.
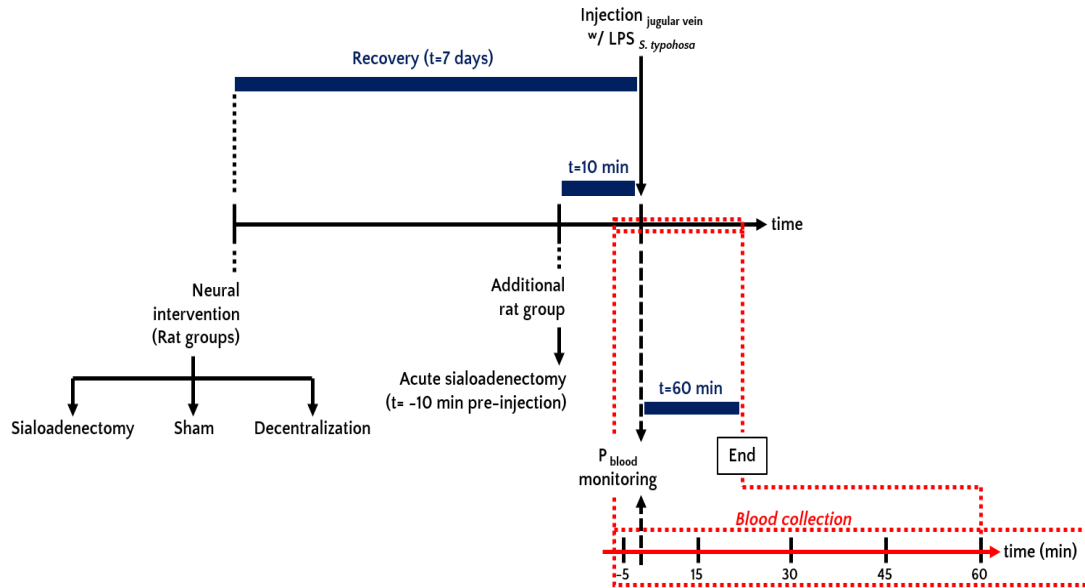
Figure 1-4. Timeline of experimental procedure to increase knowledge about effect of sialoadenectomy in inflammation.

Rats underwent neural interventions before being challenged with bacterial lipopolysaccharide (LPS). On the day of challenge, blood pressure was recorded, and blood samples were taken 5 minutes before challenge (-5), and 15, 30, 45, and 60 minutes post-challenge. Downstream analyses included blood cell counts and neutrophil activity assays.

In an attempt to elucidate the mechanism responsible for these observations, our group analyzed blood cell counts and neutrophil activity. Blood cell counts showed the same tendency across all time points and in all groups, and while neutrophil activation was diminished in ganglionectomized and sialoadenectomized rats, the difference between these and the other groups suggested that active neutrophils, contributed little to the hypotensive response to endotoxin[29].

Response to endotoxin in control rats indicated that there is an initial decrease in blood pressure followed by a gradual increase, towards a basal, normal blood pressure[29]. Because rats in which SMG had been removed showed no blood pressure recovery (non-reparative effect) for up to 60 min, these results further supported our postulate that the SMG contained a factor(s) that countered the hypotensive effect of endotoxic shock[29]. Furthermore, ganglionectomized rats

showed the same non-reparative effect, supporting the hypothesis that sympathetic nervous control on the SMG was required for an anti-inflammatory factor(s) to be active following shock[29].

Another line of experiments was concomitantly done to elucidate if mast cells release of Tumor necrosis factor (TNF), a cytotoxic factor, was an important player in the anti-inflammatory effect. Mast cells reside in epithelial and mucosal tissues, where they warn the immune system when local trauma or infection strike[30]. The granules contained within these cells contain histamine, TNF, proteases, and diverse inflammatory mediators[30]. Mast cells can have destructive effects in allergic reactions mediated by IgE, a receptor found in their surface[30].

In these experiments, rats were sensitized to *N. brasiliensis* and 30 days post-sensitization interventions included: 1. decentralization, 2. sialoadenectomy, 3. both procedures on the same animal, 4. ganglionectomy, 5. sham, 6. no intervention[31]. Mast cells were isolated 7 days post-intervention and mixed with chromium labelled WEHI-164 cells; a cell type sensitive to human TNF and widely used in short term cytotoxicity assays[31].

In agreement with previous results, decentralized rats showed significantly decreased mast cell-mediated TNF-dependent cytotoxicity, supporting the idea that SMG produced an anti-inflammatory factor that had effects beyond dampened neutrophil activity[24]. Additionally, data suggested that such factor(s) activity was controlled by the central nervous system[31] (see **Figure 1-5**). Interestingly, results showed that cytotoxic activity of mast cells from sialoadenectomized rats was also significantly reduced[31] (see **Figure 1-6** A). Since this rat group had no SMG, this observation suggested for the first time that SMG in untreated animals produced a factor that promoted mast cell-mediated inflammation[31] (see **Figure 1-6** B). Untreated animals also showed increased neutrophil production of reactive oxygen species and chemotaxis (see **Figure 1-6** C)[24]. Whether a SMG-produced pro-inflammatory factor was involved in neutrophil pro-inflammatory activity remains to be discovered. Remarkably, mast cells from ganglionectomized animals showed unchanged cytotoxic activity when compared with controls[31]. Since sympathetic

communication to the gland would come from the superior cervical ganglia and this rat group had

ganglia removed, this observation suggested for the first time that communication between the

CNS and SMGs could also use an alternate route and that CNS was able to elicit the glands to

release the putative pro-inflammatory factor that enhanced mast cell TNF-mediated cytotoxicity[31]

(see **Figure 1-6** D).
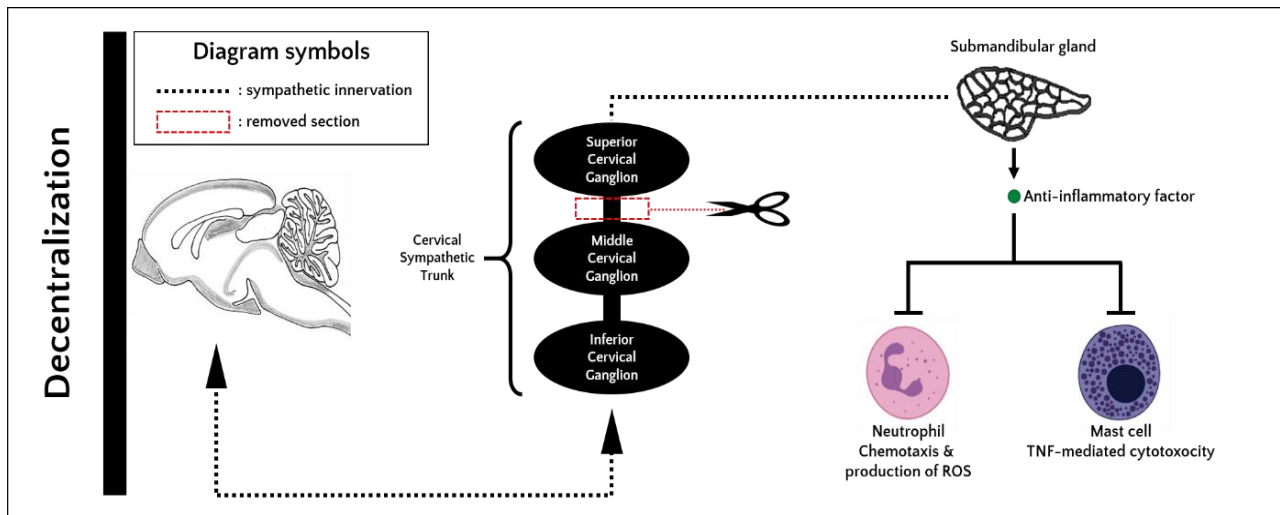
Figure 1-5. Decentralized rats lose the ability of the CNS to inhibit the release of an anti-inflammatory factor from submandibular glands.

Data suggested that the anti-inflammatory factor dampened neutrophil and mast cell pro-inflammatory activity. *Neutrophil and mast cell representations were obtained from BioRender.com*

Because we were interested in the anti-inflammatory factor(s), from this point on,

decentralization was chosen as our gold standard model, the only one shown to elicit the anti-

inflammatory effect associated with the SMG. With the object of defining the early (<1 h) and late

(>1h) anti-inflammatory effects of decentralization, the lab did a time course study using

decentralized and sham rats and collecting BALF, mast cells, neutrophils, and alveolar

macrophages (ALM) to perform functional analyses[32]. *In vitro* TNF cytotoxic assay using ALMs

stimulated with LPS showed that ALMs from decentralized rats had a significantly lower release

of TNF after 4 and 8 hours[32]. At the same time points, circulating neutrophils and their associated

phagocytic activity was also significantly dampened on decentralized rats[32]. These results

suggested that the anti-inflammatory effect tied to decentralization was linked to a functional

downregulation of neutrophils and macrophages[32].
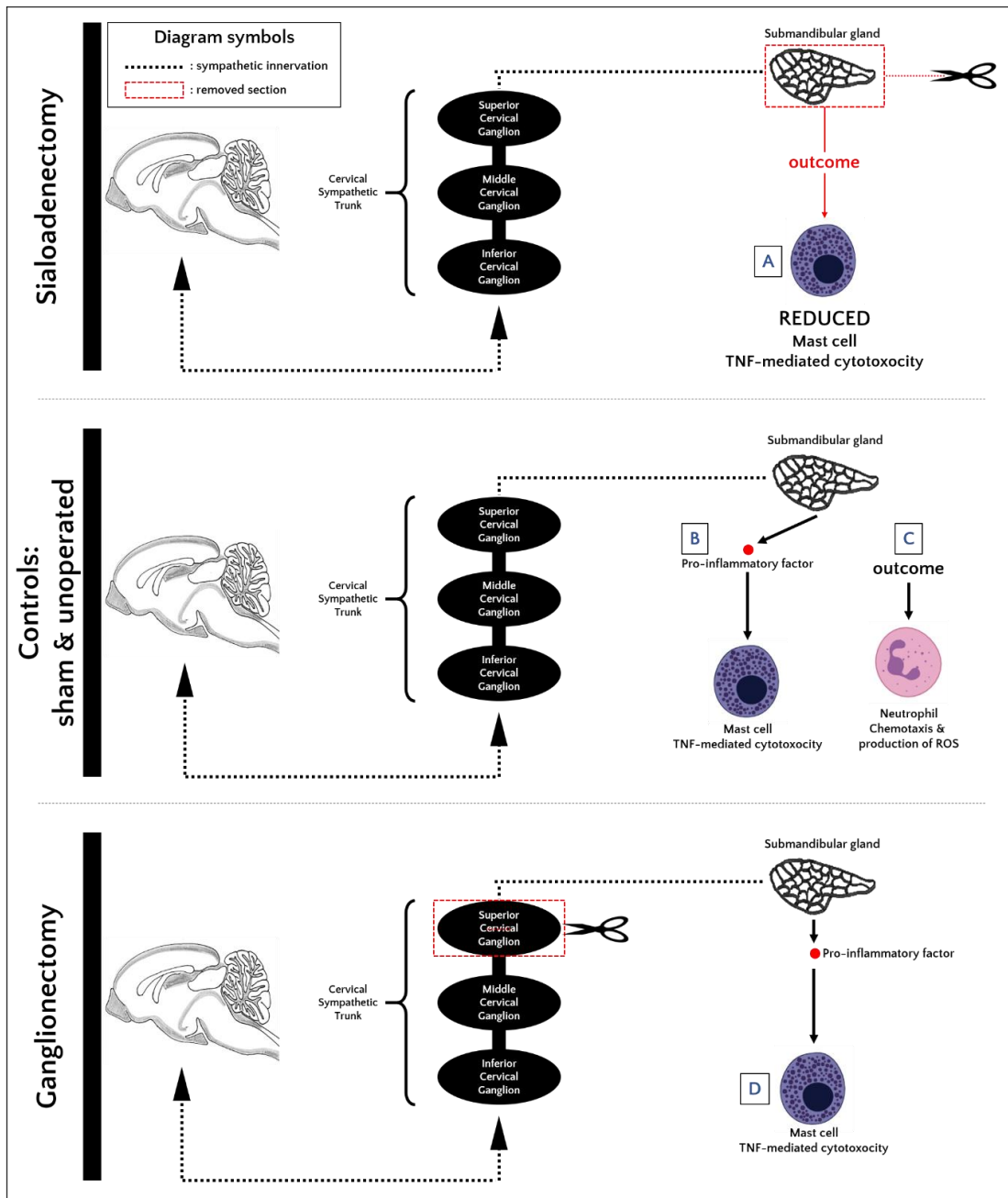
Figure 1-6. Controls and non-decentralization surgical interventions suggested that post-antigen challenge rats released a pro-inflammatory factor(s) from submandibular glands under CNS control.

Sialoadenectomized rats markedly reduced mast cell TNF-mediated cytotoxicity post-antigen challenge (A). Sham and unoperated rats showed an increase in pro-inflammatory activity. Mast cell TNF-mediated cytotoxicity increased (B), which tied with observations from sialoadenectomized rats (A) suggested that, upon insult, submandibular glands secreted pro-inflammatory factor(s) under CNS control. Control groups also showed an increase in neutrophil chemotactic activity, as well as unaltered ability to produce ROS (C). Interestingly, ganglionectomized rats also showed increased mast cell TNF-mediated cytotoxicity post-antigen challenge (D). This observation suggested that the CNS signalled the SMG through an alternate route to release the pro-inflammatory factor(s). *Neutrophil and mast cell representations were obtained from BioRender.com*

Based on these observations, attention then focused on identifying the factor(s) responsible for

this anti-inflammatory activity. The Befus group knew that the SCG innervated SMG. In addition,

14

it was known that SMG released several factors with endocrine and exocrine activity. Such factors facilitate tissue repair in the oral cavity, gastrointestinal tract, and downstream organs[33]. Additionally, the glands are known to secrete factors into the bloodstream[34], and our group had published work suggesting that at least one of these had immunomodulatory activity when posed with a threat, like anaphylaxis.

An elegant and yet simple experimental methodology was devised to identify the factor(s) responsible for the anti-inflammatory activity. Rats were sensitized to *N. brasiliensis* and, after recovery, their SMG harvested and frozen for later extraction of the anti-inflammatory factor(s)[35]. SMG extracts were firstly separated by size using molecular weight exclusion filters[35]. Sialoadenectomized, sensitized rats were given different sieved fractions of the SMG extracts prior to being exposed to LPS to induce shock[35]. A fraction containing molecules <3,000 Da protected these rats from undergoing hypotension upon exposure to LPS[35]. Fractions containing larger molecules were not protective; therefore, the anti-inflammatory factor(s) was in the <3,000 Da portion of the SMG extract[35]. Of note, when the fractions were not supplemented with protease inhibitors, the anti-endotoxic activity was lost; therefore, our group speculated that the factor(s) was a polypeptide[35].

Secondly, the <3,000 Da fraction was run through a reverse phase-high performance liquid chromatography platform[35]. Fractions were collected at different times and rats were given these fractions and then exposed to LPS[35]. It was noted that a fraction collected at 15.5 min had significant protection against hypotension[35]. After lyophilizing the fraction, electron spray mass spectrometry (ES-MS) determined the peptide to be XDIFEGG, where X stood for an undetermined amino acid[35]. However, ES-MS results identified the peptide at 738.5 Da, and DIFEGG is 636.8 Da[35]. It was established that X was a threonine (T), since this amino acid provides the additional Daltons to match that obtained by ES-MS[35]. On this basis, the peptide was named Submandibular Gland Peptide-T (SGP-T)[35]. Our group made synthetic SGP-T and used it

in *in vivo* endotoxic shock and anaphylactic models[35]. SGP-T significantly reduced the hypotensive response to insult in both models, suggesting that this was the long searched anti-inflammatory factor[35]. Moreover, a search of the rat genome database determined that this polypeptide domain is a fragment of <u>sub</u><u>m</u>andibular <u>r</u>at 1 (SMR1)[35], a protein also being studied by a group in The Institut Pasteur (Paris, FR) who speculated that SMR1 was a prohormone and that following post-proteolytic processing, some domains had endocrine functions[36]. This group showed in rats that SMR1 was androgen-regulated and observed, under provoked stress, an increase of an SMR1-derived pentamer (peptide: $_{29}$QHNPR$_{33}$) in blood that was taken up by target tissues[36]. They suggested that this pentamer could be synthesized and used in response to environmental stress[36].

Ensuing studies by our group established that SGP-T-derived fragment FEG and its D-isomeric analog, feG, retained the previously observed anti-hypotensive ability, as well as preventing disruption of intestinal motility and diarrhoea post anaphylaxis in rats[37]. In fact, even when protein translation normally incorporates L-amino acids and excludes D-amino acids[38], feG was more effective than both SGP-T and FEG[37]. So, further studies focused on the anti-inflammatory activity of feG. One study determined that leukocytes treated with feG or amidated feG, feG-NH$_2$, did not bind to heart atrial slices coming from LPS-treated rats[39]. This result indicated that treatment with these factors during inflammation could result in impeded leukocyte adhesion in the inflamed heart, in turn, reducing heart tissue damage[39]. Furthermore, the result suggested that a SMG-derived protein, SMR1, had the potential to modulate cardiac inflammation[39].

Concomitant analyses were also made on rat intestinal anaphylaxis models using SGP-T, FEG, and feG[40]. All three peptides prevented immediate LPS-mediated disruption of migrating motor complexes, a normal trait of smooth muscle cells in the gastrointestinal tract observed between meals and whose function is to move material down the digestive tube[40]. Also, the late (18 h) response to LPS, in the form of extravasation of leukocytes into peritoneum, was prevented by

feG[40]. This result added evidence that feG was a potent anti-inflammatory peptide, with activity not exclusive to pulmonary tissue in rats, but also in cardiac and intestinal tissues. A subsequent study to investigate FEG/feG using an *in vitro* intestinal anaphylaxis model suggested that these two tripeptides interacted with a receptor(s) in the intestine through which the anti-inflammatory effects were elicited[41].

Further animal studies of feG noted that this isomeric form was effective when administered orally[37,39,40], an appealing and advantageous property in drug delivery[42]. It was then important to test feG on human cells. Human neutrophils from healthy individuals were isolated and *in vitro* functional assays on oxidative burst, phagocytosis, movement, adhesion, and effect on expression of co-stimulatory molecules CD11b (a receptor on neutrophils that regulates adhesion and migration) and CD16 (a surface receptor that triggers neutrophil degranulation) were evaluated after activation with platelet activating factor (PAF) and treatment, or not, with feG[20]. PAF-activated human neutrophils exposed to feG had reduced movement and adhesion, as well as binding of antibodies to CD16[43]. Interestingly, binding of antibodies to CD11b was only reduced by 34%; yet, it may be enough to significantly reduce movement of neutrophils[43]. These results suggested that <u>in humans</u>, the anti-inflammatory activity of feG could be mediated by its interaction with CD11b and CD16 on neutrophils and putatively altering their activity in inflammatory responses[43].

To verify our findings, our group synthesized the putative control tripeptide, fdG, to test if a change in the amino acid sequence would elicit the same effect, and compared it to feG[44]. In comparison to fdG, feG had an anti-inflammatory effect *in vitro*, *ex vivo*, and *in vivo* contributing to the evidence that this tripeptide, putatively released under neural regulation, has the potential to ablate type I inflammatory effects on challenged airways[44]. Subsequent experiments showed that feG had the ability to reduce generation of reactive oxygen species by circulating neutrophils, providing one possible explanation for the anti-inflammatory mechanism of the tripeptide[45].

Ongoing research from other groups continued shedding light into the diverse roles SMR1 played in rats. A group in The Northwestern University Medical School (Chicago, USA) observed that in a model of erectile dysfunction, the gene coding for SMR1, *Vcsa1*, was significantly downregulated in penile tissues[46]. Across the Atlantic Ocean, the Institut Pasteur group studying SMR1-derived pentapeptide QHNPR, hereon referred to as sialorphin, showed that it modulated male rat sexual behavior[47] and was a mediator of pain perception[48]. In 2006, they published results about its human isofunctional domain found in human protein PROL1, opiorphin (peptide: $_{22}$QRFSR$_{26}$)[49]. On that same year, a group in The Albert Einstein College of Medicine (New York City, USA) observed that sialorphin played a role in erectile function[48]. They noted that yet another isofunctional domain is found within human protein SMR3A (peptide: $_{23}$QRGPR$_{27}$), that this protein could be a biomarker of erectile dysfunction, and that a potential therapeutic approach to erectile dysfunction could include increasing human SMR3A gene and protein expression[50]. In 2007, a review from our group summarized our anti-inflammatory findings of SMR1-derived SGP-T and recognized for the first time that Vcsa1, the rat gene that coded SMR1, was absent in the human genome[51]. This review presented a comparison between a gene cluster in rat chromosome 14 and a gene cluster in human chromosome 4[51]. These clusters were known in both species as the Variable Coding Sequence (VCS) multigene family[52]. The VCS family contained genes that coded for proteins expressed in glandular and secretory tissues[51]. Remarkably, human SMR3A and PROL1 were part of the human VCS family, just as SMR1 was within the rat's VCS gene cluster[51]. At the time, there was no known human homolog to SGP-T (see **Table 1-1**).

In ensuing experiments to better characterize the SMR1 protein in rats, our group developed two polyclonal antibodies (named 216 and 219) to SMR1, each targeting a different domain of the protein; antibody 216 was raised against SGP-T, while 219 was raised against SMR1 sequence $_{105}$PLSNPPTQLLSTEQ$_{118}$[53]. Both were IgG purified and used for WB analyses of major rat salivary glands, saliva, prostate, penis, testis, lung, and plasma[53].

Table 1-1. Functional protein domains in rat SMR1 have human homologs within proteins coded by the Variable Coding Sequence multigene family, present in both species.

Rat sialorphin (QHNPR) is located close to the amino terminus of SMR1, has analgesic and NEP inhibitory properties and therapeutic potential in erectile dysfunction. Human opiorphin (QRFSR) is located close to the amino terminus of PROL1, has analgesic and NEP inhibitory properties, and is speculated to have therapeutic effects in erectile dysfunction, the latter being a trait also for human SMR3A. Rat SGP-T (TDIFEGG) is located close to the carboxyl-terminus of SMR1 and has anti-inflammatory activity.

	Organism			
	Rat		**Human**	
Protein (length)	SMR1 146 amino acids (aa)		PROL1 248 aa	SMR3A 134 aa
Protein domain	$_{29}$QHNPR$_{33}$ (*sialorphin*)	$_{138}$TDIFEGG$_{144}$ (*SGP-T*)	$_{22}$QRFSR$_{26}$ (*opiorphin*)	$_{23}$QRGPR$_{27}$
Activity of protein domain	Analgesic NEP inhibitor Modulator of erectile physiology	Anti-inflammatory	Analgesic NEP inhibitor Modulator of erectile physiology	Modulator of erectile physiology

Interestingly, SMR1 in SMG was present at different apparent molecular weights (12 to 35 kDa) and isoelectric points (pI 4 to 7)[53]. The predicted molecular weight for the protein is 16 kDa and it was known that a cleaved product of 12 kDa occurred *in vivo*[52]. These data suggested that the protein was post-translationally modified. *N*-glycanase treatment of SMG extracts provided evidence that SMR1 is N-glycosylated *in vivo*[53]. Moreover, through immunoprobing our group detected the presence of SMR1 in parotid and sublingual glands, as well as in urogenital tissues, where SMR1-derived sialorphin was known to play a role in sexual behavior and erectile function[53]. More importantly, previous research had shown how SGP-T and its derived peptides decreased pulmonary inflammation, so lung tissue was screened for the presence of SMR1. Interestingly, this revealed several differently sized forms of SMR1, none of which changed after treatment with *N*-glycanase, suggesting different post-translational modifications to the protein were tissue-specific[53].

In experiments aimed to determine whether SMR1 release was under autonomic regulation, rats were given either a sympathomimetic or a parasympathomimetic agent[53]. Previous research showed that sialorphin, cleaved from near the amino terminus of SMR1, was released under acute

stress and sympathetic stimulation[54]. SGP-T, however, is a fragment close to the carboxyl-terminus of SMR1 and seeing that SMR1 was post-translationally modified, our group investigated if SMR1-derivates were differentially secreted upon different autonomic nervous stimulation. Not surprisingly, under sympathetic stimulation less saliva with higher protein content was secreted[53]. Of note, the sympathetic nervous system is activated under acute stress circumstances[55]. Antibody 216, raised against SGP-T, detected in these saliva samples several forms of the protein at different molecular weights and isoelectric points, and showing a similar pattern to that observed in extracts of SMG[53]. Moreover, molecular filtration of saliva and subsequent ELISA assays indicated that small peptides (<3000 Da) containing SGP-T were present in all rats stimulated with either sympathomimetic or parasympathomimetic agents. This led to postulates that (a) SMR1 is synthesized in SMG and released into saliva under autonomic stimuli, and (b) SMR1-derived peptide sialorphin has analgesic and erectile functions, while SGP-T has anti-inflammatory activity[53].

Because preclinical evidence on synthetic FEG, and feG were supportive and raised no safety issues, feG was tested on human subjects in a phase 1 study and then in a phase 2a study in mild atopic asthma. In 2012, results from a human trial using feG showed that this peptide had no significant effect on airways responses to inhaled allergen challenge (non-published data). Our group already knew that there was no equivalent gene to SMR1 in the human genome, so an *in-silico* analysis of gene(s) encoding proteins containing TDIFEGG, or SGP-T, in humans was already underway. Based on the analysis, our group proposed that a possible human isofunctional protein candidate was **h**uman CABS1 (**h**CABS1), which contained a domain proximal to the carboxyl-terminus, TDIFELL. Our group was intrigued to note that the *hCABS1* gene, which codes for this protein, is located in a cluster that seems to be conserved across homologous chromosomes (rat – chromosome 14, human – chromosome 4[18]). hCABS1 is physically adjacent to genes that code for isofunctional proteins of rat SMR1, SMR3a/b, PROL1. The significance of this shared chromosomal location with regards to transcriptional expression is unclear.

A new molecule to characterize

The production of polyclonal antibodies (pAbs) to hCABS1 was contracted to the biotech company GenScript Biotech (Piscataway, NJ, USA). Two New Zealand rabbits were immunized, each with one peptide sequence of 14 amino acids from two regions of hCABS1. The first region, aa 184-197 (DEADMSNYNSSIKS) corresponds to a predicted beta sheet of hCABS1. The second section, aa 375-388 (TSTTETDIFELLKE) contained the human anti-inflammatory peptide sequence (underlined). The antibodies were labelled H2.0 and H1.0, respectively.

To identify if, just as SMR1 in rats, hCABS1 was also present in the SMG, our group used the newly developed pAbs to hCABS1. Human SMG samples were collected, lysed, and supplemented with protease inhibitors before being separated by electrophoresis and immunoprobed using WB.

In 2015, we showed the first evidence of hCABS1 transcript in SMG and parotid glands, in addition to testes[18]. A highlight was that mRNA of the SMG was found in both male and female subjects[18], consistent with observations that opiorphin peptides derived from human gene *PROL1* are found in female and male saliva[49]. Furthermore, protein was also observed in extracts of SMG, lungs and as expected, in testes[18]. WB using H2.0 suggested that the protein was processed into several derivates and that the predicted and expected molecular weights of the major forms did not match, just like Calvel's and Kawashima's groups had observed when studying SMR1 in rats and mice, respectively[18].

To investigate whether the putative anti-inflammatory peptide sequence of hCABS1 was active, peptides TDIFELL, TDIFELLK, and FELL were synthesized. The experiment included fdG and feG as negative and positive controls, respectively[18]. To test their anti-inflammatory properties, an intestinal antigen challenge model was used. Briefly, rats were sensitized to OVA using Pertussis toxin as an adjuvant, and 4-7 weeks later were euthanized for collection of the terminal ileum, which was placed in an organ bath with a force displacement transducer. In the organ baths, ileum was treated with the peptide to be tested for 10 min, then the sensitizing antigen,

OVA, was added and the contractile response of the ileum measured. Results showed that hCABS1-derived peptides, FELL and TDIFELLK inhibited the antigen-induced ileal contraction to a magnitude similar to that of feG[18].

In another experimental model, the peptides were studied for their ability to inhibit the inflammatory cell influx into BALF of mice following intranasal exposure to LPS. FELL, TDIFELL, and TDIFELLK decreased the number of total leucocytes and neutrophils by more than half of those observed in fdG-treated (negative control) mice[18]. Alveolar macrophages in BALF , however, decreased in the same fashion as neutrophils only in mice treated with TDIFELL and TDIFELLK[18].

The significance of these experiments is that hCABS1, was identified as a human isofunctional homolog protein to SMR1 for its anti-inflammatory peptide activity. hCABS1's anti-inflammatory sequence appears to be TDIFELL and it has anti-inflammatory and anti-anaphylactic effects in animal models. hCABS1 in human SMG is present in both males and females at apparently similar levels, which provides evidence that hCABS1 has more functions than only supporting spermatogenesis. Putatively, one such function is to reduce inflammation upon exposure to insults.

To further investigate the similarities between SMR1 in the rat and hCABS1, we tested if hCABS1 release in humans was also under neural control. To test this hypothesis, we initiated a collaboration with a research team in Texas led by Dr. Thomas Ritz who has used various protocols to assess psychosocial stress. Various biomarkers of stress could be measured in saliva, and this would allow us to assess whether hCABS1 levels were under autonomic control (stress, see below)[56]. The focus of the Texan group on stress in humans, and our interest in hCABS1 were complementary. We used three experimental approaches to evaluate the effect of stress on the levels of hCABS1 protein in saliva.

Stress and saliva

Stress is a heterogeneous and complex condition, and care must be take in its definition. Dr. Hans Selye was a clinician scientist who first described the physiological aspects of stress. He noted that organisms exposed to stressors, insults that can be categorized as physical or psychological stimuli, rapidly activate the autonomic nervous system and a subsequent cascade of neuroendocrine responses that confer coping ability(-ies) to the organism by deviating from and extending normal physiological regulation[57,58]. Normally, these biological responses are transient and extinguished shortly after the stressor is no longer around[57]. However, dysregulation of the biological stress response(s) can have wide-reaching effects and is one way stressors can have a negative effect[59]. Of note, the effects of stress differ as a function of the duration of the biological stress response. Acute stress and its effects are encompassed in a period lasting from minutes to hours, while chronic stress is defined as stress that persists for several hours per day for weeks/months[59]. In our collaboration with Dr. Ritz we addressed both acute and chronic stress using cohorts of University students.

We evaluated hCABS1 levels in saliva because secretion of many factors from the salivary glands is controlled by autonomic nerves,[60] making it an appealing fluid to determine if hCABS1 was under neural control. Saliva has been used as a diagnostic fluid because it can be collected relatively easily in a non-invasive fashion, when compared to blood and serum collection. These characteristics reduce anxiety and discomfort in donors, whilst increasing the probability of acquiring repeated samples over time[61]. Saliva is a mixed product, derived primarily from the 3 pairs of major salivary glands (parotid, sublingual, and submandibular) and the 600 to 1,000 minor salivary glands situated in the regions of labial, buccal, palatal, and retromolar oral mucosa[62] (see **Figure 1-7**). Major salivary glands excrete saliva from acini into long branched ducts; this structure is surrounded by myoepithelial cells which are contractile and controlled by the autonomic nervous system (see **Figure 1-7**). Garrett and Emmelin postulated that these cells can compress the acini and ducts and assist in saliva flow[63]; however, to date there is no evidence
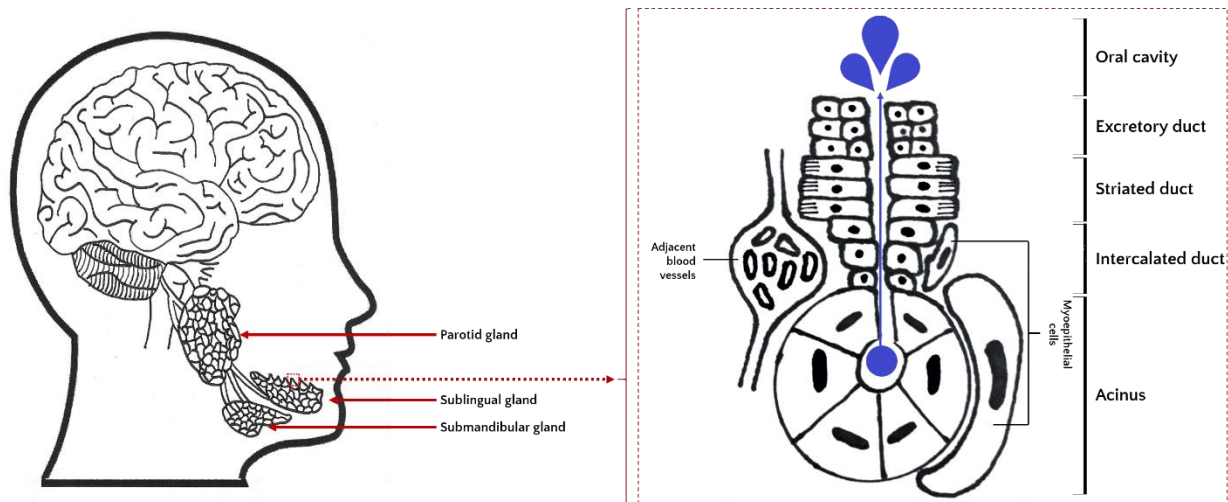
Figure 1-7. Location of the salivary glands within a human head and general diagram of an acinus terminating in an excretory duct.

In salivary glands, a primary saliva fluid (blue) is made in the acinus, which is connected to a canal system consisting of intercalated, striated, and excretory ducts and which modify saliva before it exits to the oral cavity. Acini comprise either serous or mucous cells. Myoepithelial cells surround acini and intercalated ducts.

that their presence is required for secretion to happen[62]. Of note, saliva is composed of 99% water and 1% dissolved organic and inorganic compounds[64]. This 1% fluctuates from person to person and in the same subject as a function of time[64]. Various ions and other molecules compose the inorganic fraction[64]. The organic fraction contains polypeptides and products from body secretions (urea, uric acid, creatinine) and putrefaction (putrescine, cadaverine, lipids)[64]. It is, then, this 1% that interests us, since it contains biological markers, like hCABS1, that can be indicators of disease or stress (see [21]).

Stress and hCABS1

To investigate baseline levels of hCABS1 in saliva, we collected a weekly sample for a period of 5 weeks from 64 participants (study 1)[21]. Each collection was accompanied by a validated questionnaire on negative affect[21]. To evaluate the levels of hCABS1 in acute stress, 16 participants underwent the Trier Social Stress Test (study 2)[21]. Briefly, individuals were asked to answer a baseline questionnaire on stress anxiety and depression; then given 5 minutes to prepare a speech to present in front of two "experts in presentation skills", upon entering the presentation room,

participants were made aware of the presence of a videorecorder and were told to deliver their speech standing[21]. Afterwards, they were asked to perform a mental arithmetic challenge for 5 minutes[21]. Throughout the speech and challenge the "experts" kept a neutral facial expression and provided no encouragement[21]. Saliva samples were collected 15 minutes and just before delivering the speech, then just after the arithmetic challenge and 15, 30, and 45 minutes post-stress[21]. At these time points, participants also completed a questionnaire on momentary negative affect (see **Figure 1-8**)[21]. Finally, to evaluate hCABS1 protein expression in saliva under chronic stress, a protocol designed to capture sustained academic pressure was designed with a collection of saliva from 19 students during their final exam period (study 3)[21]. Firstly, during the middle of the semester, a point when little stress was expected; then two collections, one at the early and the other at the late examination period[21]. At each collection point the students completed a psychological questionnaire package[21].
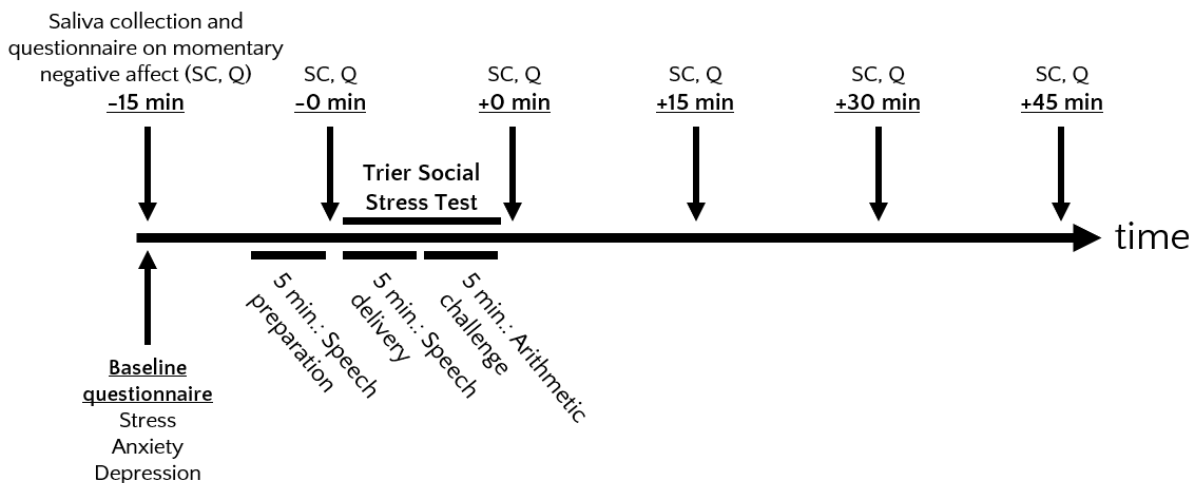
Figure 1-8. Protocol designed to evaluate hCABS1 expression in an acute stress scenario (study 2).

Subjects provided saliva samples and answered questionnaires on negative affect and perceived momentary stress at six time points during the study. 15 min and just before (-0) stress challenge (Trier Social Stress Test), and just after (+0), and 15, 30, and 45 min post-stress challenge.

When separating saliva samples through 1D-e and immunoprobing for CABS1 using our polyclonal antibody H2.0, we observed a 27 kDa variant that seemed to be stable over time at baseline (study 1)[21]. Once it was established that this form of hCABS1 was readily detected in saliva, we evaluated the acute stress samples (study 2). In these, the 27 kDa variant positively

correlated with perceived momentary stress levels[21]. Remarkably, samples from a small portion of individuals who self reported not feeling affected by the stressor had immunoreactive variants smaller than 27 kDa (<27 kDa) suggesting that these <27 kDa forms were indicators of resilience to stress[21]. Evaluation of changes of hCABS1 protein expression under chronic stress (study 3) showed no significant changes in the 27 kDa stress-associated band[21].

Overall, these results in human subjects suggested that hCABS1 is under control of the autonomic nervous system, indicated that hCABS1 in saliva can be a biomarker of acute stress and, potentially, of resilience to stress. Considering also hCABS1 gene chromosomal location, presence of anti-inflammatory domain, tissue distribution, and several observed protein variants, our data suggests that hCABS1 is an isofunctional homolog to rat SMR1 (see **Table 1-2**).

		Protein containing anti-inflammatory domain	
		Rat SMR1	Human CABS1
Trait	Gene found in Vcs multigene family	✓	✓
	Protein anti–inflammatory domain TDIFExx close to carboxyl terminus	✓ xx=GG	✓ xx=LL
	Protein in testes, submandibular gland, and saliva	✓	✓
	Various protein moieties observed in 1D and 2D Western blots	✓	✓
	Protein reactive to acute stress	✓	✓

Table 1-2. Evidence suggests that hCABS1 domain TDIFELL is a functional homolog to rat SMR1-derived SGP-T (TDIFEGG).

Rationale for this dissertation studies

To validate whether hCABS1 can be used as a biomarker of stress and begin elucidating its presence in different body compartments and its function, we needed to ensure that our research tools, antibodies targeting hCABS1, were specific. Previous characterization of pAbs H1.0 and H2.0 included WB analyses of recombinant hCABS1 overexpression cell lysate ($_r$hCABS1 OEL) and negative control lysate (NCL). Several discrete bands corresponding to different molecular

weights were detected by these pAbs. Based on these data, gel segments of an electrophoretically separated rhCABS1 OEL predicted to contain rhCABS1 were analyzed via MS-seq at the Alberta Proteomics and Mass spectrometry Facility (Edmonton, AB, CA). Results showed that rhCABS1 was detected in all-but-one of the analyzed segments (11 kDa)[18]. At the time, these observations provided confidence in the specificity of our pAbs and allowed us to proceed with their use in the study of hCABS1 in human-derived samples.

In WB, H2.0 indicated the occurrence of hCABS1 in human SMG, testes, lung, and saliva[18,21]. The multiple discrete bands observed in WB suggested that hCABS1 was post-translationally processed, perhaps through proteolytic digestion. Moreover, ≤27kDa putative variants of hCABS1 in saliva seemed to be associated with distress[21]. To validate these results, human SMG lysate and saliva were analyzed by MS-seq. Results did not identify hCABS1 among the proteins in these samples, thus raising questions about our initial conclusions with rhCABS1 OEL and our pAbs. Subsequent WB analysis showed that H2.0 also detected bands in NCL, suggesting that in addition to hCABS1, H2.0 detects other protein(s), making it essential to further characterize the immunoreactivity of our pAbs and, through evidence, support or refute our initial conclusions about hCABS1, its various forms, and association with distress.

At the same time, we thought about future analyses of saliva samples from different cohorts. This led to discussion of alternatives to WB analysis that would allow for high-throughput screening. We found a capillary nano-immunoassay platform (CNIA), Wes™, that used frugal volumes of antibody stocks, an appealing trait to us given the finite quantities of pAbs. We used our saliva samples and pAbs to compare CNIA to WB and, in doing so, developed a protocol for a high-throughput platform should future studies of hCABS1 take place.

We recognized that pAb batches are different from one another, and that specific batches of pAbs are finite, jeopardizing reproducibility in immunoprobing techniques. Throughout the first years of my postgraduate program, it became evident that development of monoclonal antibodies

(mAbs) to hCABS1 was a necessity for future research and characterization of hCABS1. Therefore, mAbs targeting hCABS1 were developed by a third-party company, with the hybridoma cell lines currently stored in the Canadian Biosample Repository (Edmonton, AB, CA). The generation of these mAbs and their use in determining expression profiles in biospecimens was pivotal in visualizing which cells/tissues express hCABS1 in humans.

We also investigated other aspects of the protein. Researchers in Japan and France had speculated CABS1 in other species contained intrinsically disordered domains[1] and bound to calcium[1,4,5]. We used available *in silico* online tools to analyze the human protein sequence of hCABS1. Our focus was the structure of the human protein, its putative co-factor binding sites, location of its disordered domains, and the conservation of TDIFELL across species. TDIFELL is a sequence within CABS1 that has anti-inflammatory activity[18]. This *in silico* work was initiated following our observations of immunoprobed hCABS1 in human-derived samples using our pAbs to hCABS1.

The work encompassed in this dissertation would not have been possible without valuable contributions by our collaborators. Dr Thomas Ritz and Dr David Rosenfield from the Southern Methodist University (Dallas, TX, USA) have provided human saliva samples from stress-induced individuals and have statistically analyzed whether our immunoprobing results associate with their validated questionnaires on stress and anxiety. Dr Michiko Watanabe and her research colleagues at the Case Western Reserve School of Medicine (Cleveland, OH, USA) have performed immunohistochemical assays on human submandibular glands using our pAbs to hCABS1, while Dr Lakshmi Puttagunta and Ms. Sarah Canil have performed immunohistochemical assays on human testes at the Alberta Precision Laboratories (Edmonton, AB, Canada). Dr Marcelo Marcet-Palacios provided guidance and expertise in several aspects of the dissertation, especially in performing the majority of *in silico* analyses of hCABS1. Finally, Dr Aron Gonshor and Dr Robert Buck from GB Diagnostics (Montreal, QC, CA) have aided in the development of mAbs to hCABS1.

Hypotheses

1. Calcium-binding protein, spermatid-associated 1 (hCABS1) is found in human submandibular glands lysates, saliva supernatant, and blood serum (**Figure 1-9**, 4)

2. Antibodies raised against hCABS1 sequence $_{184}$DEADMSNYNSSIKS$_{197}$ detect a variant(s) of the protein in saliva supernatant that is/are a biomarker(s) of acute psychosocial distress (**Figure 1-9**)

Objectives

1. To characterize polyclonal and monoclonal antibodies of hCABS1 using immunoprobing techniques on complex human biological samples

2. To validate the presence of hCABS1 in human-derived samples by optimizing protein isolation to facilitate mass spectrometry analysis

3. To validate the study of saliva-derived hCABS1 in acute stress

4. To contribute to the body of knowledge of hCABS1 by analyzing the protein sequence using *in silico* tools
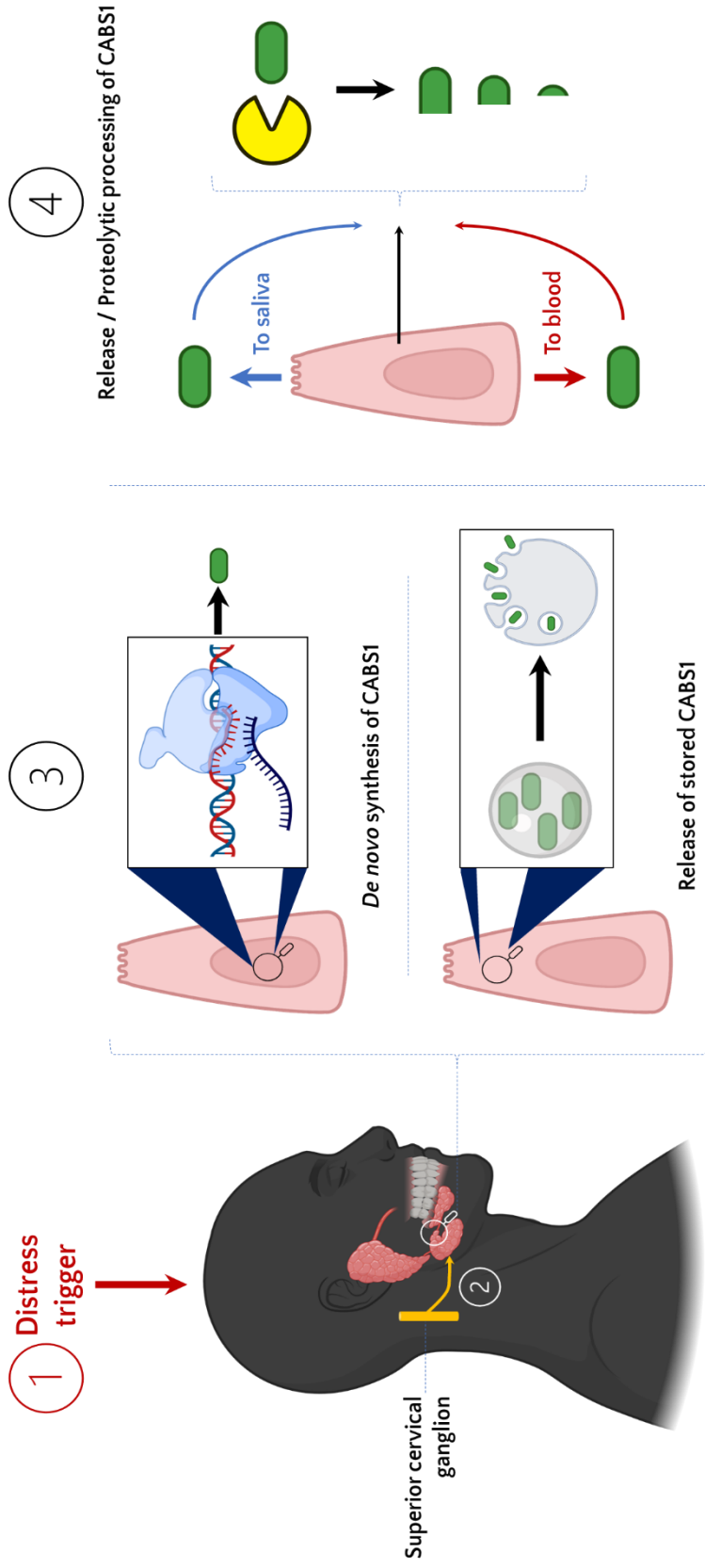
Figure 1-9. Conceptual model.

Magnifying lenses represent zooming into the compartment where they are placed. Pink diagrams in panel (3) are representative of submandibular glands (SMG) cells. In the face of distress (1), the submandibular salivary glands (SMG), innervated by the superior cervical ganglia (2), may increase transcription of CABS1 gene (3, upper panel) or release of internally stored CABS1 protein (3, lower panel). Since SMG can release factors into saliva and into blood, CABS1 may be released in full form, or proteolytically digested (4). The digested polypeptides may have functional roles yet to be elucidated. *Figure made with Biorender.com*

Chapter 2 : Characterization of polyclonal antibodies raised against synthetic peptides of human CABS1

Preamble

In 2016 our group used two pAbs to study hCABS1, H1.0 and H2.0. Up to that point, only H2.0 had been used in studies indicating that hCABS1 was present in human SMG, testes, and lung[18]. The following year, a publication showed presence of hCABS1 in saliva supernatant in WB probed with H2.0[21]. The latter article implied that hCABS1 could be a biomarker of distress and resilience to stress, a novel trait that motivated further studies. Alas, finite availability of H2.0 required the production of two new pAbs, H2.1 and H2.2, raised against the same immunogen that was used to produce H2.0.

This chapter characterizes the WB profiles of all pAbs available to our group in a transient overexpression cell lysate, human SMG, saliva, and serum. Of note, number of experiments (n) is indicated in figure captions. Furthermore, to aid in sequencing hCABS1 from human-derived samples, a 2D-e method was developed to resolve proteins in saliva supernatant. Finally, through a fruitful collaboration with Dr Michiko Watanabe, we conducted the first immunohistochemical studies of hCABS1 in SMG.

Hereafter, I use the word "variant(s)" to denote putative hCABS1 bands of different molecular size detected in WB. In the context of this dissertation, it refers to one of the portions into which something is divided. Moreover, to avoid repetition, I use the term 'form(s)' to refer to 'variants'.

Tuesday, February 18, 2020

To whom it may concern,

We fully support that this chapter of Eduardo's MSc thesis contains images from immunohistochemical analyses of human submandibular glands performed in Case Western Reserve University (Cleveland, OH, USA) by Yong Qiu Doughman and Dr Michiko Watanabe with samples provided by GlaxoSmithKline through Dr Stephen J. Lewis. The polyclonal antibodies to human Calcium-binding protein, spermatid-associated 1 (hCABS1) used in these analyses were provided by Dr Dean Befus from the University of Alberta (Edmonton, AB, CA).

Interpretation of immunohistochemical results was a collective effort including Dr Watanabe, Mrs. Doughman, Dr Befus, and Mr. Reyes Serratos. Dr Befus and Eduardo held several meetings where they discussed the physiology of submandibular glands, cell types that were positive for hCABS1, and results of studies with pre-immunization sera (negative controls). Subsequent electronic correspondence between Dr Watanabe and Dr Befus gave confidence in data interpretation, ultimately leading to the design of two posters presented at the University of Alberta (2018) and the Collegium Internationale Allergologicum conference in Mallorca, Spain (2018).

Respectfully yours,

Michiko Watanabe
Professor Emeritus of Pediatrics, Genetics, Anatomy
Case Western Reserve School of Medicine

Yong Qiu Doughman
Research Assistant
Case Western Reserve School of Medicine

Stephen J. Lewis
PhD, Professor
Division of Pulmonology, Allergy and Immunology
Case Western Reserve School of Medicine

A. Dean Befus
Professor Emeritus
Alberta Respiratory Centre
University of Alberta

Eduardo Reyes Serratos
MSc Candidate
Alberta Respiratory Centre
University of Alberta

Introduction

Calcium-binding protein, spermatid-associated 1, known as hCABS1, is a protein that in humans is encoded by gene *CABS1* located in Chromosome 4, 'q' arm, region 1, subregion 3, sub-band 3 (4q13.3)[d]. The gene has two exons, separated by one intron; however, it is the first exon that contains the coding sequence. The translated protein, 395 amino acids (aa) long, is speculated to have four phosphorylation sites (aa 273, 287, 319, 376)[65]. CABS1 was first identified in rodents in 2009 by two independent research groups working on spermatogenesis-related projects[1,4]. Both groups reported CABS1 in rodents that year. At that time, the homolog human protein was called *testis development protein NYD-SP26*[1,4]. In their seminal contributions to the knowledge of CABS1, they reported the protein to be expressed in testis, specifically in spermatids[1,4], and to be localized subcellularly in the mitochondrial inner membrane[1]. CABS1 properties included susceptibility to protease degradation[1], phosphorylation[1], intrinsically disordered domains[1], and an ability to bind calcium[1,4]. The latter was predicted to elicit important roles in calcium signalling and storage in mature sperm[4]. Although these seminal publications suggested that the protein was specific to males, further research proved the presence of *CABS1* gene transcript in female rhesus macaque uteri[13], Angus heifer oviductal epithelial cells[14], and human labial salivary glands[16].

Our interest in <u>h</u>uman CABS1 (<u>h</u>CABS1) began when we looked for a gene in the human genome that encoded a peptide domain that had anti-inflammatory properties in rats, TDIFEGG[18]. In rats, the domain was within the carboxyl-terminus of protein SMR1 that is coded by gene *Vcsa1*, which is part of the Variable Coding Sequence (VCS) multigene family, a gene cluster conserved across species[51]. Humans lack a homolog to rat gene *Vcsa1*. Our search for a human gene coding for a similar anti-inflammatory domain led us to the gene h*CABS1*, which translates a protein that

---

[d] Coding DNA sequence location within human chromosome 4: 70'334,981 – 70'337,116

contained TDIFELL[18]. Interestingly, the domain is within the carboxyl-terminus of hCABS1 and the gene is located within the human VCS multigene family.

To study hCABS1 at the protein level, we generated two polyclonal antibodies (pAbs), named H1.0 and H2.0. H1.0 targeted the anti-inflammatory domain close to the carboxyl-terminus of hCABS1, while H2.0 targeted a predicted beta sheet in the middle of hCABS1. Since our group had previously demonstrated that rat SMR1 was expressed by the submandibular glands (SMG), and was under sympathetic nervous system (SNS) control, the logical path was to test whether hCABS1 was also expressed in the SMG and influenced by the SNS.

With H2.0 used in WB, our group reported the presence of hCABS1 in testis, lung, and both male and female salivary glands[18]. These samples showed several discrete bands in WB[18], which could indicate that hCABS1 is proteolytically cleaved[66]. To test sympathetic control over hCABS1 expression we studied saliva samples from three cohorts where psychosocial stress was assessed[21]. Psychosocial stress is an activator of SNS[67], the SMG is proven to be regulated by SNS[60], and saliva is a biological fluid reflecting the proteomic changes induced by stress via the SNS[56]. WB analyses of these saliva samples using H2.0 showed that levels of a 27 kDa immunoreactive form (putatively hCABS1) positively correlated with self-reported anxiety stress[21]. Moreover, <27 kDa bands were present in individuals that self reported lower stress when challenged, leading to the hypothesis that the presence of these bands was an indicator of resilience to stress[21]. Altogether, these observations led our group to suggest that hCABS1 in saliva is a physiological biomarker of distress.

Nonetheless, the noun *biomarker* should only be applied to a molecule objectively quantified and assessed as a marker of either a normal biological process, a pathogenic process, or a pharmacological reaction to a given therapeutic intervention[68]. Our group's initial findings are suggestive of hCABS1 being a biomarker based on what our pAbs indicate on WB, but this assertion requires careful evaluation. At present, we have grown cautious about our past

observations and recognize that the use of pAbs as a research tool has both advantages and limitations. pAbs can be more sensitive than monoclonal antibodies (mAbs); as such, they can give a higher signal in immunoprobing techniques[69]. pAbs, however, can be less specific than mAbs by containing clones that bind to proteins different than the intended target[70]. With these factors in mind, if one intends to use antibodies as a research tool for biomarker discovery, it is of capital importance to validate such antibodies, whether pAbs or mAbs, in all techniques that involve them[71,72].

This chapter describes the characterization of four pAbs produced for our group; H1.0, H2.0, H2.1, and H2.2 in WB analyses of a transient overexpression cell lysate model, human saliva and serum, and human SMG (SMG), the latter also analysed by immunohistochemistry. We also detail two approaches to treat human-derived saliva prior to mass spectrometry sequencing (MS-seq) in an effort to detect hCABS1. Similarly, we analyse MS-seq results of the transient overexpression cell lysate, the only sample where hCABS1 has been detected by MS-seq to date. Overall, we sought to challenge and improve our previously established methodologies of SDS-PAGE and WB to detect hCABS1, and discuss results from studies using the new pAbs in the context of most recent published observations.

Methodologies

The study, entitled 'Anti-inflammatory proteins and biomarkers of stress' (University of Alberta internal ID: Pr00001790), was approved by the Research Ethics Office, University of Alberta (Edmonton, AB, CA).

Polyclonal antibodies to hCABS1

Rabbit polyclonal antibodies were custom made against two different regions of hCABS1 (GenScript Biotech, Piscataway, NJ, USA). Polyclonal antibody H1.0 was raised against hCABS1 amino acids (aa) 375-388 TSTTE<u>TDIFELL</u>KE (underlined anti-inflammatory domain). Polyclonal antibodies H2.0, H2.1, and H2.2 were raised against hCABS1 aa 184-197

DEADMSNYNSSIKS. Two commercial antibodies were also used, each in a single WB experiment. sc-136594, an affinity-purified rabbit antibody raised to a domain of hCABS1 located near the N-terminus (Santa Cruz Biotechnology, Dallas, TX, USA), NBP1-31573, an affinity-purified rabbit polyclonal antibody raised to hCABS1 aa 157 to 395 (Novus Biologicals, Centennial, CO, USA).

Western blot controls

Pre-immunization sera (PimmS) from each rabbit used to produce our pAbs were used as negative controls, and blocking controls were performed by incubating each pAb with the peptide used to create the pAb (immunizing peptide) in 10X amounts for 18 h (T = 4°C) before WB were performed. Samples containing a recombinant hCABS1 with a FLAG tag were probed with ANTI-FLAG ® M2, a mouse monoclonal antibody targeting FLAG sequence DYKDDDDK (Sigma-Aldrich, Oakville, ON, CA).

Transient overexpression cell lysate controls

A recombinant hCABS1 (rhCABS1) overexpression cell lysate (OEL) produced in Human Embryonic Kidney 293T (HEK293T) cells (OriGene Technologies Inc., Rockville, MD, USA) was purchased for WB. HEK293T was immortalized using SV40 large T antigen[73]. It is widely used to produce recombinant proteins by transfection of vectors containing potent viral promoters (e.g., CMV promoter) (see **Figure 2-1**). The negative control cell lysate (NCL) originates from HEK293T cells with the same vector but lacking a CABS1 cDNA insert.
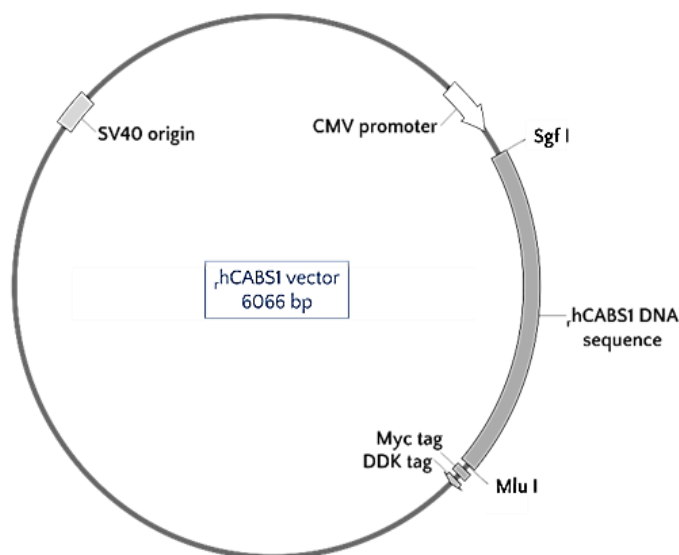
Figure 2-1. Plasmid used to generate recombinant Calcium-binding protein, spermatid-associated 1 in HEK293T cells (OriGene cat. #RC208496).

Important features in the vector include SV40 origin, to replicate in mammalian cells, CMV promoter, to express the cloned cDNA (i.e., rhCABS1 DNA sequence), and the sequence to add Myc and DDK tags in the carboxyl end of the recombinant protein. Restriction enzymes Sgf I and Mlu I were used to cut the plasmid and insert cloned cDNA. *Plasmid diagram generated using SnapGene Viewer*

Collection of human samples

Submandibular gland

Fresh human submandibular glands (SMG) samples were obtained from patients undergoing surgical removal of local squamous carcinomas. Each SMG was homogenized at 4ºC using as diluent Radio Immunoprecipitation Assay (RIPA) buffer (Tris-HCl (pH 7.4) – 50 mM, NaCl – 150 mM, EDTA – 1 mM, 1% NP40, 0.25% sodium deoxycholate) supplemented with protease inhibitor cocktail (Sigma-Aldrich – cat. #P8340). Post-homogenization, samples were centrifuged, separating the mix into three layers: a pellet, a middle supernatant, and a floating debris layer. The middle layer was collected, aliquoted and aliquots were stored at -80ºC. Prior to downstream analyses, determination of total protein concentration for each sample was done using a Pierce™ BCA Protein Assay Kit (Thermo Scientific, Waltham, MA, USA).

Serum

Human serum was obtained as described in a protocol from ProImmune Limited[74]. Briefly, a vacutainer tube containing no additive was used to collect 10 mL of whole blood from a donor. Collected blood was incubated for 45 min to allow clotting. Subsequently, the tube was centrifuged at 1500 x g and 21ºC for 15 minutes. Supernatant (serum) was carefully aspirated, transferred into 300 µL aliquots (new micropipette tips were used between aspirations), and stored at -80ºC until used. Prior to downstream analyses, determination of total protein concentration for each sample was done using a Pierce™ BCA Protein Assay Kit (Thermo Scientific).

Four experiments were carried out using human serum. In each experiment, an aliquot retrieved from -80ºC was used to create serial dilutions (total protein (µg): 15, 1.5, 0.15, 0.015) to load in each lane of a 12% polyacrylamide (PA) gel.

Saliva

Unstimulated whole saliva from a single individual was collected using the passive drool technique protocol (Salimetrics LLC, Carlsbad, CA, USA)[75] over the course of 15 days. Over the

course of the collection period, the individual exercised for, at least, 1 hour in the evenings prior to collection, slept a minimum of 7.5 h, had a set breakfast, brushed, and flossed teeth, and post-teeth cleansing waited 1.5 h before whole saliva collection. Samples were frozen at -20°C immediately after collection. When the collection period finalized, all collected samples were thawed and pooled. The resulting pool was centrifuged at 1500 x g and 4°C for 20 minutes. The supernatant was collected and transferred into aliquots. The pellet was resuspended in modified RIPA buffer (Tris-HCl (pH 7.4) – 50 mM, NaCl – 150 mM, EDTA – 1 mM, 1% NP40, 3% SDS, 1% sodium deoxycholate) and stored at -80°C.

Some supernatant aliquots were subjected to an amylase removal treatment adapted from Deutsch et al.[76] Briefly, 500 mg of potato starch, which can interact with alpha amylase by affinity adsorption, was loaded into a 1 mL syringe attached to a 0.45 μm PVDF filter. 350 μL of molecular biology grade water were passed through the column to moisturize the substrate. Once moist, 500 μL of saliva supernatant were passed through the column. The eluate was considered amylase-free saliva (see **Figure 2-2**). To elute adsorbed proteins, a solution of 3% ($^v/_v$) β-mercaptoethanol and 10% ($^m/_v$) SDS was ran through the column and collected in a tube.

Prior to downstream analyses, determination of total protein concentration for each sample was done using a Pierce™ BCA Protein Assay Kit (Thermo Scientific).
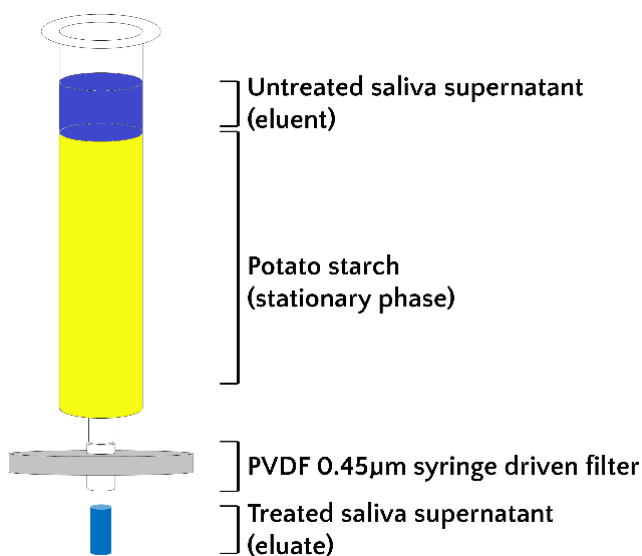
Figure 2-2. Amylase removal device.

Saliva supernatant, collected post-centrifugation, was passed through a syringe filled with potato starch and connected to a filter. Eluate was considered amylase-free saliva supernatant.

One dimensional (1D) SDS-polyacrylamide gel electrophoresis (SDS-PAGE)

The TGX™ FastCast™ 12% Acrylamide Kit (Bio-Rad, Mississauga, ON, CA) was used to prepare 1.5 mm thick gels the day prior to an experiment[77]. Polymerization took 30 min. Polymerized gels were then wrapped in a Kimwipe, placed inside a Ziploc bag, submerged in molecular grade water, and placed at 4°C until the experiment.

The first task to perform on the day of the experiment was buffer preparation. 1X SDS-PAGE running buffer was prepared from a 10X stock (1L 10X stock solution: Trizma base – 250 mM, Glycine – 1.92 M, SDS – 35 mM).

Afterward, samples were supplemented with Laemmli sample loading buffer (Bio-Rad) to a final concentration of 1X and brought to volume with RIPA buffer supplemented with 10 mM DTT and P8340 protease inhibitor cocktail. Subsequently, samples were boiled for 5 minutes before being loaded into the gel. As a reference, Chameleon Duo pre-stained protein standards (Li-cor Biosciences, Lincoln, NE, USA) were loaded on each gel alongside the samples.

During electrophoresis, samples were firstly run at 100 V until they reached the bottom of the stacking gel; once there, running voltage was increased to 125 V until sample buffer reached the bottom of the gel. Downstream procedures included gel staining with Blue Silver dye and subsequent MS-seq analyses, or WB (described below).

Two dimensional (2D) SDS-PAGE of human saliva supernatant

For every 2D SDS-PAGE experiment, enough human saliva supernatant sample aliquots to give 200 μL were combined, protein was precipitated with acetone (protocol Acetone precipitation of saliva supernatant (preparation for 2D SDS-PAGE) described in Appendix B of this dissertation) and resuspended in 125 μL of rehydration buffer (Bio-Rad). This was now considered to be the protein-containing solution.

A detailed 2D SDS-PAGE protocol is described in "Appendix B– 2D-e protocol for MS-seq analysis" of this dissertation. Briefly, the whole volume of protein-containing solution was pipetted along the length of one lane of a rehydration/equilibration tray. Then, a 7 cm immobilized pH gradient (IPG) strip was placed facing down onto the resuspended sample. Mineral oil was added on top and the IPG strip was left overnight to rehydrate. The next day, the rehydrated IPG strip was placed on Bio-Rad's i12 7 cm focusing tray, covered with mineral oil and carefully placed on the PROTEAN® i12™ IEF system (Bio-Rad). Software protocol '7 cm, pH 3-10 G' (detailed steps on Appendix B) was selected to run overnight. The next day the IPG strip underwent sequential 10 min washes with equilibration buffers (500 mL stock solution: urea – 6 M, glycerol – 3.26, SDS – 70 mM, Tris-HCl buffer (pH 8.8) – 16.7 mL, BTV with $H_2O_{deionized}$): Equilibration buffer #1 (add 100 mg of DTT to 10 mL of stock solution), and Equilibration buffer #2 (add 400 mg of iodoacetamide to 10 mL of stock solution). Once an IPG strip was equilibrated, it was taken to the biosafety cabinet and positioned on top of a 12% PA resolving gel and next to a wick soaked in 3 µL of molecular weight markers solution (see **Figure 2-3**). The resolving gel was placed in a vertical SDS-PAGE chamber, covered with 1X SDS-PAGE running buffer (recipe described above), and ran at 100 V until the blue dye reached the bottom of the gel. From this point   on,
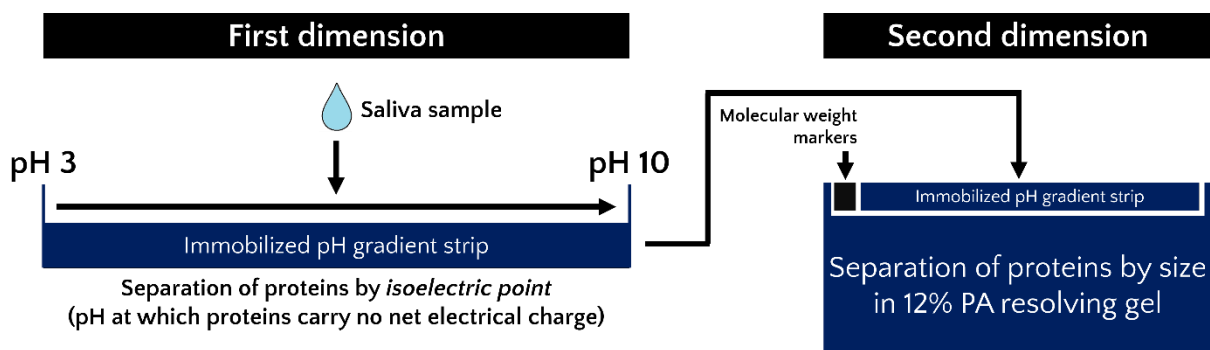
Figure 2-3. 2D SDS-PAGE pipeline diagram.

Prior to first dimension separation, proteins from saliva samples are precipitated and then resuspended in rehydration buffer. This solution was then used to rehydrate immobilized pH gradient (IPG) strips. Rehydrated strips were placed in an electrical current to separate proteins by isoelectric point. Once done, the IPG strip was placed atop a 12% polyacrylamide gel next to a wick soaked with molecular weight markers solution. Proteins were then subjected to an electrical current that induces separation by their linearized size.

downstream procedures included gel staining with Blue Silver dye and subsequent mass spectrometry sequencing (MS-seq) analyses, or WB (described below).

Western blot analysis

The day of the experiment, 1X WB running buffer (1L 1X working solution: Trizma base – 40 mM, Glycine – 300 mM, Methanol – 200 mL) was prepared and placed at 4°C.

For WB, electrophoresed samples in gels were placed in a cassette containing fiber pads, filter papers, and a 0.45 μm pore-sized nitrocellulose membrane (see **Figure 2-4**). The cassette was placed in a WB vertical transfer chamber along with an ice pack on the side. 1X WB transfer buffer was added until the cassette was covered. Transfer was done at a constant amperage of 0.5 A for 1 hour.

Figure 2-4. WB tank transfer cassette setup.

The gel must be placed on the cathode side of the cassette, while the membrane must be on the anode side as proteins, negatively charged, will travel to the anode.

After protein transfer, the cassette was opened and all, but the nitrocellulose membrane, was discarded appropriately. The nitrocellulose membrane was placed inside an opaque WB box and washed 2X rapidly (<1 min) with double distilled water before adding enough Odyssey (PBS) blocking buffer (Li-cor Biosciences) to cover the membrane. Membrane blocking was done at T_{room} for 1 h. Once blocked, blocking buffer was discarded and the membrane was immunoprobed overnight at 4°C with the antibody(-ies) pertinent to the experiment at the working concentration detailed in **Table 2-1**. The antibody diluent solution (ADS) was composed of half 1X PBS supplemented with 0.05% Tween 20, and half Odyssey (PBS) blocking buffer. Of note, to block our pAbs the immunizing peptide was added in 10X ($^{ng}/_{\mu L}$) amounts to ADS containing the pAb to

be blocked and incubated overnight at 4°C before being used to immunoprobe a membrane. After overnight membrane immunoprobing, the antibody solution was appropriately discarded, and the membrane was washed as detailed in **Table 2-2**. Li-cor Biosciences secondary antibodies were diluted 1:10,000.

Table 2-1. WB antibody working concentrations.

Pre-immunization serum (PimmS) corresponding to each of our hCABS1 pAbs were diluted to the same working concentration used when immunoprobing with the pAbs to hCABS1. Blocked pAbs refer to hCABS1 pAbs blocked with their immunizing peptide. Commercial antibodies sc-136594, NBP-31573 (both target: hCABS1) and Anti-FLAG (target: DYKDDDDK domain) were diluted as suggested by their manufacturers.

Antibody ID	Immunoprobe working concentration ($\frac{ng}{\mu L}$)
H1.0	
PimmS H1.0	3
Blocked H1.0	
H2.0	
PimmS H2.0	3
Blocked H2.0	
H2.1	
PimmS H2.1	2
Blocked H2.1	
H2.2	
PimmS H2.2	2
Blocked H2.2	
sc–136594	1
NBP–31573	10
Anti–FLAG	10

Table 2-2. Immunoprobed membrane washing steps and solutions.

Wash step	Washing solution	Time of wash (min.)
1.1		5
1.2	PBS 1X + 0.05% Tween 20	5
1.3		5
Incubation with secondary antibody	50% – PBS 1X + 0.05% Tween 20, 50% – Odyssey blocking buffer (PBS), Secondary antibody (1 : 10,000)	60
2.1	PBS 1X + 0.05% Tween 20	10
2.2		10
3.1	PBS 1X	10

For the experiments shown in **Figure 2-18** and **Figure 2-19** the membranes were stripped from immunoprobes (either H1.0, H2.0, or their PimmS) using harsh stripping buffer (100 mL working solution: SDS 10% – 20 mL, Tris HCl, pH 6.8, 0.5M – 12.5 mL, β-mercaptoethanol – 0.8 mL, $H_2O_{distilled}$ – 67.5 mL). Briefly, the buffer was warmed to 50°C and poured into a box containing the nitrocellulose membranes. The box was placed in an orbital incubator (T=50°C) for 45 min. The solution was discarded appropriately, and the membrane rinsed under running distilled water for 2 min. Subsequently, membranes were washed 3 times (t_{wash}=5 min.) with 1X PBS supplemented with 0.05% Tween 20. Membranes were then blocked with Odyssey blocking buffer (PBS) for 1 hour (T_{room}) and re-probed with H1.0, H2.0 or their PimmS at a working concentration of 0.3 $^{ng}/_{\mu L}$.

Once membranes were washed, WB were captured in an Odyssey scanner and bands were visualized in ImageStudio Lite v.5.2 (Li-cor Biosciences). For all WB images, curves were adjusted for the 700 and 800 nm channels to K=1. For both channels the Grayscale black on white setting was selected, rendering a bright background and dark immunoreactive bands. Maximum and minimum values were then adjusted to reduce background signal and allow optimum visualization of bands (see **Figure 2-5**).
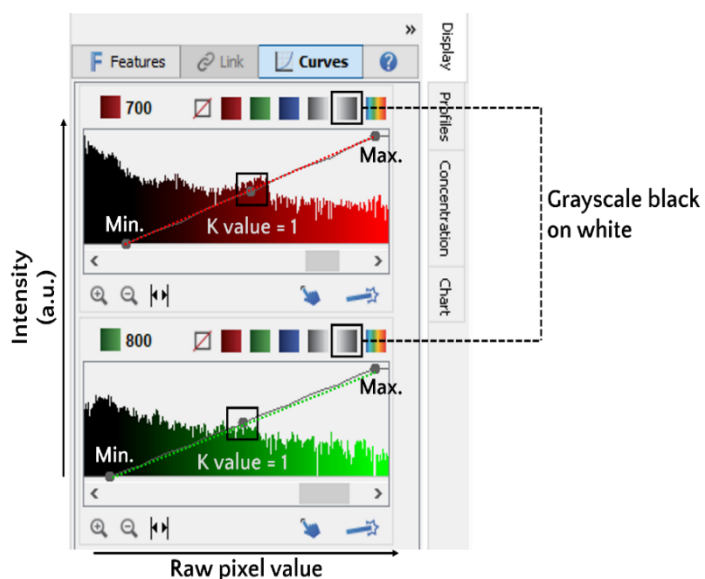
Figure 2-5. ImageStudio Lite Curves window under the Display panel.

Emission signal at 700 nm and 800 nm were captured in independent channels and shown in red (above) and green (below). Plots show signal intensity in arbitrary units (a.u.) against the raw grey pixel values (Raw pixel value). The grayscale selection icon is highlighted in black boxes and labelled Grayscale black on white.

Statistical analysis of SMG immunoreactive bands

In WB of SMG lysates, whenever a hCABS1 immunoreactive band was detected with two or more antibodies, one-way ANOVA was performed to determine if the molecular weights of said bands were statistically different. Molecular weight in kilodaltons (kDa) was determined using Li-cor software. Observed hCABS1 variants in independent WB experiments were categorized by size in kDa for H1.0 (n=5), H2.0 (n=5), H2.1 (n=6) and H2.2 (n=4). P-values correction was performed via post-hoc Holm-Šídák tests. A graph was created showing all SMG bands detected with our pAbs and indicating which hCABS1 variants are likely the same protein detected by more than one pAb (see **Figure 2-13**).

Mass spectrometry sequencing (MS-seq) analyses

Samples of interest were separated by SDS-PAGE as described above and stained using Blue Silver dye (recipe and protocol in Appendix B). Gels were then cut at the equivalent position of immunoreactive WB bands (when separating in 1D-e) or spots (when separating in 2D-e) and sent for analysis to the Alberta Proteomics and Mass Spectrometry Facility (University of Alberta, Edmonton) for in-gel trypsin digestion and MS-seq analysis through a bottom-up approach (**Figure 2-6**). This facility uses an LTQ Orbitrap XL Hybrid Ion Trap-Orbitrap mass spectrometer (Thermo Fisher Scientific). Data is processed using Proteome Discoverer v.1.4 (Thermo Fisher Scientific) using the Sequest (Thermo Fisher Scientific) database search algorithm which creates
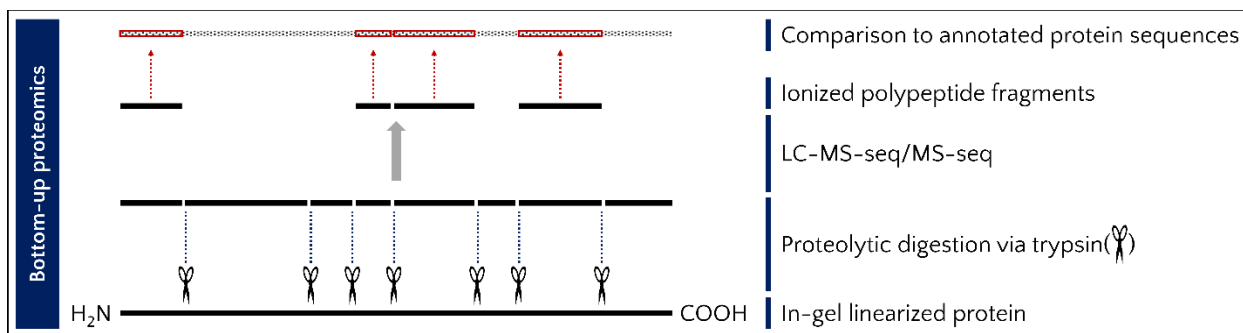
Figure 2-6. Bottom-up approach used for MS-seq identification of proteins.

Linearized proteins were cleaved by trypsin, passed through liquid chromatography (LC), then ionized to go through two sequential MS-seq analyses. Identified polypeptide fragments were compared to an annotated database.

a list of the proteins found in the evaluated sample. To make the list, a protein must have ≥2 tryptic peptides identified by MS-seq.

OEL and NCL samples were separated in 1D-e. MS-seq data retrieved from these transient overexpression cell lysates was analysed to determine if $_r$hCABS1 was present/absent in OEL or NCL. If present, the relative abundance (r.a.) signal of $_r$hCABS1 in each of the MS-seq analysed gel segments was retrieved. A graph was created where all r.a. values were graphed in the y-axis, while the x-axis indicated the range of molecular weight (kDa) belonging to each gel segment (see below, **Figure 2-11**). This range was determined by screening the proteins in each gel segment and determining the protein size range within each segment.

Human saliva was separated in 1D-e and 2D-e. MS-seq data retrieved from human saliva separated by 1D-e was analysed solely to determine if hCABS1 was present/absent. Human saliva separated by 2D-e was also analysed to determine if hCABS1 was present/absent, but also to determine whether there were protein candidates that could be interacting with pAbs to hCABS1 H1.0 and H2.0 (WB of 2D were made only with these two pAbs). Based on 2D-e-WB immunoprobing with H1.0 and H2.0, we selected 12 spots that aligned with immunoreactive spots.

Because our group is interested in identifying a 27 kDa protein associated with stress[21], we focused on MS-seq results from spots that represented that molecular weight (**Figure 2-20** F, G, H, I). Proteins that were present on, at least, 3 of these spots were further analysed. We retrieved their amino acid sequences from the online database UniProtKB[78] and used online tools for sequence alignment Clustal Omega[79] and MView[80] to compare their linear amino acid sequences to the domain used to produce H2.0 (hCABS1 a.a.: $_{184}$DEADMSNYNSSIKS$_{197}$), the pAb that detects this 27 kDa band in WB of human saliva[21]. Only proteins with domains containing amino acids with similar physicochemical properties (see [81]) than those in hCABS1 a.a. 184-197 domain were

considered potential interactors with our pAbs, in turn potentially being the 27 kDa band associated with stress.

Immunohistochemical analyses

Human SMG was obtained from patients whose cancer justified their removal (gift from GlaxoSmithKline and Dr Stephen Lewis, Case Western Reserve University, Cleveland, OH). Tissue was fixed in 10% buffered formalin and embedded in paraffin. For immunohistochemical analysis, sections were deparaffinized, rehydrated, and microwaved for 10 min in 10 mM sodium citrate (pH 6) for antigen retrieval (i.e., heat induced antigen retrieval, HIER). Subsequently, sections were blocked for 30 min (T_{room}) in PBS containing 5% bovine serum albumin and 0.1% Triton-X 100 (i.e., blocking buffer). Blocked slides were incubated overnight (T=4°C) with the immunoprobe to test (H1.0, H2.0, H2.1, H2.2, or PimmS) diluted $1/_{200}$ in blocking buffer. The next day, immunoprobed slides were washed with PBS and incubated for 2 h (T_{room}) with secondary antibody (goat anti-rabbit IgG H+L conjugated with Alexa Fluor 488, Thermo Scientific). Subsequently, slides were washed with PBS and mounted in VECTASHIELD® HardSet™ antifade mounting medium with DAPI (Vector Laboratories, Burlingame, CA, USA). Images were acquired with a Retiga EXi, Fast 1394 digital camera (Teledyne Photometrics, Tucson, AZ, USA) attached to a Diaphot 200 inverted phase contrast microscope (Nikon, Minato, Tokyo, JP) and evaluated using Q-Capture imaging software (Teledyne Photometrics).

Results

Before re-evaluation of previously established methodology

The established SDS-PAGE protocol in our group stated that when evaluating biological samples of human origin we loaded up to 25 μg of total protein into each well of a PA gel, and that downstream WB experiments should immunoprobe membranes at a concentration of 3 $^{ng}/_{μL}$ (for

H1.0 and H2.0), or 2 $^{ng}/_{\mu L}$ (for H2.1 and H2.2). The results in this section reflect what was observed when following these stipulations.

Blocked pAbs and pre-immunization sera immunoblotting controls

To evaluate samples of interest in WB, we assessed the specificity of our pAbs by (1) blocking each pAb with its own immunizing peptide, and (2) blotting membranes with pre-immunization sera (PimmS) from the rabbits that produced each pAb. We evaluated the immunoprobing pattern of OEL, NCL, and SMG with blocked pAbs and observed that blocked H1.0 and H2.2 did not detect bands in any of the tested samples (**Figure 2-7** A, D). In OEL, blocked pAbs H2.0 and H2.1 detected a dim band at 70 kDa but no bands in NCL or SMG (**Figure 2-7** B, C). We did not evaluate protein transfer efficiency or used a housekeeping protein to assess protein loading.
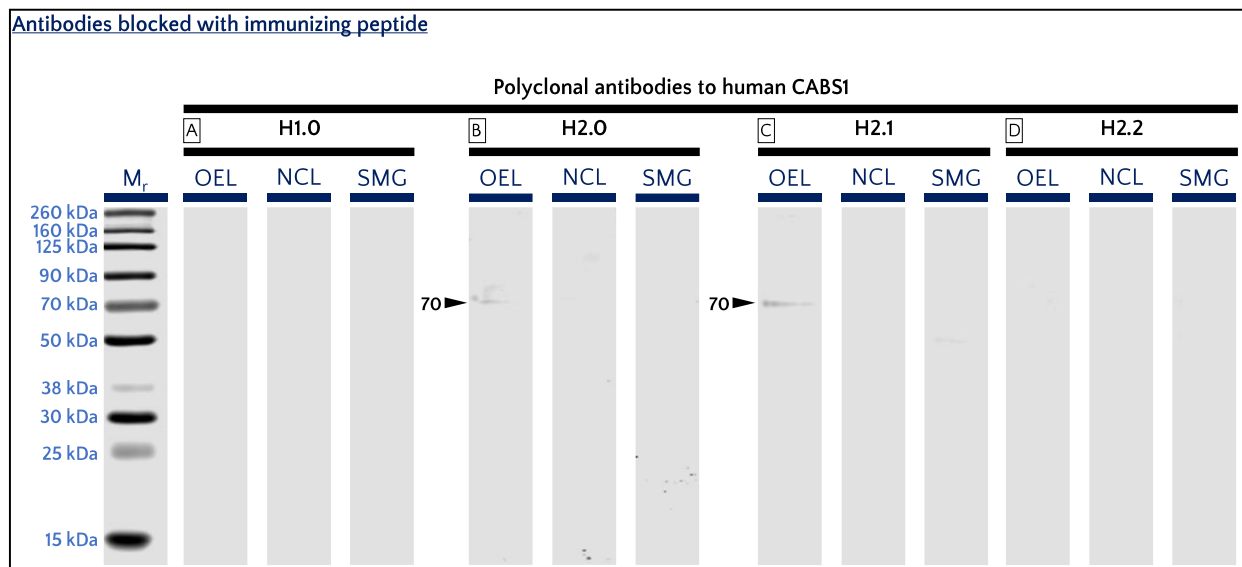
Figure 2-7. WB using blocking controls of pAbs to hCABS1.

Each pAb was blocked with the synthetic peptide used to immunize the rabbit host. pAbs H2.0 and H2.1 still detected 70 kDa bands in $_r$hCABS1 overexpression cell lysate (OEL). Negative control cell lysate (NCL) did not produce any bands. For comparison, a molecular mass reference (M_r) shows the range of protein sizes in kilodaltons (kDa) that can be present along a gel lane. Images are representative of two experiments for H1.0 and a single experiment for H2.0, H2.1 and H2.2.

As another negative control, we performed WB of biological samples using PimmS from the same rabbits that produced our pAbs. Human saliva and SMG were probed with PimmS of H1.0 and

H2.0. No bands were detected in these experiments by our pAbs to hCABS1 (**Figure 2-8** A, B). OEL and NCL were probed with PimmS of H2.1 and H2.2, no bands were detected (**Figure 2-8** C, D). Of note, OEL and NCL were never immunoprobed with PimmS of H1.0 and H2.0.
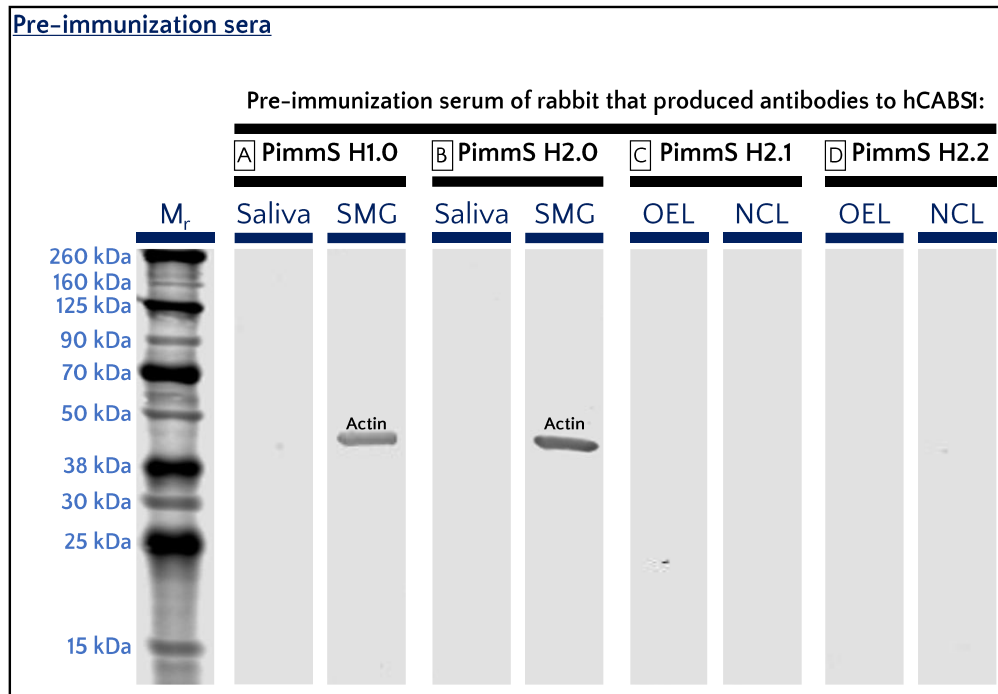
Figure 2-8. WB using pre-immunization sera (PimmS) from the rabbits that produced our pAbs to hCABS1.

PimmS H1.0 and H2.0 used to immunoprobe human submandibular gland (SMG) or saliva did not produce any bands. PimmS H2.1 and H2.2 used to immunoprobe $_r$hCABS1 overexpression cell lysate (OEL) or negative cell lysate (NCL) controls did not produce any bands. For comparison, a molecular mass reference (M_r) shows the range of protein sizes in kilodaltons (kDa) that can be present along a gel lane. Images are representative of two experiments for saliva and a single experiment for SMG in PimmS H1.0 and H2.0, and a single experiment for OEL and NCL in PimmS H2.1 and H2.2

Evaluation of pAbs to hCABS1 when screening transient overexpression cell lysates

As an additional control to test the specificity of our pAbs to hCABS1, we used a $_r$hCABS1 OEL and its NCL (characteristics described in methodology). WB analyses using H1.0 showed bands at 84 and 67 kDa for OEL and had no immunoreactivity with NCL (**Figure 2-9** A). Interestingly, in addition to bands at 84 and 67 kDa in OEL, H2.0 recognized three bands at 55, 34 and 21 kDa. These three bands were also observed at the same positions in NCL (**Figure 2-9** B). H2.1 detected

bands at 84 and 55 kDa bands in OEL, with the 55 kDa band appearing in NCL, as well as faint bands at 76 and 47 kDa (**Figure 2-9** C). H2.2 showed bands at 84, 67, 55 and 47 kDa in OEL, and in NCL bands at 55 and 47 kDa (**Figure 2-9** D). In OEL, pAb NBP1-31573 rendered a thick band at 84 kDa, followed by what seemed to be a smear until 67 kDa, and two discrete bands at 55 and 47 kDa. In NCL, this pAb detected a faint band at 55 kDa (**Figure 2-9** E). Interestingly, WB analysis using an anti-FLAG antibody showed identical banding pattern to H1.0 with bands at 84 and 67 kDa for OEL, and no immunoreactivity for NCL (**Figure 2-9** F). Thus, we speculated that in WB H1.0 specifically detects hCABS1.
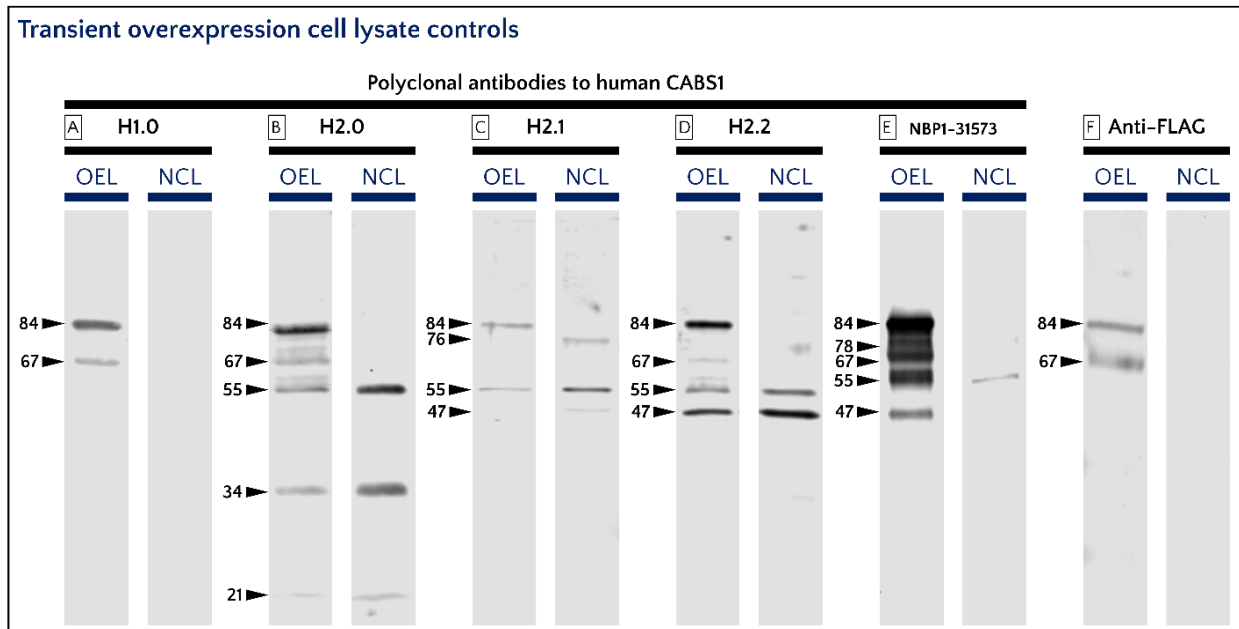
Figure 2-9. WB of ᵣhCABS1 transient overexpression cell lysate (OEL) and its negative control cell lysate (NCL) immunoprobed for hCABS1.

Our four pAbs and one commercial antibody to hCABS1 were used to immunoprobe the transient overexpression cell lysate controls. An anti-FLAG antibody targeting a domain attached to the carboxyl-terminus of ᵣhCABS1 in OEL was used as an additional control. Arrows to the left side of each antibody column indicate the molecular weight in kilodaltons of bands in OEL and NCL for each evaluated antibody. Images are representative of 16 experiments for H1.0, 8 experiments for H2.0, 17 experiments for H2.1, 18 experiments for H2.2, and a single experiment for NBP1-

We thought that increased 1D-e resolution using a gradient gel (4-20% PA) could show that H2.0, H2.1, and H2.2 detected bands in OEL and NCL were at similar-but-different apparent location in WB. We immunoprobed OEL and NCL with H2.2 using said gel and found that, still, WB-detected bands were located at the same apparent molecular weight across these samples (**Figure**
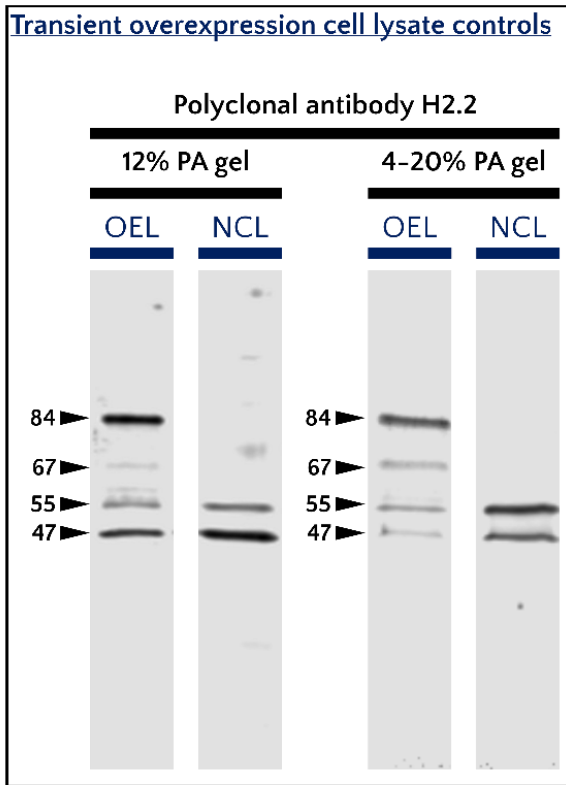
Figure 2-10. Increase of resolution via electrophoresis matrices does not separate homolog bands in OEL and NCL detected by pAb H2.2.

This data suggests that bands detected by pAb H2.2 in OEL and NCL correspond to the same proteins, presumably apresent in both cell lysate (*PA: polyacrylamide*). Images are representative of 18 experiments for 12% PA gel and a single experiment for 4-20% PA gel.

2-10), raising the possibility that some of the clones contained in H2.0, H2.1, and H2.2 were not specific to hCABS1.

Given immunoreactivity in NCL with H2.0, H2.1, and H2.2, we conducted full lane MS-seq of NCL and OEL. MS-seq analysis did not detect $_r$hCABS1 in NCL. OEL, however, showed that gel regions between 120 and 22 kDa, and 17 and 11 kDa contain $_r$hCABS1 (**Figure 2-11**). We then analysed which proteins were present in both OEL and NCL. A list of the 387 proteins
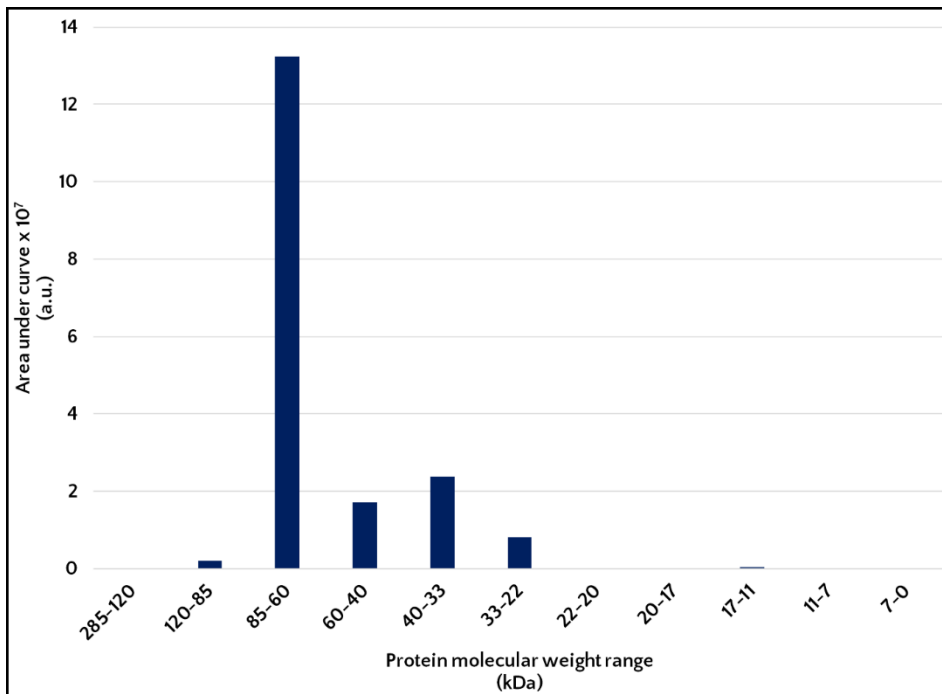
Figure 2-11. $_r$hCABS1 relative abundance in mass spectrometry sequencing analysed PA gel segments of an OEL sample.

A 12% PA gel lane containing electrophoresed OEL was cut into 11 segments. Each segment was analysed by MS-seq. $_r$hCABS1 is present in five segments ranging from 120 to 22 kDa and one segment ranging from 17 to 11 kDa.

present in both samples can be found in – MS-seq detected proteins in transient overexpression cell lysates and human saliva.

Evaluation of hCABS1 in human submandibular gland

Our group had previously shown WB using H2.0 that indicated that SMG extracts and saliva were sources of hCABS1[18,21]. To confirm these findings, we immunoprobed SMG and saliva using all available hCABS1 pAbs, some of which were raised to different domains of the protein. WB of SMG extract using H1.0 detected bands at 127, 100, 57, 52, 46, 33, 27, and a band that was present intermittently across experiments at 22 kDa (**Figure 2-12** A). H2.0 detected bands at 106, 71, 52, 33, 27, and 22 kDa (**Figure 2-12** B). H2.1 showed immunoreactive bands at 92, 71, 52, 40, and 27 kDa (**Figure 2-12** C). Lastly, H2.2 showed bands at 79, 70, 52, and 47 kDa (**Figure 2-12** D).
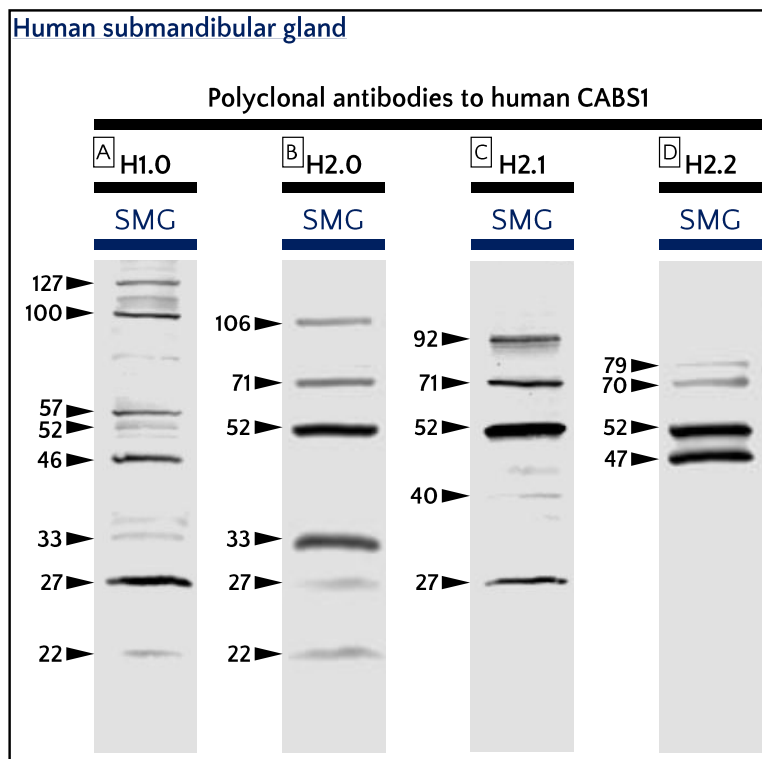
Figure 2-12. Representative WB of SMG immunoprobed for hCABS1.

Each pAb to hCABS1 detected diverse bands in the same SMG sample. Molecular weight in kilodaltons of the detected proteins is to the left of each column. Images are representative of 5 experiments for H1.0, 5 experiments for H2.0, 6 experiments for H2.1, and 4 experiments for H2.2.

We noticed that five bands at similar apparent molecular weight were consistently recognized by more than one of our pAbs in SMG. H1.0, H2.0 and H2.1 detect a 27 kDa form. H1.0 and H2.0 detect a 33 kDa band. H1.0 and H2.2 detect a 47 kDa protein. All antibodies are reactive with a 52 kDa protein, and H2.n-series antibodies bind to a 70 kDa polypeptide. One-way ANOVA and

subsequent Holm-Šídák posthoc test to correct for false discovery rate indicates that the apparent molecular weights of the previously listed hCABS1 bands are not significantly different across pAbs (**Figure 2-13**). This approach suggests that the same hCABS1 variants, namely at 27, 33, 47, 52, and 70 kDa, are being detected by more than one of our pAbs in SMG.
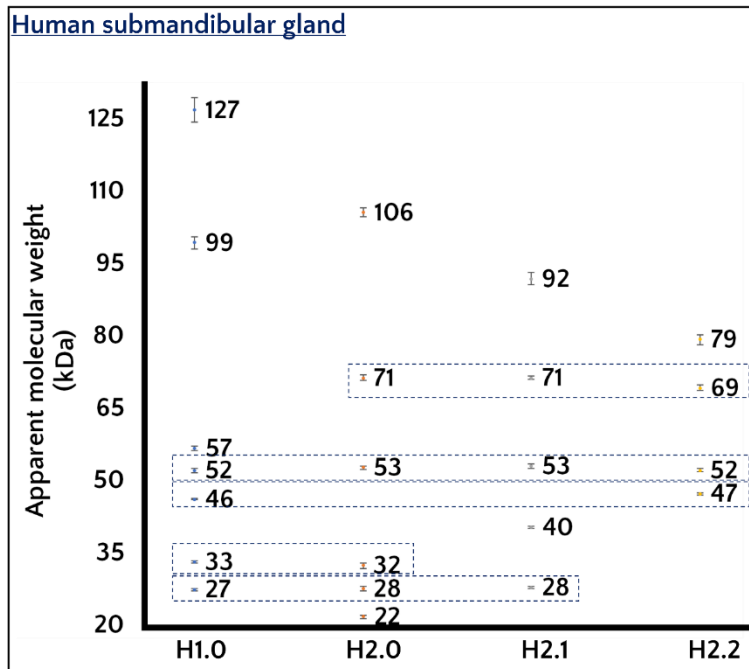
Figure 2-13. Representation of consistently observed bands when immunoprobing SMG with our pAbs to hCABS1.

Apparent molecular weight in kiloDaltons (kDa) is noted next to each point in the graph representing the mean (±SD) molecular weight of each band. pAbs to hCABS1 are on the horizontal axis.

Immunostaining of human submandibular gland sections with pAbs H1.0 and H2.1 (each tested independently) yielded a punctate pattern throughout the cytoplasm of all duct cells (**Figure 2-15** A, green), a pattern also observed in longitudinal sections (**Figure 2-15** B, green). pAbs H2.0 and H2.2 (tested independently) yielded a particulate pattern in the cytoplasm of specific duct cells in transverse sections of small ducts (**Figure 2-15** C, green). Interestingly, when observed in longitudinal sections of the larger ducts that have pseudostratified epithelia, these pAbs stained the cytoplasm of duct cells on the abluminal side, i.e., away from the lumen and adjacent to the basal surface (**Figure 2-15** D, green). Analyses of transverse sections of SMGs immunostained with PimmS rendered no signal (**Figure 2-14** A, B).

Immunohistochemistry: Human submandibular gland

H1.0 and H2.1
(target: hCABS1)

H2.0 and H2.2
(target: hCABS1)

Transversal view

Longitudinal view
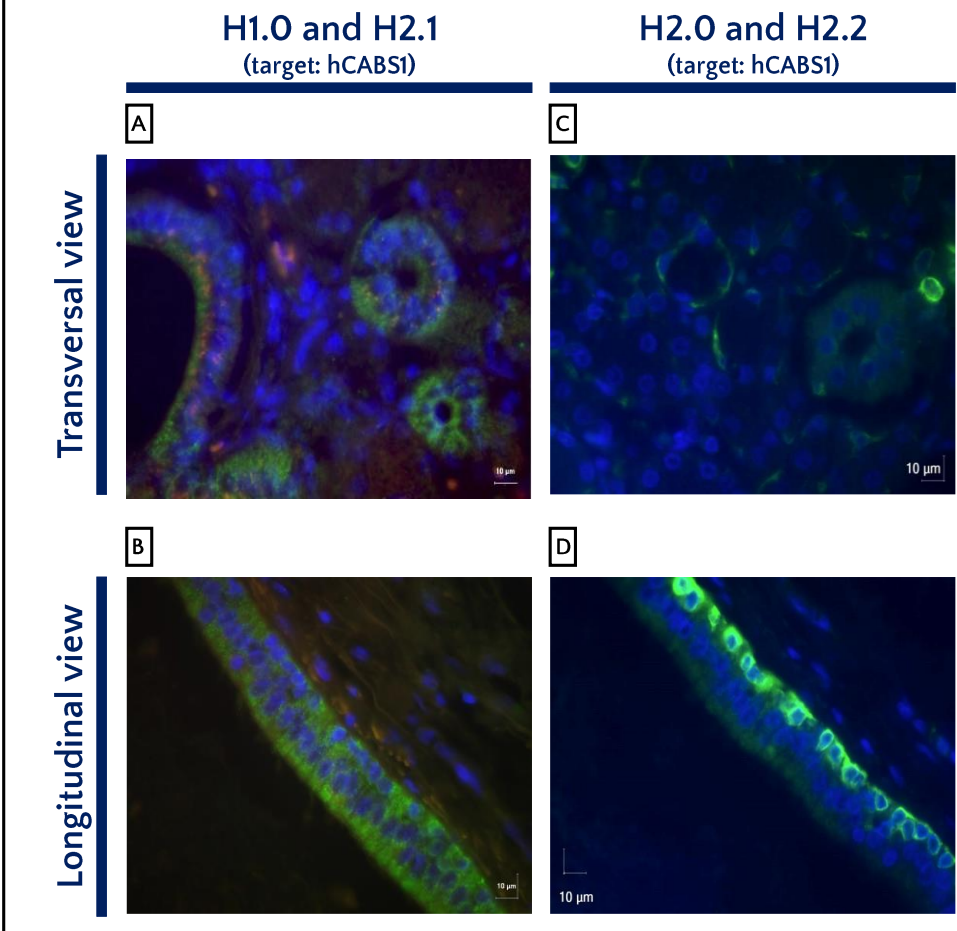
Figure 2-15. Human submandibular gland slides immunoprobed with pAbs to hCABS1.

Antibodies H1.0 and H2.1 give a different signature (green) than H2.0 and H2.2. DAPI (blue) was used to visualize cell nuclei. Red is autofluorescence. *Immunohistochemical experiment done by Mrs. Yongqiu Doughman. Image analysis done by Dr. Michiko Watanabe.*

Immunohistochemistry: Human submandibular gland

PimmS (H1.0 and H2.1)

PimmS (H2.0 and H2.2)

Transversal view
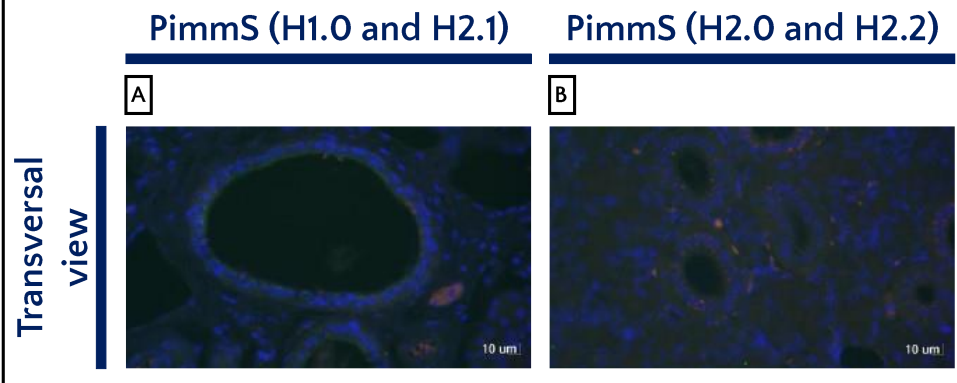
Figure 2-14. Human submandibular gland slides immunoprobed with pre-immunization serum (PimmS) from the rabbits that produced pAbs to hCABS1.

All PimmS produced the same signal (no green). DAPI (blue) was used to visualize the cell nuclei. Red is autofluorescence. *Immunohistochemical experiment done by Mrs. Yongqiu Doughman. Image analysis done by Dr. Michiko Watanabe.*

53

Evaluation of hCABS1 in human saliva

In human saliva supernatant, WB using H1.0 detected an immunoreactive band at 54 kDa (**Figure 2-16** A). H2.0 detected immunoreactive bands at 83, 27, and was the only pAb that detected bands at 19, 14, and 11 kDa in some saliva samples (**Figure 2-16** B). H2.1 detected bands at 83 and 54 kDa (**Figure 2-16** C). H2.2 detected a doublet at 62 and 54 kDa (**Figure 2-16** D). A commercial pAb to hCABS1, sc 136594, also detected a doublet at 58 and 51 kDa (**Figure 2-16** E).

Given that we were interested in the ability of pAb H2.0 to detect bands that were associated with stress, namely the 27, 19, 14, and 11 kDa variants[21], it was essential to validate our findings with mass spectrometry sequencing of the proteins present in those regions of the gel. A saliva sample known to give a strong 27 kDa band in WB was ran in a 12% PA gel and the section corresponding to 27 kDa, plus two gel segments, one above and one below, were sent for MS-seq analysis. Results did not detect hCABS1. However, we were aware that high abundance in saliva of some proteins, like alpha amylase, could conceal polypeptides present in lower abundance[76,82].

To submit to MS-seq analysis a saliva sample free of alpha amylase, we modified a protocol for removal of alpha amylase in saliva, first established by Deutsch et al.[76], and described in the methodology section of this chapter. Firstly, we immunoprobed with H2.0, the pAb that detected 27 and <27 kDa bands in human saliva, the fractions obtained at each step of alpha-amylase removal treatment. Untreated saliva supernatant immunoprobed with H2.0 gave bands at 83, 54, 42, 37, 27, 24, 19, and 12 kDa (**Figure 2-17** A). Treated saliva supernatant gave bands at 83, 54, a faint band at 37, and a doublet at 24 kDa (**Figure 2-17** B). The elution from the bound fraction in the amylase removal column yielded a single band at 54 kDa (**Figure 2-17** C). Finally, we also decided to immunoprobe whole saliva pellet to determine whether it also contained hCABS1 and found bands at 83, 56, 54, 50, and 27 kDa (**Figure 2-17** D). After visualizing that post-amylase removal the 27 kDa and <27 kDa bands disappeared, but other bands remained (compare **Figure**

2-17 A and B), we decided to get rid of amylase from saliva supernatant, separate it by size via electrophoresis, and send the entire gel lane for MS-seq analysis. Alpha amylase was not present among the proteins identified in the results, however hCABS1 was still not detected. We then sent an entire gel of un-treated saliva supernatant for MS-seq. Results still did not show hCABS1. Of note, to this day the saliva pellet has not been sent for MS-seq analysis. These results were interesting to us, as we were expecting to detect hCABS1.
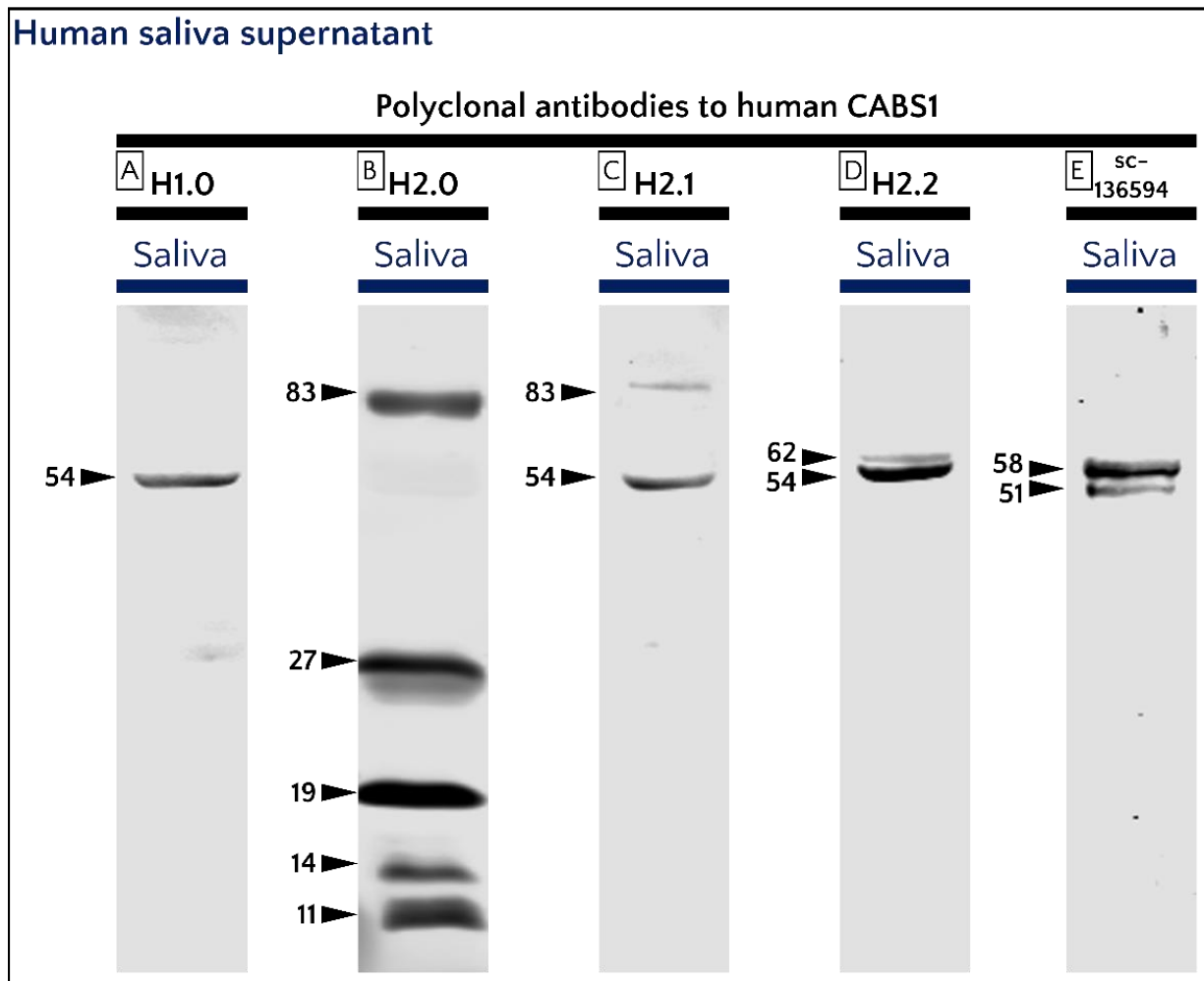
Figure 2-16. WB of human saliva supernatant immunoprobed for hCABS1.

Molecular weight in kilodaltons (kDa) of detected proteins are to the left of each column. pAb H2.0 is the only antibody that detects a band at 27 kDa that correlates with psychosocial stress, and <27 kDa bands that have been associated to resilience to stress. When compared to H2.0, all other pAbs detect less presumed variants of hCABS1. Images are representative of 9 experiments for H1.0, 11 experiments for H2.0, 4 experiments for H2.1 and 4 experiments for H2.2.
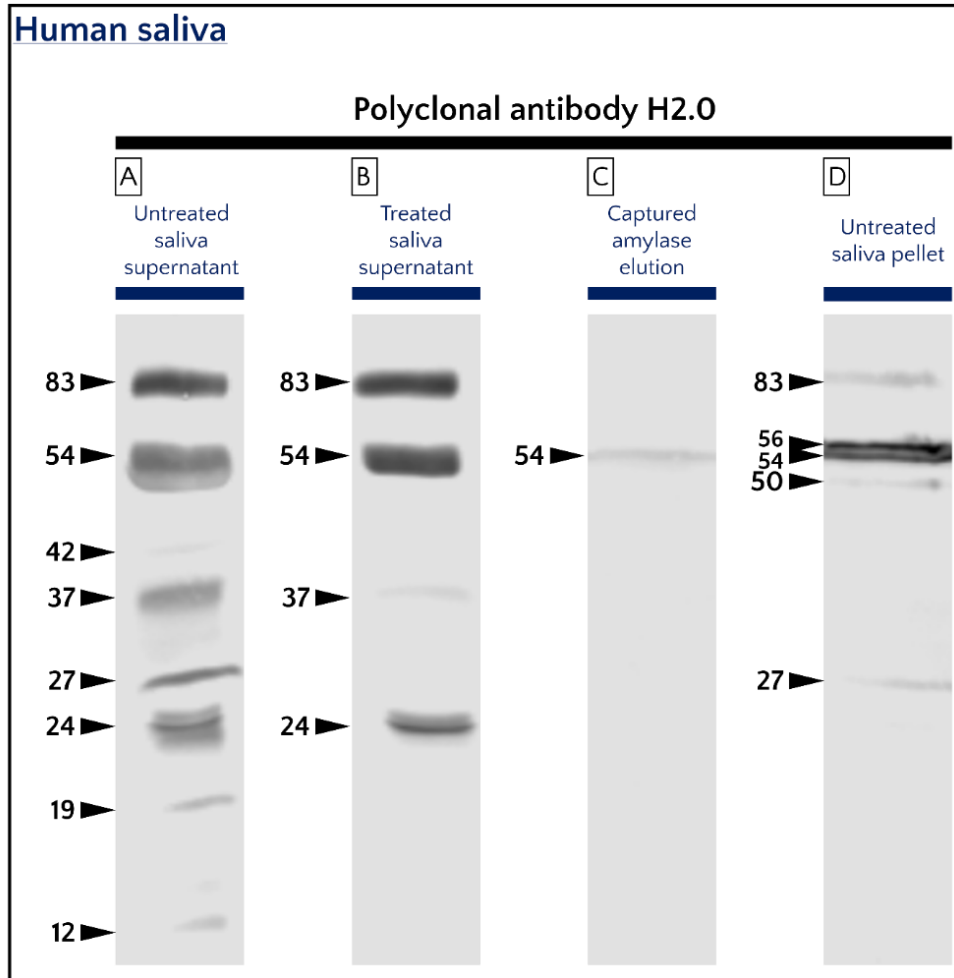
Figure 2-17. WB of human saliva supernatant treated/not treated to remove α-amylase, captured amylase elution, and saliva pellet (obtained post-centrifugation) immunoprobed for hCABS1 with pAb H2.0.

Untreated saliva supernatant gave more putative hCABS1 immunoreactive variants than treated sample. This data also indicates that a 54 kDa protein detected by H2.0 binds to potato starch, just as α-amylase. Interestingly, pellet from whole saliva seems to contain several forms of hCABS1. Images are representative of a single experiment.

We postulated that increasing resolution in our gels, i.e., separation of proteins within the gel, would be a valuable strategy for detecting hCABS1 in saliva via MS-seq. Thus, we developed a 2D-e protocol allowing firstly for the separation of proteins by their isoelectric point, and secondly by their molecular weight. Once optimized, we analysed by 2D-e a reference saliva sample, and subsequently performed WB with H1.0, H2.0, and their PimmS.

When immunoprobing with H1.0 at 3 $^{ng}/_{\mu L}$, we observed three spots of interest, namely at an apparent molecular weight of 72 kDa (pH range 5.5-5.7), at 54 (pH range 6.9-7.3), and at 46 kDa (pH range 5.2-6.1) (**Figure 2-18** A). WB using PimmS (H1.0) at 3 $^{ng}/_{\mu L}$ rendered a bigger spot at 53 kDa (pH range 5.3-6.4) (**Figure 2-18** B). Thus, indicating that this antibody working concentration may be giving non-specific spots at ~53 kDa. Alternatively, immunoprobing with H1.0 at 0.3 $^{ng}/_{\mu L}$ gives dimmer spots also at 72 kDa (pH range 5.9-6.1), and at 46 kDa (pH range 5.9-6.5) (**Figure 2-18** C). Immunoprobing with PimmS (H1.0) at 0.3 $^{ng}/_{\mu L}$ gave no spots (**Figure 2-18** D). Notably, the ~53 kDa spot was not observed at this immunoprobe working concentration. Therefore, we consider that 0.3 $^{ng}/_{\mu L}$ is the optimum concentration to
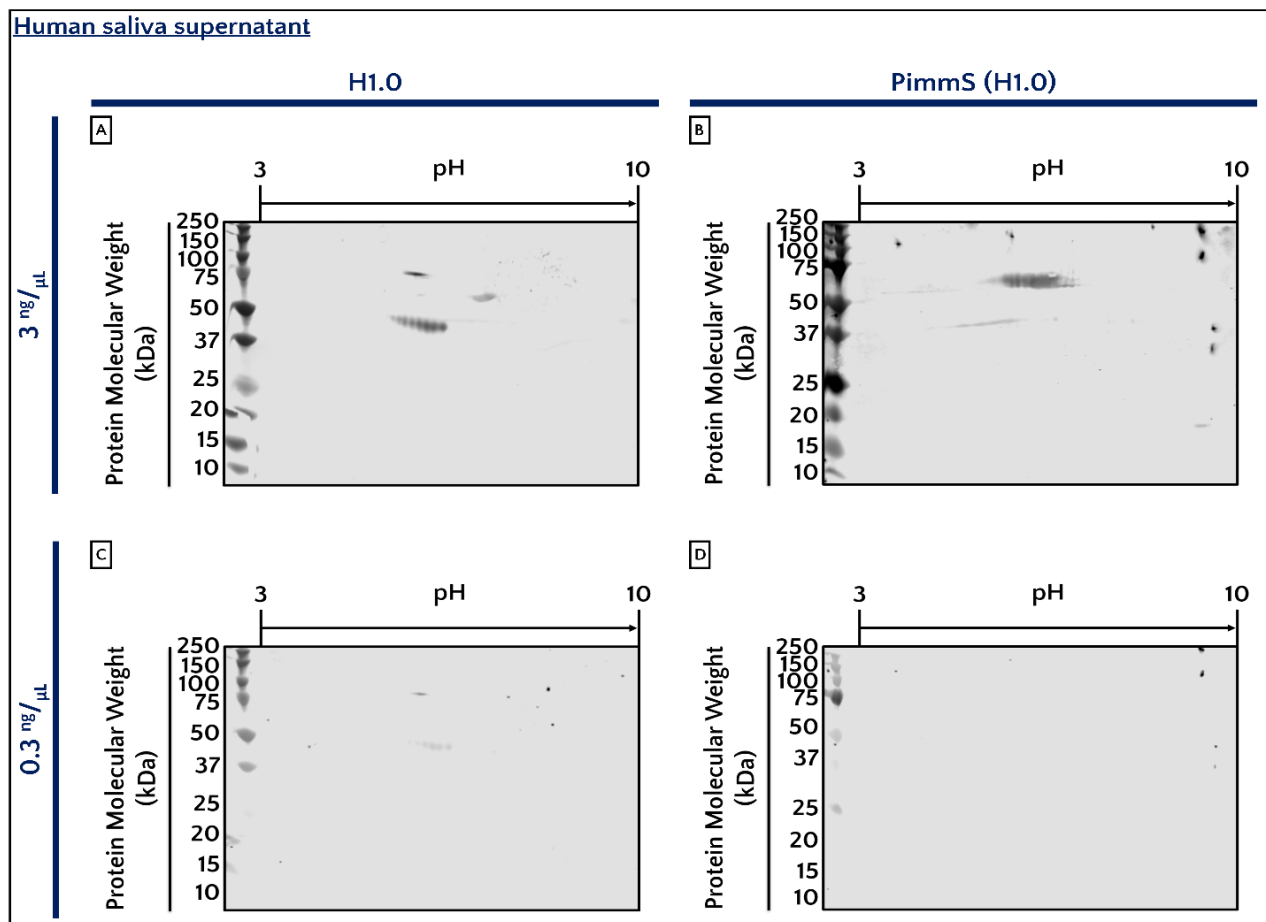
Figure 2-18. WB of human saliva supernatant separated by 2D-e and immunoprobed with H1.0 and pre-immunization serum from the rabbit that produced H1.0 (PimmS (H1.0)).

Concentration ($^{ng}/_{\mu L}$) at which each immunoprobe was used to blot the membrane is indicated in blue to the left. Each blot has a molecular weight marker to its left for reference. Images are representative of s ingle experiment for each condition.

immunoprobe human saliva with H1.0 and postulate that the aforementioned spots at 72 and 46 kDa represent true hCABS1.

WB of human saliva supernatant resolved by 2D-e and immunoprobed with H2.0 at $3\ ^{ng}/_{\mu L}$ yielded five spots of interest, namely at 84 kDa (pH range 4.8-6.6), at 56 kDa (pH range 5.2-6.7), at 33 kDa (pH range 5.1-5.7), and two regions at 28 kDa (pH range 5.2-7.5 and 8.1 to 8.7) (**Figure 2-19** A). When immunoprobing with PimmS (H2.0) at $3\ ^{ng}/_{\mu L}$, we observed seven regions that were immunoreactive. These were 62 kDa (pH range 6.0-6.2), two regions at 53 kDa (pH range 4.8-4.9 and 5.9-6.4), 51 kDa (pH range 6.6-7.3), 35 kDa (pH range 4.4-5.1), and two regions at 23 kDa (pH range 5.6-8.2 and 8.8-9.3) (**Figure 2-19** B). It was clear that just as with H1.0,
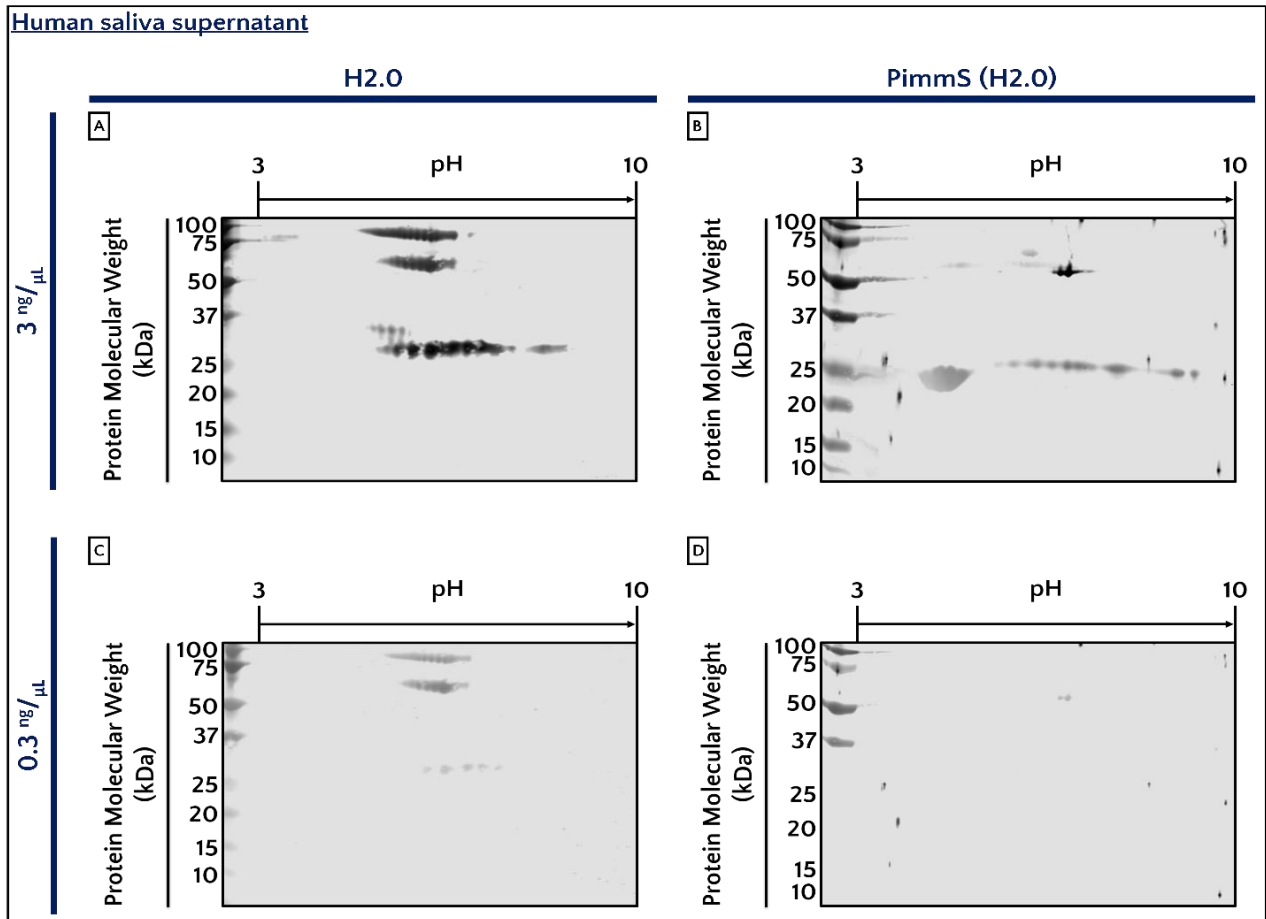
Figure 2-19. WB of human saliva supernatant separated by 2D-e and immunoprobed with H2.0 and pre-immunization serum from the rabbit that produced H2.0 (PimmS (H2.0)).

Concentration ($^{ng}/_{\mu L}$) at which each immunoprobe was used to blot the membrane is indicated in blue to the left. Each blot has a molecular weight marker to its left for reference. Images are representative of a single experiment for each condition.

immunoprobing at a working concentration of 3 $^{ng}/_{\mu L}$ yielded non-specific spots. Instead, immunoprobing with H2.0 at 0.3 $^{ng}/_{\mu L}$ yielded only three regions (dimmer) at equivalent locations as those observed when probing at 3 $^{ng}/_{\mu L}$. These were at 84 kDa (pH range 5.3-6.9), at 56 kDa (pH range 5.6-6.9), and at 28 kDa (pH range 6.1-7.5) (**Figure 2-19** C). WB using PimmS (H2.0) at 0.3 ng/µL gave two dim spots at 51 kDa (pH range 6.8-7.0) (**Figure 2-19** D). We consider that, just as H1.0, the optimum working concentration for H2.0 is also 0.3 $^{ng}/_{\mu L}$ and that this pAb detects putative hCABS1 variants at 84, 56, and 28 kDa.

We decided to use data from 2D-e-WB immunoprobed with H1.0 and H2.0 at 0.3 $^{ng}/_{\mu L}$ to determine which spots of a gel containing the same saliva sample separated by 2D-e should be sent for MS-seq. Twelve spots were sent for MS-seq analysis (**Figure 2-20**). Overall, 48 proteins were detected (see full list – MS-seq detected proteins in transient overexpression cell lysates and human saliva). However, hCABS1 was not detected. Recent analysis of the location of spots sent for MS-seq suggest that some do not reflect the exact location that is immunoreactive in WB, most notably the 27 kDa variant(-ies) that we believe are associated with stress[21].

Nonetheless, we evaluated all proteins in the region that we thought was representative of 27 kDa (**Figure 2-20** F, G, H, I) and screened them as described in Methodology. Briefly, proteins that were present in at least three of these spots were further analyzed by comparing their amino acid sequences to the hCABS1 domain used to produce H2.0. If a section of these proteins aligned with the H2.0 domain (see Appendix C – MS-seq detected proteins in transient overexpression cell lysates and human saliva, **Figure C-2** - **Figure C-10**), we considered them candidate potential interactors with H2.0. Under this criterion, we found eight potential protein interactors (**Table 2-3**). Again, we believed that these MS-seq evaluated spots were equivalent to those that gave an immunoreactive spot in WB using H2.0.
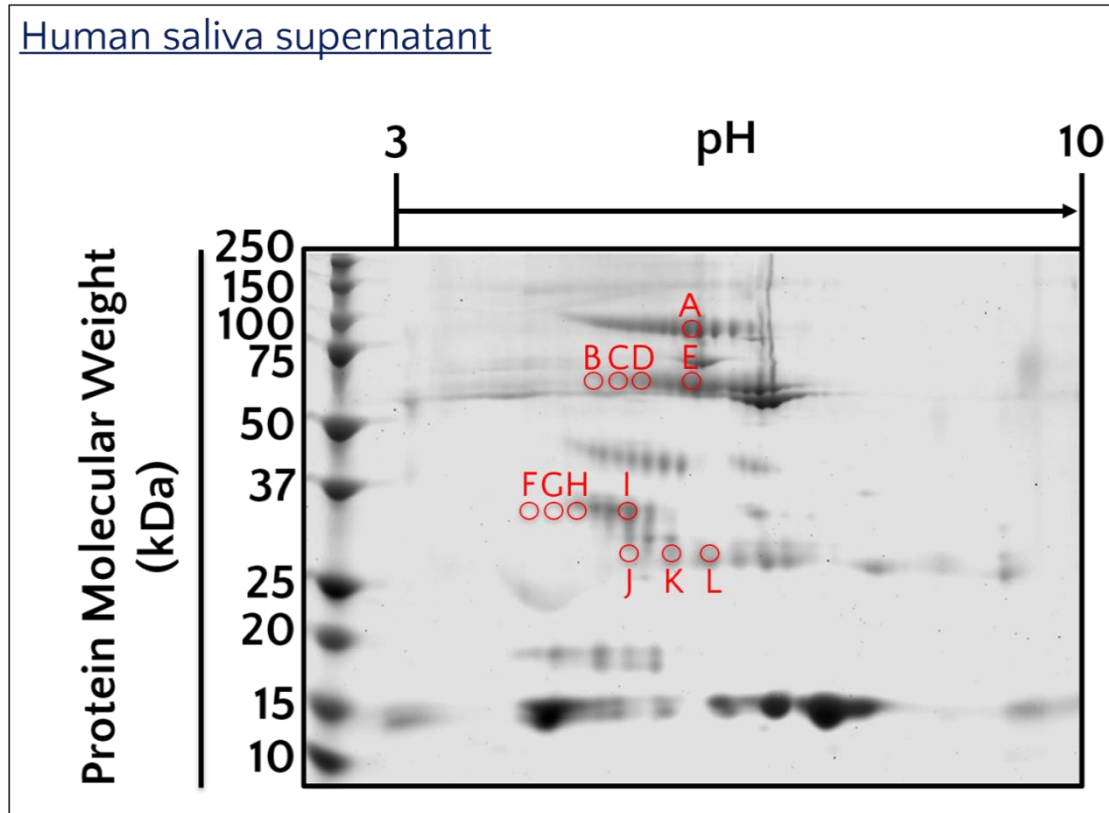
Figure 2-20. Blue silver stained gel of human saliva supernatant separated by 2D-e.

Red circles indicate the spots that were excised to be analysed by MS-seq. 85-98 kDa: A (pH 6.0-6.1); 68-64 kDa: B (pH 4.9-5.1), C (pH 5.2-5.3), D (pH 5.5-5.6), E (pH 6.0-6.1); 33-29 kDa: F (pH 4.3-4.4), G (pH 4.5-4.7), H (pH 4.8-4.9), I (pH 5.3-5.4); 25-24 kDa: J (pH 5.3-5.5), K (pH 5.7-5.9), L (pH 6.1-6.3). A full list of all proteins found in these locations can be found in – MS-seq detected proteins in transient overexpression cell lysates and human saliva. Image is representative of two experiments.

Potential proteins also being recognized by pAbs to hCABS1	
Name	Accession
BPI fold–containing family A member 2	Q96DR5
Zymogen granule protein 16 homolog B	A0A0C4DGN4
Carbonic anhydrase 6	P23280
Zinc–alpha–2–glycoprotein	P25311
Clusterin	E7ERK6
Cystatin SN	P01037
Protein LEG1	Q6P552
Prolactin–inducible protein	P12273

Table 2-3. List of MS-seq detected proteins present in all four excised 2D-e gel spots F, G, H, I (see Figure 2-20), corresponding to 33-29 kDa across a pH range of 4.3-5.4.

During gel excision, these spots were thought to be representative of 27 kDa. Accession numbers are in accordance to UniProt KB notation.

Of the proteins listed in **Table 2-3**, Carbonic anhydrase 6 (CA6) shares a similar domain to the immunogen used to produce pAb H2.0 (see **Figure C-4**) and has been associated to hypoxia-induced stress[83]. To test if H2.0 was interacting with CA6, we used H2O to probe a recombinant CA6 overexpression cell lysate (rCA6 OEL) and compared its profile to the OEL negative control cell lysate (NCL) and of saliva supernatant. H2.0 detects a single band at 55 kDa, in rCA6 OEL, but the bands is also present in NCL. In saliva supernatant, H2.0 detects bands at 83, 60, 32 and 27 kDa (**Figure 2-21** H2.0). Probing rCA6 OEL with an anti-FLAG antibody targeting the tag adjacent to rCA6 carboxyl terminus shows two bands at 42 and 38 kDa (**Figure 2-21** Anti-FLAG monoclonal antibody).
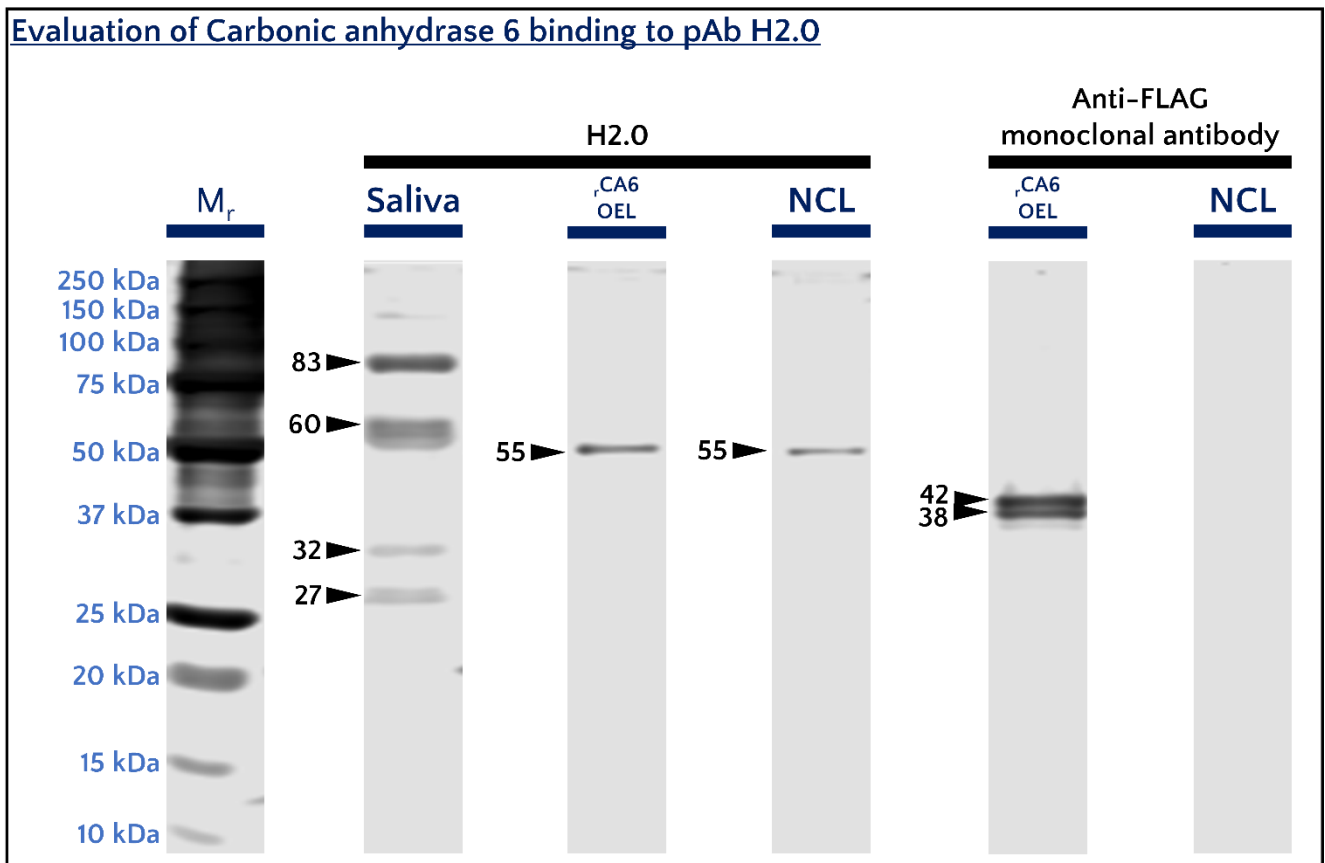
Figure 2-21. Polyclonal antibody H2.0 does not detect carbonic anhydrase 6 in WB.

A molecular mass reference (M_r) shows the range of protein sizes in kilodaltons (kDa) that can be present along a gel lane. Molecular weights in kDa are shown next to black arrows. Probing antibodies are shown in black font atop lanes. Probed samples were saliva, Recombinant carbonic anhydrase 6 overexpression cell lysate ($_r$CA6 OEL), and its inherent negative control cell lysate (NCL). Images are representative of a single experiment.

After re-evaluation of previously established methodology

The introduction of a capillary nano-immunoassay platform, described in "**Chapter 3 : A method to study protein biomarkers in saliva using and automated capillary nano-immunoassay platform (Wes™)**", employs rigorous antibody and sample amount titrations to find the combination that gives the least background noise. I translated this methodology into WB to evaluate if our published results were representative of hCABS1. The WB results in this section reflect what was observed when titrating pAbs working concentrations and in-gel sample amounts. We firstly decided to use the titration methodology in human serum, as we also wanted to evaluate if hCABS1 was present in blood. Secondly, we evaluated pAbs H1.0 and H2.0 in WB of saliva, as we have published results with these pAbs (see [18,21,66]).

Evaluation of hCABS1 in human blood serum

Other groups had described the presence of CABS1 in testes of rats[1], mice[4], and pigs[5]. Our group had observed presence of CABS1 in lung, testes, and SMG of human origin[18]. Since we speculated that hCABS1 is an isofunctional homolog to rat(r) SMR1, and cleaved domains of rSMR1, a protein produced in submandibular glands, have been proven to be present in rat's blood[53,54], it was important to study if hCABS1 was present in human blood. A single WB of human serum and plasma immunoprobed for hCABS1 showed the same band pattern in both sources (data not shown), hence the subsequent experiment was done only with serum. WB of titrated human blood serum (0.015, 0.15, 1.5, and 15 µg) and titrated immunoprobes (H1.0 and H2.0, and their pre-immunization sera: 3, 0.3, 0.03 $^{ng}/_{\mu L}$; H2.1 and H2.2, and their pre-immunization sera: 2, 0.2, 0.02 $^{ng}/_{\mu L}$) were performed (n=1).

It was clear that immunoprobing with 3 $^{ng}/_{\mu L}$ of pAb gave non-specific bands, since a similar banding pattern was obtained when probing with our pAbs to hCABS1 and with their PimmS, the latter used as a putative negative control, expected to not produce bands (**Figure 2-22** A, B, G, H, M, N, S, T). On this basis, all WB of human serum immunoprobed at a concentration of 3 $^{ng}/_{\mu L}$
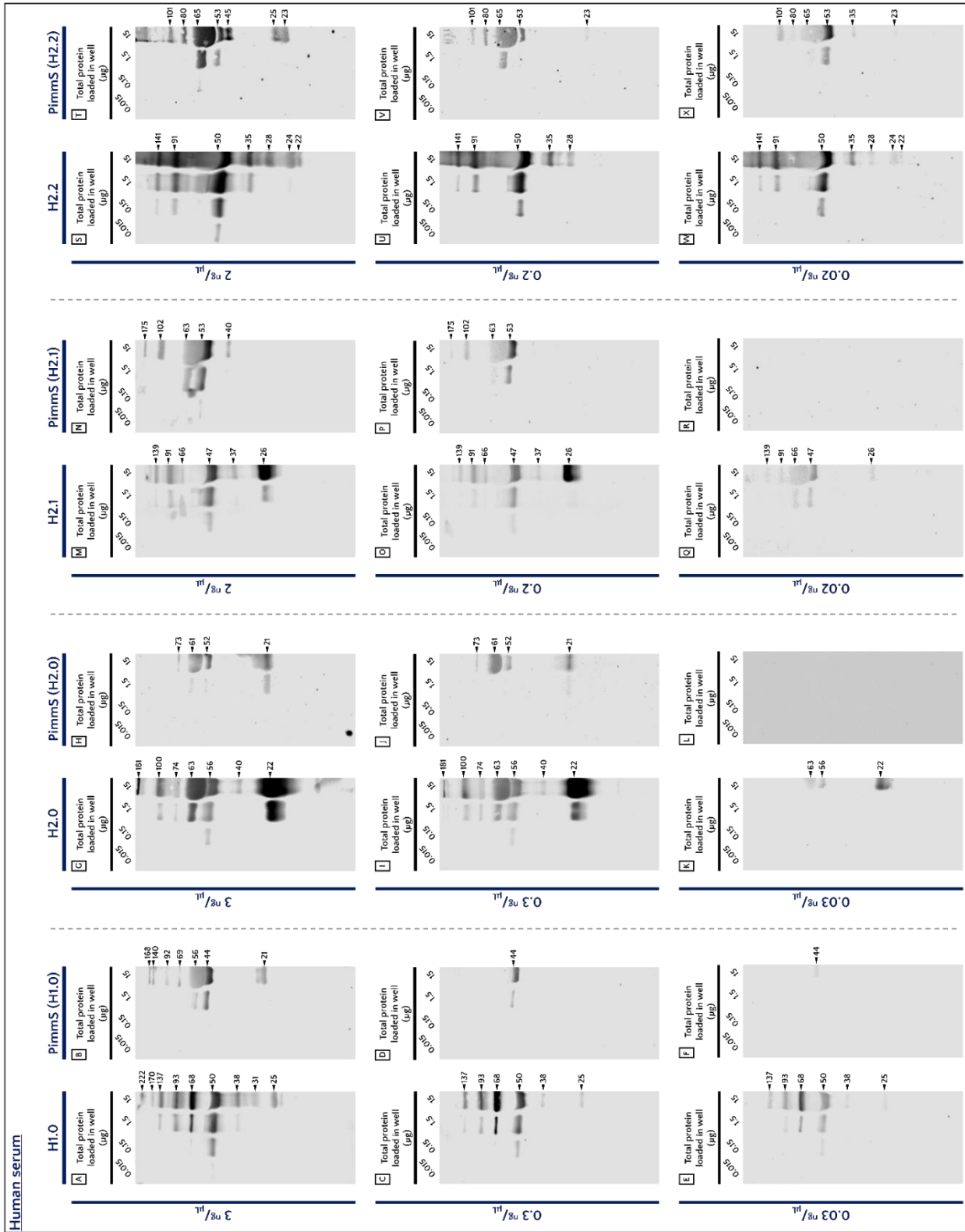
Figure 2-22. Human serum immunoprobed with pAbs to hCABS1 (Hn.m) and pre-immunization serum from the rabbit that produced Hn.m (PimmS (Hn.m)).

Concentration ($^{ng}/_{\mu L}$) at which each immunoprobe was used to blot the membrane is indicated in blue to the left. Molecular weight in kDa of the detected proteins is indicated to the right of each blot. Images are representative of a single experiment for each condition.

63

of pAbs were not reliable to discern which bands were representative of hCABS1. Moreover, upon evaluating WB immunoprobed at lower antibody or PimmS concentrations (0.3/0.2 and 0.03/0.02 $^{ng}/_{\mu L}$), we realized that the migration pattern from wells loaded with 15 µg of total protein indicated protein overload, especially between 70 and 50 kDa (**Figure 2-22** C, I, J, O, P, U, V, E, Q, W, X). Therefore, all wells containing 15 µg of total loaded protein were also unreliable. All wells loaded with 0.15 and 0.015 µg were too dilute, rendering little to no signal, just as immunoprobes with pAbs at 0.03/0.02 $^{ng}/_{\mu L}$. Given these excluding criteria, we decided to look at wells loaded with 1.5 µg of total protein and immunoprobes at a concentration of 0.3/0.2 $^{ng}/_{\mu L}$.

On this basis, WB of human serum using H1.0 detected bands at 137, 93, 68, and 50 kDa (**Figure 2-22** C), while PimmS (H1.0) detected a band at 44 kDa (**Figure 2-22** D). WB of human serum using H2.0 detected bands at 100, 74, 63, 56, and 22 kDa (**Figure 2-22** I), while PimmS (H2.0) detected a faint band at 21 kDa (**Figure 2-22** J). WB of human serum using H2.1 detected bands at 91, 66, and 47 kDa (**Figure 2-22** O), while PimmS (H2.1) detected a faint band at 63 and another at 53 kDa (**Figure 2-22** P). Finally, WB of human serum using H2.2 detected bands at 141, 91, and 50 kDa (**Figure 2-22** U), while PimmS (H2.2) detected a band at 65 kDa (**Figure 2-22** V).

Evaluation of hCABS1 in human saliva

Just as we had noticed with serum, it seemed that loading wells with 22 µg of total protein affected the migration pattern. Moreover, immunoprobing at concentration of 3 $^{ng}/_{\mu L}$ seemed to give excessive signal in our WB reading system (**Figure 2-23** A, B, G, H), while 0.03 $^{ng}/_{\mu L}$ seemed to be too dilute to consider (**Figure 2-23** E, F, K, L). Given these constraints, we focused on wells loaded with 2.2 µg of total protein and WB immunoprobed at a concentration of 0.3 $^{ng}/_{\mu L}$ using 1D-e gels.

Human saliva supernatant immunoprobed with H1.0 gives a single band at 56 kDa (**Figure 2-23** C), yet PimmS (H1.0) detects two bands at 64 and 59 kDa (**Figure 2-23** D), raising suspicions to
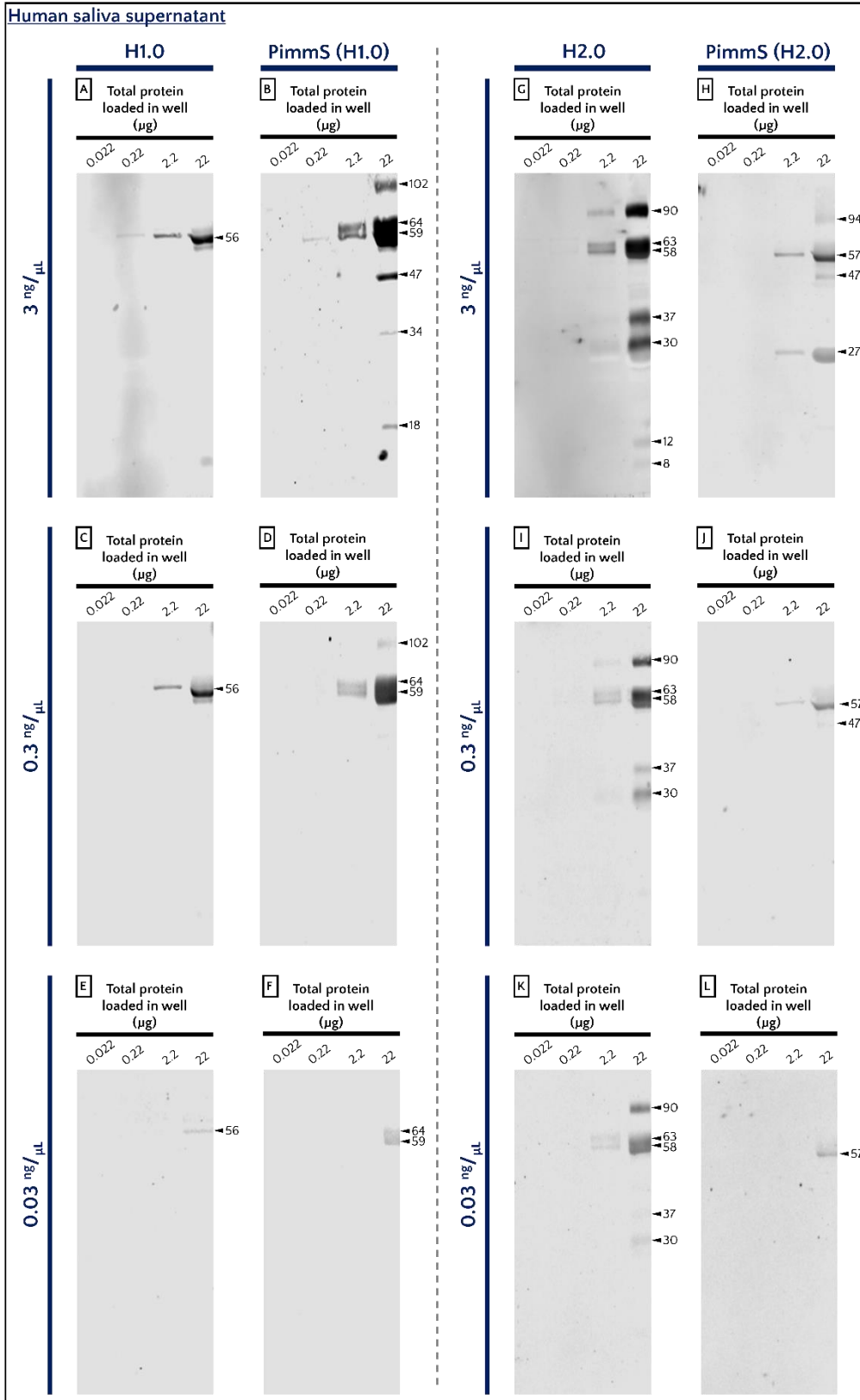
Figure 2-23. Human saliva immunoprobed with pAbs to hCABS1 (Hn.m) and pre-immunization serum from the rabbit that produced Hn.m (PimmS (Hn.m)).

Concentration ($^{ng}/_{\mu L}$) at which each immunoprobe was used to blot the membrane is indicated in blue to the left. Molecular weight in kDa of the detected proteins is indicated to the right of each blot. Images are representative of a single experiment for each condition.

65

whether H1.0 truly detects hCABS1 in saliva. H2.0 detects a band at 90 kDa and a doublet at 63 and 58 kDa (**Figure 2-23** I), while PimmS (H2.0) detects a single band at 57 kDa (**Figure 2-23** J). These results suggest that in WB H2.0 detects true hCABS1 in saliva at 90 and 63 kDa, in turn implying that previous affirmations about stress-associated bands thought to be hCABS1 (− A novel biomarker associated with distress in humans: calcium-binding protein, spermatid-specific 1 (CABS1)) need to be re-evaluated.

Discussion

In this chapter, I have shown that in analyses before methodology revaluation, I observed different WB profiles than after methodology revaluation. Previous studies evaluated up to 25 μg of protein from SMG or human saliva and then immunoprobed with a pAb working concentration of 3 $^{ng}/_{μL}$ (for H1.0 and H2.0) or 2 $^{ng}/_{μL}$ (for H2.1 and H2.2). At these conditions, WB controls, namely blocked pAbs and PimmS, as expected showed no signal, yet these results will be challenged below. WB analyses of SMG lysates showed an abundance of bands when evaluated with our pAbs, out of which five bands, consistently detected by two or more of our pAbs, could be indicative of true hCABS1 in this sample. These bands were observed at 27, 33, 47, 52, and 70 kDa. In saliva, pAbs H1.0, H2.1, H2.2 and commercial pAb sc-136594 detect a band at ~54 kDa, with H2.2 and sc-136594 detecting a doublet at this location. pAb H2.0 gave a different WB profile in saliva, with bands at 27, 19, 14, and 11 kDa, all of which had been associated to psychosocial stress[21]. Notably, H2.0 and H2.1 detected an additional band at 83 kDa in this sample. Notably, the majority of WB shown in this chapter lack presence of a housekeeping protein, typically used as a loading control. We decided against using housekeeping proteins in our WB because initial evidence suggested that hCABS1 variants were present across a wide range of molecular weights. Ideally, a loading control (housekeeping protein) has a significantly different molecular weight than that of the POI, but with putative hCABS1 variants present throughout the WB, we chose not

to use a housekeeping protein. We now recognize that total protein evaluation would circumvent this limitation, but at the time these WB were performed, we lacked the necessary reagents, like Ponceau dye.

Pre-methodology revaluation studies of transient overexpression cell lysates (OEL and NCL) immunoprobed at the same pAb working concentration, 3 or 2 $^{ng}/_{\mu L}$, but only up to 5 μg of protein loaded. This change was made chiefly because of Ab limited availability and high cost. In WB of OEL, all pAbs to hCABS1 and an anti-FLAG pAb detect a band at 84 kDa, and all but H2.1 detected a band at 67 kDa. In addition to these bands, H2.n pAbs and commercial pAb NBP1-31573 detected a band at 55 kDa. H2.2 and NPB1-31573 detected an additional band at 47 kDa, and H2.0 is the only pAb detecting additional bands in OEL at 34 and 21 kDa. WB of NCL immunoprobed with H1.0 and anti-FLAG gave no bands, while H2.n and NBP1-31573 produced a 55 kDa band. Additionally, H2.0 produced bands at 34 and 21 kDa, H2.1 at 76 and 55 kDa, H2.2 at 55 and 47 kDa and NBP1-31573 at 55 kDa.

All bands detected in NCL with H2.n pAbs and NBP1-31573 were at the same molecular weight as those observed in OEL when using the same pAbs. MS-seq analysis of OEL indicated that segments of the gel analogous to those immunoreactive in WB even with H2.n pAbs contained $_r$hCABS1, while MS-seq of NCL did not identify $_r$hCABS1.

Post-methodology revaluation studies using human serum and saliva suggest that using 3 or 2 $^{ng}/_{\mu L}$ as a working concentration, produced non-specific bands. Moreover, the amount of total protein loaded in SDS-PAGE gels for evaluating human samples, i.e., up to 25 μg, contributed to the production of non-specific bands. Titration with our two pAbs and their PimmS suggested that using 10 times less antibody (0.3 $^{ng}/_{\mu L}$ for H1.0 and H2.0 or 0.2 $^{ng}/_{\mu L}$ for H2.1 and H2.2) and loading 10 times less total protein, produced WB bands that might be hCABS1. In serum, H1.0 detected bands at 137, 93, 68 and 50 kDa, albeit this last band could be non-specific because PimmS (H1.0) detected a band at a similar position (44 kDa). pAb H2.0 detects bands in serum

at 100, 74, 63, 56, and 22 kDa. H2.1 detected bands at 91 and 47 kDa; but just as with H1.0, this last one could be non-specific because a band at a similar location (53 kDa) was detected by PimmS (H2.1). pAb H2.2 detected bands at 141, 91 and 50 and, once again, this last band is also picked up by PimmS (H2.2). Analyses of saliva after methodology revaluation were done only with H1.0, H2.0, and their PimmS because we published studies on saliva with these pAbs (see [21,66]). Just as in serum, using 10 X less pAb and loading 10 X less protein into gels gave bands in pAbs and no bands in PimmS, in turn suggesting that bands observed with pAbs in these conditions were representative of true hCABS1. H1.0 detected a band at 56 kDa; however, PimmS (H1.0) detected a doublet in the same region (64 and 59 kDa). Based on this analysis, H1.0 is not detecting hCABS1 in saliva. In turn, H2.0 detects a faint band at 90 kDa and a doublet at 63 and 58 kDa. PimmS (H2.0) detected a band at 57 kDa, suggesting that the form ~57 kDa may not be hCABS1 and that, if present, hCABS1 in saliva is detected by H2.0 at 90 and 63 kDa. Finally, we showed the two different immunohistochemical profiles that our pAbs give when analyzing SMG. On one hand, H1.0 and H2.1 stain the majority of the cytoplasm in all SMG duct cells. On the other hand, H2.0 and H2.2 only stain particles of specific SMG cells on the abluminal side of the ducts.

Before re-evaluation of previously established methodology

Previous findings from our group indicated that hCABS1 protein expression is not exclusive to the testes; as it is also expressed in submandibular gland lysate[18], lung tissue[18], and saliva[21]. Moreover, WB analyses of these samples with pAb H2.0 showed several discrete bands of different molecular weight sizes (kDa)[18,21]. Our study evaluating induction of psychosocial stress in human participants found a positive correlation between one band in saliva, 27 kDa, with stress[21]. Furthermore, discrete bands <27 kDa were present in samples from individuals that reported resilience to stress[21]. For these reasons it was important to visualize the different molecular sized variants of hCABS1, a readout that WB analysis offers, as opposed to other antibody-based techniques, e.g., ELISA. Above all, it was quintessential to further characterize our pAbs and

confirm or refute their specificities to hCABS1. It was important for us to set WB controls, references to which we could compare the immunoreactivity profile of each pAb. To this effect, we used blocked pAbs and PimmS. On one hand, the signature of pAbs versus that of blocked pAbs, i.e., blocking each purified pAb with the peptide used to immunize the rabbit that produced it, can be an indicator of which WB bands are specific to the immunizing peptide. Alternatively, PimmS contains a mixture of various naturally occurring antibodies that are reactive to diverse antigens. In WB, PimmS are an ideal control, as they reflect the immunoreactivity from pre-existing antibodies in the rabbits. Thus, comparing the immunoreactivity of our pAbs with that of their PimmS shed light on which signals were most likely induced by immunization with the peptide(s). We assumed the stock concentration of all PimmS to be 13 $^{mg}/_{mL}$ based on a document from Sigma-Aldrich detailing rabbit IgG concentration in normal serum[84] and diluted PimmS to the same working mass concentration used with our pAbs to hCABS1 when performing WB. We recognize that while PimmS and blocked pAbs offer an indicator of pAb specificity, ultimately pAb pull down and MS-seq could provide the most reliable answer concerning specificity of the pAbs.

Controls suggest that pAb mixes H2.0, H2.1 and H2.2 contain cross-reactive antibodies

We assessed OEL, NCL, and SMG with blocked pAbs to test Ab specificity. Blocked H2.0 and H2.1 detected a band in OEL at 70 kDa (**Figure 2-7** B, C) and detected no bands in NCL or SMG. This band possibly corresponds to a smear detected in OEL by non-blocked H2.0 above 67 kDa (**Figure 2-7** B), yet there is no corresponding band in non-blocked H2.1 OEL (**Figure 2-9** C). Blocked H1.0 and H2.2 did not detect bands in OEL, NCL, or SMG (**Figure 2-7** A, D). Overall, this data indicates that H2.0 and H2.1 may contain antibodies that are not specific to hCABS1 because these subsets of antibodies were not blocked by the immunizing peptide.

When we immunoprobed with PimmS, we obtained no signal in the evaluated samples. Notably, we characterized the WB profile of PimmS (H1.0 and H2.0) in human saliva and SMG early in the development of this dissertation project. In **Figure 2-8** A and B, we observed that WB of saliva

and SMG using PimmS (H1.0 and H2.0) did not detect bands. At the time, we considered SMG and saliva to be positive for hCABS1 since previous work suggested that their profiles in WB when using H1.0 and H2.0 were specific[18,21]. When these two experiments were performed, the saliva and SMG samples used had been stored at -80ºC for over 2 years, potentially jeopardizing the integrity of the proteins present in the samples and perhaps explaining why no bands were detected. In contrast, recent work titrating relatively fresh human saliva and pAb concentrations in WB (**Figure 2-23** B, H) showed that PimmS (H1.0 and H2.0) can detect potentially non-specific bands at the same pAb working concentration, 3 $^{ng}/_{\mu L}$, and amount of total protein loaded in **Figure 2-8** A, B, i.e., 22 µg.

We performed a better evaluation for PimmS (H2.1 and H2.2) by analysing the band profile that these gave on OEL and NCL. Neither PimmS (H2.1 and H2.2) detected bands on these samples (**Figure 2-8** C, D). Intriguingly, H2.1 and H2.2 antibodies detected discrete bands in NCL that PimmS (H2.1 and H2.2) did not, raising questions about the identity of these proteins present in NCL (**Figure 2-9** C (76, 55, 47 kDa), and D (55, 47 kDa)). What's more, WB analysis of NCL using H2.n antibodies and commercial pAb NBP1-31573 detected bands at equivalent locations as those seen in OEL (**Figure 2-9** B (55, 34, 21 kDa), C (55 kDa), D (55, 47 kDa), E (55 kDa)). To determine whether the equivalent bands were at the same apparent molecular weight, we used a gradient gel and theorized that increased resolution would show that these bands were at similar, but different, apparent molecular weights. Nevertheless, they were at the same location given this analysis (**Figure 2-10**, pAb H2.2 (55, 47 kDa)). Notice, however, that those bands in OEL are dimmer than the ones found in NCL (**Figure 2-9** B, C, D). Also, H1.0 and an anti-FLAG mAb did not detect any bands in NCL.

Taking all these data into account we speculated the following. It is possible that HEK293T cells, the host used to produce OEL and NCL, express hCABS1 constitutively. This could explain why NCL produces bands in WB immunoprobed with H2.n pAbs. Our MS-seq data on NCL did not

contain hCABS1, suggesting that these cells do not produce hCABS1 in a constitutive manner, or at levels detectable by MS-seq. Speculating about the H2.n observed dimmer equivalent bands in OEL, when compared to NCL, we wonder if $_r$hCABS1 down-regulates the expression of proteins, other than hCABS1, that surprisingly react with our H2.n pAbs. The number of MS-seq detected proteins in OEL is less (403) than the number of proteins detected in NCL (560), suggesting that the cells containing an overexpression vector produce a less diverse proteome, putatively because the translation machinery in the cell is being used to overexpress, in our case, $_r$hCABS1. In an attempt to find which proteins could be interacting with our pAbs, we identified the ones present in both cell lysates (– MS-seq detected proteins in transient overexpression cell lysates and human saliva). We found 387 possible candidates. It was clear, then, that an attractive approach to identify the proteins also detected by H2.n antibodies, was by IP followed by MS-seq. Future analyses of these samples could shed light on understanding what our antibodies detect. Finally, why is it that H1.0 and anti-FLAG do not detect bands in NCL while our other pAbs do? The overexpression system uses a vector that ultimately expresses a recombinant protein containing a FLAG sequence (DYKDDDDK) adjacent to the carboxyl terminus. This is relevant because the WB profile of OEL using H1.0, a pAb raised to a domain in the carboxyl terminus of hCABS1, is the same as that of an anti-FLAG antibody (**Figure 2-9** A, F). Interestingly, multiple bands in OEL were immunoreactive with our anti-CABS1 pAbs, suggesting that HEK293T has inherent proteolytic mechanisms that cleave $_r$hCABS1. MS-seq analyses of OEL suggested that there is a higher abundance of $_r$hCABS1 in a range between 85-60 kDa, but also the protein is present in lower molecular weight ranges, albeit in lower abundance (**Figure 2-11**). If random proteolytic activity was degrading $_r$hCABS1, then all MS-seq evaluated gel segments could have given a positive hit for $_r$hCABS1. Yet, it was only specific segments of the gel that contained the protein (**Figure 2-11**). Still, why is it that H1.0 and anti-FLAG antibodies do not detect lower molecular weight hCABS1 bands? We hypothesize that these smaller variants of hCABS1 have lost the

carboxyl terminus of the protein. As such, neither H1.0 nor anti-FLAG can detect them, but H2.n antibodies, having been raised to a middle domain of hCABS1, interact with them.

In submandibular glands, pAb-based Western blots suggest that there are five hCABS1 variants

While characterization of our pAbs using OEL and NCL provides an insight into the profile of our pAbs, we recognize that the profile is from an overexpression cell system. Proteomic analysis of tissue extracts, like SMG, is relevant as it can uncover tissue and disease specific markers[85] that may not be seen in cell line systems. To our knowledge, we are the only research group to has evaluated hCABS1 protein in human-derived samples. WB of SMG assessed for hCABS1 produced a complex profile (**Figure 2-12**). Our group previously published that H2.0 detected bands in female and male SMG lysates at 20, 27, 33, 51 and (sometimes) 103 kDa[18]. In my hands, SMG probed with H2.0 detected bands at 22, 27, 33, 52, 71, and 106 kDa (**Figure 2-12** B), aligning with our published observations. Further analyses with H1.0, H2.1 and H2.2 led me to propose that only some of those bands were specific for hCABS1 in SMG. The rationale for this involved comparison of immunoreactive bands using different pAbs targeting the same protein. This approach was based on the international workshop on T. spiralis antigens, held in 1991, where WB using pAbs and mAbs targeting the parasite were compared[86]. Based on a consensus, the attendees developed a strategy to identify with a high probability which bands were representative of the parasite[86]. Likewise, we compared our SMG WB and identified five bands that were consistently recognized by, at least, two of our pAbs. Following this logic, our pAbs detected five forms of hCABS1 in SMG lysate at 27, 33, 47, 52, and 70 kDa (**Figure 2-13**).

Tissue lysates are heterogeneous and rigorous protocols on sample preparation are pivotal to ensure reproducible, precise, and representative data[85,87]. Prior to WB analysis of SMG, we prepared our samples by homogenization using RIPA buffer supplemented with P8340 protease inhibitor cocktail. RIPA buffer is widely used in WB because of its efficacy to solubilize a wide

range of nuclear, cytoplasmic and membrane-bound proteins[88]. It is also compatible with protease and phosphatase inhibitors, downstream protein quantitation assays and minimizes protein interactions[88]. P8340 inhibits serine, cysteine, acid proteases, and aminopeptidases[89]. Thus, we tried to ensure that all proteins within the tissue were solubilized and proteases present in the homogenate were inactivated. Additionally, when performing SDS-PAGE, we added SMG homogenate to sample buffer containing SDS, among other compounds. Once mixed, the tube containing it was immediately placed on a heating plate at 95°C for 5 min. This heating step denatured active proteases present in the sample, in turn inactivating them completely[90]. The fact that we heated samples rapidly after collection acted in our favor, as it has been recognized that even when SDS unfolds proteins, it is not effective at doing so with certain proteases[91]. If some proteases are active, there is a time window in which proteins present in the sample run the risk of being degraded. It has been noted that 1 pg of protease is capable of significantly degrading protein content if the sample is not heated immediately once in sample buffer[92]. Thus, we had been careful to try to have our results reflect forms of hCABS1 that were processed in vivo rather than during the manipulation of samples in the experiment.

Notably, H2.0 detected WB bands in SMG from female and male subjects[18]. Our group also published the presence of hCABS1 transcript in SMG and parotid glands of female and male individuals[18]. Moreover, two independent studies showed the presence of hCABS1 transcript in labial salivary glands of female patients diagnosed with Sjögren's syndrome[16,17]. Further studies on different human-derived samples obtained from female and male individuals could tell us whether hCABS1 is a sexually dimorphic molecule. This is important because SMR1, a molecule that contains an isofunctional domain to hCABS1's $_{380}$TDIFELL$_{386}$ anti-inflammatory domain, is sexually dimorphic in rats[36,49,51,54,93].

hCABS1 presence in submandibular gland is endorsed by immunohistochemical analyses

To validate and further our understanding of the cellular and subcellular localization of CABS1 in SMG we used immunohistochemical analysis in collaboration with Dr. Michiko Watanabe. Our results showed that H1.0 and H2.1 stained the entirety of the cytoplasm in all duct cells (**Figure 2-15** A, B), while H2.0 and H2.2 stained only the abluminal cytoplasm of specific duct cells (**Figure 2-15** C, D). Seeing that H2.1 and H1.0 immunostained similarly was perhaps surprising since H1.0 was raised to a different epitope than all H2.n antibodies. We speculate that clones present in H2.1 are targeting an available hCABS1 epitope that is present in forms that antibody clones in H1.0 detect. In contrast, clones in H2.0 and H2.2 may detect an epitope that is only present in other hCABS1 variants and localized predominantly in abluminal cells, although we can not rule out that these differences in some way reflect lack of specificity for CABS1 in our pAbs. With no signal retrieved on slides immunoprobed with PimmS (**Figure 2-14** A, B) we had increased confidence in that the signal given by our pAbs was staining hCABS1 (**Figure 2-15** A, C).

Immunohistochemistry preserves tissue architecture and protein antigenicity, in theory, without compromising secondary or tertiary structure[94]. To do so, the fixation of tissue is a pivotal step and must be done immediately after surgical excision[95]. 'Ischemia time', the period between surgical removal and tissue fixation[95], must be reduced. Ischemia results in DNA, RNA and protein degradation, tied to activation of tissue enzymes and autolysis[96]. Non-coagulating fixatives like 10% buffered formalin, used in our study of SMG, intend to preserve tissue morphology and maintain antigenicity of target molecules[95]. 10% buffered formalin is widely used in histopathological studies and works by forming hydroxymethyl groups on reactive amino acids, ultimately cross linking peptides[95]. While it provides superb preservation of tissue architecture, formalin fixation can conceal epitopes[97], in turn reducing antigenicity[95]. This issue has been addressed by the introduction of heat induced epitope retrieval (HIER) into the immunohistochemical field[94]. Among other benefits, HIER ensures that certain antibodies

previously known to not give a signal with formalin-fixed tissues, give exceptional staining[98]. Since these steps were followed in our immunohistochemical analyses, we speculate that slide preparation before immunoprobing with our pAbs was done properly. The ultimate test, then, came when immunoprobing slides. A negative control, one where no signal is expected, in immunohistochemistry can be to make slides undergo the same treatment but omit adding primary antibody (see [99]). Yet, we considered that with the advantage of PimmS availability, it was important to compare their immunohistochemical profiles to that of our pAbs. We acknowledge that pAbs can cross-react with proteins containing epitopes similar to those found in our protein of interest (POI)[69]. Still, increased sensitivity is a strength of pAbs when compared to mAbs, as their signal is amplified on account of several antibodies contained in the pAb mix binding to more than one antigenic target putatively belonging to the POI[69,100].

With regards to antibody specificity, validation is commonly done in WB platforms, where the presence of a single band in agreement with the predicted molecular weight of the POI is indicative of a specific antibody[95,101]. However, this is not necessarily unequivocal evidence that the antibody(-ies) binds to the POI, as other immunoreactive protein(s) could have a similar molecular weight to that of the POI[95]. It is complicated with $_r$hCABS1 because WB of OEL shows immunoreactivity at 84 and 67 kDa (**Figure 2-9** A, F) which differs from the predicted molecular weight of hCABS1, 43 kDa. Furthermore, immunogenic epitopes are uncovered differently in WB when compared to immunohistochemistry[95]. In SDS-PAGE, a step prior to WB, denatures and linearizes proteins by destroying secondary and tertiary structures[95,102]. In tissue fixation, a step prior to immunohistochemistry, these structures are unaffected[94]. Therefore, sample preparation prior to exposure of antibody differs for each technique and epitope exposure of the target protein differs, potentially influencing the capacity of an antibody(-ies) to bind to its intended target in a specific manner[101]. Hence, WB results can't be used to predict antibody specificity in IHC and validation should be done in a technique-specific manner[101] as we have done.

pAbs targeting hCABS1 detect several bands in saliva supernatant, but mass spectrometry validation has been unsuccessful

We previously published that in saliva a consistent immunoreactive band was found at 27 kDa using H2.0 antibody[10]. Its intensity increased as participants self-reported to be stressed[21]. Bands at 18, 15, and 12 kDa were present in participants that were not affected by stress, raising the hypothesis that the presence of these low molecular weight bands could be a biomarker for resilience to stress[21]. The WB profile in saliva when using other pAbs to hCABS1 did not show the presence of any of these bands. H1.0, H2.1, H2.2, and commercial pAb sc-136594 detected a band at ~54 kDa (**Figure 2-16** A, C, D, E). H2.2 and sc-136594 detected a doublet at this location (**Figure 2-16** D, E). Interestingly, H2.0 and H2.1 detected an additional band at 83 kDa (**Figure 2-16** B, C), a location similar to that observed in WB of OEL (**Figure 2-9** B, C) where we believe the most prominent hCABS1 variant migrates in 12% PA gels.

Nonetheless, as opposed to OEL, we have not been successful in detecting hCABS1 by MS-seq analysis of saliva supernatant samples. Our initial attempt was to separate total protein from saliva using 1D-e SDS-PAGE followed by MS-seq. Initially, we sent only a section of the gel corresponding to 27 kDa for MS-seq. While hCABS1 was not detected, we noticed that an abundance of immunoglobulin was present, which is not surprising given that the apparent molecular weight of immunoglobulin light chain is ~25 kDa[103]. Thinking that there may be more than one variant of hCABS1 in saliva and that we might had missed it, we submitted a whole lane analysis of saliva for MS-seq, yet no hCABS1 was detected. In both occasions, alpha amylase, an abundant protein in saliva, was detected.

With the preamble that amylase could be masking the detection of low abundant biomarkers[76], like hCABS1, we found a treatment to remove amylase[76], treated freshly collected saliva and analyzed it using H2.0 in WB. An abundance of bands was observed in untreated supernatant (**Figure 2-17** A), including those associated to stress, i.e., 27, 19 and 12 kDa[21]. After amylase

removal, those bands disappeared (**Figure 2-17** B). A subsequent in silico analysis to see if hCABS1 and amylase are predicted to interact showed that they do not, in turn suggesting that hCABS1 should have eluted from the amylase capturing column, as opposed to being adsorbed to it. Then, why did these bands that we thought were variants of hCABS1 disappear after treatment? Moreover, why did they not re-appear when we eluted the proteins captured in the potato starch column and immunoprobed them with H2.0 (Compare **Figure 2-17** A to C)? A possible explanation is that these forms of hCABS1 may also interact with potato starch, a molecule formed by amylose and amylopectin[104], and that the solution used to elute the captured molecules was not effective in separating these hCABS1 variants from the starch substrate. We recognize that this experiment should have been performed more than once, yet low availability of H2.0 prevented us from repeating this study.

Still, these results indicated that some forms of hCABS1 were present in treated saliva supernatant. Notably, the 83 kDa variant that aligned with the H2.0-detected form in OEL (compare **Figure 2-17** B to **Figure 2-9** B) was still present post-treatment to remove amylase. Thus, we passed saliva supernatant through the potato starch column and submitted this sample for MS-seq analysis. We were successful in removing amylase, but still, this attempt did not detect hCABS1 via MS-seq. Is it possible, then, that hCABS1 is in such low abundance that even when removing amylase, we cannot detect it via MS-seq? Given this, we sought a technique that increased the resolving power; the ability to separate adjacent proteins from each other in a matrix in a way that those in greater abundance would not mask those in lower abundance. Accordingly, we used 2D-e, a technique that allowed for increased in-gel resolving power.

Increasing gel resolution prior to sequencing did not validate hCABS1 occurrence in saliva supernatant, but exposed potential proteins that could be cross-reacting with our pAbs

For 2D-e, one must firstly concentrate the protein content from a sample in a pellet and re-suspend this pellet in 2D-e resuspension buffer. To concentrate protein from saliva supernatant,

acetone precipitation that was able to precipitate 85 µg of total protein was used, well within the range of 50-100 µg required by our platform (see Appendix B – 2D-e protocol for MS-seq analysis, Table 2.1). The pellet resuspended entirely in the manufacturer's resuspension buffer; therefore, we speculated that the entirety of precipitated proteins entered the gel matrix. Indeed, when comparing our stained gel to those in literature, we found that the profile of stained proteins was similar (compare **Figure 2-20** to Figure 2[105], Figure 1[106]) and if anything, showed less protein smearing. However, the latter may reflect loss of protein content during precipitation. In fact, a group that performed 2D-e of saliva and compared different precipitation methods showed that protein recovery with acetone was less effective than precipitating with TCA/acetone/DTT[105]. Nonetheless, we obtained enough total protein (i.e., 85 µg), and decided to do 2D-e-WB using H1.0, H2.0 and their PimmS.

Initially, we used a working concentration of 3 $^{ng}/_{µL}$, as our WB protocol in the past had used. However, PimmS also gave a strong signal at this working concentration (compare **Figure 2-18** A to B, and **Figure 2-19** A to B). We devised to probe using 10X less pAb, i.e., 0.3 $^{ng}/_{µL}$. We stripped the membranes and re-probed them at the new working concentration. We obtained signal from membranes probed with H1.0, but not with PimmS (H1.0) (compare **Figure 2-18** C to D) and H2.0, but not PimmS (H2.0) (compare **Figure 2-19** C to D). These results suggested that the locations in the membrane where we got a signal were, in theory, representative of hCABS1 in saliva. We used this information to select twelve in-gel spots that we speculated could contain hCABS1 and submitted them for MS-seq analysis (see **Figure 2-20**). Results showed that hCABS1 was not present in the submitted spots. We wondered if our pAbs, especially H2.0, were detecting proteins other than hCABS1. We had sent four gel spots corresponding to, what we believed, represented the 27 kDa hCABS1 variant in 2D-e (see **Figure 2-19** C, bottom spots; **Figure 2-20** F, G, H, I). We analyzed the protein profile and speculated that proteins present in at least three spots were being detected by H2.0. We found eight potential candidates following MS-seq, but not hCABS1 (**Table 2-3**). A subsequent in-depth analysis of the range of pH and

molecular masses encompassed by each spot (F-I), suggested that we evaluated proteins with an anticipated range between 29 and 33 kDa.

Of the eight candidate proteins, carbonic anhydrase 6, zinc-alpha-2-glycoprotein, cystatin SN, and prolactic-inducible protein have been also reported to occur in saliva on 2D-e-MS-seq evaluation in independent studies[83,106–108]. What's more, carbonic anhydrase 6 and cystatin SN have also been linked to induced acute stress in the form of hypoxia[83]. In our 2D-e gels spots seem to be present at 27 kDa, even though their predicted molecular weights are: carbonic anhydrase 6 - 35 kDa, and cystatin SN - 16 kDa. These could be the identities of the protein(s) detected by H2.0. Only Hardt et al. clearly noted the in-gel observed apparent molecular weight at which these proteins were found[107]. Our observations differ in that his group detected carbonic anhydrase at two spots, 48 (pI 6.02) and 50 kDa (pI 6.21)[107], while we detected it between 29 and 33 kDa and across pH 4.3 and 5.4. Our observations align with the theoretical molecular mass of carbonic anhydrase 6, 33.6 kDa; but his observations fall closer to the molecule's theoretical pI, 6.5[107]. From Figure 5 in Hu et al. 2D-e pattern of whole saliva we calculated that carbonic anhydrase was found in spots encompassed inside a range of pH 6.9 – 8.0, all of which were at an apparent molecular weight of 28 kDa[108], an observed molecular weight that falls close to our observations of carbonic anhydrase 6.

From Figure 5 of Hu et al.[108], we calculated that cystatin SN was detected at 14 kDa and within a pH range encompassing 7.2 – 9.0, relatively consistent with the molecule's predicted molecular mass and pI of 14 kDa and 6.9, respectively. From Figure 1 of Ghafouri et al.[106], we calculated that cystatin SN was detected at <15 kDa and within a pH range of 5.8 – 6.0. In our platform, we found cystatin SN at a higher molecular mass location, 29 to 33 kDa, and at a relatively more acidic location than where it is predicted to occur, pH 4.3 – 5.4. From these comparisons, we speculate that our methodology requires further optimization, namely because it appears that characterized proteins, like carbonic anhydrase 6 and cystatin SN, seem to migrate to gel locations not

consistent with their predicted molecular weight. Yet, our results reflect what our antibodies see in our conditions. Thus, these results can be used to generate hypotheses. One hypothesis can be that H2.0 is detecting carbonic anhydrase 6 and/or cystatin SN.

A western blot of recombinant carbonic anhydrase 6 overexpression cell lysate (rCA6 OEL) suggests that H2.0 does not interact with rCA6 in this sample. rCA6 OEL contains a recombinant version of CA6 with a FLAG tag adjacent to the protein's carboxyl end. Comparison of the western blot profile generated in saliva by H2.0 (**Figure 2-21**, saliva: 83, 60, 32, 27 kDa) does not align with the profile generated in rCA6 OEL by probing with an anti-FLAG antibody (**Figure 2-21**, rCA6 OEL: 42, 38 kDa).

After re-evaluation of previously established methodology

Even when we propose that these two proteins could be interacting with H2.0 and could be the identity of the 27 kDa and, putatively, <27 kDa bands that we have associated with stress, the variable results that we have among our pAbs and biological samples are still unresolved. With the introduction of capillary nano-immunoassay into our research tools to study hCABS1, came the advent of a methodology to optimize this platform's signal. This protocol uses a dilution series for protein and primary antibody(-ies) and calls for the evaluation of signal. We decided to use this titration methodology in WB to assess if our pAbs were giving non-specific signals. Using this approach, we decided to compare the profiles of our pAbs to that of their PimmS when analyzing human serum and saliva supernatant.

Careful titration methodology suggests that our pAbs detect four hCABS1 variants in serum

Human serum is the supernatant portion obtained from a centrifuged blood sample, if no anti-coagulant agent(s) are introduced and the blood is allowed to clot[109]. Blood can be a reflection of ongoing physiological conditions[110]. Body cells shed products into blood that have the potential to become markers of an individual's physiological state, in turn making it an ideal fluid for clinical

diagnostics[110]. Under the premise that blood contains molecules originating from SMG[54,111–113] and/or testes[114,115], we looked for presence of hCABS1 in serum, as we have reported the presence of hCABS1 in these sources and lung[18]. We decided to probe serum with all our pAbs and their PimmS using our titration methodology to determine which working concentrations were optimum for assessing this biological fluid in WB.

Review of our results showed that when evaluating blood serum, we need to load 1.5 $\mu g_{\text{total protein}}$ into 12% PA gel wells, and immunoprobe at working concentrations of 0.3 $^{\text{ng}}/_{\mu L}$ (for H1.0 and H2.0) or 0.2 $^{\text{ng}}/_{\mu L}$ (for H2.1 and H2.2). At these conditions, we believe that representative hCABS1 bands are found at 137, 93, and 68 kDa for H1.0 (**Figure 2-22** C), 100, 74, 63, and 56 kDa for H2.0 (**Figure 2-22** I), 91 kDa for H2.1 (**Figure 2-22** O), and 141 and 91 kDa for H2.2 (**Figure 2-22** U). While our pAbs showed more bands at these conditions, bands detected by their PimmS at the same location, qualitatively, were considered non-specific (**Figure 2-22** D, J, P, V). We recognize that the discrepancy in molecular weights between these equivalent PimmS-detected and pAb-detected bands seems to be enough to think that they represent a different protein altogether (E.g., H1.0 50 kDa band (**Figure 2-22** C) vs PimmS (H1.0) 44 kDa band (**Figure 2-22** D)). Repetition of WB analysis of human serum with our pAbs and their PimmS at these optimized conditions can help us determine whether these bands are at representing proteins of the same molecular weight. PimmS aside, whether some pAbs are detecting the same hCABS1 variant(-ies) remains to be determined.

Altogether, this serum analysis suggested that hCABS1 is present in blood, which led us to speculate that this protein could be released by SMG, testes, and lung into the bloodstream. If this is true, the presence of hCABS1 in SMG of female individuals[18] makes us wonder whether the levels of molecule in blood vary as a function of sex. Interesting research in other mammals have shown that Cabs1 transcript is present in the female reproductive system of rhesus macaques[13] and heifers[14]; protein presence remains to be evaluated. A further question that arises from these

observations is whether CABS1 production is exclusive to reproductive tissue, SMG, and lungs, or are other organs producing and shedding it into the bloodstream? WB evaluation of serum from female participants can help us determine (1) if the protein is present, and (2) if the expression of the variants of hCABS1 that we have observed in males is the same in females.

With regards to our optimization protocol for WB, serial dilution of sample, thus dilution of available antigen, has proven to be an essential step prior to assessment of samples[116]. Attempting to optimize a WB protocol, a 0.5 log serial dilution of hamster brain homogenate was made and prepared for SDS-PAGE and subsequent WB[116]. While retaining a fixed antibody working concentration, Lee et al. showed how WB sensitivity, i.e., output signal, increased with greater sample amount[116] in a similar form as we show in human serum (**Figure 2-22** A, G, M, S). In contrast to Lee et al., we also did a serial dilution of our pAbs and we compared their WB profiles to those of each of their PimmS. Several WB studies compare pAbs and PimmS to show the increase in immunoreactivity after several immunization boosts ([117–121]).

The titration strategy challenged our original interpretation of WB profiles in saliva supernatant

Once the titration methodology was established, we decided to assess saliva supernatant in WB using two antibodies we had published results with, H1.0 and H2.0, as well as to probe the same saliva sample with PimmS of these pAbs. We probed membranes using antibody working concentrations of 0.3 $^{ng}/_{\mu L}$ and on wells with a total protein content of 2.2 μg, as these conditions gave defined bands. Under these restrictions, pAb H1.0 detected a protein that was also identified by PimmS (H1.0) (**Figure 2-23** , compare C to D). In fact, PimmS (H1.0) showed a doublet at the equivalent location, suggesting that the band identified by H1.0 is not specific for hCABS1. This pattern was seen across all combinations of sample amount and antibody concentration in H1.0 evaluation of saliva supernatant (**Figure 2-23** A, B, C, D, E, F). Evaluation of saliva supernatant using H2.0 and PimmS (H2.0) suggests that this pAb detected two proteins at 90 and 64 kDa, a

pattern not shared with PimmS (H2.0) (**Figure 2-23**, compare I to J). Thus, that the lower molecular mass forms ($\leq$ 27 kDa) detected by H2.0 at conditions where SDS-PAGE wells were loaded with up to 25 µg of total protein and membranes were probed with an antibody concentration of 3 $^{ng}/_{µL}$ may not be representative of hCABS1. We have published that hCABS is a biomarker of stress given that a 27 kDa band detected in WB by H2.0 was positively correlated to self-reported stress, and posed that the occurrence of < 27 kDa bands, also detected by H2.0, were indicators of stress resilience[21]. The re-evaluation of our methodology posed a new hypothesis to be tested. Namely, is stress eliciting the occurrence of hCABS1 in saliva supernatant (see [21,66]) based on PimmS WB patterns in this biofluid?

In our post-methodology re-evaluation WBs of human serum and saliva supernatant, PimmS at the highest concentration (3 or 2 $^{ng}/_{µL}$) detected bands that appear at the equivalent location as those detected by their pAb counterparts. McNeilly et al. identified similar results when evaluating *E. coli* protein EspA with pre and post-immunization serum from a calf immunized with this protein[117]. The WB profile clearly shows a fainter band at the equivalent location in the pre-immunization WB and an intense band on the WB probed with post-immunization serum (Figure 3[117], EspA). This pattern was also observed in Nataro et al. WB evaluation of lysate from bacteria strain HB101(pJPN31) with serum from volunteers from before and after known exposure to the bacteria[120]. A clear band was observed in the WB probed with pre-immunization serum (Figure 5[120], D); albeit, this may have been because the volunteer had been exposed to the same bacteria before the experiment. This article also mentions the presence of high molecular weight bands present in both the antiserum and pre-immunization serum from rabbits exposed to the bacteria, and speculates that these bands represent low-affinity antibodies targeting ubiquitous *E.coli* antigens[120]. Similarly, it is possible that bands detected by our PimmS and pAbs are a fraction of low affinity antibodies targeting ubiquitous human proteins that contain common antigenic determinants to the ones we used as immunogens. This could explain why even after antigen-affinity purification of rabbit antiserum we still got putatively non-specific antibodies in

our pAbs. In fact, a BLAST® Protein[122] analysis to determine which annotated proteins in the human genome database contain similar motifs to our H2.n pAbs immunogen (hCABS1 a.a.: $_{184}$DEADMSNYNSSIKS$_{197}$) encountered 132 proteins that share, at least, 4 continuous common amino acids, 51 of which correspond to sequences in immunoglobulins. This analysis supports the idea that our H2.n pAbs could be detecting proteins other-than-hCABS1, even when they were affinity purified. The same analysis done for our H1.n pAbs immunogen (hCABS1 a.a.: $_{380}$TSTTETDIFELLKE$_{396}$) encountered 167 proteins sharing at least 4 continuous common amino acids. Out of these proteins, only 2 are immunoglobulins. With lesser cross-reactivity to immunoglobulins, it is less likely that this antibody could be detecting immunoglobulins in saliva in a non-specific manner, something that H2.0 could be doing. Moreover, this suggestion implies that hCABS1 is not present in saliva or, if present, is not detected by either H1.0 or MS-seq.

Rabbits, the host species that produced all our pAbs, also express CABS1

Rabbits and humans (host and antigen source species) are mammals and both produce CABS1. Factually, the hCABS1 antigens used for immunizing the rabbits that produced our pAbs are similar to domains present in rabbit CABS1 (**Figure 2-24**). Because of this, it is possible that, at one point during the production of our pAbs, the rabbit produced antibodies to endogenous CABS1. GenScript's ongoing immunogen boosts during pAb production should, in theory, have kept the immune response against our hCABS1 peptides active. However, it is unknown to us whether naturally occurring positive and negative selection of B cells in the rabbit suppressed the existence of B cells that produced antibodies to hCABS1 and, if so, what the effect was in the final pAb mix we obtained. It is possible that rabbits did not give us the best pAbs in response to our hCABS1 immunogens. Nonetheless, while WB data using our pAbs is questionable, our data on immunohistochemistry suggests that our pAbs are a suitable research tool for this immunoprobing technique.

Figure 2-24. Sequence alignment of human (h, *Homo sapiens*) CABS1 and rabbit (r, *Oryctolagus cuniculus*) CABS1-isoform X1.

hCABS1 is used as the reference sequence. rCABS1-isoform X1 covers 99.5% of hCABS1 length. However, the percentage of residues that are the same in rCABS1 with respect to hCABS1 is 65.6%. Residues enclosed in red dotted boxes indicate sections of hCABS1 used to produce polyclonal antibodies H1.0 and H2.n in New Zealand rabbits. Consensus row at 100% consensus threshold shows sets of residues that are either the same across both species, or share a predefined physicochemical property. Consensus patterns (%) are based on sets of residues that share a predefined property based on the classification by W.R. Taylor. u: tiny, s: small, h: hydrophobic, p: polar

Summation: Western blot profiles of polyclonal antibodies

In our WB system, bands that are considered to represent hCABS1 are (by sample): in OEL at 84 and 67 kDa, in SMG at 71, 52, 47, 33 and 27 kDa, in saliva at 90 and 64 kDa, and in serum at 139, 91, 71 and 63 kDa (**Table 2-4**, samples listed by column from left to right). Overall, only a band averaged at 70 kDa occurred in OEL, SMG and serum. Two bands averaged at 91 and 64 kDa occurred in saliva and serum. Other bands seemed to be sample-specific. These are: one band in serum at 139 kDa, one band in OEL at 84 kDa, and four bands in SMG at 52, 47, 33 and 27 kDa (**Table 2-4**, two rightmost columns).

While the comprehensive titrations of antibody and antigen re-evaluations were only performed once, altogether, results indicate that our previous WB may not have been optimized and that the conclusions reached in our publications require reappraisal. Because our four pAbs identify different bands in WB, we postulate that each pAb differs in the prominence of clones recognizing specific epitopes, and together with post-translational processing of hCABS1, multiple bands are detected. Moreover, our data suggests that hCABS1 is processed differently in different tissues and bodily fluids. Despite attempts using 2D-e, we have been unsuccessful in confirming that any of the bands are hCABS1 by MS-seq. Thus, an explanation for our observations is that our pAbs are not specific for hCABS1, despite being affinity purified with their immunogen.

Given the equivocal nature of our pAbs results, to identify hCABS1 and its potential molecular forms in multiple tissues and fluids, we developed monoclonal antibodies to different regions of CABS1 and tested these in WB, immunohistochemistry, and immunoprecipitation coupled with MS-seq (see Chapter 4).

Table 2-4. Average molecular weights (MW) detected by pAbs targeting hCABS1 per sample.

Each cell represents the mean of a band's molecular weight in kilodaltons (kDa) detected by pAbs described in this chapter at, putatively, the same region.

Transient overexpression cell lysate controls

Human submandibular gland (SMG)

Human saliva

Human serum

hCABS1 OEL	NCL	hCABS1 OEL excluding NCL detected bands	SMG	SMG excluding inconsistent bands	Saliva pre-optimization	Saliva post-optimization	Serum post-optimization	All bands	Sample(s) where band occurs
Average MW (kDa)	Average MW (kDa)	Average MW (kDa)	Average MW (kDa)	Average MW (kDa)	Average MW (kDa)	Average MW (kDa)	Average MW (kDa)	Average MW (kDa)	
-	-		127		-		139	139	Serum
-	-		106		-				
-	-		96		-				
84	-	84	-		83	90	91	91	Saliva, serum
-	76		-		-			84	OEL
67	-	67	71	71	-		71	70	OEL, SMG, serum
-	-		57		60	64	63	64	Saliva, serum
55	55		52	52	54			52	SMG
47	47		47	47	51			47	SMG
-	-		40		-				
34	34		33	33	32			33	SMG
-	-		27	27	27			27	SMG
21	21		22		19				
-	-		-		14				
-	-		-		11				

Chapter 3 : A method to study protein biomarkers in saliva using and automated capillary nano-immunoassay platform (Wes™)

Preamble

In 2016-2017, our group recognized we had a finite amount of pAbs targeting hCABS1. At the time, we aimed to validate if hCABS1 was a biomarker of psychosocial distress in saliva. With a limited amount of antibodies and saliva samples we looked for alternative platforms that would use minimal amounts of reagents to complete this milestone. An appealing option presented when the Plastic Surgery research laboratory at the University of Alberta acquired a state-of-the-art capillary nano-immunoassay (CNIA) platform, Wes™. Like Western blot (WB), samples are separated by electrophoresis and immunoprobed with an antibody(-ies) targeting protein(s) of interest. This chapter details the methodology to evaluate our saliva samples in Wes™.

For our experiments, when compared to WB, Wes™ utilized 16.5X less antibody stock; similarly, sample volume is also significantly less in CNIA, yet it depends on the concentration of the original sample. Careful controls must be conducted prior to running analyses in CNIA. In our case, we established a Reference Saliva (Refsal) sample that was loaded on every plate to allow the interexperimental evaluation of our results.

The work presented in this chapter is product of a collaboration with Drs Thomas Ritz and David Rosenfield from the Southern Methodist University (SMU; Dallas, TX, USA), and Drs Marcelo Marcet-Palacios and Dean Befus from the University of Alberta. Dr Ritz performed a validated psychosocial stressor test, the Trier Social Stress Test (TSST) on a pool of students from SMU and collected the saliva samples evaluated in this article. Dr David Rosenfield performed statistical analyses of experimental results. Drs Marcelo Marcet-Palacios and Dean Befus provided guidance in the design of the methodology and the redaction of this article.

To illustrate how CNIA can positively impact biomarker discovery, we used Dr Ritz TSST samples, immunoprobed them with antibodies to hCABS1 H1.0 and H2.0, and compared CNIA's readout with WB results of the same samples (published in 2017, see [21]).

A version of this chapter has been published as:

<u>Reyes-Serratos, E.</u>, Marcet-Palacios, M., Rosenfield, D., Ritz, T., Befus, A.D. (2020). A method to study protein biomarkers in saliva using an automated capillary nano-immunoassay (Wes™). *Journal of Immunological Methods*, 479, 112749. https://doi.org/10.1016/j.jim.2020.112749

Title: A method to study protein biomarkers in saliva using an automated capillary nano-immunoassay platform (Wes™)

Authors: Eduardo Reyes-Serratos[1], Marcelo Marcet-Palacios[1,2], David Rosenfield[3], Thomas Ritz[3], A. Dean Befus[1]

Affiliations: [1] Department of Medicine, Alberta Respiratory Centre, University of Alberta, Edmonton, Alberta, Canada; [2] Northern Alberta Institute of Technology, Edmonton, Alberta, Canada; [3] Department of Psychology, Southern Methodist University, Dallas, Texas, United States of America

Corresponding author: Eduardo Reyes-Serratos. University of Alberta, 567 Heritage Medical Research Center. Edmonton, AB. Canada. T6G 2S2. reyesser@ualberta.ca

Highlights

- We analyzed levels of human CABS1 in saliva in a study of acute stress

- We used capillary nano-immunoprobing assay Wes™ and compared it to Western Blot

- Wes™, replicates previous Western blot results of elevated hCABS1 in acute stress

- Wes™ has higher sensitivity, specificity, throughput, uses less sample, antibodies

- This extends our previous evidence that saliva hCABS1 is a biomarker of stress

Abstract

Traditional immunoprobing techniques like Western blot continue to play a crucial role in the discovery and validation of biomarkers. This technique suffers from several limitations that affect reproducibility and feasibility for large-scale studies. Modern immunoprobing techniques have addressed several of these limitations. Here we contrast the use of Western blot and an automated capillary nano-immunoassay (CNIA), Wes™. We provide evidence highlighting the methodological advantages of Wes™ over Western blot in the validation of a novel biomarker, Calcium binding protein, Spermatid associated 1 (hCABS1). While Wes™ offers a faster, more consistent approach with lower requirements for sample and antibody volumes, variations in expected molecular weights and computational algorithms used to analyze the data must receive careful consideration and assessment. Our data suggests that CNIA approaches are likely to positively impact biomarker discovery and validation.

Keywords: Capillary nano-immunoassay; Wes™; saliva; CABS1; stress; biomarker(s); immunoprobing; Western blot

Introduction

Validated biomarkers are objective indicators of a clinical outcome that can be measured accurately and reproducibly. Biomarkers can be physiological and/or biochemical processes, molecular reactions, or molecules themselves. The quest for molecular biomarkers as predictors of clinical outcome(s) has gained momentum over the past two decades[123]. Selection of the biological specimen to be used as the sample source, as well as defining the target molecule (protein, RNA, DNA) are important considerations in design of the protocol and instruments used for biomarker measurement[124]. A limitation in studying and establishing biomarker candidates is that the levels of some candidate molecules are hard to detect and/or quantify[125]. Therefore, optimization of accurate and reproducible quantitative techniques is of great importance in establishment and evaluation of novel biomarkers.

91

Commonly used samples for biomarker studies include biological fluids like serum, plasma, or urine. Among them, saliva is a desirable source because its collection is non-invasive, requires minimal equipment and training, in turn minimizing costs, and can be processed with relative ease[126,127]. However, as saliva is not sterile and is subject to microbial contamination, proper collection techniques are needed to help ensure sample quality[126,127], and sensitive and specific assays are required to measure biomarkers in saliva.

A candidate biomarker in saliva that promises to be an indicator for psychological stress is human Calcium binding protein, Spermatid associated 1 (hCABS1)[21]. Other groups have characterized this protein in rat[1], mouse[4], and porcine testes[5] and recorded higher than estimated molecular weight for this protein using gel electrophoresis and Western blot. Such observations led to suggestions that CABS1 is an intrinsically disordered protein[1], highly susceptible to proteolytic cleavage.

To study hCABS1, we produced antibodies to two different regions of the protein, assuming that proteolytic maturation might produce polypeptides of different sizes and containing different epitopes. Western blot analyses of human saliva[21], submandibular gland, testes, and lung identified discrete hCABS1-derived variants[18], leading us to speculate that hCABS1 is selectively processed by proteases. We established that hCABS1 contains an anti-inflammatory peptide motif[18]. Moreover, we found that in saliva a 27 kDa hCABS1 form was positively correlated with self-reported anxiety and stress[21]. Interestingly, the occurrence of variants of hCABS1 <27 kDa in saliva was associated with lower self-report of stress, leading to speculations about a possible role in stress resiliency [21].

To validate the clinical relevance of these observations on hCABS1 in saliva, we sought to establish an immunoassay with higher throughput than Western blot that would be sensitive and accurately determine the levels of various forms of hCABS1 in human saliva. In this manuscript, we describe a method to assess the levels of salivary hCABS1, a candidate biomarker of psychological stress,

using the automated capillary nano-immunoassay (CNIA) Wes™ platform. Wes™ was selected because the volume of our antibodies was limited, and we needed to evaluate different-sized forms of hCABS1.

Materials and methods

Polyclonal antibodies to hCABS1

Two polyclonal antibodies (pAb) were raised in New Zealand rabbits to two regions of hCABS1 protein. H1.0 was produced against a 14-mer polypeptide sequence at the carboxyl end of hCABS1 and containing a putative anti-inflammatory sequence (underlined) *TSTTETDIFELLKE* (aa T375-E388)[18]. Additionally, a section of hCABS1 corresponding to a beta sheet (aa D184-S197) was used to create polyclonal antibody H2.0 using the 14-mer polypeptide DEADMSNYNSSIKS. The polyclonal antibodies were affinity-purified using their immunizing peptide[18].

Human recombinant CABS1 and cell lysate controls

A recombinant human CABS1 overexpression cell lysate (rhCABS1 OEL) was used as a positive control. It was produced by OriGene Technologies Inc. (Rockville MD) by inserting a True Open Reading Frame (TrueORF) clone containing the hCABS1 sequence into Human Embryonic Kidney 293T (HEK293T) cells. Cell lysate of HEK293T containing an empty TrueORF plasmid was used as a negative control (NCL). Both rhCABS1 OEL and NCL had a protein stock concentration of 1 mg/mL.

Collection and protein determination of saliva supernatant

Sixteen participants (mean age 33.6 [SD=15.0]; 6 women) completed the Trier Social Stress Test (TSST)[128], which is a standardized psychosocial stressor with evaluative threat, in which participants are required to give a 5-min free speech and complete an oral 5-min mental arithmetic test in front of an audience of the experimenter and two confederate "evaluators".

Saliva samples (Salivettes, Sarstedt, Germany) were provided at six time points during the test; 15 minutes and just before (-0) exposure to the stressor, and just afterward (+0), 15, 30, and 45 minutes post-exposure to the stressor, as previously described[21]. Samples were frozen and sent for analysis, where they were thawed and centrifuged at 1500 rcf and 4°C for 20 minutes. Supernatants were collected, mixed by pipetting, aliquoted, and stored at -80°C until analysis.

We established a Reference saliva (Ref. sal.) to use as a standard for comparing the expression of hCABS1 across samples. We pooled 200 mL of whole saliva using the passive drool methodology from SalivaBio (Salimetrics) from an individual who self-reported low levels of psychological stress and had a similar diet and exercise routine on days when samples were collected. On every day of collection, saliva was immediately placed at -20°C. Once 200 mL was collected, all aliquots were thawed and centrifuged at 1500 rcf and 4°C for 20 minutes. Afterward, we transferred the pooled supernatant to a sterile glass bottle, mixed by pipetting, and stored 50 µL aliquots at -80°C.

For all saliva samples, determination of total protein concentration was done using a Pierce™ BCA Protein Assay Kit (Thermo Scientific).

CNIA immunoprobing Analysis

Wes™ loads less than 300 nanoliters of sample into a capillary and electrophoretically separates the proteins by either size or pI, based on the kit that the user purchases[129]. Separated proteins are probed with a primary antibody targeting the protein of interest. This is followed by treatment with a secondary Horseradish peroxidase-conjugated antibody. Subsequently, the chemiluminescent substrate is added on nine occasions and a CCD camera captures the emission of light. Chemiluminescence intensity is assessed through electrophoretograms generated by Compass for SimpleWestern software v3.1.7 (ProteinSimple, San José, CA). In its default mode, the software defines peaks within the electrophoretogram directly related to the amount of protein

bound to the primary antibody. Each peak has an area under the curve that can be used to quantify the signal given by the sample.

In the case of size-separating matrices, the user must load a molecular weight ladder in one capillary. Samples are compared to this ladder to estimate the size of the target protein. Additionally, each sample is mixed with a Fluorescent Master Mix (FMM) containing three fluorescently labeled proteins (internal markers) used as a control for protein migration within each capillary. The outcome is an electrophoretogram showing chemiluminescent signals as a function of estimated protein molecular weights.

Initially, we assessed the levels of hCABS1 in rhCABS1 OEL, NCL, and saliva in Wes using H1.0 and H2.0. Firstly, we performed titrations to optimize the signal-to-noise ratio as a function of sample and antibody concentrations. As per manufacturer's suggestions, the optimum signal occurs when it is maintained over the course of the experiment, background noise is below 2000 chemiluminescence arbitrary units (a.u.), signal-to-noise ratio is greater than 10, and peak resolution is clear.

To prepare the different concentrations of our samples, all dilutions were mixed with the appropriate amount of FMM and 0.1X sample buffer. We diluted rhCABS1 OEL and CL to attain final concentrations of 50, 10 and 20 µg/mL, while Ref. sal. samples were diluted to 500, 100 and 20 µg/mL. Samples were vortexed and heated at 95°C for 5 minutes, centrifuged and stored on ice until they were loaded into the Wes™ plate. hCABS1 antibodies H1.0 and H2.0 were diluted in Wes™ antibody diluent to attain concentrations of 300 ng/µL, 60 ng/µL, 12 ng/µL, 6 ng/µL and 3 ng/µL.

Once we optimized the Ref. sal. sample concentration and antibody amounts; we ran our TSST cohort saliva samples. They were evaluated on two occasions, on different Wes™ plates and on different days.

TSST saliva data analysis

In Wes™, saliva electrophoretograms showed hCABS1 peak at 60 kDa using H1.0 and at 34 kDa when we used H2.0. All plates where saliva was tested were loaded with two wells containing Ref. sal., used to normalize samples tested on different plates. The immunoreactive peaks produced by the TSST samples were normalized to Ref. sal. 60 kDa peak, when using H1.0, and to the 34 kDa peak when using H2.0 using the following formula:

$$\frac{A_{\text{cohort saliva sample}}}{A_{\text{Reference saliva sample}}} = \text{ratio of expression relative to the Ref. sal.}$$

After normalizing all values for each of the six TSST assessment points, we averaged the values of each sample that were obtained on each of the two occasions in which they were assessed. Timepoints without values, either because there was no signal or because sample was limited, were set to missing values. The resulting variables were submitted as dependent variables to a repeated measures Mixed effect model (MEM) analysis including time as independent variable, age, gender, and group (asthma, healthy control) as covariates[21]. Different error-covariance matrices were examined, and the matrix which best fit the data (Toeplitz) was used for analyses. For exploratory purposes, means comparisons were undertaken with the Least Significant Difference method, which is equivalent to no correction for multiple comparisons.

Results

Optimization of Wes™ running parameters for the detection of hCABS1 variants

To assess the capability of our antibodies to detect various forms of hCABS1 we used recombinant hCABS1 overexpression cell lysate (rhCABS1 OEL) and its negative cell lysate (NCL) as controls. After performing titrations, we concluded that the best total protein concentration of antigen to load per capillary was 10 µg/mL at pAb concentrations of 3 µg/mL (H1.0) and 12 µg/mL (H2.0).

We observed that both antibodies (H1.0 and H2.0) detected two variants at 65 and 94 kDa in rhCABS1 OEL (**Figure 3-1** A, B), whereas these peaks were not detected in NCL (**Figure 3-1** C, D). To further assess antibody specificity, we ran capillaries without sample but with the antibodies at the mentioned concentrations. We identified a non-specific peak at ~230 kDa that is produced when our antibodies bind to an internal marker protein from the Wes™ system ("internal marker peak", **Figure 3-1** A, B, C, D). This reactivity has been detected with other antibodies as well [130].
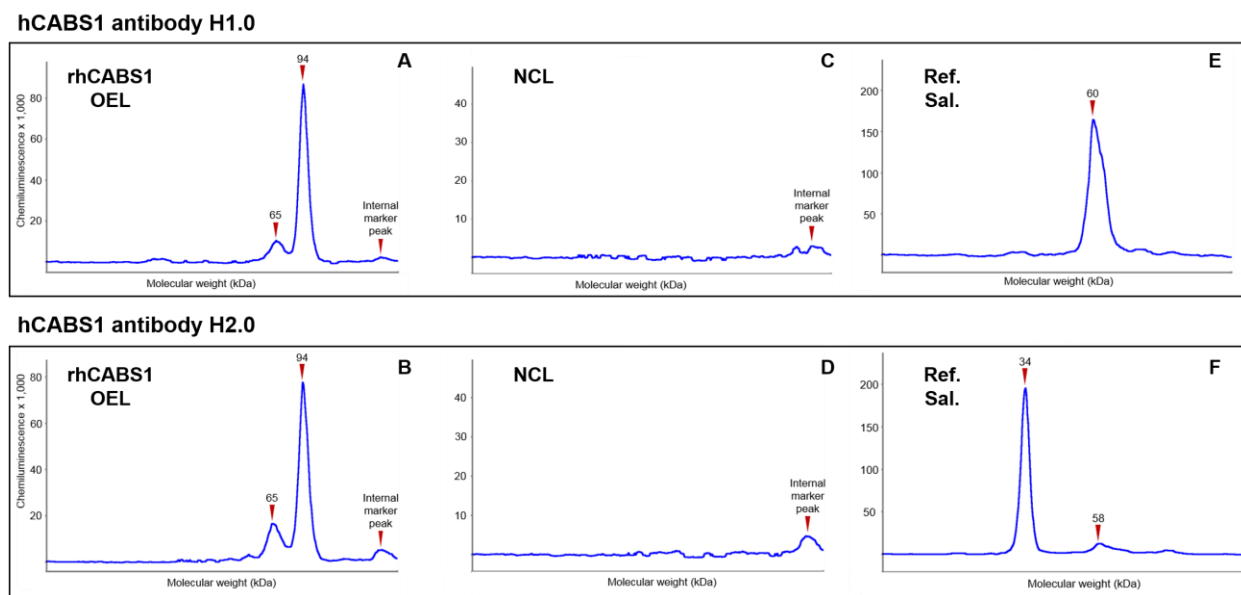
Figure 3-1. In Wes, hCABS1 overexpression cell lysates render a different immunoreactive pattern than human saliva when using antibodies to hCABS1 raised against different parts of the protein.

Both antibodies, H1.0 and H2.0, detect hCABS1 variants at 94 and 65 kDa in a recombinant hCABS1 overexpression cell lysate (rhCABS1 OEL) (A, n=4; B, n=4) and no hCABS1 variants negative control cell lysate (NCL) (C, n=4; D, n=4). In rhCABS1 OEL and NCL, both antibodies interact with a protein used in Wes as an internal marker peak. In a reference saliva sample (Ref. Sal.) used to optimize Wes running parameters, H1.0 detects an hCABS1 variant at 60 kDa (E, n=19), and H2.0 detects two hCABS1 variants at 58 and 34 kDa (F, n=19).

Since our interest lies in the levels of hCABS1 in saliva, we optimized running conditions in Wes™ by using Ref. sal. and pAb H1.0 and H2.0 at different concentrations. Using Ref. sal. under the Wes™ default running protocol, we obtained optimum signal-to-noise ratio at 500 µg/mL and pAb concentrations of 12 µg/mL (H1.0) and 6 µg/mL (H2.0). Interestingly, each antibody rendered a different pattern. H1.0 detected hCABS1 at 60 kDa, and H2.0 at 34 kDa (**Figure 3-1** E, F).

Next, we optimized the use of Wes™ in saliva samples from a stress cohort of 16 patients. Using the default running parameters in the Wes™ platform, some cohort samples produced little-to-no signal when assessed (**Figure 3-2** A). To increase the sensitivity of detection for hCABS1 using Wes™, we modified the default running protocol by increasing the amount of stacking matrix and

hCABS1 antibody H2.0
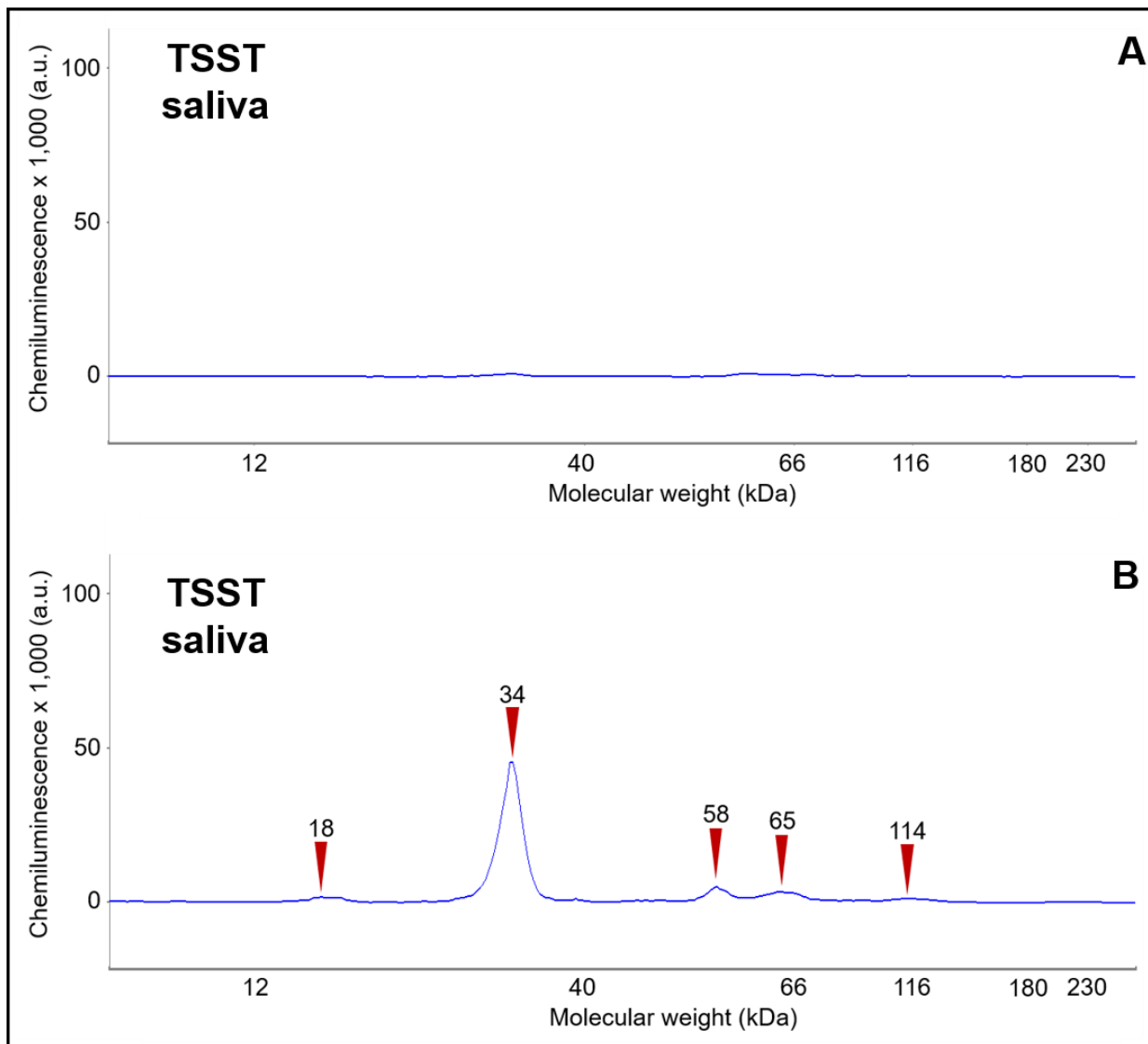
Figure 3-2. Increasing stacking matrix and sample quantity in the capillary, as well as primary antibody incubation time, enhances signal of protein-of-interest.

(A) Electrophoretogram of TSST cohort human saliva screened with hCABS1 antibody H2.0 generated by running default Wes protocol. No signal of hCABS1 is observable (B) Electrophoretogram of the same saliva sample screened with H2.0 generated by modifying Wes running protocol. hCABS1 H2.0-expected 34 kDa variant is observed, along with additional forms at 18, 58, 65, and 114 kDa

sample into the capillary, as well as exposure time to the hCABS1 antibodies (**Table 3-1**). These modifications increased sensitivity, resulting in detection of five variants of hCABS1 when using H2.0 at 18, 34, 58, 65, and 114 kDa (**Figure 3-2** B); the most prominent peak at 34 kDa.

Table 3-1. CNIA running protocols can be changed to increase signal-to-noise ratio and detection of the protein of interest.

Parameters that need to be modified are the time (t) of sample and stacking matrix loading into the capillary, and of primary (1°) antibody exposure

	Default Running Protocol	Modified Running Protocol
t sample load	9 sec.	12.6 sec.
t stacking matrix load	15 sec.	21 sec.
t 1° antibody exposure	30 min.	90 min.

Immunoprobing in Wes™ replicates Western blot observations

We previously reported that in Western blot, antibody H2.0 detected a 27 kDa variant of hCABS1 in the TSST saliva cohort (see [21], Fig 1). We observed that immediately after exposure to the stressor, levels of this 27 kDa hCABS1 form increased (see [21], Fig 1, +0 min) and later decreased (see [21], Fig 1, +15, 30, 45 min) to levels similar to before exposure to the stress test (see [21], Fig 1, -0 min). MEM analysis established that levels of hCABS1 in saliva significantly differed when comparing time points -0, +15, +30, +45 min to time point +0 min, while there was no difference between time points -15 and +0 min.

When evaluating the same TSST saliva samples with H2.0 in Wes™, we observed that the 34 kDa detected protein followed the same pattern as the 27 kDa band in Western Blot, increasing significantly following stress and returning to baseline levels thereafter (**Figure 3-3** A; see 21, Fig. 3). Using antibody H2.0 to detect hCABS1, we observed that the standard deviation of the 34 kDa Wes™ signal at every timepoint of saliva collection was significantly lower than the standard deviation of the 27 kDa Western blot signal ($p < 0.007$). Given different methodologies in estimating the molecular size using WB and CNIA, we speculate that the 27 kDa WB band and 34 kDa CNIA peak correspond to the same protein (see discussion).

Furthermore, we previously reported that through an exploratory analysis we found an apparent association between lower self-reports of stress and saliva variants of hCABS1 of sizes 18 and 12 kDa detected through Western blot and the use of H2.0[21]. Interestingly, 15 saliva TSST samples showing this pattern in Western blot also showed in Wes™ the occurrence of a small peak at 18 kDa hCABS1 when using H2.0 to immunoprobe (**Figure 3-2** B).

H1.0 and H2.0 detect different variants of hCABS1 in saliva; H1.0-detected forms do not correlate with stress

Evaluation of TSST saliva samples with antibody H2.0 in Wes™ detected a form at 34 kDa that is sensitive to stress induction. In contrast, antibody H1.0 only detected a variant of hCABS1 of 60 kDa in all samples. Levels of this 60 kDa hCABS1 salivary form were lower immediately before the TSST and increased immediately after the test (**Figure 3-3** B, -0 and +0 min., respectively).

However, this change was not significant. Significant changes were observed between samples collected 15 minutes post-stress exposure and 15 minutes pre-stress exposure, as well as immediately after exposure to stress (**Figure 3-3** B, +0 versus -15, and +15 min.). After marked decrease at 15 minutes post-stress, levels of the 60 kDa variant fluctuated thereafter (**Figure 3-3** B). Thus, using H1.0 in Wes™ there was no significant increase of hCABS1 in saliva after exposure to acute stress in the TSST. Our TSST samples have not been probed for hCABS1 using H1.0 in Western blot.

Discussion

In previous studies using Western blot to analyze cell lysates and saliva we showed that hCABS1 is present in several discrete variants of different molecular sizes[18,21]. Western blot has several limitations, such as a relatively large amount of sample and antibody required, as well as low

A

Capillary nano-immunoassay
H2.0

$\dfrac{\text{Area}_{\text{34kDa peak, saliva TSST}}}{\text{Area}_{\text{34kDa peak, saliva reference}}}$

Stress test

Timepoint of saliva collection
(min.)

B

Capillary nano-immunoassay
H1.0

$\dfrac{\text{Area}_{\text{60kDa peak, saliva TSST}}}{\text{Area}_{\text{60kDa peak, saliva reference}}}$

Stress test

Timepoint of saliva collection
(min.)
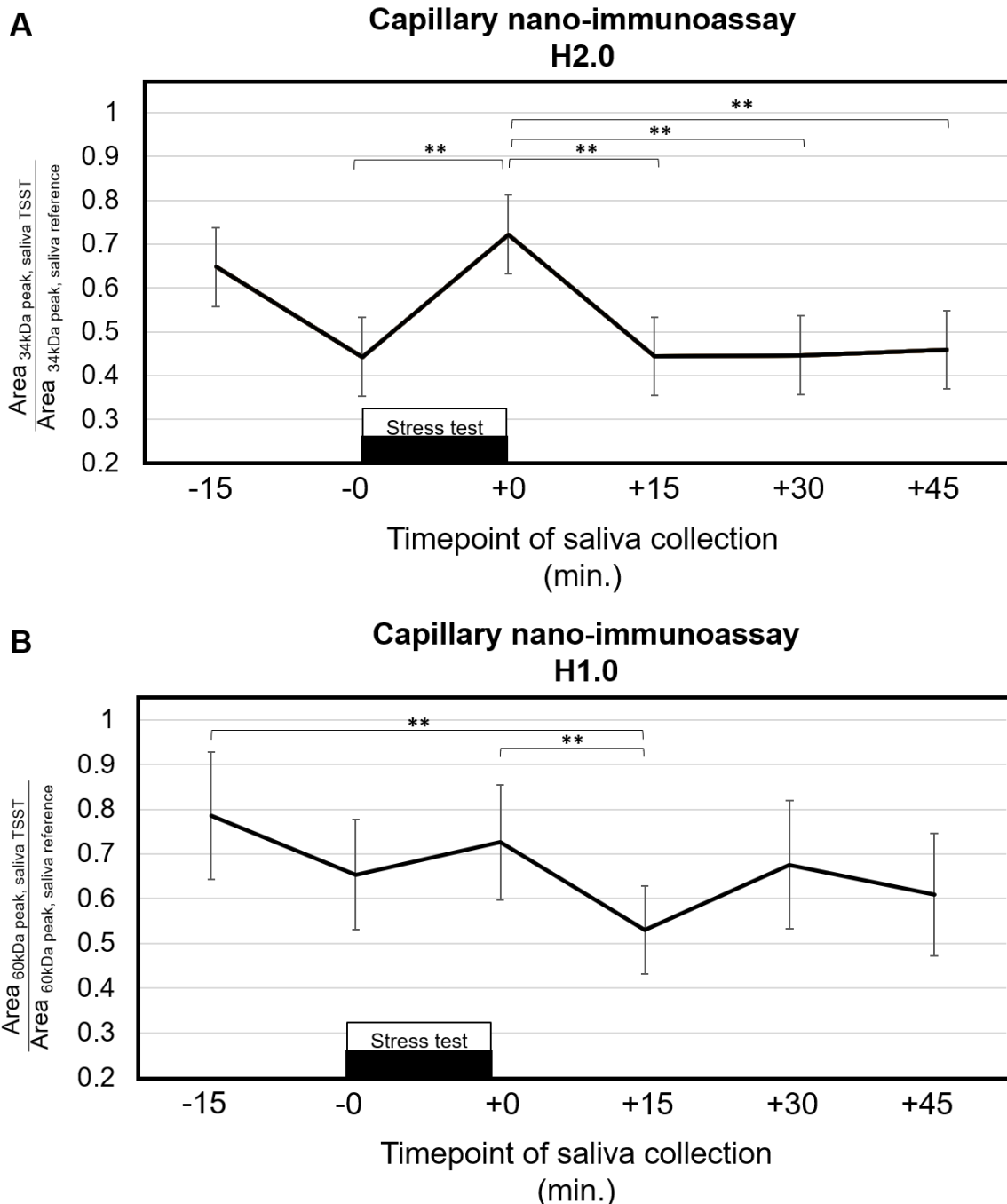
Figure 3-3. Capillary nano-immunoassay replicates Western blot readings as observed when replicating the TSST saliva analyses with hCABS1 antibody H2.0.

Interestingly, in CNIA salivary hCABS1 variants detected with H1.0 show a different trend to forms detected with H2.0 in the same TSST saliva samples. Saliva samples from 16 volunteers subjected to the Trier Social Stress Test (TSST) collected at six timepoints were immunoprobed for hCABS1 using antibody H2.0 and assessed using CNIA or Western blot. In both, Western blot and CNIA, we observed a trend in increase of salivary hCABS1 levels when comparing levels just before stress induction (-0 min.) to just after stress (+0 min.). When using H2.0, both immunoprobing techniques showed that salivary hCABS1 levels descend to similar-to-pre-stress levels after 15 min. (A) All saliva samples rendered a 34 kDa peak of chemiluminescent signal. The area under each peak was normalized to that of a homolog peak in a reference saliva sample. Differences were observed when comparing time points relative to measurement immediately after stress test (+0 min.). (B) Using hCABS1 antibody H1.0 every saliva sample rendered a 60 kDa peak of chemiluminescent signal. The area under each peak was normalized to that of a homolog peak in a reference saliva sample. These 60 kDa forms show no association to stress. Nevertheless, differences were observed when comparing time points relative to 15 min. post-stress. ***P<0.01*

throughput. Because our antibodies were custom made and their stock was limited and our sample volumes were low, we became interested in approaches that could identify the differently sized hCABS1 variants, while having the added value of using relatively small volumes of both antibodies and samples. This would allow further characterization of their association with clinical endpoints. We investigated the use of Wes™ to identify the various variants of hCABS1. To compare both immunoprobing techniques, we used saliva samples from a stress cohort. Wes™ replicated our previous observations in Western blot with H2.0 antibody.

Selection of positive and negative control samples was important to confirm specificity in Wes™. We used an overexpression HEK293T-based cell lysate as our control and optimized Wes™ by performing titrations; i.e., using a combination of different amounts of total antigenic protein and different antibody concentrations. We observed that in Wes™ the optimum total protein concentration per capillary in our control cell lysates was 10 µg/mL. In contrast to previous reports, where HEK293 cell lysates were assessed by Wes™ at a concentration of 200 µg/mL[131], we attained better peak resolution by diluting the cell lysate further. Once optimized, we observed that both hCABS1 antibodies detected a major peak at 94 kDa and a minor peak at 65 kDa in rhCABS1 OEL (**Figure 3-1** A, B). By contrast, in Western blot analyses of rhCABS1, H1.0 detected two bands at 83 and 66 kDa, and H2.0 also detected those bands in addition to three other bands at at 53, 31, and 21 kDa (data not shown). The differences in protein sizes between Western blot and Wes™ platforms likely involve the use of different separation matrices in the two methods. Western blot utilizes polyacrylamide and Wes™ uses benzophenone. ProteinSimple, the parent company of our CNIA platform, has established that the estimated sizes of proteins in the Wes platform differ by up to 20% from those estimated using Western Blot[132].

In contrast to cell lysates, saliva sample analyses in Wes™ required higher protein concentrations (e.g. 500 µg/mL) to give a signal. This aligns with previous observations, where the same saliva sample concentration was used to assess Nerve Growth Factor and Calcitonin gene-related

peptide in CNIA[133]. When compared to saliva analysis in Western blot, in which we loaded samples at a concentration of 625 µg/mL ($25µg/40µL_{well}$[21]), in Wes™ we loaded samples at a lower concentration (500µg/mL). However, in CNIA we obtained optimum results with higher antibody concentrations than those used in Western blot. For instance, saliva analyses in Western blot using H2.0 required us to dilute the antibody to 3 µg/mL, while Wes™ saliva analyses required 6 µg/mL. Nevertheless, in Wes™ the overall volume of antibody stock needed to attain the concentration to assess all samples was 16.5 times less than that needed to assess the same number of samples in Western blot.

During optimization of Wes™ protocol for saliva, we modified the running parameters to obtain an improved signal for our stress samples (**Table 3-1**). Once optimized, H1.0 detected a single peak at 60 kDa and H2.0 detected a peak at 34 kDa (**Figure 3-1** E, F). In some TSST samples, additional smaller peaks at 18, 58, 65, and 114 kDa were detected (**Figure 3-2** B). In contrast, Western blot analyses of saliva using H1.0 detected a band at 54 kDa (data not shown), while H2.0 detected bands at 102, 51, 33, 27, 18, 15, and 12 kDa[21].

We were particularly interested in the effect of psychological stress in salivary hCABS1 because previously, using Western blot (H2.0 antibody), we reported a strong association between the expression of a 27 kDa form of salivary hCABS1 and distress[21]. Our results in Wes using H2.0 antibody validated our previous studies in Western blot of increases of hCABS1 in saliva after exposure to stress in samples from a TSST cohort. This trait was observed in the 34 kDa peak in Wes™ which shows the same pattern as the 27 kDa band in Western blot (**Figure 3-3** A; see [21], Fig. 3). In our past study, we also observed an apparent link between resilience to stress and conspicuous 18 and 12 kDa bands of hCABS1 in saliva[21]. In Wes™, after optimizing the running protocol, we noticed that in 31% of the TSST samples an 18 kDa small peak was detected (**Figure 3-2** B). Fifteen of the 18 kDa Wes™-detected samples also showed in Western blot the occurrence of the 18 and 12 kDa hCABS1 forms linked to resilience to stress. While the Wes™ software appears

to detect the signal of a possible resilience-associated form of hCABS1 in saliva, the signal is small and dwarfed by the 34 kDa prominent peak detected by H2.0 in the Wes™ platform (**Figure 3-2 B**). In that respect, Western blot seems to detect these stress resilience-associated variants of hCABS1 more obviously. In contrast to H2.0, Wes™ results of TSST saliva analyses with H1.0 did not show a significant association between levels of hCABS1 and exposure to stress (**Figure 3-3 B**). Antibody H1.0 was not used to study TSST in Western blot.

Interestingly, Wes™ analyses of rhCABS1 OEL and saliva showed peaks corresponding to hCABS1 proteins of different sizes. We observed a similar pattern in Western blot[18,21]. hCABS1 has a predicted molecular weight of 43 kDa and Western blot analyses of rhCABS1 OEL detect its major form at almost twice this estimate, 83 kDa (data not shown). rhCABS1 OEL comes from an artificial expression system meant to overexpress the recombinant protein and be used as a positive control. Nevertheless, our observations align with the higher-than-predicted molecular weight of CABS1 in other species[5,21]. Studies of CABS1 in rat provided evidence that it is an Intrinsically Disordered Protein (IDP)[1]. IDPs have, among other traits, a large proportion of charged acidic amino acids, which may affect the migration pattern of the protein in a reducing environment [1], such as the environment in SDS-PAGE and Wes™. As a comparison, e-cadherin, a known IDP whose predicted molecular weight is 100 kDa, has been observed at 110 kDa in Western blot and 166 kDa in Wes™ when immunoprobing A549 human lung cells[134]. Another trait of IDPs is their hypersensitivity to protease degradation[1]. We speculate that hCABS1 undergoes proteolytic maturation, which may explain why we see different-sized variants of the protein in saliva, as well as in human submandibular gland lysates, lung, and testes[18,21]. We hypothesize that these hCABS1-derived polypeptides have different functions, such as an anti-inflammatory role[18], and a role associated with distress[21], reinforcing the need for further studies of hCABS1.

Availability of techniques with high sensitivity and specificity is paramount to explore novel candidate molecules and their associations with human traits. Thus far, we have successfully

characterized our antibodies to hCABS1 in Wes™, providing a high throughput immunoprobing platform that is conservative of our antibody stock and sample volumes. Wes™ can be used to study diverse cohorts to properly assess the protein of interest in a fast turnaround time. One must be mindful, however, of the cost involved in optimization of protocols. Once optimization is completed, the high number of samples that can be assessed in a short period of time (e.g., 72 samples/day in Wes™), plus the specificity of the platform make it a suitable method for clinical biomarker validation. Association between validated molecular biomarkers and clinically relevant outcomes is important for developing novel diagnostic tests to be used by health workers in the front line and ultimately improve human quality of life.

Acknowledgements

Supplemental information (Chapter III)

CNIA analyses of OEL and NCL using pAbs to hCABS1 H1.0, H2.0, H2.1, and H2.2 show the same chemiluminescent profile. Our data indicates that under optimized conditions (**Figure 3-4**, red lines in all graphs) all pAbs detect in OEL a peak corresponding to a protein of 96 kDa, and a smaller peak corresponding to a protein of 65 kDa. When evaluating NCL with H1.0 or H2.0 we obtained no chemiluminescent signal, indicating that in this platform under optimum conditions our pAbs do not interact with the proteins present in NCL (**Figure 3-4** A, B, NCL). When evaluating NCL with H2.1 the data indicates that proteins present in NCL may interact with H2.1, yet the chemiluminescent signal attained in NCL is minor than the signal obtained in OEL (**Figure 3-4** C). When evaluating NCL using H2.2 under optimized conditions (red line) we detected one peak corresponding to a protein of 51 kDa; however, the chemiluminescent signal of such a protein is much lower than that obtained when evaluating OEL with H2.2 (**Figure 3-4** D).
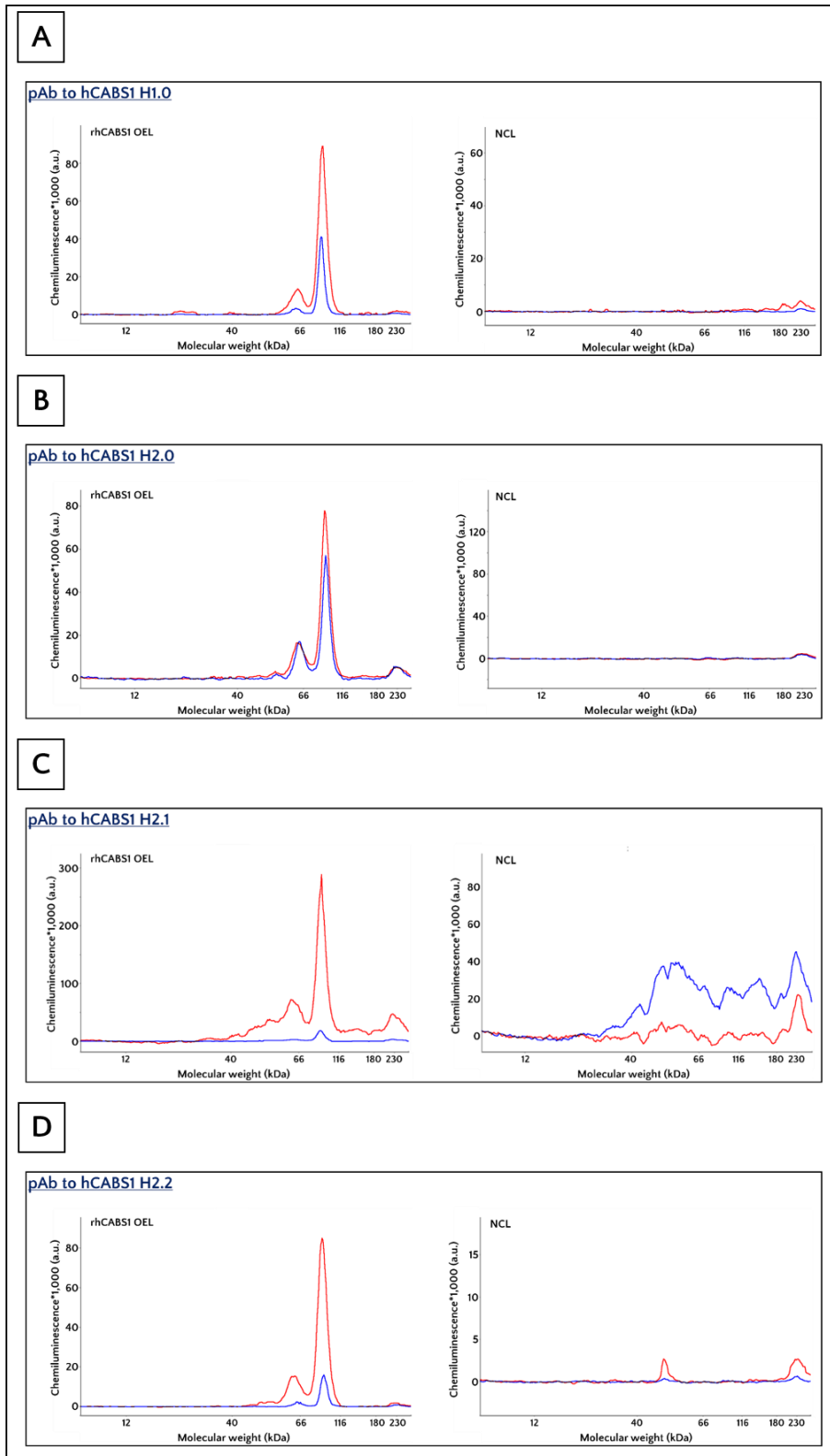
Figure 3-4. Electrophoretograms of ᵣhCABS1 overexpression cell lysate (OEL) and negative control cell lysate (NCL) evaluated with pAbs to hCABS1 (A) H1.0, (B) H2.0, (C) H2.1, and (D) H2.2.

All graphs indicate molecular weight (kDa) in the horizontal axis and chemiluminescent signal (a.u.) in the vertical axis. Blue lines represent experiments ran under non-optimized conditions, while red lines represent experiments ran under optimized conditions.

Chapter 4 : Characterization of monoclonal antibodies targeting human calcium-binding protein, spermatid-associated 1

Preamble

Our experimental and *in silico* data suggest that hCABS1 is proteolytically processed into discrete forms[18,21]. We developed two polyclonal antibodies (pAbs) to hCABS1, H1.0 and H2.0. 'H2.0', a pAb raised to a middle domain in hCABS1 (a.a.: $_{184}$DEADMSNYNSSIKS$_{197}$)[18], detects a protein in human saliva supernatant that positively correlates with perceived distress[21]. In WB (WB) this protein has an apparent molecular weight of 27 kDa[21], and when analyzed using capillary nano-immunoassay (CNIA), of 35 kDa[66]. Interestingly, only in Western blot (WB) of saliva supernatant does H2.0 detect proteins <27 kDa that may be indicative of resilience to stress[21]. To date, a biomarker of resilience to stress has not been discovered, but our data suggests that forms of hCABS1 could be such a biomarker.

We had also established that hCABS1 contains an anti-inflammatory domain, TDIFELL, similar to the one in rat SMR1, TDIFEGG[37,43,51,135]. To study this domain in hCABS1, we created 'H1.0', a pAb raised to a 14 amino acid hCABS1 sequence found at the carboxyl terminus of the protein that encompasses the anti-inflammatory site (a.a.: $_{375}$TSTTE<u>TDIFELL</u>KE$_{388}$, underlined anti-inflammatory domain)[18]. In CNIA of human saliva supernatant, H1.0 detects a protein at an apparent molecular weight of 60 kDa[66]. Using H1.0 to detect hCABS1 or its fragments, we were unable to establish a correlation with perceived distress[66].

Collectively, these interesting observations in saliva using two pAbs targeting different regions of hCABS1, the realization of the finite nature of our pAbs, and increasing concerns about their specificity due to an inability to sequence hCABS1 from saliva, led us to the creation of monoclonal antibodies (mAb) to hCABS1.

The creation of these mAbs was contracted to GenScript, the company that created our pAbs to hCABS1. The company also synthesized a peptide library for hCABS1 for us. This library encompassed 20-mer sections of hCABS1 (**Table 4-1**). Thus, to more fully characterize hCABS1 and its multiple molecular forms, we selected three immunogens for the production of mAbs, namely: the stress-associated immunogen located in the middle of hCABS1 (**Figure 4-1**, **M**iddle), the anti-inflammatory immunogen located in the carboxyl terminus of hCABS1 (**Figure 4-1**, **C**OOH - carboxyl terminal), and the entire recombinant ($_r$) hCABS1. Further ELISA analyses done by our collaborator in the United States, Gonshor-Buck diagnostics (GBD), using the hCABS1 peptide library (**Table 4-1**) suggests that the mAb created using full $_r$hCABS1 targets hCABS1 a.a. $_{41}$ITSEGDHVTSVNEYMLESDF$_{60}$ domain (GBD proprietary data not provided), close to the amino terminus (**Figure 4-1**, **N**H$_2$ - amino terminal).
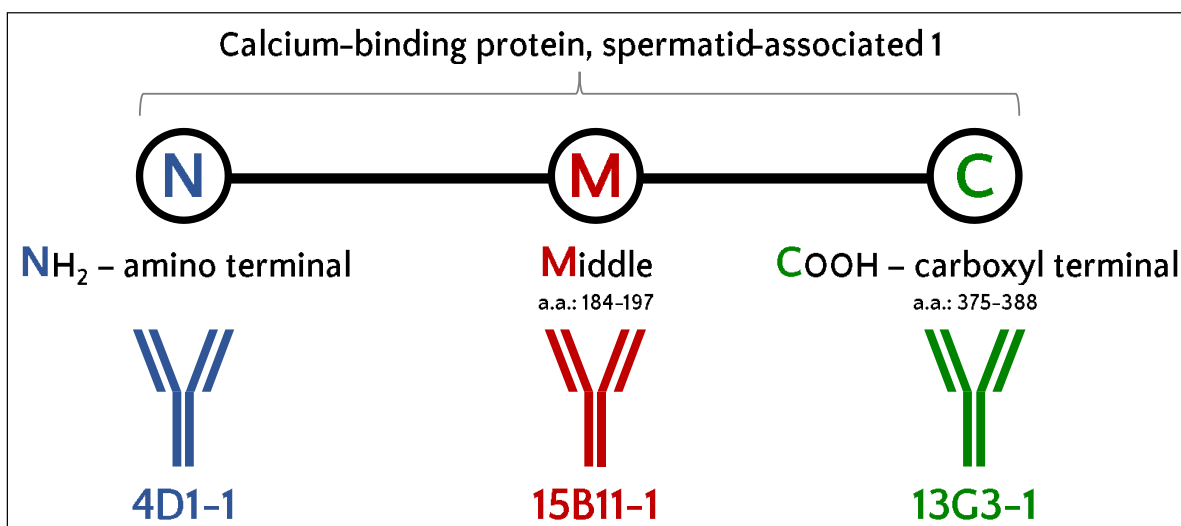
Figure 4-1. Immunogens used to produce monoclonal antibodies to Calcium-binding protein, spermatid-associated 1 (CABS1).

Antibody 15B11-1 was raised against a middle domain of CABS1 (amino acids (a.a.) 184-197) that was previously used to produce a polyclonal antibody that detected Western blot bands associated with psychosocial distress. Antibody 13G3-1 was raised to a domain containing a.a. sequence $_{380}$TDIFELL$_{386}$, a putative anti-inflammatory domain of CABS1. Antibody 4D1-1 was raised against the entire recombinant CABS1 protein. Further evaluation using ELISA indicates that 4D1-1 targets a domain (a.a. 41-60) near the amino terminal.

GenScript used the three immunogens (**Figure 4-1**) to inoculate five BALB/c mice per immunogen and begin mAb production. During mAb production, GenScript performed their own quality control assays; however, at two points we analyzed samples of the antibodies provided by

GenScript to confirm that appropriate immunoreactivities were being selected (**Figure 4-2** A, B). Briefly, after the third inoculation to BALB/c, antisera from all mice were collected and sent to our group at the University of Alberta (U of A) and to our collaborator, Gonshor-Buck Diagnostics (GBD). At the U of A, we performed WB using a reference saliva sample, an overexpression cell lysate for hCABS1, and its negative control cell lysate. GBD developed an in-house ELISA assay to evaluate the immunoreactivity of antisera using the peptide library of hCABS1. Data analysis from U of A and GBD aided in the selection of a single mouse per immunogen, i.e., 3 mice, to continue mAb production. When GenScript derived 10 hybridomas from each mouse spleen, these were cultured, and supernatants (n=30, 10 per immunogen) were sent to the U of A and GBD for analysis. These analyses led to the selection of five clones per immunogen for further development and one clone for each immunogen was selected for amplification and purification of mAbs 15B11-1, 13G3-1 and 4D1-1 (**Figure 4-1**). GenScript provided us with purified mAbs from selected clones and with cell lines from 30 clones (5 clones x 2 duplicates x 3 immunogens = 30 clones). Presently, these samples are stored at the Canadian Biosample Repository (Edmonton, Alberta, Canada)[136].

The acquisition of these mAbs, each targeting a different domain within hCABS1, assisted us in validating our work using pAbs. I established an optimized WB methodology to evaluate human-derived samples, the data of which is shown in this chapter. Of note, number of experiments (n) is indicated in figure captions. During the duration of these experiments, I had the opportunity to mentor Ms. Tarana A. Mangukia, who ultimately immunoprecipitated $_r$hCABS1 from a transient hCABS1 overexpression cell lysate. Her data has opened a new line of research for hCABS1, that is IP of hCABS1 from human-derived biofluids. Additionally, collaboration with Dr. Lakshmi Puttagunta from the Department of Laboratory Medicine and Pathology at the University of Alberta and Ms. Sarah Canil from Alberta Precision Laboratories generated the first immunohistochemical analysis image of human testis using mAb 15B11-1.

Table 4-1. Peptide library of hCABS1.

Eighteen protein segments, each 20 amino acids long, were synthesized and sent to GBD to assist in their in-house ELISA tests.

hCABS1 protein segment (# a.a.)	Mass (mg)	Purity (%)	Observations	hCABS1 sequence	Solvent	Concentration Mass / $V_{solvent}$ (mg/mL)	pH	hCABS1 protein segment (# a.a.)
1 - 20	4.6	91.1	Resuspended in 1.0 mL of solvent	MAEDGLPKIYSHPPTESSKT	H$_2$O	4.6	5.0	1 - 20
21 - 40	4.1	98.8	Resuspended in 1.0 mL of solvent	PTAATIFFGADNAIPKSETT	DMSO	4.1	7.0	21 - 40
41 - 60	4.9	87.1	Resuspended in 1.0 mL of solvent	ITSEGDHVTSVNEYMLESDF	DMSO	4.9	7.0	41 - 60
61 - 80	4.1	94.2	Resuspended in 1.0 mL of solvent	STTTDNKLTAKKEKLKSEDD	H$_2$O	4.1	5.0	61 - 80
81 - 100	4.0	89.5	Resuspended in 1.0 mL of solvent	MGTDFIKSTTHLQKEITSLT	DMSO	4.0	7.0	81 - 100
101 - 120	4.9	94.2	Resuspended in 1.0 mL of solvent	GTTNSITRDSITEHFMPVKI	H$_2$O	4.9	5.0	101 - 120
121 - 140	4.9	88.6	Resuspended in 1.0 mL of solvent	GNISSPVTTVSLIDFSTDIA	DMSO	4.9	7.0	121 - 140
141 - 160	4.5	86.5	Resuspended in 1.0 mL of solvent	KEDILLATIDTGDAEISITS	DMSO	4.5	7.0	141 - 160
161 - 180	4.5	88.8	Resuspended in 1.0 mL of solvent	EVSGTLKDSSAGVADAPAFP	H$_2$O	4.5	5.0	161 - 180
181 - 200	4.7	96	Resuspended in 1.4 mL of solvent	RKKDEADMSNYNSSIKSNVP	H$_2$O	3.4	5.0	181 - 200
201 - 220	4.6	96.5	Resuspended in 1.0 mL of solvent	ADEAVQVTDSTIPEAEIPPA	3% ammonia water	4.6	9.5	201 - 220
221 - 240	4.8	85.7	Resuspended in 1.0 mL of solvent	PEESFTTIPDITALEEEKIT	DMSO	4.8	7.0	221 - 240
240 - 260	20.0	Crude	Resuspended in 1.6 mL of solvent	TEIDLSVLEDDTSAVATLTDS	H$_2$O	12.5	5.0	240 - 260
261 - 280	4.5	86.5	Resuspended in 1.4 mL of solvent	DEKFITVFELTTSAEKDKDK	H$_2$O	3.2	5.0	261 - 280
281 - 300	4.1	90.2	Resuspended in 1.0 mL of solvent	REDTLLTDEETTEGASIWME	DMSO	4.1	7.0	281 - 300
301 - 320	4.0	99.3	Resuspended in 1.4 mL of solvent	RDTANEAETHSVLLTAVESR	H$_2$O	2.9	5.0	301 - 320
320 - 340	4.9	93.3	Resuspended in 1.0 mL of solvent	RYDFVVPASIATNLVEESSTE	H$_2$O	4.9	5.5	320 - 340
340 - 360	4.9	94.8	Resuspended in 1.0 mL of solvent	EEDLSETDNTETVPKITEPFS	H$_2$O	4.9	5.0	340 - 360
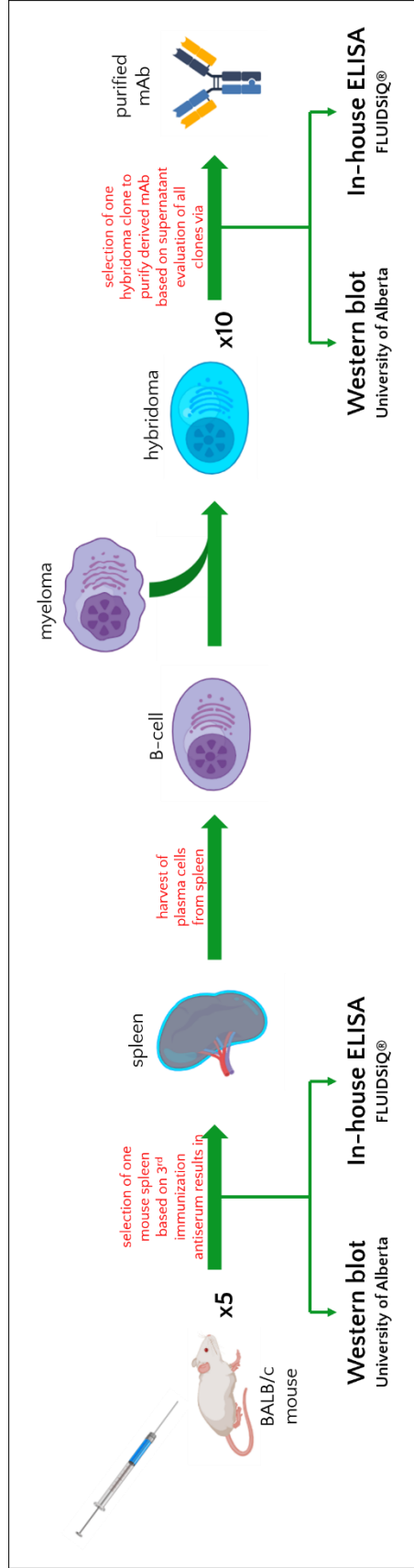
Figure 4-2. Pipeline followed to produce mAbs to hCABS1.

Five BALB/c mice per immunogen described in **Figure 4-1** were used to produce antiserum. After the third inoculation, antiserum was sent to the University of Alberta (U of A) and GBD for in-house tests. A collective decision led to the selection of one mouse spleen per immunogen. Limiting dilution was used to isolate single plasma cells from each spleen. Each plasma cell was expanded and fused with a myeloma. Selective media was used to isolate hybridomas (10 independent per immunogen, each a parental clone). Each parental clone was expanded, and supernatant was sent to the U of A and GBD for in-house tests. Data analysis led to the selection of a single parental clone per immunogen to be used to produce and purify mAbs. *Graphics were retrieved from BioRender.com*
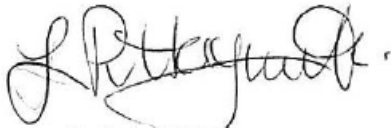
To whom it may concern,

We fully support that this chapter of Eduardo's PhD thesis contains an image from immunohistochemical analysis of human testis performed in the Alberta Precision Laboratories (Edmonton, AB, Canada) by Ms. Sarah Canil. The monoclonal antibody targeting human Calcium-binding protein, spermatid-associated 1 (antibody ID: 15B11-1) used in this experiment was provided by Dr. Dean Befus from the University of Alberta (Edmonton, AB, CA).

Interpretation of immunohistochemical results was a collective effort including Dr. Lakshmi Puttagunta, Ms. Canil, Dr. Befus, Dr. Marcelo Marcet-Palacios, and Mr. Reyes-Serratos.

Respectfully yours,

Lakshmi Puttagunta
Professor at the Department of Laboratory Medicine &
Pathology
University of Alberta
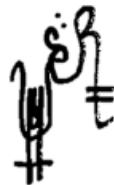
Sarah Canil
Laboratory Scientist
Alberta Precision Laboratories

Marcelo Marcet-Palacios
Assistant Adjunct Professor
Department of Medicine
Division of Endocrinology and Metabolism
University of Alberta

A. Dean Befus
Professor Emeritus
Alberta Respiratory Centre
University of Alberta

Eduardo Reyes-Serratos
PhD Candidate
Alberta Respiratory Centre
University of Alberta

To whom it may concern,

We fully support that this chapter of Eduardo's PhD thesis contains Western blot images from immunoprecipitation (IP) experiments of human Calcium-binding protein, spermatid-associated 1 overexpression cell lysate and human saliva supernatant.

The experiments were performed at the Heritage Medical Research Centre (Edmonton, AB, Canada) by Ms. Tarana A. Mangukia, who was initially trained by Mr. Eduardo Reyes-Serratos and quickly showed proficiency in performing wet lab experiments. Ms. Mangukia performed immunoprecipitation experiments with minimal input from Mr. Reyes-Serratos. Resulting eluates from IP experiments were analyzed via Western blot.

Interpretation of Western blot results was a collective effort between Ms. Mangukia and Mr. Reyes-Serratos.

Respectfully yours,

Tarana A. Mangukia
Honors undergraduate student
Faculty of Chemistry
University of Alberta

Eduardo Reyes-Serratos
PhD Candidate
Alberta Respiratory Centre
University of Alberta

Marcelo Marcet-Palacios
Assistant Adjunct Professor
Department of Medicine
Division of Endocrinology and Metabolism
University of Alberta

A. Dean Befus
Professor Emeritus
Alberta Respiratory Centre
University of Alberta

Introduction

External body of knowledge of CABS1 ties its occurrence to the male urogenital tract, but novel research challenges this dogma

Studies of CABS1 in rats, mice and pigs identified its presence at specific developmental stages during spermiogenesis, the transformation of spermatids into spermatozoa[1,4,5]. Moreover, RNA analyses of several tissues indicated that CABS1 transcript was restricted to testes and the main olfactory epithelium[1]. However, protein was only detected in testes[1,4,5]. CABS1 was detected in the mitochondria, cytoplasm, and flagellum of sperm[1,5]. In porcine sperm, CABS1 protein was also found in the acrosome, where it may play a pivotal role in the acrosome reaction when spermatozoa and oocyte fuse[5]. The first functional association of CABS1 in mice was described in 2021. A *Cabs1* knockout mouse model identified sperm with a bent tail and disturbance in expression of cytoskeleton-related proteins[11]. CABS1 deficiency was associated with subfertility of mice[11]. Altogether, this evidence suggests that CABS1 plays an indispensable role in optimum formation and function of sperm. Interestingly, murine spermatids also expressed a long, non-coding RNA of the CABS1 gene antisense, but knockdown of this anti-CABS1 did not alter sperm development, morphology or function; its significance is unknown[11].

Outside male urogenital research, *Cabs1* gene expression has been reported in macaque uterus and cattle oviductal epithelium, suggesting an association between *Cabs1* expression and estrus[13,14]. In female humans, *CABS1* is detectable in minor salivary glands[16], consistent with our findings of mRNA and protein in male and female SMG[18]. Collectively, these observations likely led the Human Genome Organisation Gene Nomenclature Committee to correct the name for CABS1 in February of 2016, from calcium-binding protein, spermatid-**specific** 1 to calcium-binding protein, spermatid-**associated** 1.

An alternate line of research put forward the use of CABS1 as a biomarker of distress in humans

In the 1980's, our group became intrigued by evidence that immune and inflammatory responses are modulated by the nervous system[137–140]. To investigate this relationship, we established an experimental model in allergen-sensitized rats by severing the sympathetic nerve trunk upstream of the superior cervical ganglia (SCG), an intervention called decentralization[20,141]. Initial data showed that decentralization decreased lung inflammatory responses to allergen challenge in sensitized rats[20]. Ultimately, we identified that the anti-inflammatory activity was dependent on the submandibular glands (SMG) regulated by the nervous system through SCG[29,142]. A heptapeptide isolated from SMG, TDIFEGG, proved to be responsible for the anti-inflammatory activity[143]. This 7-mer is found near the carboxyl-terminus of a protein called Submandibular Rat 1 (SMR1)[143], which is more abundant in male than female SMG. Work by others identified that SMR1 is a prohormone and precursor of several polypeptides, one of which has analgesic[144], sexual behavior modulating[145], and erectile function[146]. We determined that humans lack SMR1[18,53] and searched for a human protein containing the anti-inflammatory heptapeptide sequence. We identified that Calcium-binding protein, spermatid-associated 1 (CABS1) contains a homologous peptide, TDIFELL, also near its carboxyl-terminus[18]. The genes human CABS1 and rat SMR1 are located within a conserved gene cluster. Because TDIFE-GG/LL is found both in CABS1 and in SMR1, we hypothesize that an evolutionary gene translocation moved the anti-inflammatory fragment from SMR1 to primate CABS1[18,51,147].

SMR1 in rats is expressed in SMG, saliva and testes [53]. Until 2015, CABS1 had only been characterized in testes, so given that CABS1 was analog to SMR1 we postulated that human CABS1 was also present in SMG and saliva. Indeed, we confirmed that lysates of human SMG expressed CABS1 mRNA and protein[18]. Both female and male SMG lysates expressed protein at similar levels, suggesting sex-independent expression[18]. Notably, using polyclonal antibodies (pAbs)

targeting hCABS1, saliva and SMG lysates showed several forms of CABS1 that varied in kilodaltons (kDa)[18,21], similar to a diversity of processed forms of SMR1[53].

To determine if human CABS1 was under neural control as SMR1 in the rat, we used our pAbs to evaluate levels of CABS1 in saliva following psychological stress via WB analysis. As expected, our pAbs detected increased levels of a 27 kDa form after stress challenge and positively correlated to perceived momentary distress[21]. Remarkably, samples from a small portion of individuals who self-reported not feeling affected by the stressor had CABS1 forms <27 kDa in saliva suggesting that these forms were associated with resilience to stress[21]. Thus, we concluded that CABS1 is under control of the autonomic nervous system, which is promptly activated in psychological distress. Recent studies using our pAbs in a state-of-the-art immunoassay corroborated that CABS1 in saliva positively correlates with distress, although this immunoassay did not detect forms of CABS1 <27 kDa[66].

Since our research at that time point suggested that different molecular weight variants of hCABS1 were biomarkers of stress, WB was deemed the ideal technique to study hCABS1 in complex biofluids. In short, prior to WB protein homogenates are linearized and separated by size, followed by the use of antibodies that target and identify the location of a protein of interest (POI), in our case hCABS1. **Table 2-4** presented the WB profiles that our pAbs generate in a transient overexpression cell lysate system, human SMG, saliva, and serum. Questioning of the WB methodology used in previous publications from our group (see references [18,21]) led to an optimized pipeline. In turn, the bands identified in WB by our pAbs, which were considered to represent hCABS1, have been revised. Briefly, when using our pAbs, we now consider bands representative of hCABS1 to be as follows (per sample): in hCABS1 overexpression cell lysate (OEL) bands at 84 and 67 kDa, in SMG bands at 71, 52, 47, 33, and 27 kDa, in saliva bands at 90 and 64 kDa, and in serum bands at 139, 91, 71 and 63 kDa (see **Table 2-4**).

In early 2020, we received monoclonal antibodies (mAbs) that target three different domains of hCABS1 (**Figure 4-1**), diversifying our research toolkit. In contrast to pAbs, hybridoma-based mAbs are identical copies of a single antibody that binds to a single epitope[148]. This chapter describes the characterization of our novel mAbs targeting hCABS1 in WB analyses of transient overexpression cell lysates, human SMG, saliva and serum. Altogether, these data contribute to the way we should interpret WB profiles using our antibodies, and which band(s) we should consider to accurately represent hCABS1 in our WB system. The chapter also details the WB profile obtained throughout immunoprecipitation of hCABS1 from transient overexpression cell lysate and human saliva, and confirms that immunoprecipitation with mAb 4D1-1, targeting a domain close to the amino terminus, is possible. Finally, we provide the first immunohistochemical image of human testes, and describe the localization of hCABS1 protein in this compartment.

Materials and methods

The study, entitled 'Anti-inflammatory proteins and biomarkers of stress' (University of Alberta internal ID: Pro00001790), was approved by the Research Ethics Office, University of Alberta (Edmonton, AB, CA).

Monoclonal antibodies to hCABS1

Mouse-derived hybridomas produced the monoclonal antibodies described in this manuscript. Mice were immunized against specific domains of hCABS1, their spleens were harvested and spleen-derived B-cells were isolated via serial dilutions. B-cells were combined with myelomas to create hybridomas (GenScript Biotech, Piscataway, NJ, USA). Monoclonal antibody 13G3-1 was raised against hCABS1 amino acids (aa) 375-388 TSTTE<u>TDIFELL</u>KE (underlined anti-inflammatory domain). Monoclonal antibody 15B11-1 was raised against hCABS1 aa 184-197 DEADMSNYNSSIKS. Monoclonal antibody 4D1-1 was raised against the entire recombinant hCABS1 protein.

Western blot controls

For WB controls, membranes were probed with either (a) no primary antibody, just secondary goat anti-mouse antibodies (Li-cor, Lincoln, NE, USA – cat. # 926-32210) or (b) isotype antibodies to our mAbs. Mouse IgG1.κ (R&D systems, Minneapolis, MN, USA – cat. # MAB002) are isotype antibodies for mAbs 15B11-1 and 13G3-1. Mouse IgG2α.κ (Stemcell™ Technologies, Vancouver, BC, Canada – cat. # 60108) are isotype antibodies for mAb 4D1-1.

Transient overexpression cell lysate controls

Commercial source

A recombinant hCABS1 (rhCABS1) overexpression cell lysate (OEL) produced in Human Embryonic Kidney 293T (HEK293T) cells (OriGene Technologies Inc., Rockville, MD, USA – cat. # LY409727) was purchased and used in most WB described in this chapter. HEK293T was immortalized using SV40 large T antigen[73]. It is widely used to produce recombinant proteins by transfection of vectors containing potent viral promoters (e.g., CMV promoter) (**Figure 2-1**). The negative control cell lysate (NCL) originates from HEK293T cells with the same vector but lacking a CABS1 cDNA insert.

In-house source

Plasmid amplification and retrieval

To produce rhCABS1 containing a **Myc**-DDK tag (sequence: **EQKLISEEDL**AANDILDYKDDDDK) at the carboxyl end of the recombinant protein (see **Figure 2-1**), 10 µg of TrueORF rhCABS1 plasmid (OriGene Technologies Inc., Rockville, MD, USA – cat. # RC208496) was purchased. Once received, the dried plasmid was resuspended in 100 µL of Ultrapure™ DNase/RNase-free distilled water (Invitrogen, Waltham, MA, USA – cat. # 10977015). To amplify the plasmid, Subcloning Efficiency™ DH5α competent cells (Invitrogen™, Waltham, MA, USA – cat. # 18265017) were transformed with the reconstituted plasmid. Briefly, 500µg plasmid was used with a molar plasmid-to-DH5α cells ratio of 1:10, the mix was placed on

ice for 20 minutes, heat shocked at 37°C for 20 seconds, and placed on ice for 2 minutes. DH5α cells were transferred to LB broth (Sigma-Aldrich, Burlington, MA, USA – cat. # L3522) and incubated for 1 hour. After incubation, cells were plated in LB agar (Sigma-Aldrich, Burlington, MA, USA – cat. # L3147) supplemented with 25 $^{\mu g}/_{mL}$ kanamycin (Gibco™, Waltham, MA, USA – cat. # 15160054) and incubated overnight at 37°C. The next day, single colonies were selected, resuspended in LB broth supplemented with 25 $^{\mu g}/_{mL}$ kanamycin and incubated overnight.

The amplified plasmid was obtained from DH5α transformed cells using a QIAprep® Spin Miniprep kit (QIAGEN, Hilden, NRW, Germany – cat. # 27104) as per the manufacturers protocol. The concentration and purity of plasmid was determined using a NanoVue spectrophotometer (GE Healthcare, Chicago, IL, USA). Subsequently, the plasmid was placed at -80°C.

HEK293T transfection with plasmid

HEK293T cells were cultured in Dulbecco's Modified Eagle Medium (DMEM), high glucose, pyruvate (Gibco™, Waltham, MA, USA, cat. # 11995065), supplemented with 11% fetal bovine serum (FBS) and 1.1% penicillin/streptomycin. For transfection, cells were cultured in a Petri dish until ~80% confluency media was attained. Media was changed to DMEM, high glucose, pyruvate, supplemented with 1.1% penicillin/streptomycin (no FBS). To mediate the transfection in HEK293T cells, polyethyleneimine (PEI) was used (Polysciences, Inc. Warrington, PA, USA – cat. # 23966-1). 3μg of plasmid were used with a molar plasmid-to-PEI ratio of 1:3. The mix was incubated at room temperature for 30 minutes, then added in a dropwise manner to the HEK293T cells. Cells were incubated overnight (37°C and 5% CO_2) and lysed the next day (see below).

Cell lysis

After cells reached 70-80% confluence, media was removed, and cold 1X PBS solution was added to the attached cells. The dish containing cells was tilted continuously for 2 minutes before removing the PBS solution. 0.5 mL cold 1X PBS solution was added before scraping, aspirating, and transferring cells into a microfuge tube. The Petri dish was washed once again with 1 mL of

cold 1X PBS solution, the surface was scraped to retrieve remaining attached cells, and the solution was transferred to the same microfuge tube. The tube was centrifuged (2,500 rcf, 5 min., 4⁰C), the supernatant discarded, and the pellet kept. The pellet was resuspended in 1 mL of Radio Immunoprecipitation Assay (RIPA) buffer (Tris-HCl (pH 7.4) – 50 mM, NaCl – 150 mM, EDTA – 1 mM, 1% NP40, 0.25% sodium deoxycholate) supplemented with P8340 protease inhibitor cocktail (Sigma-Aldrich, St. Louis, MO, USA – cat. # P8340). The tube containing the resulting cell suspension was placed on ice and lysed using two sonication pulses (30 $^{seconds}/_{pulse}$). Subsequently, the tube on ice was placed in an orbital shaker (100 rpm, 15 min.) followed by a centrifugation cycle (14,000 rcf, 15 min, 4⁰C). The resulting supernatant, now identified as $_r$hCABS1 OEL, was transferred to a new microfuge tube and stored at -80⁰C. Protein concentration was determined using a Pierce™ BCA assay protein assay kit (Thermo Scientific™, Waltham, MA, USA – cat. # 23225).

Collection of human samples

Submandibular gland

Human submandibular glands (SMG) samples were collected in January 2017 from patients, a female and a male, undergoing surgical removal of squamous carcinoma at the University of Alberta hospital (Edmonton, Canada). Each SMG was homogenized at 4⁰C using as diluent RIPA buffer supplemented with P8340 protease inhibitor cocktail. Post-homogenization, samples were centrifuged, separating the mix into three phases. The middle phase was collected, aliquoted and stored at -80⁰C. Prior to downstream analyses, determination of total protein concentration for each sample was done using a Pierce™ BCA Protein Assay Kit (Thermo Scientific).

Blood samples

Blood serum and plasma were retrieved from a 30-year-old male in March of 2019. Human serum and plasma were retrieved as described in a protocol from ProImmune Limited[74]. For serum, a vacutainer tube containing no additive was used to collect 10 mL of whole blood. Collected blood

was incubated for 45 min to allow clotting. Subsequently, the tube was centrifuged at 1500 x g and 21°C for 15 minutes. Supernatant (serum) was carefully aspirated, transferred into 300 μL aliquots (new micropipette tips were used between aspirations), and stored at -80°C until used. For plasma, a vacutainer tube containing anticoagulant was used to collect 10mL of whole blood. Then, the tube was inverted 10 times to mix blood with anticoagulant. Immediately after, the tube was centrifuged at 1500 x g and 21°C for 15 minutes. Supernatant (plasma) was carefully aspirated, transferred into 300 μL aliquots (new micropipette tips were used between aspirations), and stored at -80°C until used.

Saliva

Unstimulated whole saliva from a human male was collected using the passive drool technique protocol (Salimetrics LLC, Carlsbad, CA, USA)[75] over the course of 15 days. Throughout the collection period, the individual exercised for, at least, 1 hour in the evenings prior to collection, slept a minimum of 7.5 h, had a set breakfast, brushed and flossed teeth, and post-teeth cleansing waited 1.5 h before whole saliva collection. Samples were frozen at -20°C immediately after collection. When the collection period finalized, all collected samples were thawed and pooled. The resulting pool was centrifuged at 1500 rcf and 4°C for 20 minutes. The supernatant was collected and transferred into aliquots. Prior to downstream analyses, determination of total protein concentration for each sample was done using a Pierce™ BCA Protein Assay Kit (Thermo Scientific).

Serial dilutions/Titration of antibody and sample amounts

Total protein concentration for each stock/undiluted sample was determined using a Pierce BCA kit (Thermo Scientific). The sample diluent in all serial dilutions consisted of 1 part 4X Laemmli sample buffer (BioRad) and 3 parts RIPA buffer supplemented with P8340 protease inhibitor cocktail (Sigma Aldrich). Prior to combining both reagents, 4X Laemmli sample buffer was supplemented with DTT to a final concentration of 50 mM$_{DTT}$ (see **Figure 4-3**).

Prior to preparing the testing samples, final sample concentration (**Equation 4-1**) and volume (**Equation 4-2**) were calculated, and initial sample volume (**Equation 4-3**), as well as sample diluent volume (**Equation 4-4**) for all samples to be tested in the dilution (**Table 4-2**). To prepare testing samples, the sample diluent was added firstly to all tubes, then the necessary amount of undiluted/stock sample was added to reach the desired testing sample concentration ([Concentration $_{sample,\ final}$], **Figure 4-3**, 1). After gently pipetting up and down, the necessary volume of this sample was transferred to the subsequent tube to achieve a 1/10 dilution with respect to the initial testing sample (**Figure 4-3**, 2). After gently pipetting up and down, the calculated amount of this sample was transferred to the final tube to achieve a 1/100 dilution with respect to the initial testing sample (**Figure 4-3,** 3).

$$[\text{Concentration}_{sample,final}] = \frac{m_{desired}}{V_{well}}$$

Equation 4-1. Calculation of final sample concentration. To calculate the amount of protein per lane divide the desired mass (m, in micrograms) by the well's volume (V, in microliters). A 10-lane gel has a well volume of 40 μL, while a 15-lane gel has a well volume of 20 μL.

$$V_{sample,\ final} = (\#\ \text{wells}_{sample} + 1)(V_{well})$$

Equation 4-2. Calculation of final sample volume. To calculate the necessary sample volume, multiply the number of wells where this sample will be tested plus one (as excedent) by the well's volume (V, in microliters). A 10-lane gel has a well volume of 40 μL, while a 15-lane gel has a well volume of 20 μL.

$$V_{sample,\ initial} = \frac{[\text{Concentration}_{sample,\ final}](V_{sample,\ final})}{[\text{Concentration}_{sample,\ initial}]}$$

Equation 4-3. Calculation of initial sample volume. To calculate the volume of stock/undiluted sample, divide the product of final sample concentration (**Equation 4-1**) and final sample volume (**Equation 4-2**) by the sample's initial concentration, previously determined using a Pierce BCA assay. Recall using the same units for each term (in concentration: mg/mL or μg/μL).

$$V_{sample\ diluent} = V_{sample,\ final} - V_{sample,\ initial}$$

Equation 4-4. Calculation of sample diluent. To calculate the necessary amount of sample diluent, subtract the initial sample volume from the final sample volume. Recall using compatible units (μL or mL).
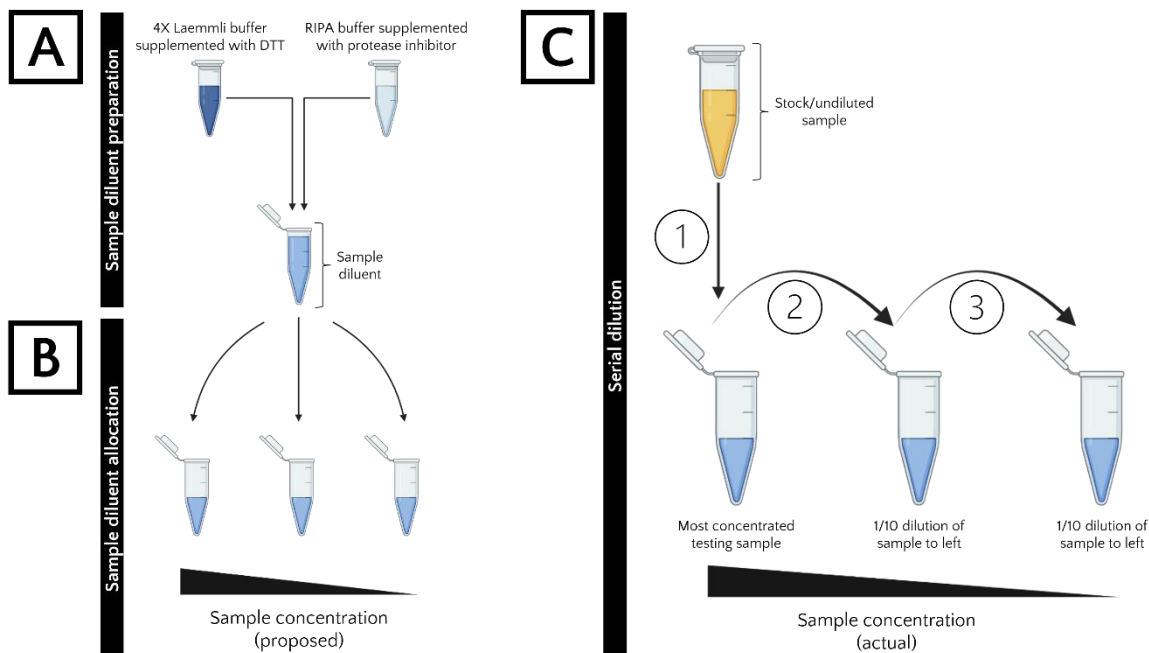
Figure 4-3. Pipeline of sample preparation in titration experiments.

(A) Sample diluent was prepared by mixing Laemmli and RIPA buffers. (B) The required volume of sample diluent was added to each of the tubes to be used in serial dilution. (C) Finally, the necessary amount of original/undiluted sample was used to do a 10-fold serial dilution. *Figure made with BioRender.com*

After serial dilutions were made, testing samples were boiled for 5 minutes, transferred to ice, centrifuged in a microfuge at 4000 rpm, vortexed in the lowest speed and loaded into their respective lane in the gel. Molecular mass reference (M_r), a molecular weight ladder was loaded in a well adjacent to the samples being tested. Ladders used in these experiments include were Precision Plus Protein All Blue Prestained protein standards (Bio-Rad) and BlueAQUA Prestained protein ladder (GeneDireX, Inc.).

One dimensional (1D) SDS-polyacrylamide gel electrophoresis (SDS-PAGE)

The TGX™ FastCast™ 12% Acrylamide Kit (Bio-Rad, Mississauga, ON, CA) was used to prepare 1.5 mm thick gels the day prior to an experiment[77]. Polymerization took 30 min. Polymerized gels were then wrapped in a Kimwipe, placed inside a Ziploc bag, submerged in molecular grade water, and placed at 4°C until the experiment.

Table 4-2. Proposed table to calculate amounts of sample and diluent in serial dilutions.

Numbers in black circles indicate the equation (and order of process) used to calculate the value in each cell. From top to bottom: Top non-shaded row is representative of the most concentrated sample, middle row is representative of a 1/10 dilution of the previous sample and bottom row is representative of a 1/10 dilution of the previous sample (1/100 of the most concentrated sample). Columns shaded in light blue contain the volumes that need to be added to their respective tube. Once calculations are made, firstly add the sample diluent to all tubes, then add the initial sample volume (coming from a sample that is more concentrated than the one you are preparing, see **Figure 4-3**).

	Sample preparation						
Sample ID	[Concentration] sample, final ($\mu g/\mu L$)	$v/_{well}$ (μL)	[Concentration] sample, initial ($\mu g/\mu L$)	V sample, final (μL)	V sample, initial (μL)	Sample ID	V sample diluent (μL)
Sample	① $\dfrac{m_{desired}}{V_{well}}$	$v/_{well}$	Determined using a Pierce BCA assay	② $(\text{\# wells}_{sample}+1)(V_{well})$	③ $\dfrac{[\text{Concentration}_{sample,final}](V_{sample,final})}{[\text{Concentration}_{sample,initial}]}$	Sample	④ $V_{sample,final}-V_{sample,initial}$
1/10 sample	① /10	$v/_{well}$	①	②	③	1/10 sample	④
1/100 sample	① /100	$v/_{well}$	① /10	②	③	1/100 sample	④

On the day of an experiment, new 1X SDS-PAGE running buffer was prepared from a 10X stock (1L 10X stock solution: Trizma base – 250 mM, Glycine – 1.92 M, SDS – 35 mM). During electrophoresis, samples were firstly run at 100 V until they reached the bottom of the stacking gel; once there, running voltage was increased to 125 V until sample buffer reached the bottom of the gel. Downstream procedures included gel staining with Blue Silver dye and subsequent MS-seq analyses, or WB (WB, described below).

rhCABS1 plasmid digestion and agarose gel electrophoresis

To verify that DH5α effectively amplified the rhCABS1 plasmid, a double digestion with restriction enzymes Bam HI and Xho I (Thermo Scientific, Waltham, MA, USA – cat. # ER0051 and ER0692, respectively) was performed. Briefly, 1 µg of plasmid was mixed with 10 units of Bam HI, 10 units of Xho I, 1X K buffer (20mM Tris-HCl (pH 8.5), 10mM $MgCl_2$, 1 mM DTT, 100mM KCl)[149] and brought to a final reaction

volume of 20 µL with Ultrapure™ DNase/RNase-free distilled water (Invitrogen, Waltham, MA, USA – cat. # 10977015). The reaction was incubated at 37ºC for 2 hours. After incubation, 2.5µL of 10X DNA loading dye (30%($^v/_v$) glycerol, 0.05%($^w/_v$) bromophenol blue) was added to the digested fragments mix. The mix was loaded into a 1% agarose gel previously placed in an electrophoretic chamber and submerged in running buffer (1X TAE (0.04 M Tris base, 0.11 %($^v/_v$) acetate, 0.2 %($^v/_v$) 0.5 M sodium EDTA), 0.01% ethidium bromide). As a molecular mass reference (M_r), a molecular weight ladder (GeneDireX®, Taoyuan, Taiwan – cat. # DM010-R500) was loaded in a well adjacent to the samples being tested. The loaded gel was run at 100 V until the dye line had travelled 80% of the gel. A UV transilluminator was used to visualize the digested plasmids.

Immunoprecipitation

For all steps involving a magnet, the magnetic stand (Invitrogen™, Waltham, MA, USA – cat. # 12321D) was placed inside a bucket containing ice.

In a microfuge tube, Pierce™ Protein A/G Magnetic Beads (Thermo Scientific™, Waltham, MA, USA – cat. # 88802) were blocked with a 5% ($^w/_v$) bovine serum albumin (BSA) aqueous solution[e] with a bead volume to BSA volume ratio of 1:1. To ensure proper bead blocking, the tube was placed on a nutating mixer and incubated for 1 hour, at 4ºC. To separate blocked beads from the BSA solution, the microfuge tube was placed on a magnetic stand. Once beads stuck to the wall of the microfuge tube closest to the magnet, the liquid fraction was aspirated and discarded. Then the beads were resuspended in Low Salt Immunoprecipitation buffer (LSIP buffer: Tris base – 50mM, NaCl – 20 mM, $MgCl_2$ – 1mM, TritonX100 – 1%, P8340 protease inhibitor – 1X; pH ~8), and vortexed to ensure homogenization.

---

[e] Mix 0.5 g $_{BSA}$ in 10 mL $_{ultrapure\ water}$, vortex, and place at 4°C overnight for complete dissolution

To test our mAbs targeting hCABS1, in-house $_r$hCABS1 OEL was used as a '*positive control sample*' given that it contained recombinant generated hCABS1 protein. In a separate microfuge tube, $_r$hCABS1 OEL was combined with mAb targeting hCABS1 with a lysate volume[f] to mAb[g] volume ratio 1.6:1. To ensure proper mixing, the tube was placed on a nutating mixer and incubated for 1 hour at 4°C. As a '*negative control sample*', another microfuge tube containing $_r$hCABS1 OEL combined with ultrapure distilled water instead of antibody was incubated, using the same ratio.

After initial incubations, each sample (i.e., *positive* and *negative* controls) was mixed with the beads' solution with a sample volume to beads volume ratio of 2:1 and incubated for 1 hour at 4°C on a nutating mixer. After incubation, the tube was placed on the magnetic stand, where Bead-Antibody-Protein Of Interest (b-a-POI) complexes stuck to the wall of the tube facing the magnet (**Figure 4-4** B). Liquid fractions were removed and saved for further WB evaluation at 4°C (**Figure 4-4** B). The tube was removed from the magnet, b-a-POI complexes were resuspended in 500µL LSIP buffer, and the entire volume was transferred to a new microfuge tube. To get rid of non-specific proteins, b-a-POI complexes underwent three washing steps. Washes consisted of placing the tube back on the magnetic stand, aspirating supernatant/wash eluate (each eluate was saved for further WB analysis) and - *except on the third/final wash step* - resuspending b-a-POI in 500µL LSIP buffer. Collected wash eluates were stored at 4°C, while b-a-POI complexes were stored at -20°C overnight. The next day, beads were resuspended in 1 part 4X Laemmli sample (BioRad) and 3 parts RIPA buffer supplemented with P8340 protease inhibitor cocktail (Sigma Aldrich). The mix was boiled at 95°C for 5 minutes and then the tube was placed on the magnetic stand. The supernatant, containing unbound antibodies and POI, was transferred to a new tube,

---

[f] $_r$hCABS1 OEL concentration was 0.32 $^{µg}/_{µL}$
[g] Working antibody concentrations were: 15B11-1 = 1.945 $^{µg}/_{µL}$, 13G3-1 = 1.006 $^{µg}/_{µL}$, 4D1-1 = 1.037 $^{µg}/_{µL}$

and supplemented with DTT to a final concentration of 12.5 mM$_{DTT}$. This sample was saved at 4°C for further WB evaluation.
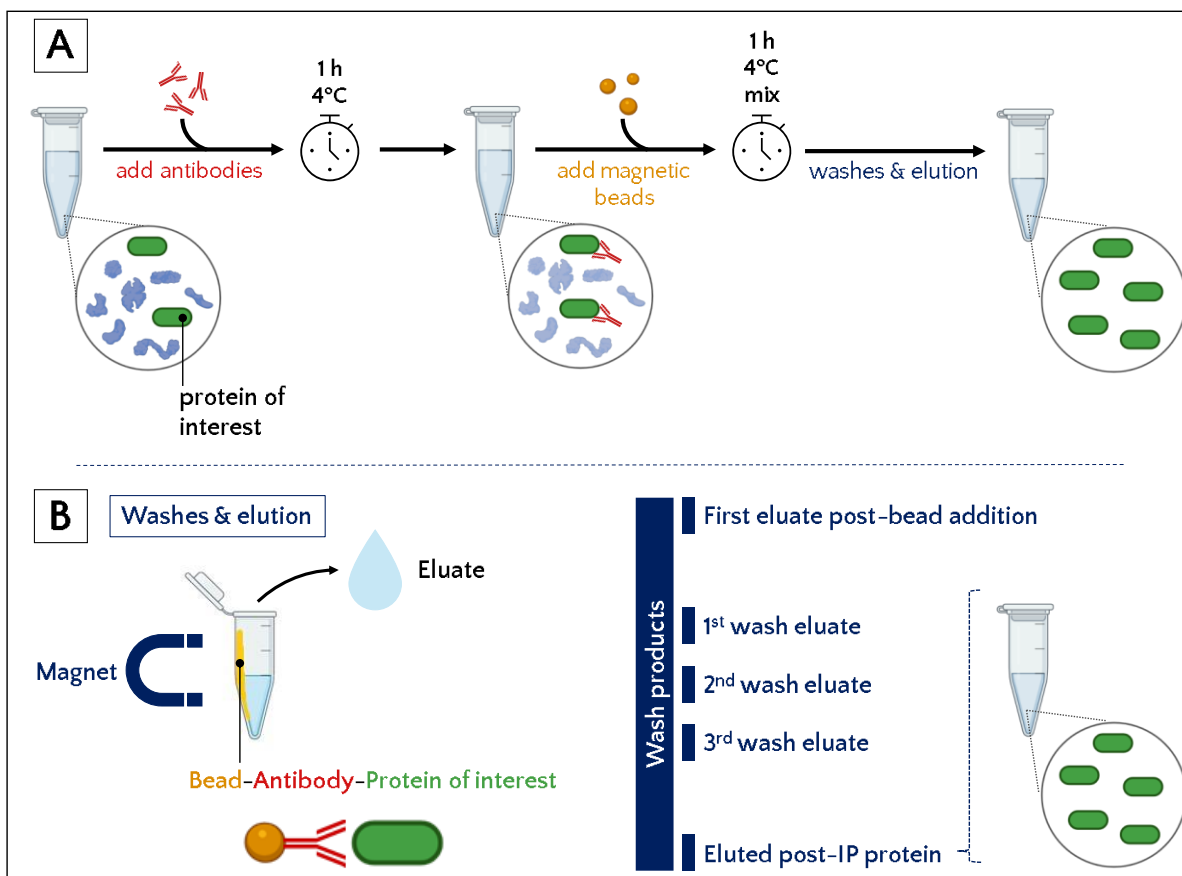
Figure 4-4. Pipeline of immunoprecipitation protocol.

(A) Summarized steps of immunoprecipitation protocol from complex samples. Protein of interest is in green, antibodies in red and magnetic beads in orange. 'Washes and elution' steps are further described in next panel. (B) Bead-antibody-protein of interest (b-a-POI) complexes are pulled into a magnet, theoretically capturing b-a-POI while eluate is transferred into another tube for downstream evaluation. Five eluates were preserved for Western blot evaluation, their given names shown to the right of panel B. IP Western blots shown in this chapter use the eluate nomenclature described here. *Figure made with Biorender.com*

WB analysis

The day of the experiment, 1X WB running buffer (1L 1X working solution: Trizma base – 40 mM, Glycine – 300 mM, Methanol – 200 mL) was prepared and placed at 4°C.

For WB, electrophoresed samples in gels were placed in a cassette containing fiber pads, filter papers, and a 0.45 μm pore-sized nitrocellulose membrane (**Figure 2-4**). The cassette was placed in a WB vertical transfer chamber along with an ice pack on the side. 1X WB transfer buffer was

added until the cassette was covered. Transfer was done at a constant amperage of 0.5 A for 1 hour.

After protein transfer, the cassette was opened and all, but the nitrocellulose membrane, was discarded appropriately. The nitrocellulose membrane was placed inside an opaque WB box and washed 2X rapidly (<1 min) with double distilled water before adding enough WB blocking buffer (1% fish skin gelatin (Truin Science Ltd., Edmonton, AB, Canada – cat.#FG800), 1X PBS, 0.1% Tween20) to cover the membrane. Membrane blocking was done at T_{room} for 1 h. Once blocked, blocking buffer was discarded and the membrane was immunoprobed overnight at 4°C with the antibody(-ies) pertinent to the experiment at the desired working concentration (**Table 4-4**). The antibody diluent solution (ADS) was composed of half 1X PBS supplemented with 0.05% Tween 20, and half WB blocking buffer. After overnight membrane immunoprobing, the antibody solution was appropriately discarded, and the membrane was washed as detailed in **Table 4-3**. Li-cor Biosciences secondary antibodies were diluted 1:10,000.

Table 4-3. Immunoprobed membrane washing steps and solutions.

Wash step	Washing solution	Time of wash (min.)
1.1	PBS 1X +0.05% Tween 20	5
1.2		5
1.3		5
Incubation with secondary antibody	50 % – PBS 1X +0.05% Tween 20, 50 % – WB blocking buffer, Secondary antibody (1 : 10,000)	60
2.1	PBS 1X +0.05% Tween 20	10
2.2		10
3.1	PBS 1X	10

Table 4-4. WB antibody working concentrations.

Isotype antibodies corresponding to each of our hCABS1 mAbs were diluted to the same working concentration used when immunoprobing with the mAbs to hCABS1. Anti-FLAG (target: DYKDDDDK domain) was diluted as suggested by its manufacturer.

Antibody ID	Immunoprobe working concentration ($^{ng}/_{\mu L}$)		
15B11–1	10	1	0.1
13G3–1			
Isotype$_{for\ 15B11–1\ \&\ 13G3–1}$ IgG1.κ			
4D1–1	10	1	0.1
Isotype$_{for\ 4D1–1}$ IgG2α.κ			
Anti–FLAG	10		

Once membranes were washed, WB were captured in an Odyssey scanner and visualized in ImageStudio Lite v.5.2 (Li-cor Biosciences). For all WB images, curves were adjusted for the 700 and 800 nm channels to K=1. For both channels the *Grayscale black on white* setting was selected, rendering a bright background and dark immunoreactive bands. Maximum and minimum values were then adjusted to reduce background signal and allow optimum visualization of bands (**Figure 2-5**). Of note, images that are evaluated together (e.g., 'mAb' vs 'no primary antibody' vs 'isotype antibody') were set to the same maximum and minimum signal values.

Post-titrations: WB image screening and selection criteria for figures in this chapter

After titrations of loaded sample amount and antibody probing concentration, resulting WBs were evaluated for banding pattern. To decrease complexity, the selection criteria of which data to show in this chapter was the maximum amount of loaded sample at which both 'No primary antibody' and 'isotype antibody' gave no signal, but at which the antibody targeting CABS1 gave a signal (**Figure 4-5**). In saliva WBs, signal was present when probing with mAbs, 'No primary antibody' and 'isotype antibody'. In blood serum WBs, signal was present when probing with mAbs and 'isotype antibody'.
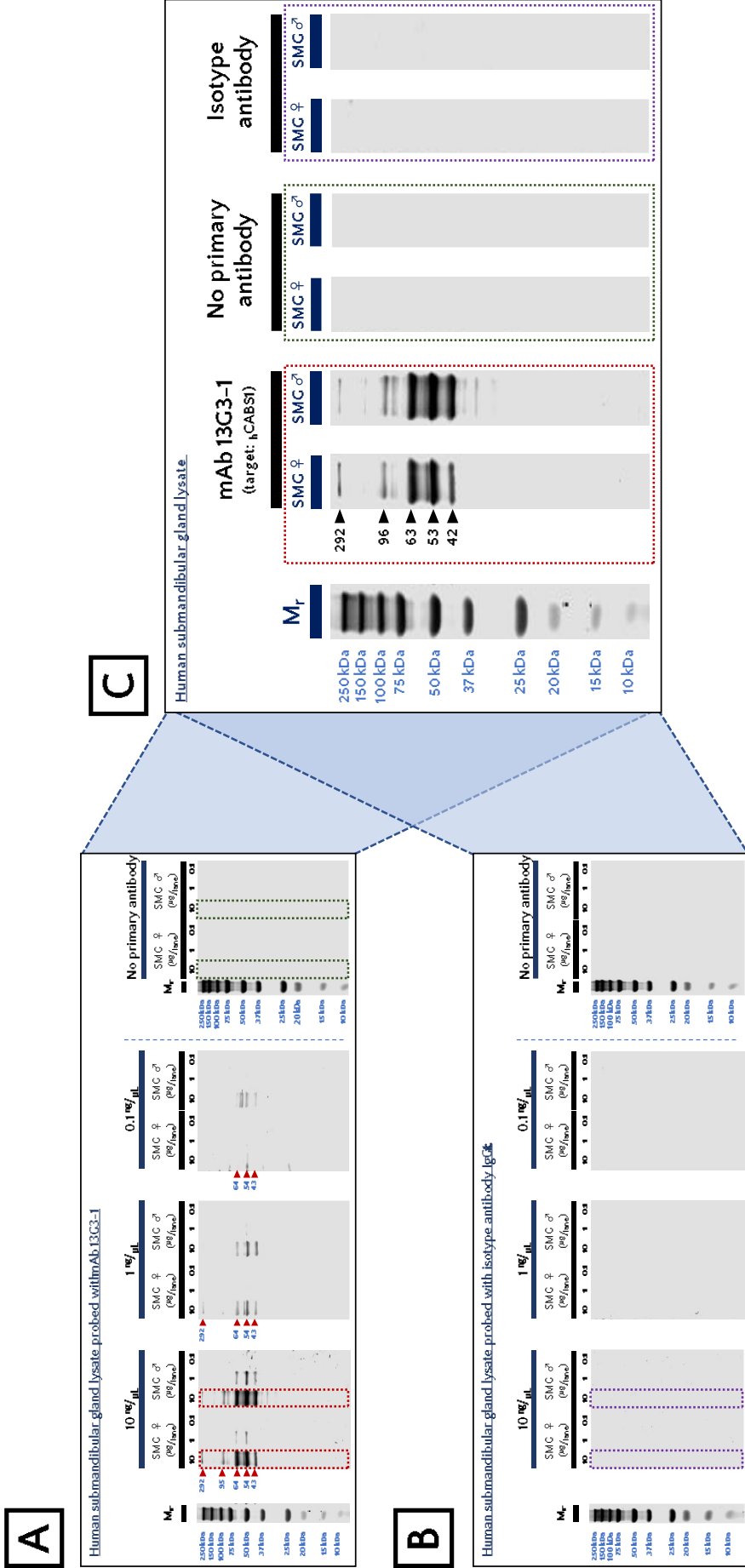
Figure 4-5. Pipeline of relevant image selection of Western blots after sample and antibody titrations.

A sample of interest, in this example human submandibular gland (SMG), was diluted in 10-fold steps resulting in 10, 1 or 0.1 μg of total protein being loaded in gel lanes. Post-Western blot, the membranes were probed with a primary antibody working concentration of either 10, 1 or $0.1\,^{ng}/_{\mu L}$ or no primary antibody (shown atop each membrane image). All membranes were exposed to a secondary antibody to generate visible bands. A molecular mass reference (M_r) placed at the left of all Western blots shows the range of protein sizes (in kilodaltons, kDa) that can be present. (A) Western blot of female (♀) and male (♂) SMG probed with monoclonal antibody (mAb) 13G3, that targets human Calcium-binding protein, spermatid-associated 1 ($_h$CABS1). Enclosed in red dashed rectangles are the lanes that show bands that interact with 13G3 and enclosed in green rectangles are lanes loaded with the same protein amount with no signal for the membrane probed with only secondary antibody. (B) Western blot of female (♀) and male (♂) SMG probed with isotype antibody (to 13G3) IgG1.κ. Enclosed in purple dashed rectangles are lanes showing no signal loaded with the same amount of protein as lanes showing signal in the 13G3 probed membrane. (C) Final figure depicting lanes that were equivalently treated except for the immunoprobe (mAbs to hCABS1, no primary antibody, isotype antibody). Dashed rectangles are color coded and indicate where each shown lane came from (red and green rectangles from panel A, and purple rectangle from panel B). Panel (A) is representative of 3 independent experiments, while panel B represents a single experiment due to isotype availability.

Molecular weight determination

All WB images included a molecular mass reference (M_r) showing proteins of known molecular mass (in kilodaltons, kDa). WB images were opened in Microsoft Paint. This program provides the pixel value of the place where the cursor is present (**Figure 4-6** A). The cursor was placed atop each M_r band, and the pixel value (of the y-axis) corresponding to each M_r band was recorded in Microsoft Excel (**Figure 4-6** B). At the same time, pixel values of bands occurring in sample lanes were recorded and kept for later calculations. M_r pixel values were then divided by 38 to be converted to centimetres (**Figure 4-6** B). The resulting dataset was used to graph molecular mass (y-axis), versus distance (x-axis) (**Figure 4-6** C). A 6th order polynomial trendline and its equation were generated.

The equation was used to calculate the molecular mass of bands occurring in samples (**Figure 4-6** D). Briefly, the previously recorded pixel values for bands in each sample were also divided by 38 to be converted to centimetres, and the resulting value was input into the equation. The output was molecular mass of the band(s) in kDa.

Immunohistochemical analysis of human testis

The testis slide was baked at 60ºC for 1 hour and then deparaffinized and retrieved on Dako Omnis fully automated IHC platform (Agilent, Santa Clara, CA, USA) using EnVision FLEX target retrieval solution, High pH (Dako Omnis) (Agilent – part # GV80411-2) at 97ºC for 30 min. Monoclonal antibody 15B11-1 (targeting hCABS1) was diluted 1/100 in EnVision FLEX antibody diluent (Agilent – part # K800621-2) and was applied for 20 min. at 32ºC followed by EnVision Flex+ Mouse LINKER (Dako Omnis) (Agilent – part # GV82111-2) for 10 min. Subsequently, EnVision FLEX, HRP.Rabbit/Mouse (Agilent – part # GV80011-2) was added for 20 min. Visualization was performed using DAB+ substrate chromogen system (Dako Omnis) (Agilent – part # GV82511-2) and counter stained with Gill I Hematoxylin formula (Leica, Wetzlar, Hesse, Germany – cat. #3801500).

Panel B — Molecular Weight Marker (Precision Plus All Blue – BioRad)

M_r (kDa)	Distance Px	Distance Cm
250	7	0.2
150	17	0.4
100	28	0.7
75	38	1.0
50	57	1.5
37	75	2.0
25	104	2.7
20	122	3.2
15	145	3.8
10	164	4.3
y	x	x'

Px → cm conversion factor: 38

Band location

Sample	Px	Cm
SMG ♀	45	1.2

Panel C

$$y = 1.6474x^6 - 25.158x^5 + 153.03x^4 - 475.2x^3 + 805.93x^2 - 748.76x + 362.69$$
$$R^2 = 0.9997$$

Panel D

$$M_{SMG\,♀\ band}\ (1.2\ cm) =$$

$$1.6474(1.2)^6 - 25.158(1.2)^5 + 153.03(1.2)^4 - 475.2(1.2)^3 + 805.93(1.2)^2 - 748.76(1.2) + 362.69$$

$$= 64\ kDa$$

Figure 4-6. Pipeline for determining molecular mass of bands observed in WB.

(A) Microsoft Paint is used to obtain the pixel (px) coordinates of bands of interest in a Western blot image. When the cursor is placed atop a band, pixel coordinates are given in the lower left paint window (location enclosed by a black dotted rectangle). The red target depicts the cursor placed over a molecular mass reference (M_r) band, and its pixel coordinate value is in red (bottom of panel A). The same applies for the green target placed over a band in the sample of interest. (B) Pixel coordinate values are entered into Microsoft Excel for each band. M_r have known molecular mass values in kilodaltons (kDa). The sample of interest, in this case human submandibular gland (SMG), doesn't. After coordinates are input, the pixel values must be divided by 38, the conversion factor between px and centimeters (cm). (C) Converted coordinates from M_r are graphed against the known molecular mass value of reference proteins. The resulting equation is shown above its R^2 value. (D) The equation is used to obtain the molecular mass of bands of interest in the sample. In this example, the converted coordinate from SMG, in cm, is input into the equation. The result is the molecular mass of the band of interest in kDa.

133

Results

Evaluation of mAbs to hCABS1 when screening transient overexpression cell lysates

To evaluate the specificity of our mAbs to hCABS1, we used a transient hCABS1 overexpression cell control, OEL, and its inherent negative control, NCL. WB analyses using 15B11-1 showed bands at 78, 53 and 47 kDa for OEL, and presence of analog bands at 53, 47 kDa in NCL, as well as bands at 38, 33, and 31 kDa (**Figure 4-7**). No immunoreactivity was observed in membranes probed with isotype antibody IgG1.κ at the same working antibody concentration as 15B11-1 or with no primary antibody (**Figure 4-7**). Antibody 13G3-1 detected bands at 78, 64 and 53 kDa in

Figure 4-7. WB of $_r$hCABS1 transient overexpression cell lysate (OEL) and its negative control cell lysate (NCL) immunoprobed with monoclonal antibody (mAb) 15B11-1, and controls (no mAb and isotype antibody IgG1.κ).

A molecular mass reference (M_r) indicates the range of protein sizes in kilodaltons (kDa) that can be present along a lane. Molecular masses in kDa are shown next to arrows in black. All lanes were loaded with 1 μg $_{total\ protein}$. Working antibody concentration for 15B11-1 and IgG1.κ was 1 $^{ng}/_{μL}$. Image is representative of two independent experiments for 15B11-1 and no primary antibody and one experiment for IgG1.κ. The shown molecular masses are the average of 2 independent experiments where the same banding pattern was observed.

OEL, and an analog band at 53 kDa in NCL (**Figure 4-8**). No bands were observed in membranes probed with no primary antibody, but OEL probed with isotype antibody IgG1.κ at the same working antibody concentration as 13G3-1 shows a band at 64 kDa (**Figure 4-8**). Antibody 4D1-1 shows a band at 78 kDa in OEL, and a faint band at 53 kDa in NCL (**Figure 4-9**). No signal was detected in membranes probed with no antibody, but a membrane probed with isotype antibody IgG2α.κ shows several bands in a smear pattern in a range between 100 and 35 kDa (**Figure 4-9**). Evaluation of these control lysates with an anti-FLAG antibody targeting aminoacidic sequence

Figure 4-8. WB of $_r$hCABS1 transient overexpression cell lysate (OEL) and its negative control cell lysate (NCL) immunoprobed with monoclonal antibody (mAb) 13G3-1, and controls (no mAb and isotype antibody IgG1.κ).

A molecular mass reference (M_r) indicates the range of protein sizes in kilodaltons (kDa) that can be present along a lane. Molecular masses in kDa are shown next to arrows in black. All lanes were loaded with 1 μg $_{total\ protein}$. Working antibody concentration for 13G3-1 and IgG1.κ was 10 $^{ng}/_{μL}$. Image is representative of two independent experiments for 13G3-1 and no primary antibody and one experiment for IgG1.κ. The shown molecular masses are the average of 2 independent experiments where the same banding pattern was observed.

Figure 4-9. WB of ᵣhCABS1 transient overexpression cell lysate (OEL) and its negative control cell lysate (NCL) immunoprobed with monoclonal antibody (mAb) 4D1-1, and controls (no mAb and isotype antibody IgG2α.κ).

A molecular mass reference (M_r) indicates the range of protein sizes in kilodaltons (kDa) that can be present along a lane. Molecular masses in kDa are shown next to arrows in black. All lanes were loaded with 1 µg $_{total\ protein}$. Working antibody concentration for 4D1-1 and IgG2α.κ was 1 $^{ng}/_{µL}$. Image is representative of two independent experiments for 4D1-1 and no primary antibody and one experiment for IgG2α.κ. The shown molecular masses are the average of 2 independent experiments where the same banding pattern was observed.

DYKDDDDK, adjacent to the carboxyl end of the recombinant hCABS1 in commercial OEL shows two bands at 78 and 51 kDa, with the 51 kDa band also present in NCL (**Figure 4-10**).

We began optimizing an immunoprecipitation protocol to capture CABS1 from biological samples. The obvious candidate sample to use for this goal was OEL, since theoretically it contains recombinant ($_r$) hCABS1. However, commercial OEL was expensive and the last two batches we received did not interact with any of our mAbs, suggesting that production of $_r$hCABS1 in those batches was not optimal. We decided to produce our own OEL by transfecting HEK293T cells with the plasmid containing the $_r$hCABS1 cassette (see Methodology). Firstly, the plasmid was
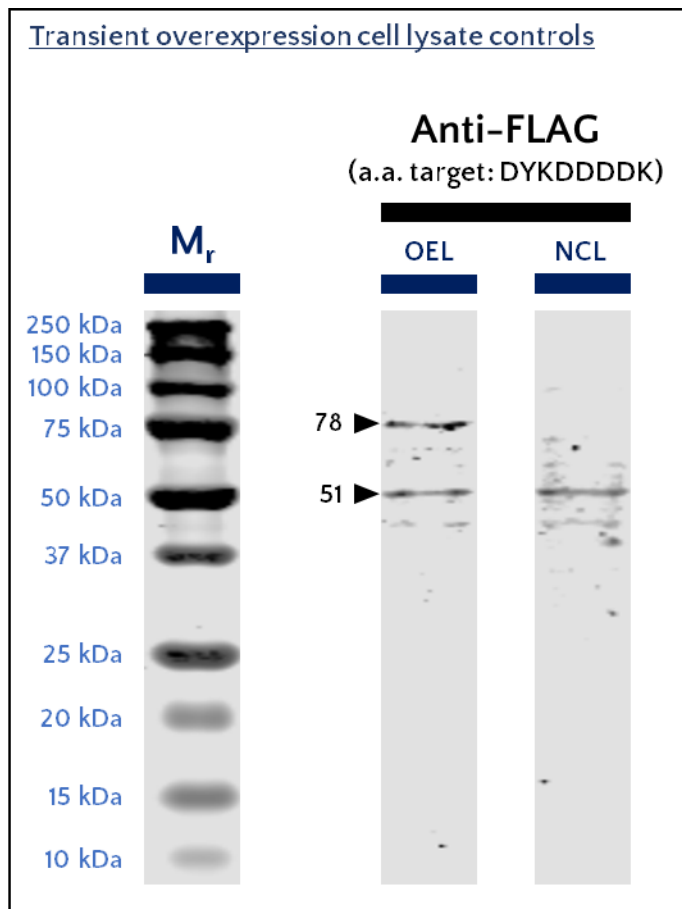
136

Figure 4-10. WB of rhCABS1 transient overexpression cell lysate (OEL) and its negative control cell lysate (NCL) immunoprobed with an Anti-FLAG monoclonal antibody.

A molecular mass reference (M_r) indicates the range of protein sizes in kilodaltons (kDa) that can be present along a lane. Molecular masses in kDa are shown next to arrows in black. All lanes were loaded with 1 µg total protein. Working antibody concentration for Anti-FLAG was 10 ng/µL. Image is representative of a single experiment.

amplified in Subcloning Efficiency™ DH5α competent cells. A minor portion of the recovered amplified plasmid was digested with Xho I and Bam HI and ran in an agarose gel to verify proper amplification. As expected, we observed post-digestion fragments at 4829 and 1237 base pairs (**Figure 4-11**). The plasmid was used to transfect HEK293T cells, which were later lysed and used in immunoprecipitation.

WB analysis of in-house produced OEL probed with 15B11-1 shows two bands at 76 and 54 kDa, but the lysate probed with an anti-FLAG antibody targeting a sequence adjacent to the C-terminus of rhCABS1 in the lysate only detects a 76 kDa band (**Figure 4-12** A). Immunoprecipitation (IP) of OEL using 15B11-1 was analysed using WB. The WB probing antibody was 15B11-1 as well. The first IP eluate after adding magnetic beads gives bands at 76, 63, 50, 30 and 25 kDa, with the 25 kDa band still present in the 1st wash eluate. The final product, eluted post-IP protein, shows bands at 143, 54, 50, 30, 25 and 22 kDa (**Figure 4-12** B). As an additional control we performed an immunoprecipitation without adding of capture antibody. A WB analysis using 15B11-1 as the probing antibody shows bands only in the first eluate post-bead addition; the bands are at 76 and 50 kDa (**Figure 4-12** C).
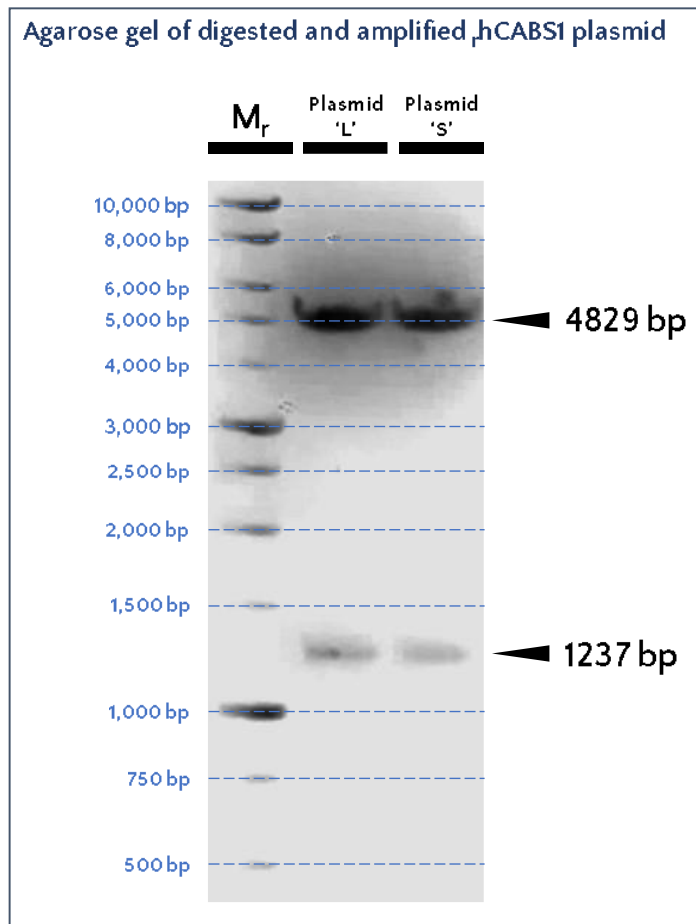
Figure 4-11. Cleavage patterns of digested rhCABS1 plasmids isolated from E. coli DH5α.

Two independent amplified plasmids, large (L) and small (S), were digested with Xho I and Bam HI. The expected fragments for this plasmid were 4829 and 1237 base pairs (bp). Presence of expected digests indicate successful amplification of the plasmid of interest. Reference molecular mass (M_r) ladder is shown on the left-most lane.

WB analysis of in-house produced OEL probed with 13G3-1 shows two bands at 76 and 54 kDa (**Figure 4-13** A). Immunoprecipitation of OEL using 13G3-1 as capturing antibody was evaluated in WB using the same antibody as probe. The first eluate post-bead addition shows three bands at 76, 54 and 25 kDa, there are no bands in the three IP washes, and the eluted protein post-IP shows three bands at 117, 54 and 25 kDa (**Figure 4-13** B).

WB analysis of in-house produced OEL probed with 4D1-1 shows a single band at 76 kDa (**Figure 4-14** A). Immunoprecipitation of OEL using 4D1-1 as capturing antibody was evaluated using WB using the same antibody as a probe. The first eluate post-bead addition shows three bands at 76, 54, and 25 kDa. The first wash shows a band at 54 kDa, and the final product, eluted protein post-IP, shows four bands at 104, 54, 46 and 25 kDa (**Figure 4-14** B).

Western blot: mAb 15B11-1 probing (a) rhCABS1 without immunoprecipitation, (b) rhCABS1 and wash eluates throughout immunoprecipitation, (c) sham control
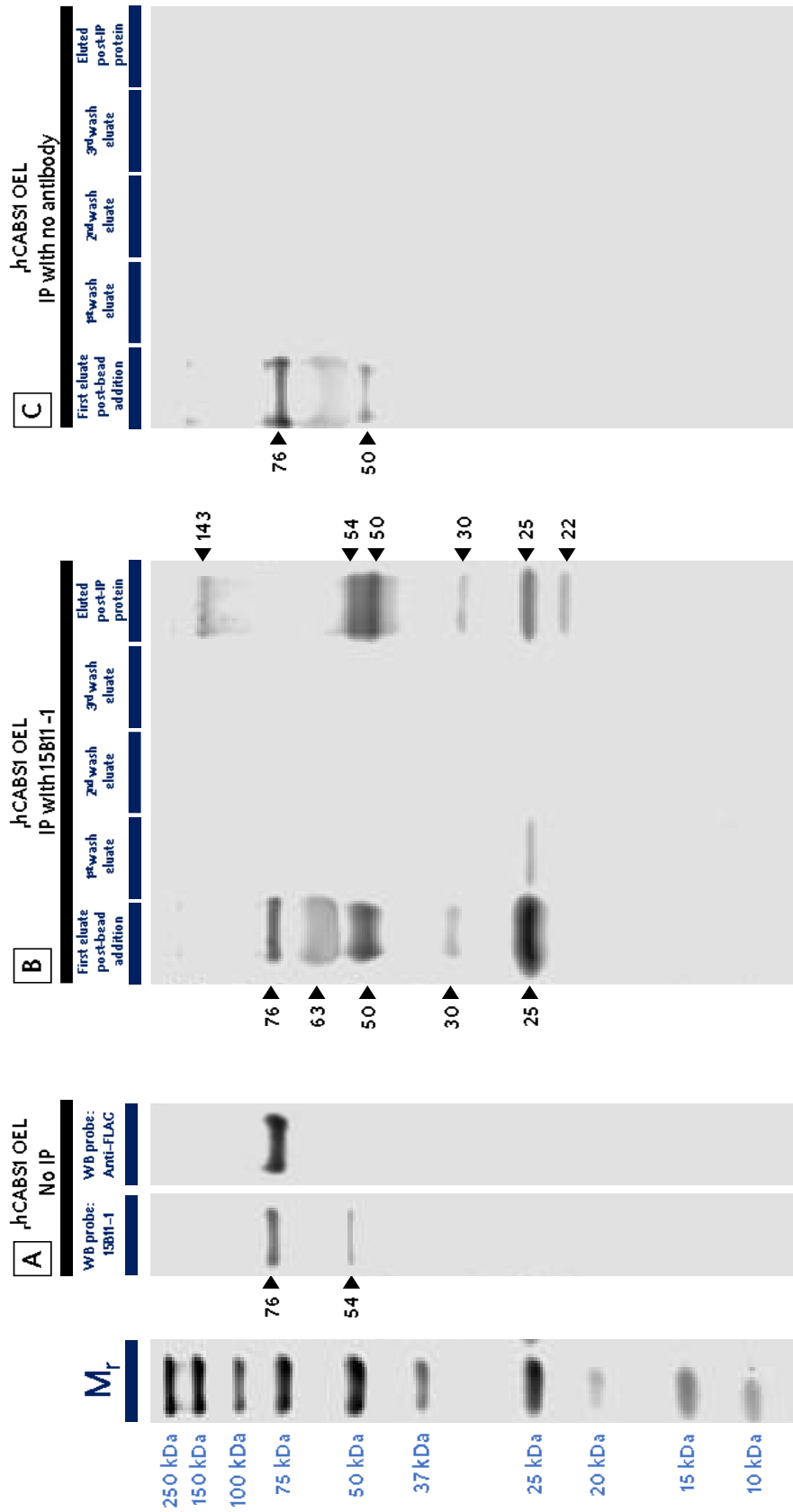
Figure 4-12. WB of immunoprecipitation (IP) experiments using mAb to CABS1 15B11-1 as capturing IP antibody and as WB probe of recombinant human Calcium-binding protein, spermatid-associated 1 (rhCABS1).

Molecular masses in kilodaltons (kDa) are shown next to arrows in black. Molecular mass reference (M_r) standards shown in the left-most lane. (A) As a reference, rhCABS1 overexpression cell lysate (OEL) without undergoing immunoprecipitation was ran adjacent to immunoprecipitation eluates and probed with the capture antibody, 15B11-1, and with an anti-FLAG antibody. (B) Shown here are the profiles of all eluates post-washing. rhCABS1 OEL immunoprecipitated with mAb 15B11-1, and the resulting elution post-IP. (C) rhCABS1 OEL immunoprecipitated with no antibody results in a band profile from the first eluate post-bead addition that matches non-IP rhCABS1. *IP and WB experiment performed once by Tarana A Mangukia, image processing and analysis done by Eduardo R.-Serratos*

139
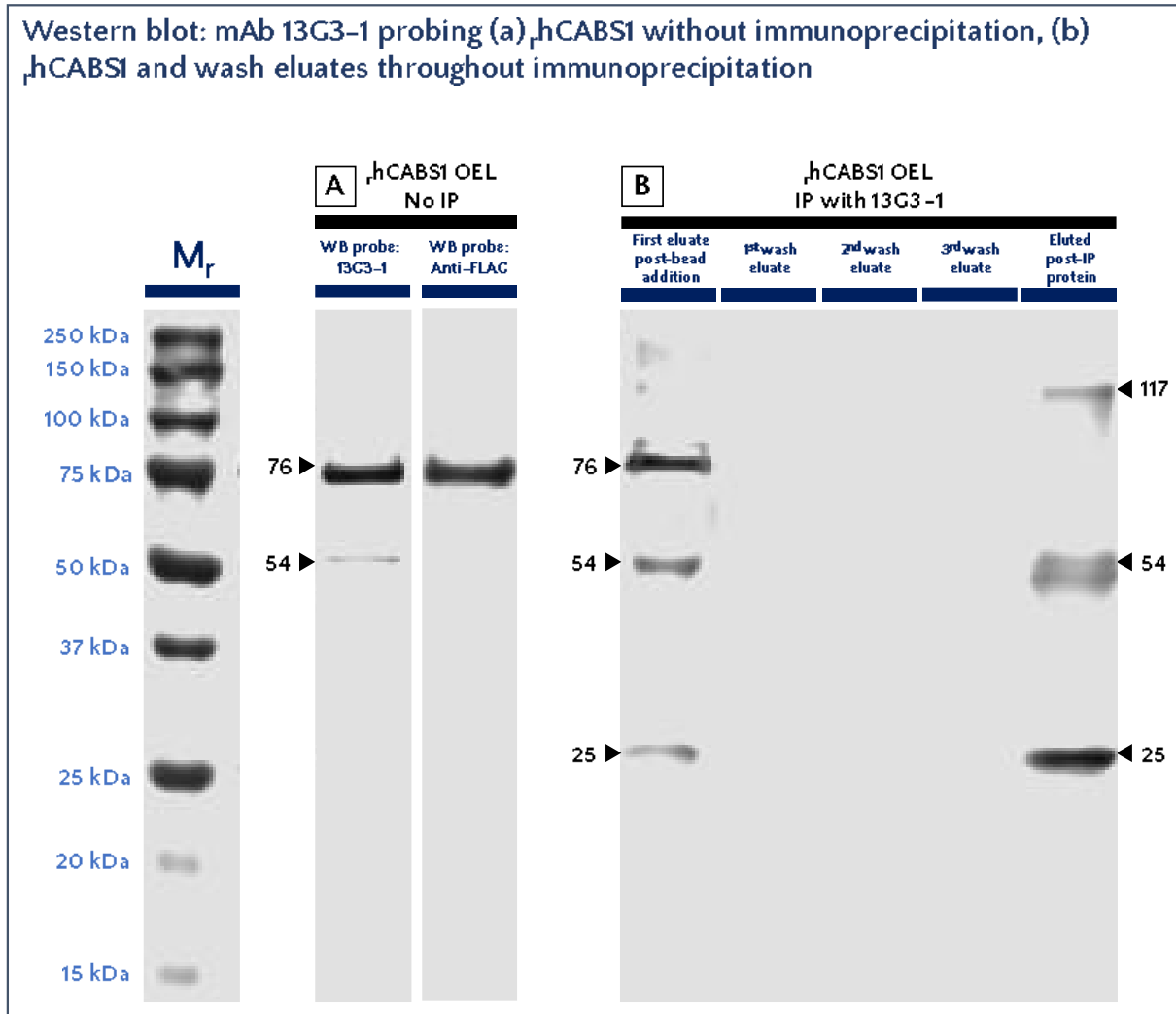
Figure 4-13. WB of immunoprecipitation (IP) experiments using mAb to CABS1 13G3-1 as capturing IP antibody and as WB probe of recombinant human Calcium-binding protein, spermatid-associated 1 (rhCABS1).

Molecular masses in kilodaltons (kDa) are shown next to arrows in black. Molecular mass reference (M_r) standards shown in the left-most lane. (A) As a reference, rhCABS1 overexpression cell lysate (OEL) without undergoing immunoprecipitation was ran adjacent to immunoprecipitation eluates and probed with the capture antibody, 13G3-1, and with an anti-FLAG antibody. (B) Shown here are the profiles of all eluates post-washing rhCABS1 OEL immunoprecipitated with mAb 13G3-1, and the resulting elution post-IP. *IP and WB experiment performed once by Tarana A Mangukia, image processing and analysis done by Eduardo R.-Serratos.*
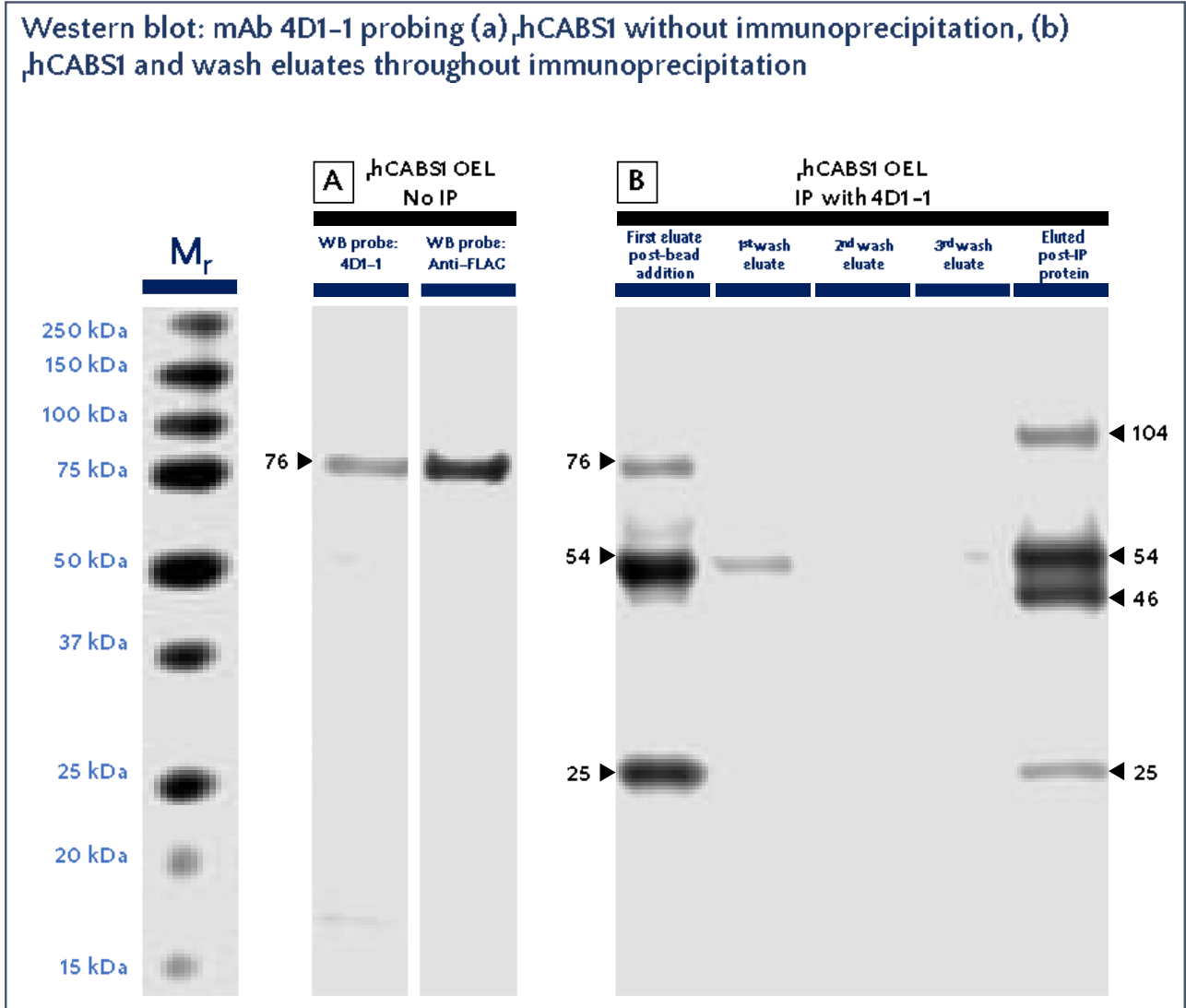
Figure 4-14. WB of immunoprecipitation (IP) experiments using mAb to CABS1 4D1-1 as capturing IP antibody and as WB probe of recombinant human Calcium-binding protein, spermatid-associated 1 (rhCABS1).

Molecular masses in kilodaltons (kDa) are shown next to arrows in black. Molecular mass reference (Mr) standards shown in the left-most lane. (A) As a reference, rhCABS1 overexpression cell lysate (OEL) without undergoing immunoprecipitation was ran adjacent to immunoprecipitation eluates and probed with the capture antibody, 4D1-1, and with an anti-FLAG antibody. (B) Shown here are the profiles of all eluates post-washing rhCABS1 OEL immunoprecipitated with mAb 4D1-1, and the resulting elution post-IP. *IP and WB experiment performed once by Tarana A Mangukia, image processing and analysis done by Eduardo R.-Serratos*

Evaluation of hCABS1 in human submandibular gland

WB evaluation of human submandibular gland lysate using pAbs targeting hCABS1 result in a complex banding pattern, and indicate that this biological compartment is a source of hCABS1 (see **Figure 2-12**,[18,21]). Thus, evaluation of SMG using our mAbs to hCABS1 could add value to our understanding of the complex banding pattern observed when using pAbs.

WB of SMG lysate using 15B11-1 detects a single band at 53 kDa in both male and female extracts. No bands were detected when probing with isotype antibody IgG1.κ at the same working antibody concentration as 15B11-1, and no bands were detected when using no primary antibody (**Figure 4-15**).
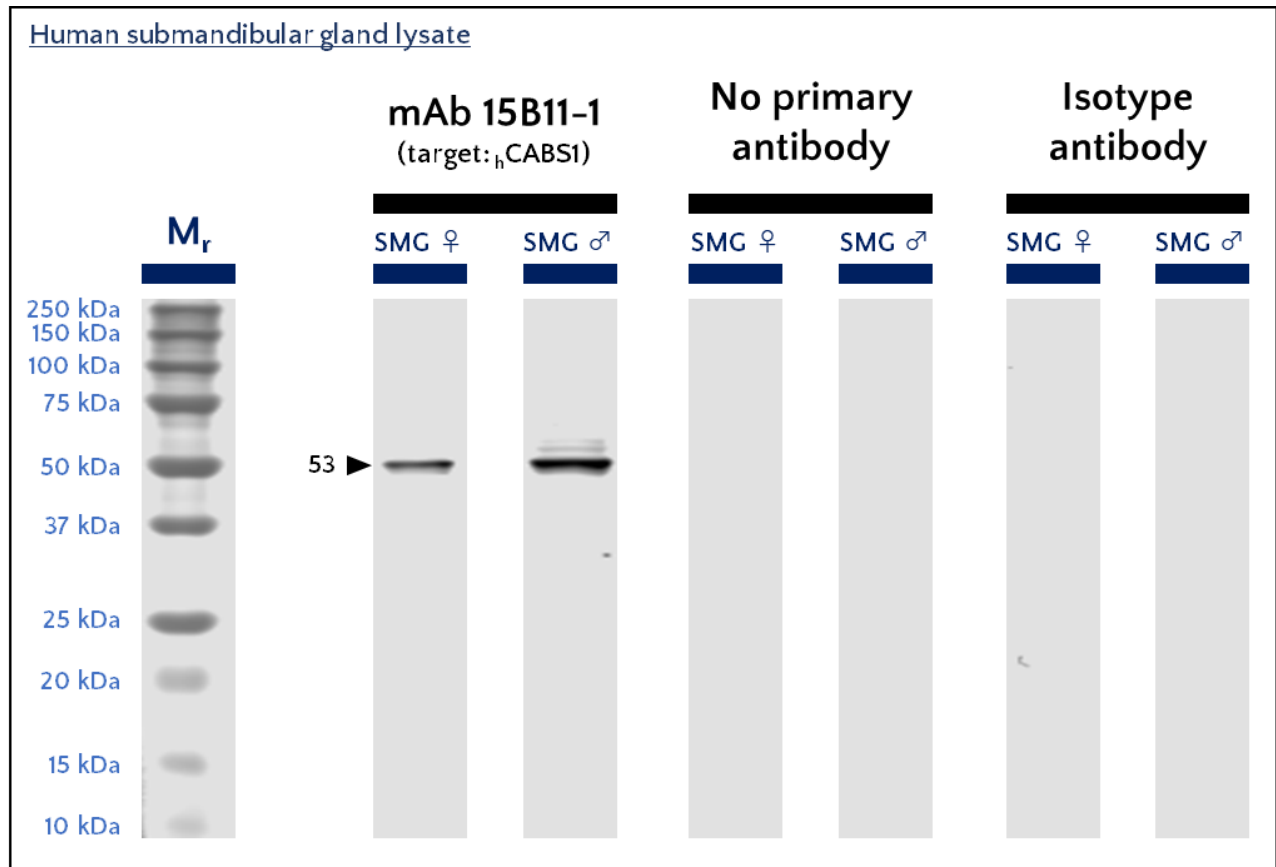
Figure 4-15. WB of female (♀) and male (♂) human submandibular gland lysates (SMG) probed with monoclonal antibody (mAb) 15B11-1, and controls (no mAb and isotype antibody IgG1κ).

A molecular mass reference (M_r) indicates the range of protein sizes in kilodaltons (kDa) that can be present along a lane. Molecular masses in kDa are shown next to arrows in black. All lanes were loaded with 10 µg $_{total\ protein}$. Working antibody concentration for 15B11-1 and IgG1.κ was 1 $^{ng}/_{µL}$. Image is representative of three independent experiments for 15B11-1 and no primary antibody, and one experiment for IgG1.κ. The shown molecular masses are the average of 3 independent experiments where the same banding pattern was observed.

WB analyses of SMG lysate using 13G3-1 as a probe consistently show three bands at 63, 53, and 42 kDa. In addition to these bands, two bands at 292 and 96 kDa were observed in a single WB experiment (**Figure 4-16**). No bands are detected when probing membranes with isotype antibody IgG1.κ at the same antibody working concentration as 13G3-1, or when adding no primary antibody (**Figure 4-16**).
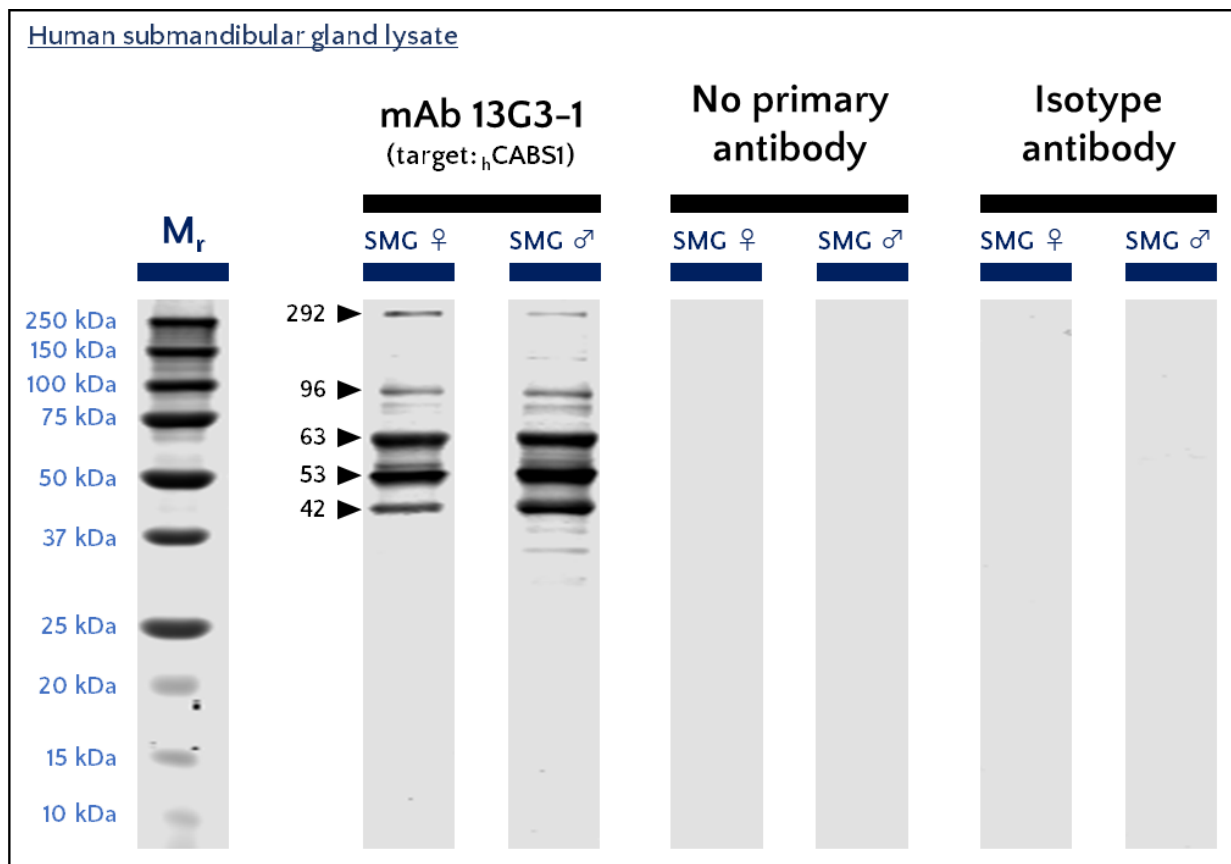
Figure 4-16. WB of female (♀) and male (♂) human submandibular gland lysates (SMG) probed with monoclonal antibody (mAb) 13G3-1, and controls (no mAb and isotype antibody IgG1κ).
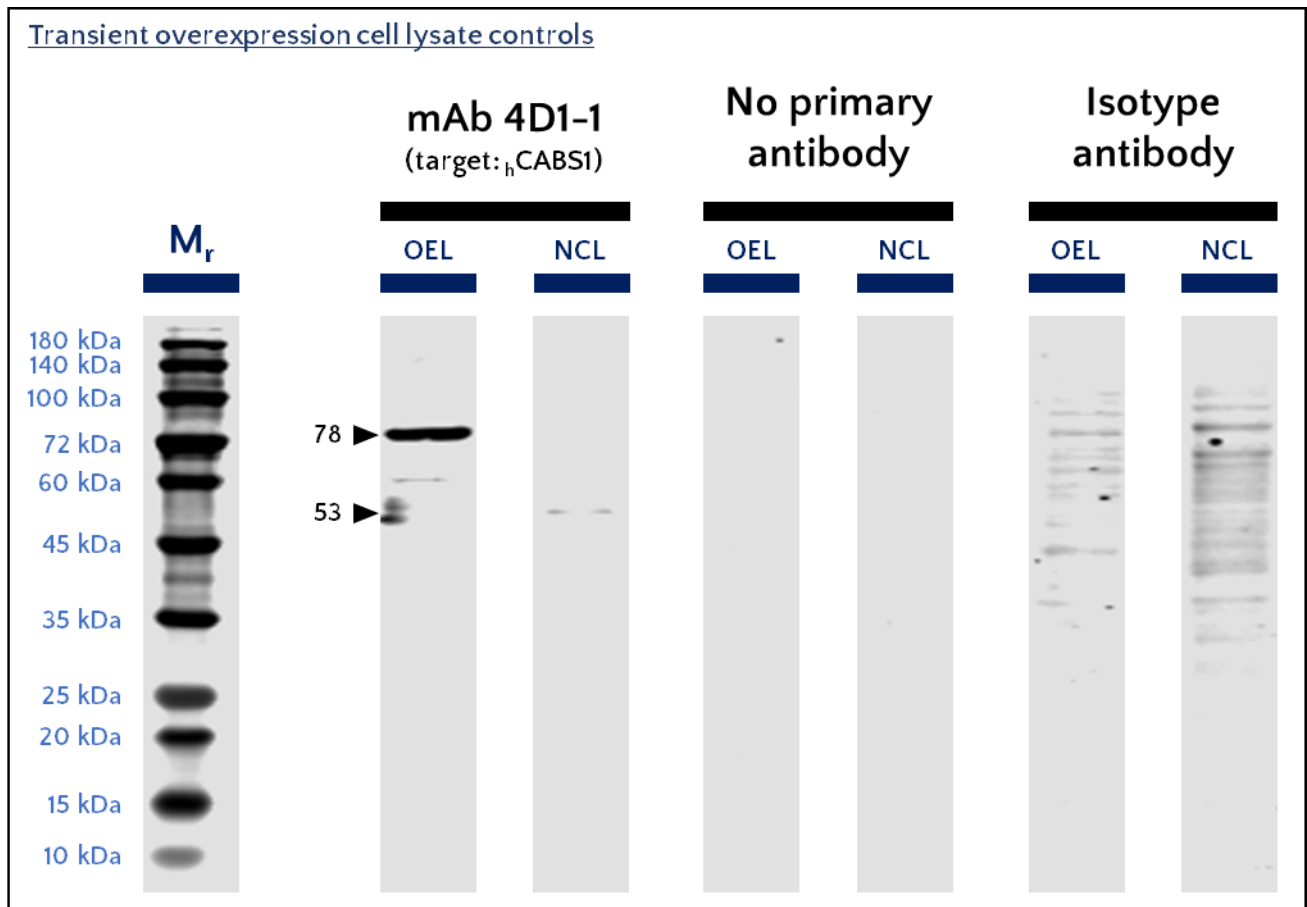
A molecular mass reference (M_r) indicates the range of protein sizes in kilodaltons (kDa) that can be present along a lane. Molecular masses in kDa are shown next to arrows in black. All lanes were loaded with 10 μg total protein. Working antibody concentration for 13G3-1 and IgG1.κ was 10 ng/μL. Image is representative of three independent experiments for 13G3-1 and no primary antibody, and one experiment for IgG1.κ. The bands at 292 and 96 kDa were seen only once. For all other bands, the shown molecular masses are the average of 3 independent experiments where the same banding pattern was observed.

WB of SMG lysate using antibody 4D1-1 detects two bands at 63 and 53 kDa in both male and female SMG, and two additional faint bands at 96 and 78 kDa are detected in the male SMG lysate

(**Figure 4-17**). No immunoreactivity was observed in WB using IgG2α.κ at the same antibody working concentration as 4D1-1, or when probing with only secondary antibody (**Figure 4-17**).
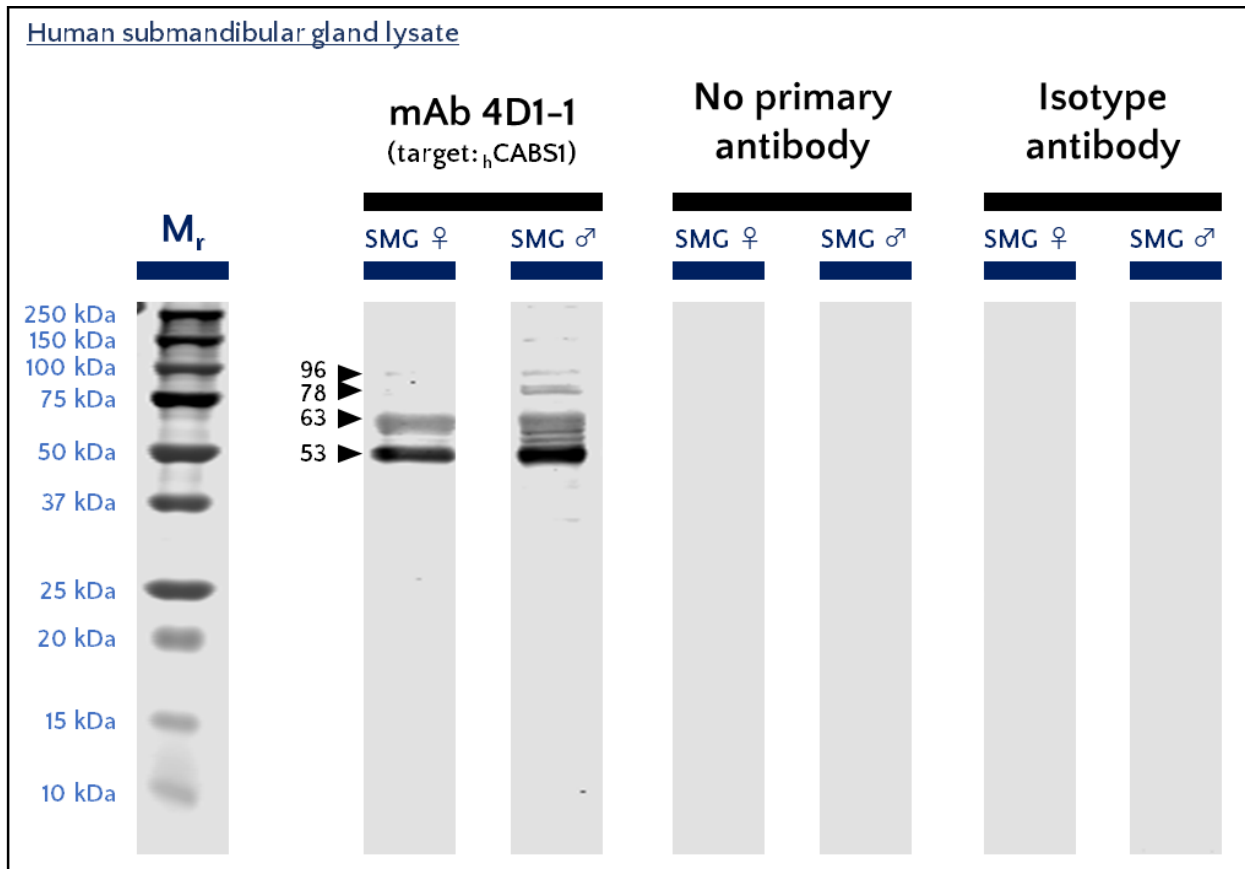
Figure 4-17. WB of female (♀) and male (♂) human submandibular gland lysates (SMG) probed with monoclonal antibody (mAb) 4D1-1, and controls (no mAb and isotype antibody IgG2α.κ).

A molecular mass reference (M_r) indicates the range of protein sizes in kilodaltons (kDa) that can be present along a lane. Molecular masses in kDa are shown next to arrows in black. All lanes were loaded with 10 µg $_{total\ protein}$. Working antibody concentration for 4D1-1 and IgG2α.κ was 10 $^{ng}/_{µL}$. Image is representative of three independent experiments for 4D1-1 and no primary antibody, and one experiment for IgG2α.κ. The shown molecular masses are the average of 3 independent experiments where the same banding pattern was observed.

Evaluation of hCABS1 in human saliva supernatant

In human saliva supernatant, WB using 15B11-1 detects five bands at 60, 56, 53, 25, and 15 kDa. The same banding pattern, except the 53 kDa band, is detected when probing with only secondary antibody, while isotype antibody IgG1.κ shows the same pattern as 15B11-1 except for the 15 kDa band (**Figure 4-18**). Saliva supernatant evaluated with antibody 13G3-1 detects four bands at 58,

56, 51 and 15 kDa. Probing the sample with only secondary antibody detects a faint band at 81 kDa, two close bands at 56 and 51 kDa, and a faint band at 15 kDa. Isotype antibody IgG1.κ detects a similar pattern to 13G3-1, 58, 56, 51 and 15 kDa, albeit with a less intense signal than our mAb (**Figure 4-19**). In saliva supernatant, antibody 4D1-1 detects three bands at 58, 56, and 51 kDa, albeit the signal from the 56 kDa band is more intense. When probing membrane only with secondary antibody and with isotype antibody IgG2α.κ at the same probing concentration as 4D1-1, two bands appear at 58 and 56 kDa (**Figure 4-20**).
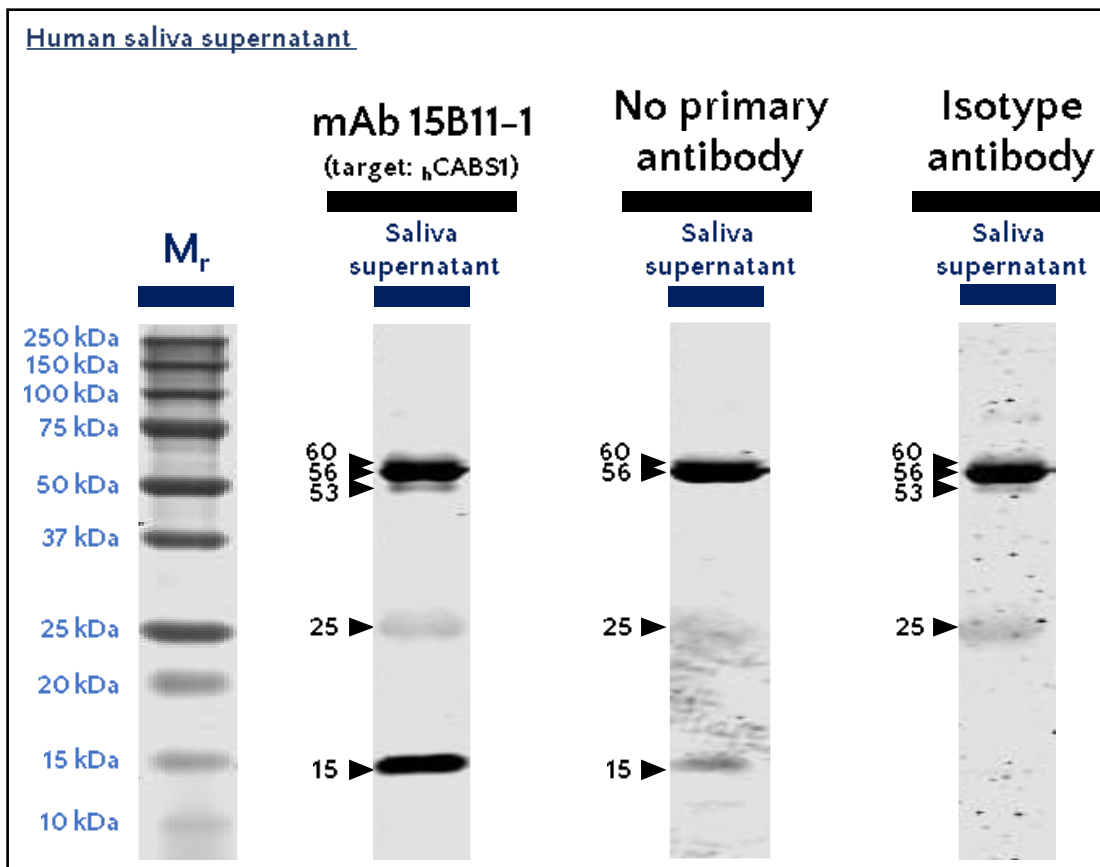
Figure 4-18. WB of human saliva probed with monoclonal antibody (mAb) 15B11-1, and controls (no mAb and isotype antibody IgG1.κ).

A molecular mass reference (M_r) indicates the range of protein sizes in kilodaltons (kDa) that can be present along a lane. Molecular masses in kDa are shown next to arrows in black. All lanes were loaded with 10 μg total protein. Working antibody concentration for 15B11-1 and IgG1.κ was 1 ng/μL. Image is representative of three independent experiments for 15B11-1 and no primary antibody, and one experiment for IgG1.κ. The shown molecular masses are the average of 3 independent experiments where the same banding pattern was observed.

Figure 4-19. WB of human saliva probed with monoclonal antibody (mAb) 13G3-1, and controls (no mAb and isotype antibody IgG1.κ).

A molecular mass reference (M_r) indicates the range of protein sizes in kilodaltons (kDa) that can be present along a lane. Molecular masses in kDa are shown next to arrows in black. All lanes were loaded with 10 μg total protein. Working antibody concentration for 13G3-1 and IgG1.κ was 10 ng/μL. Image is representative of three independent experiments for 13G3-1 and no primary antibody, and one experiment for IgG1.κ. The shown molecular masses are the average of 3 independent experiments where the same banding pattern was observed.

Two immunoprecipitation experiments using either 13G3-1 or 4D1-1 as capturing antibodies for saliva supernatant were evaluated by WB. Non-immunoprecipitated saliva supernatant probed with 13G3-1 in this experiment resulted in a similar profile to previous westerns of this sample probed with 13G3-1; i.e., two close bands at 54, 49 kDa and a band at 15 kDa (**Figure 4-21** A). After adding beads coated with our antibody and incubating with saliva supernatant, the resulting first eluate produced five bands at 204, 128, 61, 49 and 25 kDa. Subsequent washes showed consistent bands at 49 and 25 kDa that decreased in intensity as washes progressed. Finally, the resulting captured proteins post-IP produced five bands at 122, 47, 25, 24 and 15 kDa, with a smear between 122 and 47 kDa (**Figure 4-21** B). Non-immunoprecipitated saliva supernatant
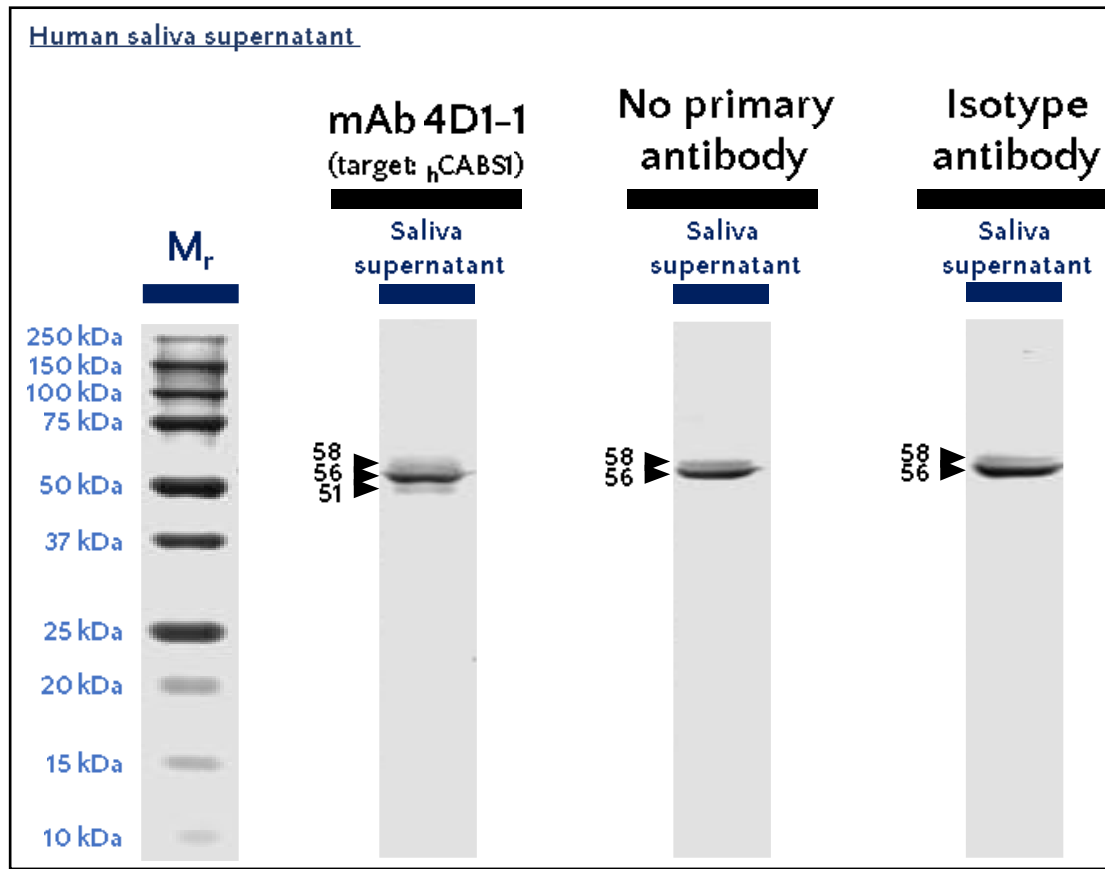
Figure 4-20. WB of human saliva probed with monoclonal antibody (mAb) 4D1-1, and controls (no mAb and isotype antibody IgG2α.κ).

A molecular mass reference (M_r) indicates the range of protein sizes in kilodaltons (kDa) that can be present along a lane. Molecular masses in kDa are shown next to arrows in black. All lanes were loaded with 10 μg total protein. Working antibody concentration for 4D1-1 and IgG2α.κ was 1 ng/μL. Image is representative of three independent experiments for 4D1-1 and no primary antibody, and one experiment for IgG2α.κ. The shown molecular masses are the average of 3 independent experiments where the same banding pattern was observed.

probed with 4D1-1 in this experiment resulted in two bands at 54 and 50 kDa (**Figure 4-22** A).

The first eluate post-bead addition gave four bands at 184, 51, 32 and 25 kDa, with washes showing

the 51 kDa band decrease in intensity as the washes progressed. The final product post-IP shows

a smear with 5 regions that could be considered to contain bands at 150, 138, 54, 45, 33 and 27

kDa (**Figure 4-22** B).
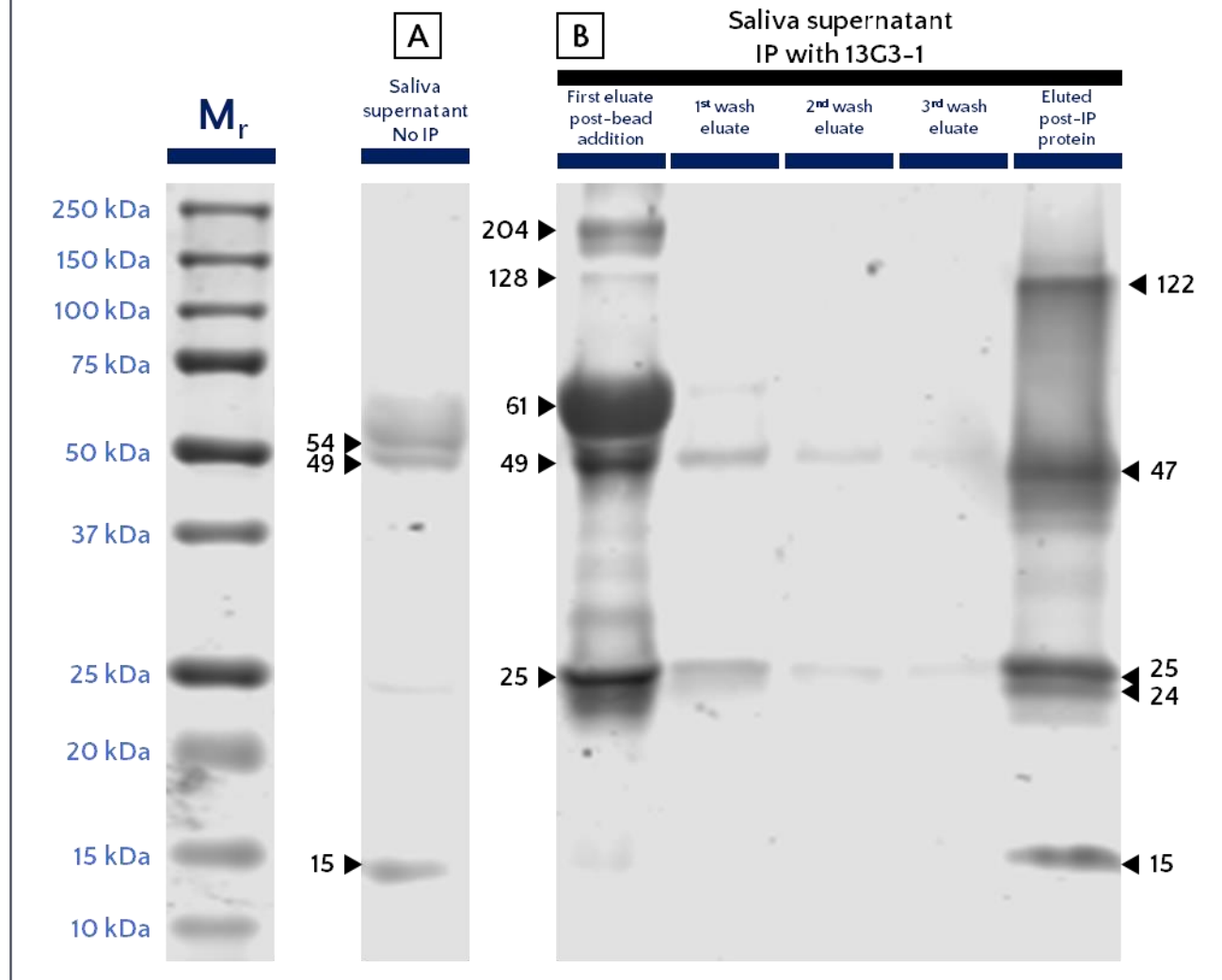
Figure 4-21. WB of immunoprecipitation (IP) experiments using mAb to CABS1 13G3-1 as capturing IP antibody and as WB probe.

Molecular masses in kilodaltons (kDa) are shown next to arrows in black. Molecular mass reference (M_r) standards shown in the left-most lane. (A) As a reference, saliva supernatant without undergoing immunoprecipitation was ran adjacent to immunoprecipitation eluates. (B) Shown here are the profiles of all eluates post-washing saliva supernatant immunoprecipitated with mAb 13G3-1, and the resulting elution post-IP. *IP and WB experiment performed once by Tarana A Mangukia, image processing and analysis done by Eduardo R.-Serratos.*

Figure 4-22. WB of immunoprecipitation (IP) experiments using mAb to CABS1 4D1-1 as capturing IP antibody and as WB probe.

Molecular masses in kilodaltons (kDa) are shown next to arrows in black. Molecular mass reference (M_r) standards shown in the left-most lane. (A) As a reference, saliva supernatant without undergoing immunoprecipitation was ran adjacent to immunoprecipitation eluates. (B) Shown here are the profiles of all eluates post-washing saliva supernatant immunoprecipitated with mAb 4D1-1, and the resulting elution post-IP. *IP and WB experiment performed once by Tarana A Mangukia, image processing and analysis done by Eduardo R.-Serratos.*

Evaluation of hCABS1 in human blood serum

We speculated that hCABS1 could be released into circulation by endocrine organs like the submandibular glands and testes. Thus, we decided to evaluate blood serum using WB and our monoclonal antibodies targeting hCABS1. The serum sample was taken from an adult male with no known comorbidities.

WB evaluation of blood serum using 15B11-1 shows a single band at 52 kDa. The same band is present when probing the membrane with isotype antibody IgG1.κ at the same working concentration, with an additional band at 25 kDa. No signal is detected when probing the
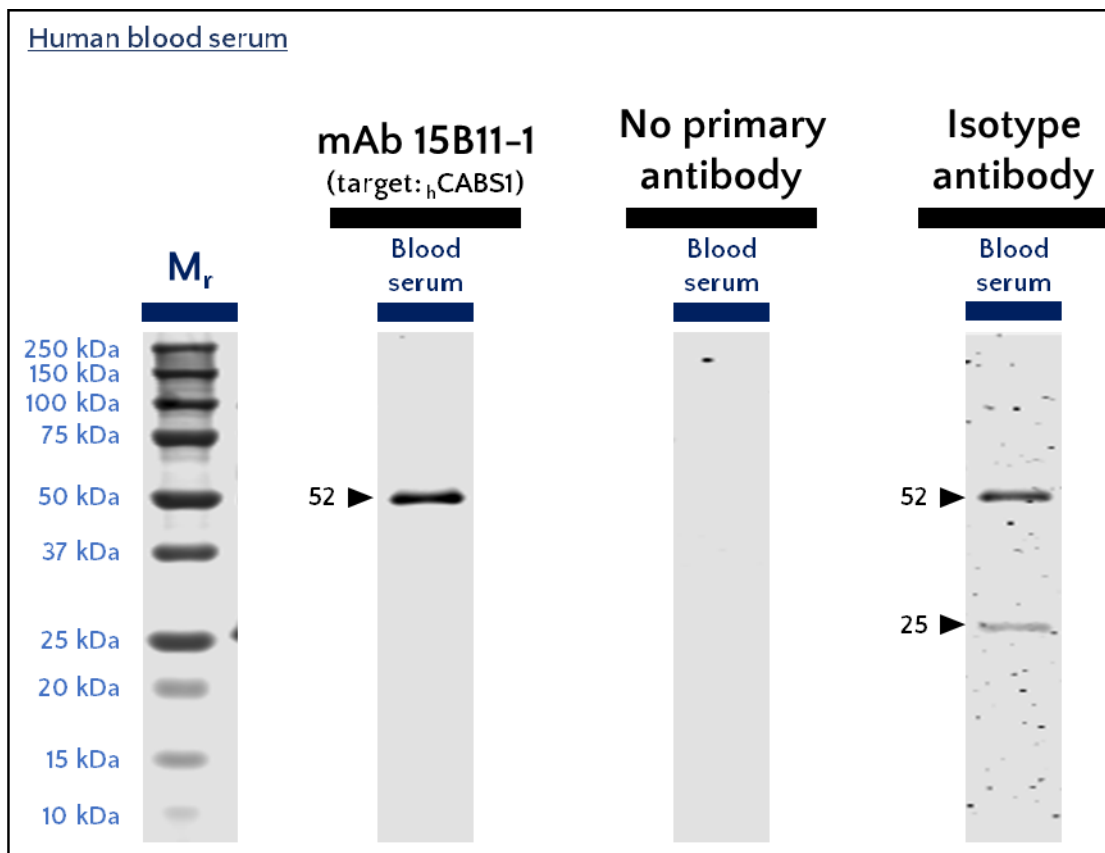
Figure 4-23. WB of human blood serum probed with monoclonal antibody (mAb) 15B11-1, and controls (no mAb and isotype antibody IgG1.κ).

A molecular mass reference (M_r) indicates the range of protein sizes in kilodaltons (kDa) that can be present along a lane. Molecular masses in kDa are shown next to arrows in black. All lanes were loaded with 1 μg total protein. Working antibody concentration for 15B11-1 and IgG1.κ was 10 ng/μL. Image is representative of three independent experiments for 15B11-1 and no primary antibody, and one experiment for IgG1.κ. The shown molecular masses are the average of 3 independent experiments where the same banding pattern was observed.

membrane with only secondary antibody (**Figure 4-23**). When probing with 13G3-1, WB experiments show two bands at 61 and 52 kDa. The 52 kDa band is also present when probing with isotype antibody IgG1.κ at the same working antibody concentration as 13G3-1. IgG1.κ also detects a band at 25 kDa. No signal is present when probing membrane only with secondary antibody (**Figure 4-24**). mAb 4D1-1 detects in blood serum two bands at 61 and 52 kDa, while its isotype antibody, IgG2α.κ, detects an analog band at 52 kDa. No signal is present when only probing with secondary antibody (**Figure 4-25**).
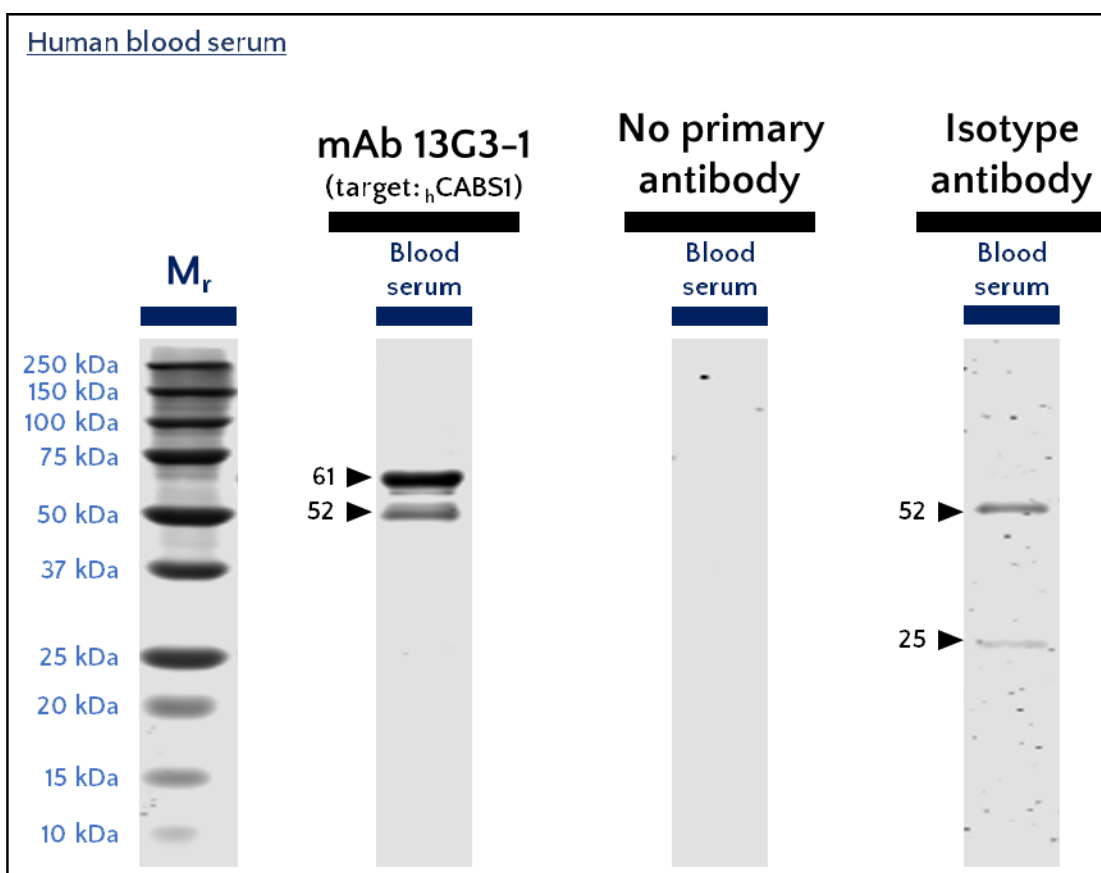
Figure 4-24. WB of human blood serum probed with monoclonal antibody (mAb) 13G3-1, and controls (no mAb and isotype antibody IgG1.κ).

A molecular mass reference (M_r) indicates the range of protein sizes in kilodaltons (kDa) that can be present along a lane. Molecular masses in kDa are shown next to arrows in black. All lanes were loaded with 1 μg total protein. Working antibody concentration for 13G3-1 and IgG1.κ was 10 ng/μL. Image is representative of three independent experiments for 13G3-1 and no primary antibody, and one experiment for IgG1.κ. The shown molecular masses are the average of 3 independent experiments where the same banding pattern was observed.

Figure 4-25. WB of human blood serum probed with monoclonal antibody (mAb) 4D1-1, and controls (no mAb and isotype antibody IgG2α.κ).

A molecular mass reference (M_r) indicates the range of protein sizes in kilodaltons (kDa) that can be present along a lane. Molecular masses in kDa are shown next to arrows in black. All lanes were loaded with 1 μg $_{total\ protein}$. Working antibody concentration for 4D1-1 and IgG2α.κ was 10 $^{ng}/_{μL}$. Image is representative of three independent experiments for 4D1-1 and no primary antibody, and one experiment for IgG2α.κ. The shown molecular masses are the average of 3 independent experiments where the same banding pattern was observed.

Immunohistochemical analysis of human testis

A pilot study on slides of human testis immunoprobed with antibody 15B11-1 shows presence of hCABS1 in Leydig cells in the interstitial space (**Figure 4-26**, arrow with line pattern), and precursors to primary spermatocytes inside seminiferous tubules (**Figure 4-26**, dark arrow). The signal generated by mAb 15B11-1 suggests that hCABS1 is present in the cytoplasm of these cells.
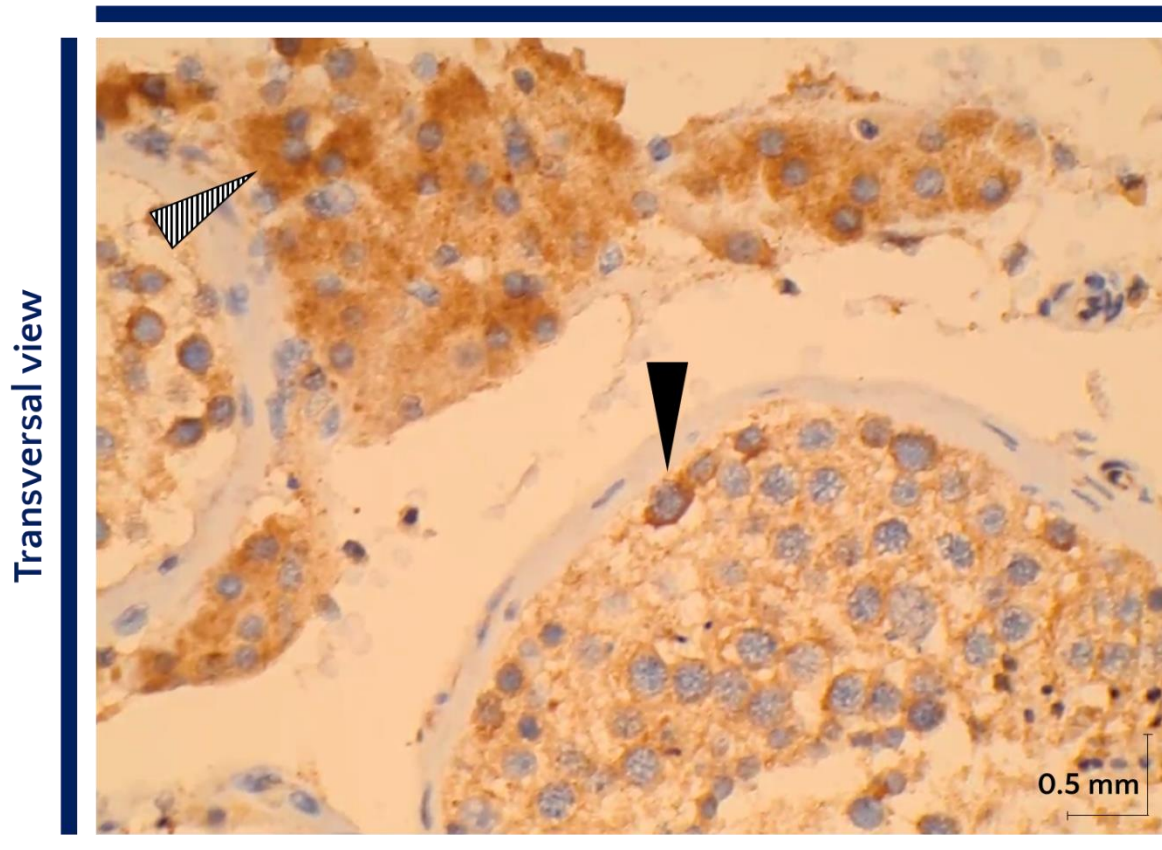
Figure 4-26. Human seminiferous tubules immunoprobed with mAb to hCABs1 15B11-1 (magnification: 200 X).

Brown signal is indicative of hCABS1 protein presence in cytoplasm of cells. Blue signal highlights cell nuclei. Cytoplasm in Leydig cells (arrow with line pattern) and primary spermatogonia (dark arrow) stains strongly for hCABS1. *Immunohistochemical experiment done by Ms. Sarah Canil. Image analysis done by Dr. Lakshmi Puttagunta*

Discussion

This chapter shows the banding pattern of our mAbs in WB in a transient $_r$hCABS1 overexpression cell lysate, its inherent negative control cell lysate, human submandibular gland lysates, saliva, and blood serum. In addition, the post-immunoprecipitation WB profiles of an in-house made $_r$hCABS1 overexpression cell lysate and saliva supernatant, and the first immunohistochemical analysis of human testicular tissue are shown. I employed the titration strategy for (a) antibody

and (b) sample amounts used in the most recent characterization of our pAbs (see Chapter 2 - After re-evaluation of previously established methodology). WB controls for our mAbs included: probing membranes with only the secondary antibody, and with isotype antibodies.

In transient hCABS1 overexpression cell lysates (OEL), a band at 78 kDa is reflective of recombinant ($_r$) hCABS1

In commercially bought CABS1 overexpression cell lysate (OEL), two bands stand out at 78 and 64 kDa. The 78 kDa band is detected by all mAbs targeting hCABS1 and a monoclonal anti-FLAG antibody[h], while the 64 kDa band is only detected by 13G3-1. Of note, the 64 kDa band was also detected by IgG1.κ, the isotype antibody of 13G3-1, albeit the signal is dimmer than that obtained when probing OEL with 13G3-1. A band at 53 kDa was detected by 15B11-1 and 13G3-1, but negative control cell lysate (NCL) detects a band of the same size, suggesting its signal is non-specific (see **Figure 4-7**, **Figure 4-8**, **Figure 4-9**, **Figure 4-10**). Thus, there is certainty that in commercially bought OEL, hCABS1 is present at 78 kDa and, potentially, at 64 kDa.

In-house made OEL also shows a band at 76 kDa when evaluated by all mAbs targeting hCABS1 and the anti-FLAG monoclonal antibody (see **Figure 4-12** A, **Figure 4-13** A, **Figure 4-14** A). An additional band at 54 kDa was detected by mAbs 15B11-1 and 13G3-1 but based on the comparison between commercially bought OEL and NCL, one can speculate that this band is non-specific (see **Figure 4-12** A, **Figure 4-13** A). Moreover, other groups have also reported non-specific immunoprecipitation of a protein at this location (~50 kDa) from HEK293 cell lysate samples[150]. Discrepancy between molecular masses between commercially bought and in-house made OEL can be attributed to the use of different molecular mass reference (M_r) standards between experiments. Overall, these data provide more certainty in that in our system, hCABS1 in OEL is present between 76-78 kDa.

---

[h] OEL produces a recombinant hCABS1 containing a FLAG sequence (a.a. DYKDDDK) adjacent to its carboxyl end.

Western blots of immunoprecipitated in-house $_r$hCABS1 OEL result in bands above 100 kDa that may represent $_r$hCABS1

Under our SDS-PAGE conditions, immunoprecipitation of $_r$hCABS1 from OEL should show in WB a band ~76 kDa. Indeed, untreated in-house made OEL probed with an anti-FLAG mAb shows a single band at that location (**Figure 4-12** A, **Figure 4-13** A, **Figure 4-14** A). However, a band detected at the top of the eluted post-IP protein lane, at 143, 117 and 104 kDa by 15B11-1, 13G3-1 and 4D1-1, respectively, may be representative of $_r$hCABS1 post-immunoprecipitation (**Figure 4-12** B, **Figure 4-13** B, **Figure 4-14** B). The discrepancy in molecular weights suggests that $_r$hCABS1 does not migrate in SDS-PAGE as intended. The first indication came from the WB pattern obtained from the first eluate post-bead addition, where a 76 kDa band, likely $_r$hCABS1, is present. This eluate is obtained after incubation of magnetic beads with the protein of interest bound to the capturing antibody. Theoretically, the magnetic beads coated in protein A/G bind to the capturing antibody creating the bead-antibody-protein of interest (b-a-POI) complex[151] (see **Figure 4-4** B). The first eluate post-bead addition should not contain protein of interest, since in theory it would be bound to the magnetic beads that are displaced close to the magnet, leaving an eluate free of protein of interest. At that point, there are two possibilities: (a) a fraction of hCABS1 is captured, while another is lost (the one present in this eluate), or (b) hCABS1 is not captured by our mAbs using this immunoprecipitation protocol.

Let us consider (a). The first wash of the b-a-POI complex results in presence of bands at either 25 or 54 kDa (**Figure 4-12** B, **Figure 4-14** B, respectively), and further washes show no bands. These two bands at 25 and 54 kDa, also detected in other wash eluates, are likely the capturing mAbs (15B11-1, 13G3-1, 4D1-1). Recall that in our WB system, we use a secondary antibody to bind to the primary antibody targeting the POI, and that our mAbs were raises in mice. The secondary antibody we use binds to mouse IgG heavy and light chain[152]. Thus, leftover capturing antibody that doesn't bind to magnetic beads is part of the first eluate post-bead addition, and when

preparing this eluate for SDS-PAGE we treat so that IgG is denatured and linearized, in turn, making it detectable by our secondary antibodies in WB at the molecular weight of IgG heavy and light chain[153]. This leaves putative hCABS1 bands, detected by 15B11-1 and 4D1-1 at 50 and 46 kDa, respectively. The predicted molecular mass of CABS1 is 43 kDa[66,147]. Other putative hCABS1 bands are detected at 143, 117 and 104 kDa by 15B11-1, 13G3-1 and 4D1-1, respectively. We suspect that the difference in molecular weight between untreated and post-IP $_r$hCABS1 OEL is due to unsuccessful release of $_r$hCABS1 from the capturing antibody. This speculation is partially backed up by mass spectrometry sequencing of b-a-POI complexes using 4D1-1 as a capturing antibody, where $_r$hCABS1 is detected, but no immunoglobulins (potentially from 4D1-1) are detected. Nevertheless, this MS-seq finding indicates that 4D1-1 is an antibody that our group can use in the future to immunoprecipitate hCABS1 from human-derived samples.

Western blots using mAbs targeting hCABS1 endorse that this protein is present in human submandibular gland

Our group has previously reported occurrence of *CABS1* transcript in SMG[18], and pAb-based WB indicated that the protein was also translated in this compartment (see reference [18] and **Figure 2-12**). Analysis of the complex profile obtained when performing pAb-based WB of SMG suggested that five variants of hCABS1 were present in that compartment, namely at ~ 70, 52, 47, 33 and 27 kDa (see **Figure 2-13**). However, mAb-based WB suggest that only three bands are reflective of hCABS1 in SMG. All our mAbs detect in SMG a band at 53 kDa, 13G3-1 and 4D1-1 detect a band at 63 kDa, and only 13G3-1 detects a band at 42 kDa (see **Figure 4-15**, **Figure 4-16**, **Figure 4-17**).

It appears that 13G3-1 and 4D1-1, which respectively target the carboxyl and amino termini of hCABS1, detect an extra variant at 63 kDa in SMG, but 15B11-1, which targets a middle region of hCABS1 does not detect this variant. Under our experimental conditions, samples are supplemented with DTT and SDS, then heated at 95°C with the intention of denaturing and

linearizing the proteins within, consequently exposing all epitopes. If the band at 63 kDa were a form of hCABS1, then all 3 antibodies should detect it. Is it possible that this variant has a modification that masks the middle segment from 15B11-1? Since 15B11-1 is a monoclonal antibody, it is expected that it will recognize a singular epitope. Antibodies recognize epitopes with a length between 9 and 22 amino acids[154], with exceptional cases of antibodies that can recognize 1 amino acid epitope[155]. If hCABS1 in SMG is expressed slightly differently at the specific location that 15B11-1 targets, then this mAb won't interact with hCABS1 in WB, despite the linearization of hCABS1. Our mAbs were created using the hCABS1 sequence reported in open access databases. To our knowledge, sequencing of hCABS1 gene or protein isolated from human SMG has not yet been done, but for human CABS1 alone, 1871 SNP variants have been reported in the database for single nucleotide polymorphisms (dbSNP) of the NCBI[156]. An analysis of these variants and the resulting protein would prove valuable for future prediction of hCABS1 variants, and potentially design of antibodies that target specific variants of hCABS1, if indeed they exist.

13G3-1 is the only antibody to detect a band at 42 kDa, a location that matches the predicted molecular weight of hCABS1[66,147]. While I was unable to isolate hCABS1 from SMG to be sequenced via mass spectrometry, work on immunoprecipitation using our mAbs may lead to successful sequencing of the protein from this compartment. Altogether, mAbs-based WB of SMG endorse the occurrence of hCABS1 in this compartment.

mAbs validation in one-dimensional SDS-PAGE followed by Western blot can't confirm that hCABS1 is present in human saliva supernatant

To validate that the signal we obtained in WB was reflective of hCABS1, we decided to probe membranes containing the same samples with (a) no primary antibody, only secondary goat anti-mouse antibody and (b) isotype antibodies to our mAbs. The WB profiles obtained when probing saliva supernatant with our mAbs, only secondary antibody, or isotype antibodies suggest that most bands detected in this biological fluid are not hCABS1.

While all 3 mAbs targeting hCABS1 consistently detect three bands in close proximity between 60 and 51 kDa, probing membranes with no primary antibody or isotype antibody deliver the same banding profile (see **Figure 4-18**, **Figure 4-19**, **Figure 4-20**). The presence of several bands with similar molecular weight may mask bands(s) reflective of hCABS1. One such abundant protein is IgG in saliva, which could account for the band at 56 kDa (heavy chain) detected by all our mAbs and for the 25 kDa band (light chain) detected by 15B11-1 and controls. Our secondary antibody, a goat anti-mouse antibody that targets heavy and light chains of mouse IgG_1, IgG_{2a}, IgG_{2b} and IgG_3[152], could be interacting with immunoglobulins in human saliva supernatant. The saliva supernatant sample used in these experiments comes from a 250 mL pool of saliva that was homogenized immediately before aliquoting. The average yield of IgG in saliva has been reported to be 2.65 $\mu g_{IgG}/mL_{saliva}$, and share comparable IgG profile to that of blood[157]. By that metric, our 250 mL pool could have contained 662.5 μg_{IgG}[152]. Contradicting this speculation is the fact Li-cor Biosciences, the company producing our secondary antibodies, cross absorbs the secondary antibodies against human to minimize cross-reactivity with human serum proteins[152]. Is it possible that saliva proteome contains proteins that share similar domains to those being targeted by the secondary antibodies (i.e., mouse IgG heavy chains)? A comparative analysis of proteins present in human and mouse saliva shows the existence of equivalent immunoglobulin chains in both organisms[158] (see reference [158], additional file 5 – rows 71, 72). Whether these proteins were used by Li-cor to generate their secondary antibodies is unknown, but if so, it may explain the cross-reactivity between saliva proteins and the secondary antibodies. Future work separating saliva supernatant via 2D-e, followed by WB could show if our mAbs detect several proteins in the range of 56-60 kDa, and comparison of the WB profiles with our controls may show which bands, if any, are representative of hCABS1. Nevertheless, current data on the bands we detect in human saliva supernatant is inconclusive and can't provide evidence that these bands are reflective of hCABS1.

Despite this appraisal, the presence of *CABS1* transcript[16,18] in salivary glands and protein in SMG[18,21] poses the question of whether CABS1 is present in saliva or not. Notice the band at 53 kDa detected by 15B11-1 and 51 kDa detected by 13G3-1 and 4D1-1. That band is not detected by the secondary antibody, and while present when probing with isotype antibodies, the signal is not as strong. Theorizing that these bands could be representative of hCABS1, we attempted to isolate hCABS1 from saliva supernatant via immunoprecipitation. As with OEL immunoprecipitation, bands at ~50 and 25 kDa are likely to be unbound (to magnetic beads) capturing antibody (see **Figure 4-21** B, **Figure 4-22** B). The outcome for both immunoprecipitations suggest that an abundance of capturing antibodies did bind to magnetic beads (**Figure 4-21** B, **Figure 4-22** B - smears at ~50 and 25 kDa). However, 13G3-1 shows the additional presence of two bands at 122 and 15 kDa (compare the 15 kDa bands between **Figure 4-21** A and B). To date, the identities of the proteins at those regions remains unsolved, but optimization of an immunoprecipitation protocol using mAb 4D1-1, which has successfully captured $_r$hCABS1 from cell lysate, and its use in saliva supernatant may validate the occurrence of hCABS1 in this compartment.

hCABS1 may be present in human serum as a single variant

The report of a single peptide encompassing 3.54% of hCABS1 sequence found in human plasma (see [159] - supplemental information PDF, row #811) supports our postulate that hCABS1 is present in blood. Our WB data further endorses this hypothesis, where mAbs 13G3-1 and 4D1-1 detect a band at 61 kDa (**Figure 4-24**, **Figure 4-25**), although 15B11-1 fails to detect it. This band could correspond to hCABS1 in blood, but as with SMG, the band is not detected with 15B11-1, the antibody targeting a middle segment of hCABS1. Why is it that the antibodies that target either end of the linearized hCABS1 protein detect the 61 kDa band and the 15B11-1, targeting a middle domain of hCABS1, does not? I postulate that the organ(s) releasing hCABS1 into the bloodstream express hCABS1 slightly differently that the canonical reported amino acid (a.a.) sequence. Recall that we generated our mAbs considering the reported hCABS1 a.a. sequence. A study of hCABS1 transcript expression across tissues would answer if the gene transcribes differently as a function

of the cells expressing it. The resulting protein(s) may have different function(s) depending on their location. Alternative splicing has been postulated as an evolution mechanism to remodel protein interactions depending on the tissues they are expressed in[160–162]. However, this hypothesis may not be correct, as *CABS1* gene has only one intron, harbored between the two exons that code for the protein. Currently unknown hCABS1 variants resulting from SNPs may be behind the inability of 15B11-1 to detect the 61 kDa band. Aside from these hypotheses, the 61 kDa band may also be reflective of human serum albumin (HSA), which accounts ~50% of the total serum proteome[163] and has a similar molecular weight, 66 kDa[164]. Under suboptimal conditions, HSA has been reported cross-react with monoclonal antibodies targeting different proteins[165].

All our mAbs detect a band at 52 kDa in serum (**Figure 4-23**, **Figure 4-24**, **Figure 4-25**). The 52 kDa band is also detected by isotype antibodies IgG1.κ (for 15B11-1 and 13G3-1) and IgG2α.κ (for 4D1-1) (**Figure 4-23**, **Figure 4-24**, **Figure 4-25**). Moreover, IgG1.κ picks up a band at 25 kDa (**Figure 4-23**, **Figure 4-24**). These bands at 52 and 25 kDa in isotype antibodies could reflect of an artifact explained by the affinity that mouse antibodies have for human immunoglobulins, which are abundant in serum. mAbs 15B11-1 and 13G3-1 are mouse-derived antibodies of subclass IgG1.κ, and mAb 4D1-1 is subclass IgG2α.κ. If the 52 and 25 kDa bands observed by isotype antibodies represent binding of our mAbs to heavy and light chains of immunoglobulins in human serum, our data suggests that contrary to what the supplier suggests, these mouse-derived antibodies cross-react with immunoglobulins present in human sera. Another explanation may be that mice, the host species that produced our antibodies, developed tolerance to their own CABS1 and that hCABS1 is a poor immunogen. Like with our pAbs (see Chapter 2 - Discussion - Rabbits, the host species that produced all our pAbs, also express CABS1), the hCABS1 peptides used for immunizing the mice to produce our mAbs have similarities to domains present in mouse CABS1 (**Figure 4-27**). However, these CABS1 sections share less continuous domains across species (human and mice) when compared to continuous sequences

shared between humans and rabbits (compare **Figure 2-24** with **Figure 4-27**, red boxes). Theoretically, GenScript's repeated immunogen boosts and use of adjuvant during mAb production should have induced antibody responses against hCABS1 peptides. Even so, it is possible that negative selection of B cells suppressed the existence of B cells that produced potent antibodies targeting hCABS1.

In stark contrast to the speculation about tolerization, another possibility to explain the occurrence of bands when probing with isotype antibodies is that mice might produce an autoantibody to endogenous CABS1. Natural autoantibodies have been reported in sera of normal humans[166] and mice[167]. If such an autoantibody exists in mice, due to the relative similarity of CABS1 overall sequence across species (**Figure 4-27**, 60.7%), this autoantibody could interact with human CABS1 in serum (see **Figure 4-23**, **Figure 4-24**, **Figure 4-25**, isotype antibody). Thus, the 52 kDa band in these figures could reflect hCABS1 if the mouse-derived isotype antibodies contain an autoantibody to CABS1.

Potential biomarkers in blood serum may be present in relative low abundance, and masked by dominant proteins like HSA and immunoglobulins[164]. Thus, I propose that future WB experiments of human serum deplete samples from HSA and immunoglobulins via relatively simple and validated methodologies[164,168] prior to probing for hCABS1. Serum samples depleted from HSA and immunoglobulins should be probed with our mAbs to hCABS1, only secondary antibody, and isotype antibodies and WB profiles should be compared with those reported in this dissertation (**Figure 4-23**, **Figure 4-24**, **Figure 4-25**).
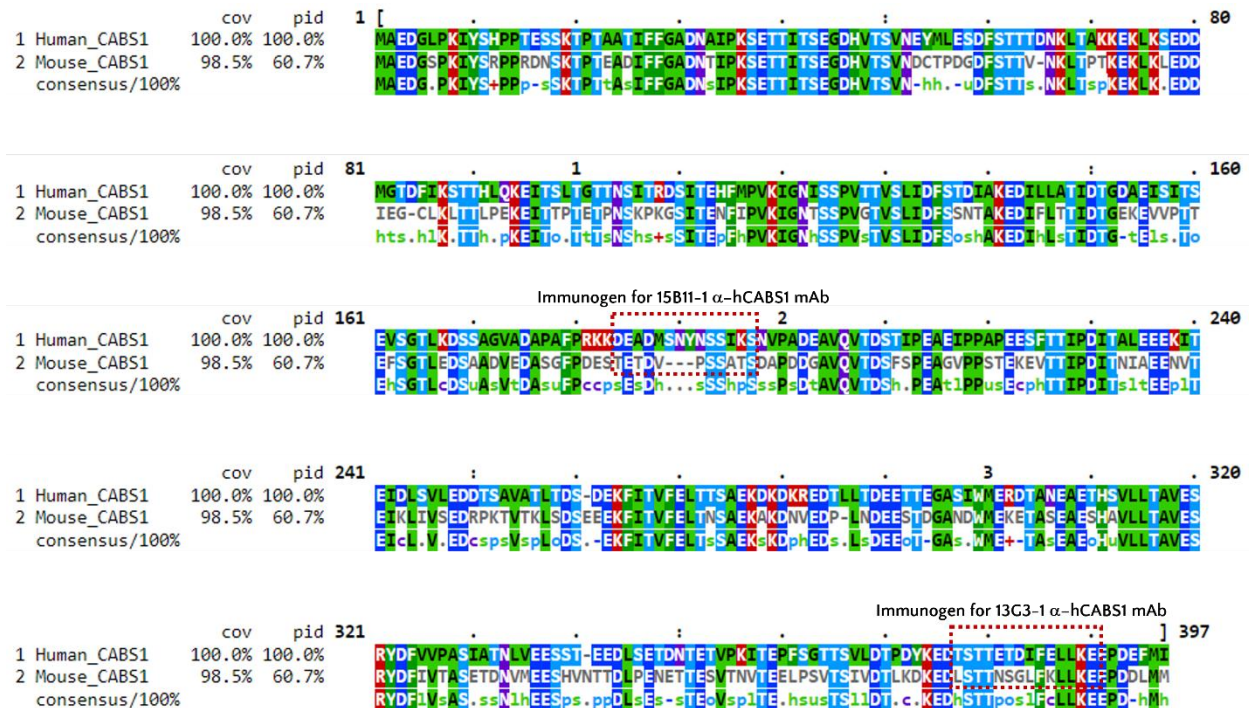
Figure 4-27. Sequence alignment of human (h, *Homo sapiens*) CABS1 and mouse (m, *Mus musculus*) CABS1.

hCABS1 is used as the reference sequence. mCABS1 covers 98.5% of hCABS1 length. However, the percentage of residues that are the same in mCABS1 with respect to hCABS1 is 60.7%. Residues enclosed in red dotted boxes indicate sections of hCABS1 used to produce monoclonal antibodies 15B11-1 and 13G3-1 in BALB/c mice. Consensus row at 100% consensus threshold shows sets of residues that are either the same across both species, or share a predefined physicochemical property. Consensus patterns (%) are based on sets of residues that share a predefined property based on the classification by W.R. Taylor. u: tiny, s: small, h: hydrophobic, p: polar

Immunohistochemical analysis of human testis indicate a different localization of hCABS1 than the one described in animal models

While hCABS1 signal seems to be present in cytoplasm of cells throughout seminiferous tubules (**Figure 4-26** lower right), the signal dramatically increases in cells immediately adjacent to the basal lamina (**Figure 4-26**, dark arrow). These strongly stained cells are likely primary spermatogonia, typically found near the basal lamina of seminiferous tubules, and characterized by an oval nuclei with condensed chromatin[169]. These cells derive from undifferentiated diploid germ cells, maintain a diploid nature, and undergo further mitotic divisions to produce primary spermatocytes[169]. Contrastingly, in mice, CABS1 protein stains with greater intensity in elongated

spermatids located close to the lumen, and not the basal lamina, of seminiferous tubules[4,11] (see reference [4] – Figure 5 e, f, and reference [11] – Figure 1 F). The same trend is observed in rat testis, where cytoplasm of spermatozoa close to the lumen of seminiferous tubules shows an abundant presence of CABS1[1] (referred to as CLPH, see reference [1] – Figure 4 C, D) and in pig testis[5] (see reference [5] – Figure 4 A, B, C). In animal models, cells staining for CABS1 suggest that this protein is present in haploid cells, as opposed to diploid cells (which our human data suggests). Overall, immunohistochemical experiments in animal models suggest that CABS1 protein is only present in elongated spermatids close to the lumen of seminiferous tubules, while our pilot study indicates that CABS1 protein in human seminiferous tubules is more abundant in Sertoli cells adjacent to the basal lamina of seminiferous tubules.

Our data also indicates that CABS1 protein is present in the interstitial space of testis, specifically in the cytoplasm of Leydig cells (**Figure 4-26**, arrow with line pattern). Leydig cells reside in the testicular interstitium and synthesize and secrete androgen hormones that are necessary for production and maturation of spermatogenic cells[169]. In mouse, rat and pig immunohistochemical analyses, CABS1 is present exclusively inside seminiferous tubules, and not in the testicular interstitium[1,4,5,11]. A potential reason that could account for discrepancy between our staining in human testis and the staining observed in animal testis is that the testicle slide used for this pilot study is representative of a male subject with an unknown malady. Thus, we recognize the human testis image we show here may not represent what occurs in a healthy testis. Further optimization of immunohistochemical methodologies in human-derived tissues will provide insight on the localization of CABS1 in the human body. Nevertheless, the presence of hCABS1 in Leydig cells is exciting. The main function of Leydig cells is to produce the androgen testosterone when luteinizing hormone (LH) is present. Whether hCABS1 expression is under control of LH and plays a role in production of testosterone remains to be elucidated.

Anomalous migration of CABS1 in SDS-PAGE may be a result of its unusual nature

Surprisingly, WB of CABS1 protein identified several forms in rodent[1,4], porcine[5] and human-derived[18,21] samples ranging from 11 to 80 kDa, given that CABS1 predicted molecular weight (MW) is ~43 kDa across species. Anomalous migration of hCABS1 in SDS-PAGE may be because of glycosylation and phosphorylation events, presence of proline residues, of acidic residues, of metal ions bound to hCABS1 during SDS-PAGE, and of intrinsically disordered domains.

Glycosylation of proteins can significantly alter apparent MW. Initial evidence suggests that hCABS1 is not glycosylated[18]; however, this should be corroborated. Moreover, rat CABS1 is target of phosphorylation[1] and human CABS1 is predicted to have phosphorylation sites[147], but these are unlikely to account for a significant MW change.

Aside from post-translational modifications, metal ions attached to hCABS1 may account for the difference between predicted and observed MW. SDS-PAGE of mouse testis-derived CABS1 appears at different molecular weights when bound, or not, to calcium ion (Ca^{2+} presence: 58 kDa, Ca^{2+} absence: 66 kDa)[4]. Like CABS1, Histidine-rich Ca^{2+}-binding protein (HCP) also exhibits anomalous migration under SDS-PAGE. It is speculated that Ca^{2+}-bound HCP is more compact than Ca^{2+}-unbound HCP[170]. This results in an accelerated migration in SDS-PAGE, in turn exhibiting a lower molecular weight[170]. Moreover, *Arabidopsis thaliana* calmodulins exposed to Ca^{2+} and separated via SDS-PAGE resolve to lower molecular weights when compared to Ca^{2+}-depleted fractions separated under the same conditions[171]. These findings agree with Kawashima et al. findings on mouse CABS1, where absence of bound Ca^{2+} results in higher molecular weight. The interaction of CABS1 with Ca^{2+} may differ across species. An EF-hand, a protein motif with great affinity for calcium ion, seems to be responsible in rats[1], while in other species the interaction is predicted to be via the high proportion of negatively charged amino acids[4,147]. While human-derived CABS1 has not been assessed for calcium binding, our computational analyses suggest that it has a calcium binding domain, which may play a role in generating different-sized

bands[147]. It is possible that under our SDS-PAGE methodology some interactions between metallic ions, like calcium, and hCABS1 in our samples are not entirely disrupted, resulting in hCABS1 variants still bound to Ca^{2+}. MW discrepancy could also be on account of a high proportion of negatively charged amino acids within hCABS1, which may confer overall negative charge to domains within the sequence. Such domains prevent proper binding of SDS to polypeptides and result in slower migration of a protein under SDS-PAGE denatured conditions[2,172].

Anomalous migration in SDS-PAGE has also been observed in proline-rich proteins (PRP)[173,174]. It is speculated that prolines affect SDS binding to proteins[175]. Prolines are 5.1% of the amino acids in hCABS1, and while they may play a role in anomalous migration, their contribution may be minimal. For comparison, a recombinant PRP, bPRP23, contained 36% prolines, had a predicted MW of 23 kDa, but an observed MW of 33 kDa[174]. Other known PRP contain far more prolines than hCABS1; for instance, basic salivary proline-rich protein 2 and salivary acidic proline-rich phosphoprotein 1/2 contain 25 and 37% prolines within their sequences, respectively. Research is needed to confirm or refute the role that prolines may play in hCABS1 SDS-PAGE migration.

Another reason is that CABS1 contains disordered domains, protein segments that lack a fixed conformation[1,147]. Disordered regions could account for discrepancies between predicted and larger observed MW[1]. With regards to smaller MW forms of CABS1, i*n silico* analysis of human CABS1 suggests an overlap between disordered and elastase-susceptible domains[147]. Disordered proteins allow exposure of protease-prone regions, as has been shown for rat CABS1[1], and could facilitate cleavage to produce multiple lower kDa CABS1 polypeptides. Thus, CABS1, just as SMR1, may be a precursor of several polypeptides with distinct biological functions.

Taken together, proteolytic sensitivity of hCABS1 on account of intrinsically disordered domains, reduced binding to SDS because of negatively charged amino acids, and potential to be bound to

Ca2+ or other metallic ions while in SDS-PAGE may be involved in the anomalous migration of hCABS1 in SDS-PAGE.

Summation: WB profiles of monoclonal antibodies

In our WB system, bands that are considered to represent hCABS1 are (by sample): in OEL at 77 and 64 kDa, in SMG at 63, 53 and 42 kDa, no bands in saliva when considering controls, and in serum a band at 61 kDa (**Table 4-5**, samples listed by column from left to right). Overall, only a band averaged at 63 kDa occurred in OEL, SMG and serum. Other bands seemed to be sample-specific. These are: two bands in SMG at 52 and 42 kDa, and a single band at 77 kDa in OEL (**Table 4-5**, two rightmost columns).

We speculate that the molecular weight difference between the bands reported above and those observed when doing WB using our pAbs to hCABS1 (see **Table 2-4**) is due to the evolving WB methodologies, shift in method to calculate molecular weight of bands, and use of different molecular mass reference (M_r) ladders. An overall appraisal of mAbs and pAbs WB band profiles is found in "Chapter 5: Debriefing – What Western blot profiles of pAbs and mAbs targeting hCABS1 indicate".

Table 4-5. Average molecular weights (MW) detected by mAbs targeting hCABS1 per sample.

Each cell represents the mean of a band's molecular weight in kilodaltons (kDa) detected by mAbs described in this chapter at, putatively, the same region. The final column contains the average MW of bands across samples.

Transient overexpression cell lysate controls

hCABS1 OEL commercial	hCABS1 OEL in-house Average MW (kDa)	NCL	hCABS1 OEL excluding NCL-detected bands Average MW (kDa)
78	76	-	77
64	-	-	64
-	-	-	
-	-	-	
51	54	53	
47	-	47	
-	-	-	
-	-	38	
-	-	33	
-	-	31	
-	-	-	
-	-	-	

Human submandibular gland (SMG)

SMG with appraisal of controls Average MW (kDa)
63
53
42

Human saliva

Saliva w/o appraisal of controls	Saliva with appraisal of controls
Average MW (kDa)	
59	-
56	-
52	-
25	-
15	-

Human serum

Serum w/o appraisal of controls	Serum with appraisal of controls
Average MW (kDa)	
61	61
52	-

All bands with appraisal of controls Average MW (kDa)	Sample(s) where band occurs
77	OEL
63	OEL, SMG, serum
52	SMG
42	SMG

Chapter 5 : Debriefing – What Western blot profiles of pAbs and mAbs targeting hCABS1 indicate

> Five years elapsed between the experiments shown in Chapter 2 and those shown in Chapter 4. During that period, refinements in methodology, use of different molecular mass references (M_r), and switch from a Li-cor molecular mass calculator to calculating band sizes (kDa) myself (see **Figure 4-6**) may have collectively influenced the varying molecular weights reported in this dissertation. However, the number of bands spread throughout a similar region in WB is similar across experiments.

The complexity of WB banding profiles observed across samples when probing for hCABS1 using pAbs led to careful revision of the methodology used to validate our novel mAbs. The International Working Group for Antibody Validation recommended four strategies to ensure that readout of antibody-dependent experiments, like WB, was reflective of the protein of interest (POI) being targeted. Particular to WB, the strategies are: (1) altering POI expression via genome editing/RNAi prior to WB, (2) use of mass spectrometry sequencing (MS-seq) to validate that a given WB signal (band) reflects occurrence of POI in a given sample, (3) comparing and contrasting WB profiles from two or more antibodies targeting the POI, and (4) modification of POI by addition of labelling tag and use of a tag-specific antibody in WB[176]. In our case, most samples are human-derived, and to date we have not found a cell line that endogenously expresses CABS1. Thus, we did not contemplate the use of genome editing strategies but diligently followed strategies (2) – (4). In most recent experiments, namely WB of serum and saliva using pAbs and all mAbs WB, we incorporated titration of (a) sample amount loaded in SDS-PAGE lanes, and (b) probing antibody amount used in WB.

In our WB system, when accounting for controls, profiles of optimized methodologies, and exclusion of inconsistent bands, pAbs targeting hCABS1 detect sample-specific bands at averaged molecular weights of 139 (serum), 84 (hCABS1 overexpression cell lysate, OEL), 52 (submandibular glands lysate, SMG), 47 (SMG), 33 (SMG) and 27 (SMG) kDa. In saliva and serum, pAbs detect two bands at 91 and 64 kDa, and a band at 70 kDa is detected in OEL, SMG, and serum (**Table 5-1**, left). Conversely, our mAbs detect less bands when accounting controls.

Four bands are sample-specific at 77 (OEL), 52 (SMG) and 42 (SMG) kDa, and a band at 63 kDa is detected in OEL, SMG, and serum (**Table 5-1**, right).

OEL produced a recombinant hCABS1 protein containing a Myc-FLAG tag adjacent to its carboxyl terminus (see **Figure 2-1**). WB using an anti-FLAG monoclonal antibody yielded bands at average molecular weights of 84 and 70 kDa with pAbs, and 77 and 63 kDa when comparing WB profiles using mAbs. Use of a labelling tag in hCABS1 and validation of WB profile using a tag-directed antibody (strategy 4[176]) reassures that these bands are representative of hCABS1 in our WB system. We speculate that difference between molecular weights (7 kDa; e.g., 84-77 = 7) may be a result of using different molecular mass reference (M_r) markers across experiments (see [177]). It is interesting that said bands (**Table 5-1**, blue cells) are encountered in the same samples, namely OEL, SMG and serum, when using different antibodies. We speculate that SMG-specific bands detected at 52 and 47 kDa by pAbs, and 52 and 42 kDa by mAbs (**Table 5-1**, orange cells) correspond to the same proteins, but lack evidence to prove this. All pAbs targeting hCABS1 synthesized by GenScript were affinity purified against the immunogen used to produce each antibody. Conversely, mAbs were captured from hybridoma supernatants via protein A/G. The existence of antibodies that theoretically target the same domain within hCABS1 and identify WB bands at putatively equivalent regions provides further confidence that those bands represent hCABS1 in a given sample.

Altogether, WB evidence provided in this dissertation suggests that in humans hCABS1 is present beyond the testicular compartment in blood serum and in SMG of both sexes (see **Figure 4-15**, **Figure 4-16**, **Figure 4-17**). MS-seq data on human-derived samples could validate these observations. Alas, we have not successfully sequenced hCABS1 from human-derived samples to date. The only sample that has shown hCABS1 occurrence is OEL (see **Figure 2-11**). Firstly, studies on blood serum depleted of abundant proteins HSA and immunoglobulins (see Chapter 4 - Discussion - hCABS1 may be present in human serum as a single) may facilitate successful

sequencing of hCABS1 in serum. Furthermore, MS-seq data of SMG could validate the occurrence of hCABS1 in that compartment. With the advent of an immunoprecipitation (IP) protocol using our mAbs, use of (a) SMG IP followed by WB to identify location of POI in SDS-PAGE gels, and (b) IP followed by MS-seq, we could validate that SMG-derived bands at those locations are representative of hCABS1.

Table 5-1. Observed Western blot bands (averaged) when probing samples with polyclonal and monoclonal antibodies targeting human Calcium-binding protein, spermatid-associated 1 (hCABS1).

Blue cells indicate bands that likely correspond to the same protein across antibodies despite different molecular weights (MW) in kilodaltons (kDa). Orange cells indicate bands that could correspond to the same protein. OEL: hCABS1 overexpression cell lysate, SMG: submandibular glands lysate. *In a capillary nano-immunoassay platform, pAbs detect OEL-derived peaks at (a) 94 and (b) 65 kDa, and saliva-derived peaks at (c) 60 and (d) 34 kDa.

Polyclonal antibodies (target: hCABS1)		Monoclonal antibodies (target: hCABS1)	
All bands — Average MW (kDa)	Sample(s) where band occurs	All bands with appraisal of controls — Average MW (kDa)	Sample(s) where band occurs
139	Serum		
91	Saliva, serum		
84 *a	OEL	77	OEL
70 *b	OEL, SMG, serum	63	OEL, SMG, serum
64 *c	Saliva, serum		
52	SMG	52	SMG
47	SMG	42	SMG
33	SMG		
27 *d	SMG		

Chapter 6 : Structural and post-translational analysis of human calcium-binding protein, spermatid-associated 1

Preamble

Monday, March 21, 2022

To whom it may concern,

We fully support that the article presented in this chapter of Eduardo's PhD thesis contains computational analyses of human Calcium-binding protein, spermatid associated 1 (hCABS1) performed by Dr Marcelo Marcet-Palacios.

This article came to be because of initial in silico work on the disordered nature of hCABS1 performed by Eduardo Reyes-Serratos. Dr Marcelo Marcet-Palacios encouraged the development of this project and, along with Eduardo, expanded the analysis using proteomic tools to understand the nature of hCABS1.

Eduardo wrote the Materials and Methods section and performed the amino acid sequence conservation analysis of CABS1 across species in its entirety. He provided its interpretation in the Results and Discussion sections, Figure 3, Supplemental Figure 1, Table 1, and Supplemental Table 1. Subsequent editorial revisions to the entire article between Dr Marcet-Palacios, Dr Befus, and Eduardo led to the submission of the manuscript to the Journal of Cellular Biochemistry.
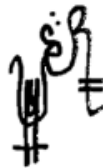
Respectfully yours,

Marcelo Marcet-Palacios
Assistant Adjunct Professor
Department of Medicine
Division of Endocrinology and Metabolism
University of Alberta

A. Dean Befus
Professor Emeritus
Department of Medicine
Alberta Respiratory Centre
University of Alberta

Eduardo Reyes Serratos
PhD Candidate
Department of Medicine
Alberta Respiratory Centre
University of Alberta

A version of this chapter has been published as:

Marcet-Palacios, M., **Reyes-Serratos, E.**, Gonshor, A., Buck, R., Lacy, P., Befus, A.D. (2020). Structural and post-translational analysis of human calcium-binding protein, spermatid-associated 1. *Journal of Cellular Biochemistry*, 121 (12), 4945-4958. https://doi.org/10.1002/jcb.29824

Title: Structural and Post-Translational Analysis of Human Calcium Binding Protein, Spermatid Associated 1.

Running Title: In Silico analysis of Human CABS1

Authors: Marcelo Marcet-Palacios[*][ψ], Eduardo Reyes-Serratos[*], Aron Gonshor[ξ], Robert Buck[ξ], Paige Lacy[*] and A. Dean Befus[*].

Affiliations: [*] University of Alberta, Alberta Respiratory Centre, Department of Medicine, Edmonton, AB. Canada. [ψ] Northern Alberta Institute of Technology, Biological Sciences, Edmonton, AB. Canada. [ξ] GB Diagnostics, 4980 Glencairn Avenue, Montreal, QC, Canada, H3W 2B2.

Corresponding author: Marcelo Marcet-Palacios. University of Alberta, 569 Heritage Medical Research Center. Edmonton, AB. Canada. T6G 2S2. marcelo@ualberta.ca

Abstract

Recently, we detected a novel biomarker in human saliva called calcium binding protein, spermatid-associated 1 (CABS1). CABS1 protein had previously been described only in testis, and little was known of its characteristics other than it was considered a structurally disordered protein. Levels of human CABS1 (hCABS1) in saliva correlate with stress, while smaller sized forms of hCABS1 in saliva are associated with resilience to stress. Interestingly, hCABS1 also has an anti-inflammatory peptide sequence near its carboxyl terminus, similar to that of a rat prohormone, submandibular rat 1 (SMR1). We performed phylogenetic and sequence analysis of hCABS1. We found that from 72 CABS1 sequences currently annotated in the National Center for Biotechnology Information protein database, only 14 contain the anti-inflammatory domain 'TxIFELL", all of which are primates. We performed structural unfoldability analysis using PONDER and FoldIndex and discovered 3 domains that are highly disordered. Predictions of 3-dimensional structure of hCABS1 using RaptorX, IonCom and I-TASSER software agreed with these findings. Predicted neutrophil elastase cleavage density also correlated with hCABS1 regions of high structural disorder. Ligand binding prediction identified Ca^{2+}, Mg^{2+}, Zn^{2+}, leucine and thiamine pyrophosphate, a pattern observed in enzymes associated with energy metabolism and mitochondrial localization. These new observations on hCABS1 raise intriguing questions about the interconnection between the autonomic nervous system, stress and the immune system. However, the precise molecular mechanisms involved in the complex biology of hCABS1 remain unclear. We provide a detailed *in-silico* analysis of relevant aspects of the structure and function of hCABS1 and postulate extracellular and intracellular roles.

Keywords: Disordered domains, CABS1, anti-inflammatory peptides, Post-translational processing, stress, resilience, *in-silico* analysis, I-TASSER, IonCom, and RaptorX.

Author contributions: All 6 authors contributed conceptually and in the design of the study. The document was written primarily by Marcelo Marcet-Palacios with contributions from Eduardo Reyes-Serratos and Paige Lacy. All figures were created by Marcelo Marcet-Palacios and Eduardo Reyes-Serratos. All authors provided editorial contributions.

Introduction

The central nervous system (CNS) has bidirectional communications with the peripheral nervous system, which in turn has functional connections with the immune/inflammatory system. To investigate the interaction between the sympathetic nervous system and the inflammatory response, we developed an animal model that involved bilateral decentralization of the superior cervical ganglia in rats, followed by an assessment of its effects on inflammation[20]. Among the observed outcomes was a marked reduction of pulmonary inflammation, including a reduction in alveolar macrophage and neutrophil influx into the airways. In experiments to understand the mechanisms involved following decentralization, we found that removal of submandibular glands (SMG) in male rats abolished the anti-inflammatory effects[31]. It was postulated that the SMG released an anti-inflammatory factor(s) and that this process was controlled by cervical sympathetic nerves[31].

Salivary glands have both exocrine and endocrine functions, with both local and systemic effects, such as in the liver[178] and mammary glands[179]. To identify the anti-inflammatory factor(s) released by SMG, we obtained extracts from rat SMG and purified a seven-amino acid peptide (TDIFEGG) using reverse phase HPLC[135] that had anti-inflammatory activity. This heptapeptide was identified within the prohormone submandibular rat 1 (SMR1)[44,135,143]. SMR1 had originally been identified in rat SMG[180] and the mRNA was localized to acinar cells[93]. Other peptides have been identified from different regions of SMR1 prohormone, including the undecapeptide VRGPRRQHNPR, hexapeptide RQHNPR and a pentapeptide QHNPR[54]. The authors established that, while the

undecapeptide and hexapeptide were found within the SMG, the pentapeptide was only found in the submandibular secretions from the primary excretory ducts, suggesting that some SMR1 proteolytic processing took place outside of the gland[54]. Treatment of rats with the sympathomimetic hormone, epinephrine, induced the presence of the hexapeptide in blood, and this was blocked by ligature of SMG ducts and blood vessels, indicating that the origin of the hexapeptide was the SMG[54]. Over the following decade, numerous reports identified several anti-inflammatory and anti-allergenic roles of SMR1-derived TDIFEGG and its derivatives in mice, rats, and sheep[51].

SMR1 is not expressed in the human genome, but a similar sequence to the SMR1 heptapeptide, TDIFEGG, is present in human calcium binding protein, spermatid-associated 1 (hCABS1), namely TDIFELL[18]. This sequence and its derivatives have anti-inflammatory activity in mouse and rat models[18]. Interestingly, several molecular forms of hCABS1 have been found in human testes, lungs, salivary gland extracts and saliva[18,21]. To determine if hCABS1 is under neural control as SMR1 is, we investigated the relationship between levels of molecular forms of hCABS1 in saliva during acute and prolonged stress[21]. We detected a 27 kDa form of hCABS1 in saliva that correlated with increased self-perceived stress, and smaller molecular forms ($\leq$20 kDa) associated with resilience to stress, data suggesting that hCABS1 is a biomarker of stress[21].

Although there has been significant progress in understanding the expression of hCABS1 and its relationship with stress, numerous unanswered questions surround the biology of this novel biomarker. This manuscript focuses on *in silico* analyses of hCABS1, including its highly disordered nature, location of Ca^{2+}, Mg^{2+}, Zn^{2+}, leucine and TPP (thiamine pyrophosphate, or vitamin B1) binding domains, posttranslational modifications like phosphorylation, catalytic processing by neutrophil elastase and components of the phylogeny of the putative anti-inflammatory peptide sequence. In addition, there is an in-depth analysis of how factors that may bind hCABS1 could participate in its putative extracellular and intracellular roles, including in

undiscovered enzymatic roles of hCABS1 intracellularly, perhaps linked to mitochondrial function.

Materials and Methods

The amino acid sequence of human CABS1 was retrieved from the annotation recorded in the Universal Protein Resource Knowledgebase, Q96KC9, and inputted into each of the predictive software described below.

CABS1 structural disordered domain prediction

The FoldIndex algorithm[181] was downloaded as a script from the developer's website and run using a Python interface. Output was a set of unfoldability predictor values of each individual amino acid based on the equation described by Prilusky *et al.*[181] which aims to discriminate between folded and intrinsically unfolded proteins. We also used the PONDR[182] (Predictor of Natural Disordered Regions) online web server. In this interface, we selected 5 algorithms, which generate scores aimed to elucidate disordered domains in a given amino acid sequence. These algorithms are VSL2, VL3, VL-XT, XL1-XT and CaN-XT. Output of each algorithm was given as a set of scores of each individual amino acid. Data obtained from FoldIndex and PONDR were used to generate graphs showing each algorithm's predictor values/scores (y-axis) for every sequence of 10 amino acids (x-axis).

3-dimensional structural prediction approaches

We used I-TASSER[183], IonCom[184], and RaptorX[185] online web servers to predict the 3-dimensional structures of hCABS1. I-TASSER provided additional information on putative cofactor-binding domains. IonCom provided additional information on presumed ion-binding domains. 3D files were downloaded from these servers in pdb format. We used PyMol[186] v.1.7.6.0 to generate visual representations of the hCABS1 molecule based on the information provided by NetPhos and

PeptideCutter, as well as to visualize the output from I-TASSER, IonCom, RaptorX. All 3D models were validated with ProSA[187] and ERRAT[188]. SwissDock was used to validate I-TASSER ligand binding predictions for TPP.

Post-translational modification analysis

We used NetPhos[189] online web server to predict serine, threonine or tyrosine phosphorylation sites in hCABS1. To predict protein kinase CK2 targets, we used Group-based Prediction System ver. 5.0[190]. To predict neutrophil elastase digestion, we utilized PeptideCutter from ExPASy.

Extracellular secretion signal peptide analysis

We used SignalP 5.0[191] web server to assess whether hCABS1 contained signal peptides.

Amino acid sequence conservation analysis

We obtained all 72 animal Calcium-binding protein, spermatid-associated (or specific) 1 annotated sequences from the protein database of the National Center for Biotechnology Information (NCBI) (**Supplemental file 1 available on the online version of this article**). We excluded sequences that were listed as 'predicted' or 'low quality'. All sequences were inputted in FASTA format into the EMBL-EBI Clustal Omega multiple sequence alignment online tool[192,193]. After online analysis, we downloaded the alignment file to visualize it on Jalview[194] v. 2.11.0.

We performed a phylogenetic analysis using the online platform www.phylogeny.fr[195], which has a pipeline that uses the MUSCLE algorithm to align sequences[196], followed by the GBlocks method to eliminate poorly aligned positions and divergent regions[197]. Refined sequences were inputted into PhyML for tree construction using a Maximum-likelihood method[198] and finally sent to TreeDyn, a software that renders the phylogenetic tree[199].

We used the Protein Variability Server[200,201] to calculate Shannon entropy values, a widely used measurement of randomness of a given data set that evaluates the conservation of amino acid

sequences[202]. For this analysis, we excluded one species that had significant insertions (*Tupaia chinensis)* in CABS1 and three species with significant deletions (*Heterocephalus glaber*, *Dasypus novemcintus* and *Fukomys damarensis*). All other species (n = 68) were aligned in Clustal Omega and a Jalview file was downloaded. Once aligned in Jalview in a way that flanking regions were shown, we selected from the most prevalent beginning of the protein (residue 20) to the most prevalent end of the protein (residue 438) and generated a FASTA file (**Supplemental file 1**). The file was then uploaded to the online PVS server and we obtained Shannon entropy graphs (see **Figure 6-4**).

Results

Assessment of hCABS1 structural unfoldability

Early postulates on hCABS1 biology have been developed from work done on other species. Rat CABS1, for example, is intrinsically disordered, explaining its hypersensitivity to proteolytic degradation[1]. Rat and hCABS1 contain similar high proportions of acidic amino acids, also a feature of intrinsically disordered proteins[1]. Thus, we postulated that hCABS1 is an intrinsically disordered protein. To further test this postulate, we performed structural unfoldability analysis of hCABS1 using two independent approaches (**Figure 6-1**). The predictor of naturally disordered regions (PONDR) software utilizes several neural networks that were trained by using well-documented disordered regions from several proteins[182]. We used five of these systems independently (VLXT, XL1_XT, CAN_XT, VL3 and VSL2) to increase the rigor of our analysis. The predicted disorder probability was plotted as PONDR Score (**Figure 6-1** A). Areas where all five neural network predictions agreed on positive values are highlighted under the curves. A hCABS1 model was created to depict the relative location of disordered regions within residues 35-42, 210-247, 286-302 and 332-360 (**Figure 6-1** A).
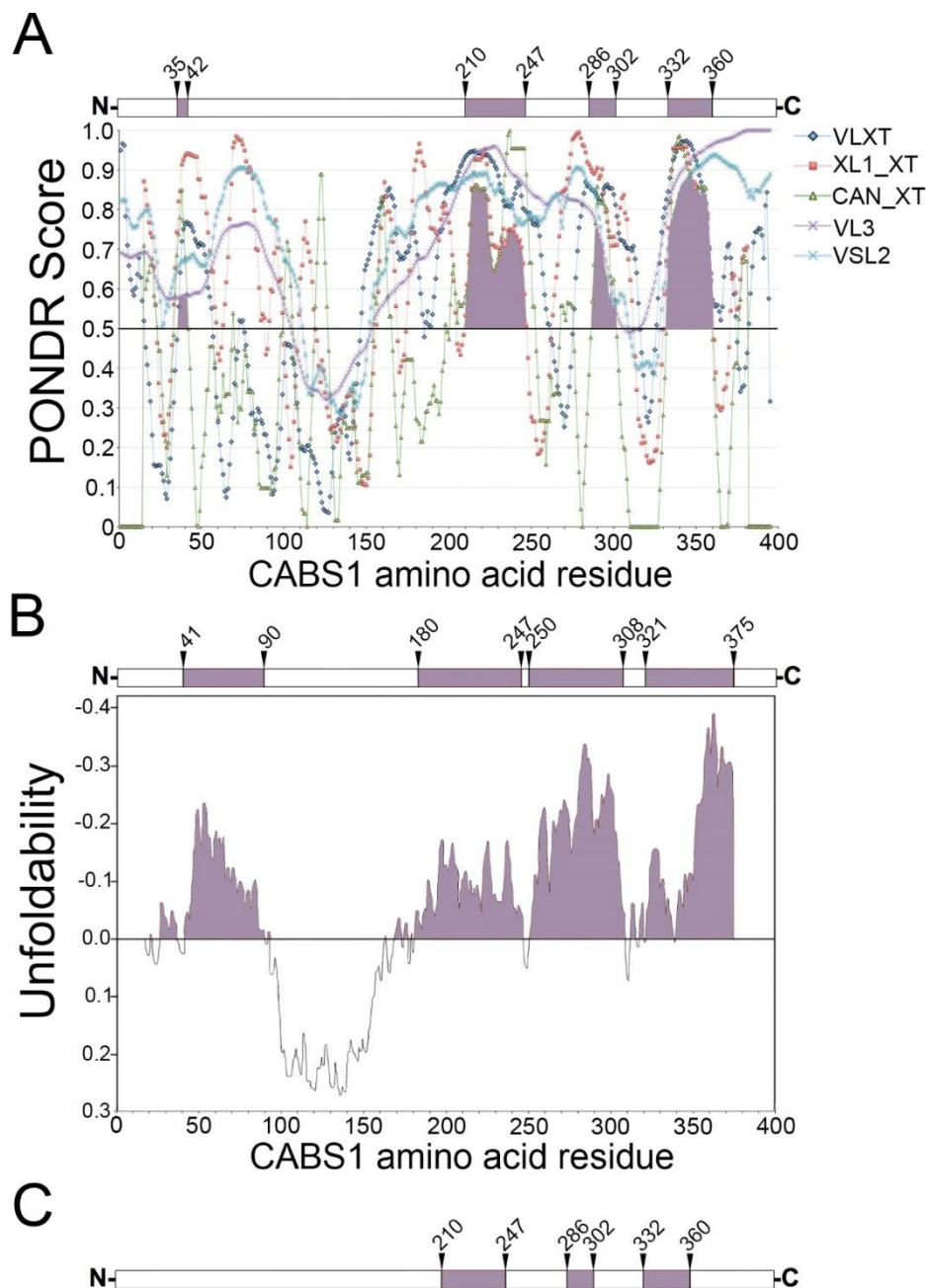
Figure 6-1. Analysis of hCABS1 disordered regions.

(A) PONDR software was used to predict unfolded regions within hCABS1 using various neural network algorithms. Five unique algorithms named VSL2, VL3, VL-XT, XL1-XT and CaN-XT were used. Areas under the curve (shaded purple) indicate regions where all five algorithms predicted unfolded regions with probabilities higher than 50%. (B) Using hydrophobicity-dependent algorithms, FoldIndex software was used to analyze hCABS1 for intrinsically unfolded sequences. hCABS1 regions with negative unfoldability index are highlighted in purple. (C) Representation of hCABS1 polypeptide indicating regions where both PONDR and FoldIndex software independently predict highly disordered sequences.

A second method used to predict whether hCABS1 sequences are intrinsically unfolded was FoldIndex. This approach, by contrast, takes into account residue hydrophobicity and net charge of the sequences[181]. Interestingly, this methodologically unrelated approach also detected four main regions with highly unfolded probabilities within residues 41-90, 180-247, 250-308 and

321-375 (**Figure 6-1** B). Regions where both approaches agreed in their predictions were residues 210-247, 286-302 and 332-360 (**Figure 6-1** C).

3-Dimensional predictions of hCABS1 structure

To validate the existence of multiple regions with highly disorder structures, we used two threading applications, RaptorX[185] and Ion Ligand Binding Site Prediction (IonCom)[184], as well as the Protein Structure and Function Predictions (I-TASSER) software[183]. The latter combines homology modeling and *de novo* (*ab initio*) prediction strategies. We used these approaches because of their reported success, and to contrast results generated from distinct strategies. While homology modeling looks at evolutionarily related structures, threading predicts likely secondary structures, and then predicts hinge points that develop into motifs, domains and later, tertiary and quaternary structures. *De novo* predictions utilize physicochemical principles only, demanding extensive computer resources.

We validated all model predictions using ProSA[187] and ERRAT[188]. ProSA analysis generated z-scores of -2.41, -2.39 and 0.19, for models generated with I-TASSER, IonCom and RaptorX, respectively. ProSA residue scores using average energy over 40-residues generated plots with high fluctuations in residue quality for all 3 models (data not shown). ERRAT analysis generated results that agreed with those by ProSA. Overall quality factors for our models were of 64.533, 8.421 and 16.887 for I-TASSER, IonCom and RaptorX, respectively. Therefore, we used the model generated by I-TASSER for all subsequent analyses.

I-TASSER identified several homology templates; however, none were of animal origin. The highest homology was identified as pleuralin-1 (PDB ID 2NBI) with a z-score of 4.90, a protein present in the marine diatom *Cylindrotheca fusiformis*. Other templates included yeast fatty acid synthase (PDB ID 2PFF) with a z-score of 1.62, and type II-C Cas9 enzyme (PDB ID 4OGC) with a z-score of 0.57 found in the bacterium *Actinomyces naeslundii*.

The hCABS1 model predicted by I-TASSER showed a molecule with minimal secondary structure (**Figure 6-2** A). Residues 210-247, 286-302 and 332-360, previously predicted to be in regions highly disordered (**Figure 6-1** C), do indeed appear as random coils in the I-TASSER model (sequences highlighted in red). The hCABS1 model predicted by IonCom also shows these three regions as random coils but predicted additional secondary structures at the N- and C-terminal ends of hCABS1 (**Figure 6-2** B). Interestingly, both the RaptorX software and IonCom predict the existence of an α-helix motif at the carboxyl terminal of hCABS1 (**Figure 6-2** A, C), which coincides with the anti-inflammatory motif TDIFELL, highlighted in green in all three models (**Figure 6-2**).
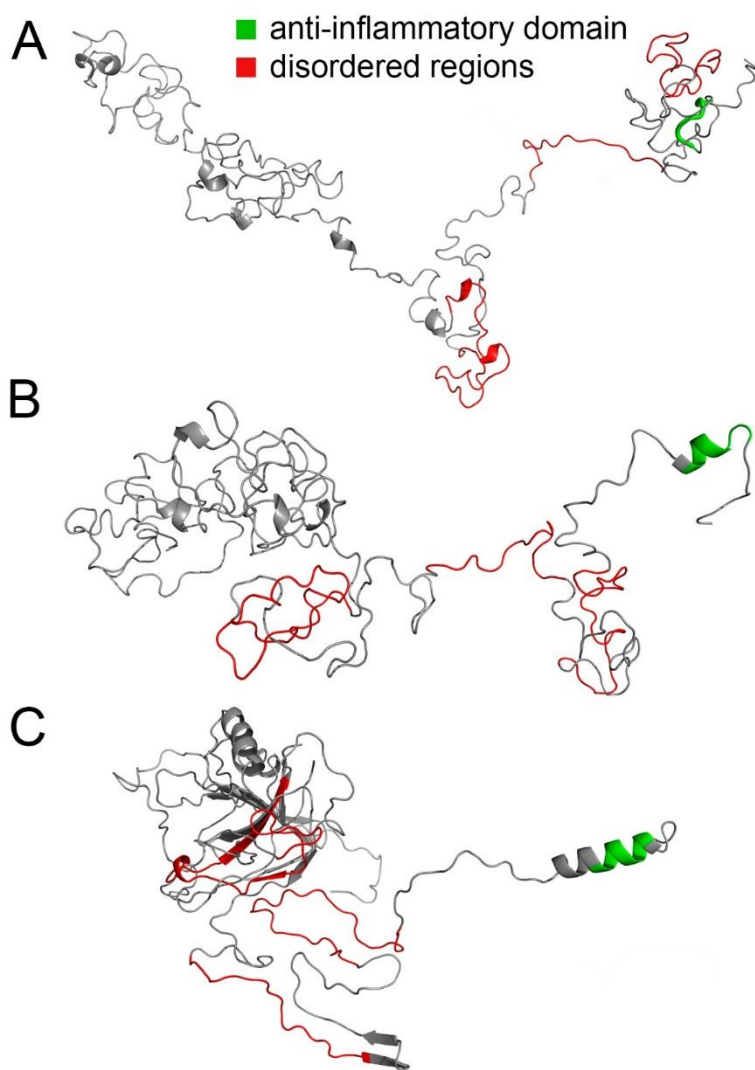
Figure 6-2. Prediction of hCABS1 3-dimensional (3D) structure.

Polypeptide segments predicted to be highly disordered are colored in red (residues 210-247, 286-302 and 332-360). The carboxyl terminal anti-inflammatory peptide sequence (380-TDIFELL-386) is labeled green. (A) hCABS1 3D structure predicted with I-TASSER software. (B) hCABS1 3D structure predicted with the IonCom software. (C) CABS1 structure predicted with the RaptorX software.

Amino acid sequence conservation of CABS1

At present, 72 CABS1 sequences have been annotated in the NCBI protein database. After analyzing them in Clustal Omega, we noted that the longest CABS1 protein sequence is 512 amino acids long, while the shortest is 156. The average length was 389 amino acids.

Species with flanking amino acid domain insertions at the amino terminus were *Acinonyx jubatus, Bubalus bubalis, Callorhinus ursinus, Camelus dromedarius, Camelus ferus, Enhydra lutris kenyoni, Eptesicus fuscus, Eumetopias jubatus, Felis catus, Lynx canadensis, Myotis davidii, Neomonachus schauinslandi, Odocoileus virginianus texanus, Phyllostomus discolor, Puma concolor, Sus scrofa, Ursus arctos horribilis, Vicugna pacos, and Zalophus californianus*. The latter also had a domain insertion in the carboxyl terminus. *Tupaia chinensis* had an insertion in the middle region at residue 115 that no other species had. Species with significant amino acid deletions were *Desypus novemcinctus, Fukomys damarensis*, and *Heterocephalus glaber*. Because of their significant insertions or deletions, we excluded these species for a subsequent Shannon entropy analysis of protein sequence conservation.

An anti-inflammatory peptide sequence of CABS1, TxIFELL, is only found in primates of the infraorder Simiiformes

The anti-inflammatory sequence TDIFELL was first identified in humans and experiments showed that FELL also had anti-inflammatory activity[18]. Thus, we categorized species containing FELL within the TxIFELL peptide as ones with the anti-inflammatory domain. Out of the 72 analyzed species, only 14 contain the putative anti-inflammatory domain 'TxIFELL', all of which were primates of the infraorder Simiiformes (**Figure 6-3**). Of note, Nancy Ma's Night monkey (*Aotus nanymaae*) and Northern White-cheeked Gibbon (*Nomascus leucogenys*) show a point mutation, T**G**IFELL, whereas all the others have TDIFELL (**Figure 6-3**, **Table 6-1**). Interestingly, a model of intestinal anaphylaxis showed that "TxI" was not necessary to elicit anti-inflammatory activity[18]. We observed that "FELL" elicited this activity and postulated that this

tetrapeptide contains the core anti-inflammatory component[18]. Moreover, a Shannon entropy analysis indicates that the anti-inflammatory sequence displays noticeably lower level of entropy in primates (**Figure 6-4**).
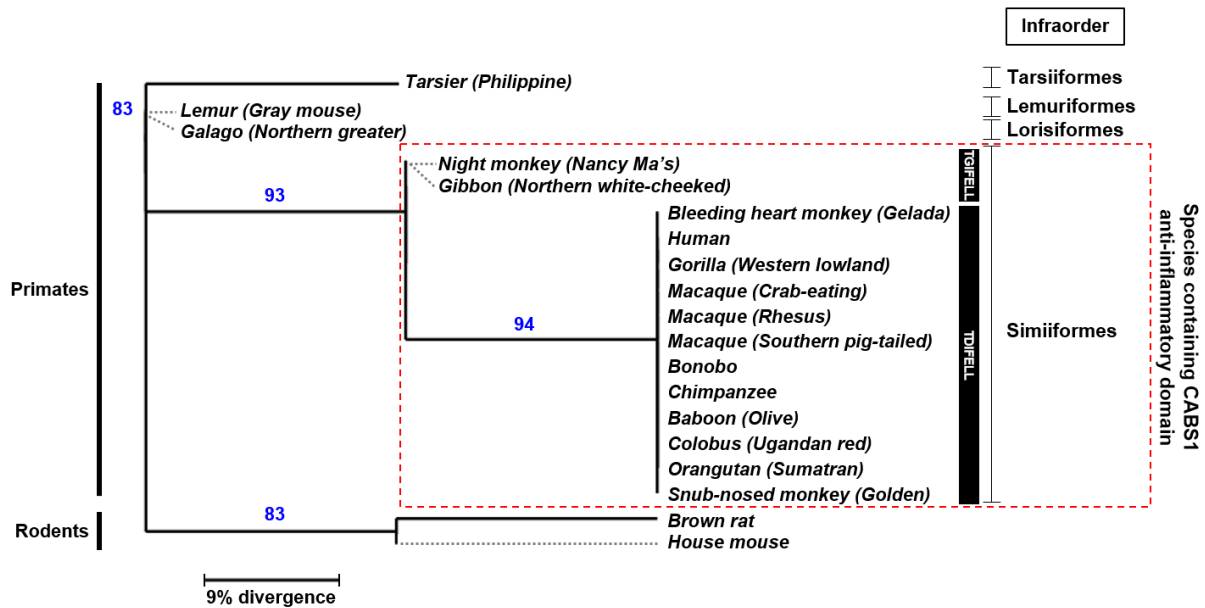
Figure 6-3. Phylogenetic tree of CABS1 using a maximum likelihood tree based on CABS1 amino acid sequences of annotated species in the NCBI protein database.

Numbers in blue indicate branch support values (%). The anti-inflammatory sequence TDIFELL is restricted to members of the infraorder Simiiformes.

Table 6-1. CABS1 anti-inflammatory domain is conserved in primate species.

Species	CABS1 anti-inflammatory domain						
Homo sapiens	380 T	D	I	F	E	L	L 386
Pan paniscus	380 T	D	I	F	E	L	L 386
Pan troglodytes	380 T	D	I	F	E	L	L 386
Gorilla gorilla gorilla	380 T	D	I	F	E	L	L 386
Pongo abelii	380 T	D	I	F	E	L	L 386
Nomascus leucogenys	381 T	G	I	F	E	L	L 387
Rhinopithecus roxellana	381 T	D	I	F	E	L	L 387
Piliocolobus tephrosceles	380 T	D	I	F	E	L	L 386
Macaca fascicularis	381 T	D	I	F	E	L	L 387
Macaca nemestrina	381 T	D	I	F	E	L	L 387
Macaca mulatta	381 T	D	I	F	E	L	L 387
Theropithecus gelada	380 T	D	I	F	E	L	L 386
Papio anubis	381 T	D	I	F	E	L	L 387
Aotus nancymaae	371 T	G	I	F	E	L	L 377

184

Current data indicates that annotated primates outside infraorder Simiiformes do not contain FELL, but FKLL. CABS1 in the testes has been characterized in the rat[1] and house mouse[4]. The peptide sequences in these rodent species in the region of the anti-inflammatory sequence in primates are SGIFKLL and SGLFKLL, respectively.
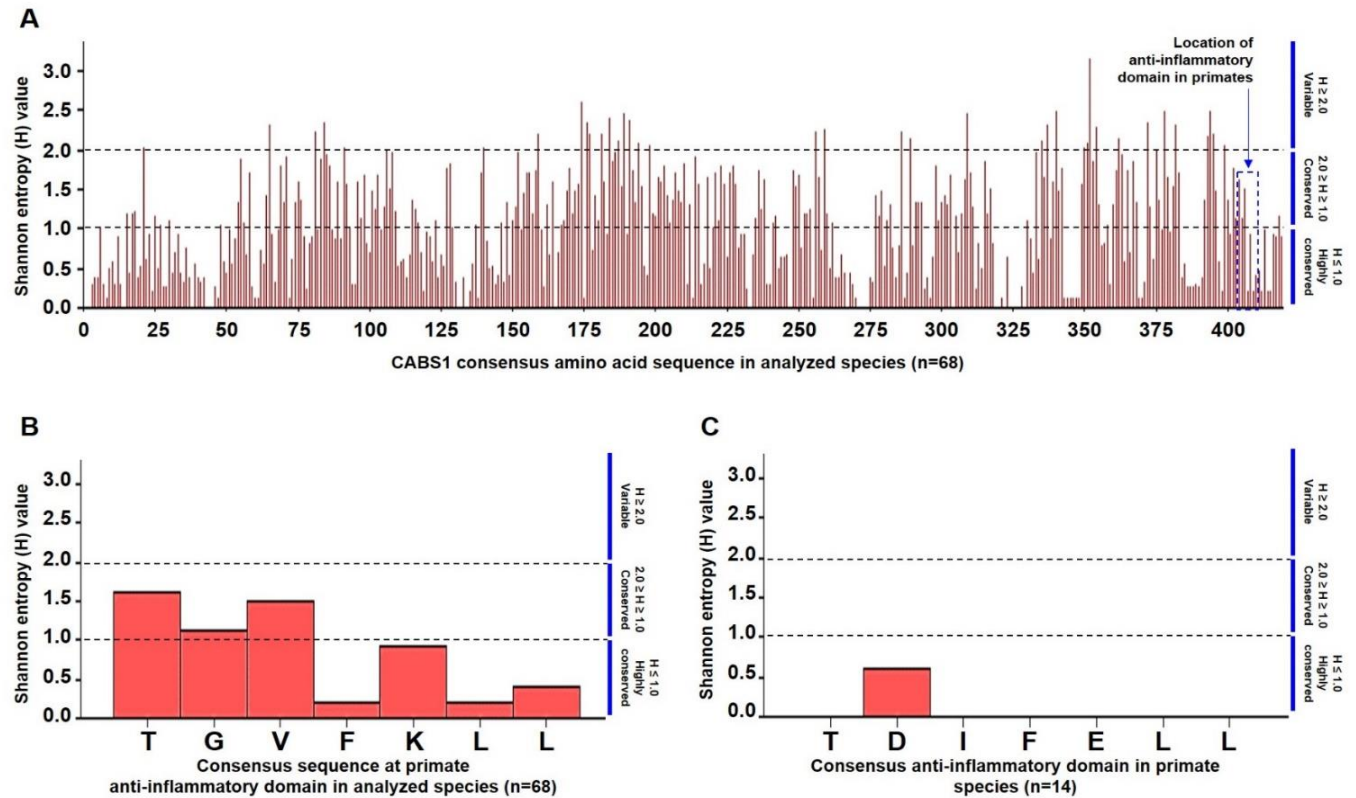
Figure 6-4. The anti-inflammatory domain TDIFELL in CABS1 is not highly conserved across all species and seems to be only associated to primates.

(A) Shannon entropy values per amino acid of CABS1 consensus sequence. (B) Shannon entropy analysis of the location of primate-associated anti-inflammatory motif in all analyzed species. (C) Shannon entropy analysis of CABS1 anti-inflammatory motif in primates of parvorders Catarrhini and Platyrrhini.

Post-translational modifications of hCABS1

NetPhos software[189] was used to predict phosphorylation sites on hCABS1. A total of 14 residues showed a score of more than 95% probability, including 13 serine (residues S43, S77, S110, S170, S245, S273, S319, S337, S338, S344, S360, S364 and S376), and one threonine residue at position T303. Because protein kinase CK2 was previously reported to phosphorylate rat CABS1[1], we used Group-based Prediction System (GPS)[190] to assess the specific contribution of CK2 on hCABS1.

GPS determined 24 residues as likely targets for CK2-mediated phosphorylation. 7 of these residues were in agreement with NetPhos (**Figure 6-5** A). These 7 residues and their scores were S43/2.0802, S77/4.682, S110/1.801, S337/4.657, S338/4.329, S344/3.127 and S376/5.097. The sites were plotted on a cartoon representation of hCABS1 and on a stick representation model of hCABS1 using the I-TASSER model developed in **Figure 6-2** A.
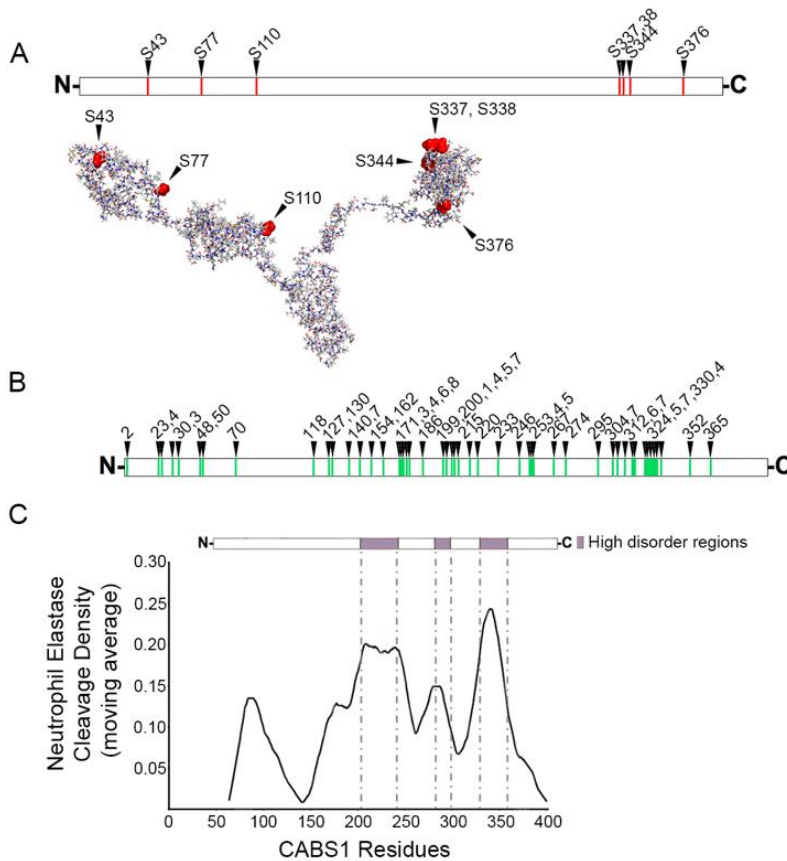
Figure 6-5. Phosphorylation and proteolytic processing of hCABS1.

(A) NetPhos and GPS were used to predict hCABS1 residues likely to be phosphorylated by protein kinase CK2. Arrowheads indicate the amino acid number in the hCABS1 sequence. The 3D structure generated by I-TASSER was used to highlight the location of these phosphorylation events. (B) PeptideCutter software was used to build a digestion map for neutrophil elastase. Arrowheads indicate the relative location of proteolytic events and the P1 residue. (C) The neutrophil elastase cleavage density represented as the moving average of cleavage sites per amino acid was plotted and compared with the image that predicts regions of high structural disorder.

Using SignalP-5.0 Server for signal peptide sequence prediction, we uploaded the FASTA sequence for hCABS1 and determined that the likelihood of a N-terminus hydrophobic signal peptide sequence was negligible (0.001). Signal peptide sequences specifically bind to the signal recognition particle (SRP) receptor on the endoplasmic reticulum (ER) membrane to allow insertion of proteins through the ER membrane and enter the ER lumenal space. Because hCABS1 lacks this sequence, it is not possible for hCABS1 to enter the ER and therefore must be translated as an uncleaved protein by ribosomes in the cell cytoplasm. This suggests that hCABS1 is secreted from salivary glands through nonclassical secretion mechanism(s) that is independent of the canonical ER-Golgi apparatus-

secretory vesicle pathway. Several nonclassical secretion pathways include membrane transporters, multivesicular bodies, exosome/microvesicle shedding, lysosome secretion, and lytic release.

Because several molecular forms of hCABS1 have been identified, the PeptideCutter software, available through ExPASy, was used to predict potential cleavage sites. The software offers *in silico* digestions for numerous proteases. We found that 15 out of 34 available enzymes did not cleave hCABS1. From the remaining 19 enzymes, only 8 are expressed in humans. In descending order, according to cleavage frequency, these enzymes are pepsin (137 cleavage sites), neutrophil elastase (48 cleavage sites), trypsin (28 cleavage sites), chymotrypsin (18 cleavage sites), Arg-C proteinase (5 cleavage sites), caspase 1 (2 cleavage sites), enterokinase (1 cleavage site) and thrombin (1 cleavage site). It is not surprising that digestive enzymes like pepsin, trypsin and chymotrypsin could cleave hCABS1 at numerous sites. Also, not surprisingly, neutrophil elastase appears to cleave hCABS1 at a high number of sites (**Figure 6-5** B). Neutrophil elastase is an aggressive protease known to digest virtually all extracellular matrix proteins, in addition to its role in proteolytic activation of several matrix metalloproteinases during inflammation[203]. The presence of neutrophil elastase in the oral cavity makes it a likely candidate for hCABS1 processing. We previously reported the presence of several hCABS1 forms in saliva using immunodetection by Western blot[18,21] and capillary nano-immunoassay[66]. To better understand the complex pattern of likely P1 residues for neutrophil elastase shown in **Figure 6-5** B, we calculated the "20 amino acid moving average" of P1 sites along the hCABS1 sequence (**Figure 6-5** C). Interestingly, cleavage site density correlated with hCABS1 regions that display highly unfolded secondary structure. This supports the hypothesis that hCABS1 is a proteolytic target of neutrophil elastase and that this enzyme may play an important role in the genesis of functionally distinct forms of hCABS1.

Cofactors and their role in hCABS1 biological function

In addition to tertiary structure, I-TASSER also predicts protein-cofactor interactions and likely polypeptide biological function. This software predicted interactions of hCABS1 with Ca^{2+} (residues 42 and 44), Mg^{2+} (residues 219 and 223), Zn^{2+} (residues 214 and 216), leucine (residues 194, 195, 257, 263 and 267) and thiamine diphosphate (residue 360) (**Figure 6-6** A). To validate hCABS1 and TPP interaction, the software SwissDock was used. Swissdock reported a Full Fitness interaction of -1043.70 kcal/mol with an estimated ΔG of -9.06 kcal/mol. Space-filling and stick
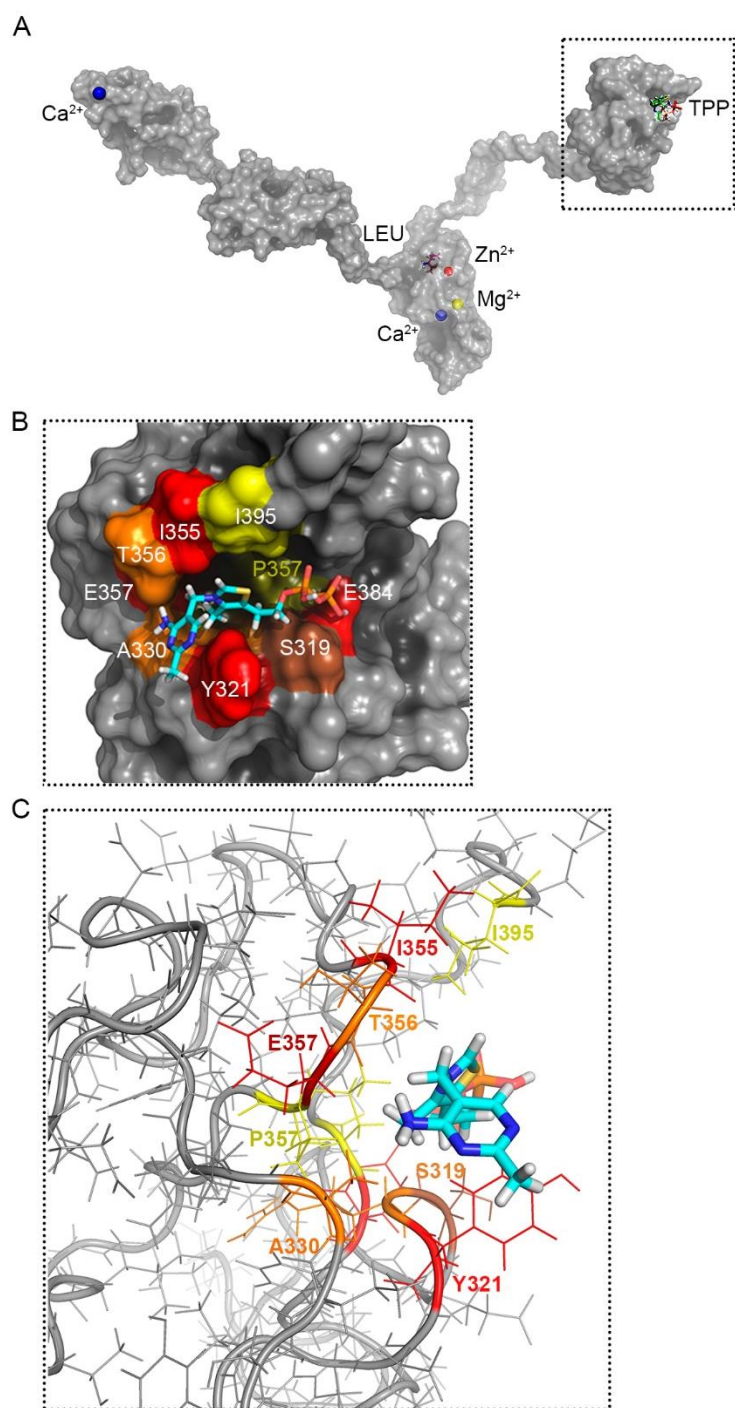
Figure 6-6. Cofactor interaction analysis.

(A) 3D structure of hCABS1 predicted with I-TASSER was used to indicate putative binding sites for calcium (Ca^{2+}, 42-43), leucine (Leu, 194, 195, 256, 263 and 267), magnesium (Mg^{2+}, 219 and 223), zinc (Zn^{2+}, 214 and 216) and thiamine diphosphate (TPP, 360). An additional Ca^{2+}-binding site was detected by IonCom (Ca^{2+}, 248-252). Square inset represents the C-terminal domain of hCABS1 with a putative TPP binding site. (B) Zoomed in region from C-terminal domain inset. I-TASSER model validation using SwissDock depicting hCABS1 residues that interact with TPP. (C) Stick model representation of B) showing a side view of the hCABS1-TPP interaction and the amino acid resides involved.

models showing amino acid residues involved in the interaction are shown in **Figure 6-6** B and C. Residues predicted to make H-bonds with TPP were: E318, S319, R320, Y321, T331, K354, I355, T356, E384, L385 and I395. I-TASSER also predicted that hCABS1 could play a role in fatty acid biosynthetic pathways; specifically, hydrolase, reductase, transferase, fatty acid synthase and dehydratase activities. Hydrolase activity would likely include palmitoyl-[acyl-carrier-protein] hydrolase, acyl-[acyl-carrier-protein] hydrolase, myristoyl-[acyl-carrier-protein] hydrolase, and oleoyl-[acyl-carrier-protein] hydrolase. Reductase activity would likely include enoyl-[acyl-carrier-protein] reductase and enoyl-[acyl-carrier-protein] reductase. Transferase activity would likely include [acyl-carrier-protein] S-acetyltransferase. Fatty acid synthase activity would likely include fatty-acyl-CoA synthase. Dehydratase activity would likely include 3-hydroxyacyl-[acyl-carrier-protein] dehydratase and 3-hydroxypalmitoyl-[acyl-carrier-protein] dehydratase.

Discussion

Acute and chronic stress play significant roles in the composition of soluble factors in saliva. While parasympathetic signals induce a water-rich salivary discharge, sympathetic stimulation induces a high protein salivary output[204]. Accessibility to saliva and the presence of cell-free DNA, several RNA forms (mRNA, microRNA and piwi-interacting RNA) and soluble or exosomic granules (exosomes, microvesicles and apoptotic bodies), make this fluid an attractive diagnostic sample source[205]. CABS1 is an exciting, novel salivary biomarker with the potential to predict stress and resilience to stress[21]. This duality is so far unique within the literature of stress biomarkers.

Our current understanding of hCABS1 presents an interesting challenge. While CABS1 has been detected in sperm and mitochondria in non-human samples, our group has identified human forms of CABS1 secreted from salivary glands. We postulate that intracellular and extracellular localization for hCABS1 may represent two very distinct functional modes. For example, secreted hCABS1 may be involved in stress and immuno-inflammatory processes, while intracellular hCABS1 may regulate energy metabolism and intracellular stress pathways (**Figure 6-7**). Our *in-*

silico evidence illustrates these two potential modes of action for hCABS1 by shedding light on interactions with cofactors like TPP, Ca²⁺ and Leu. Secretion through non-classical mechanisms and tissue-specific processing are likely to be critical components of hCABS1 biology.
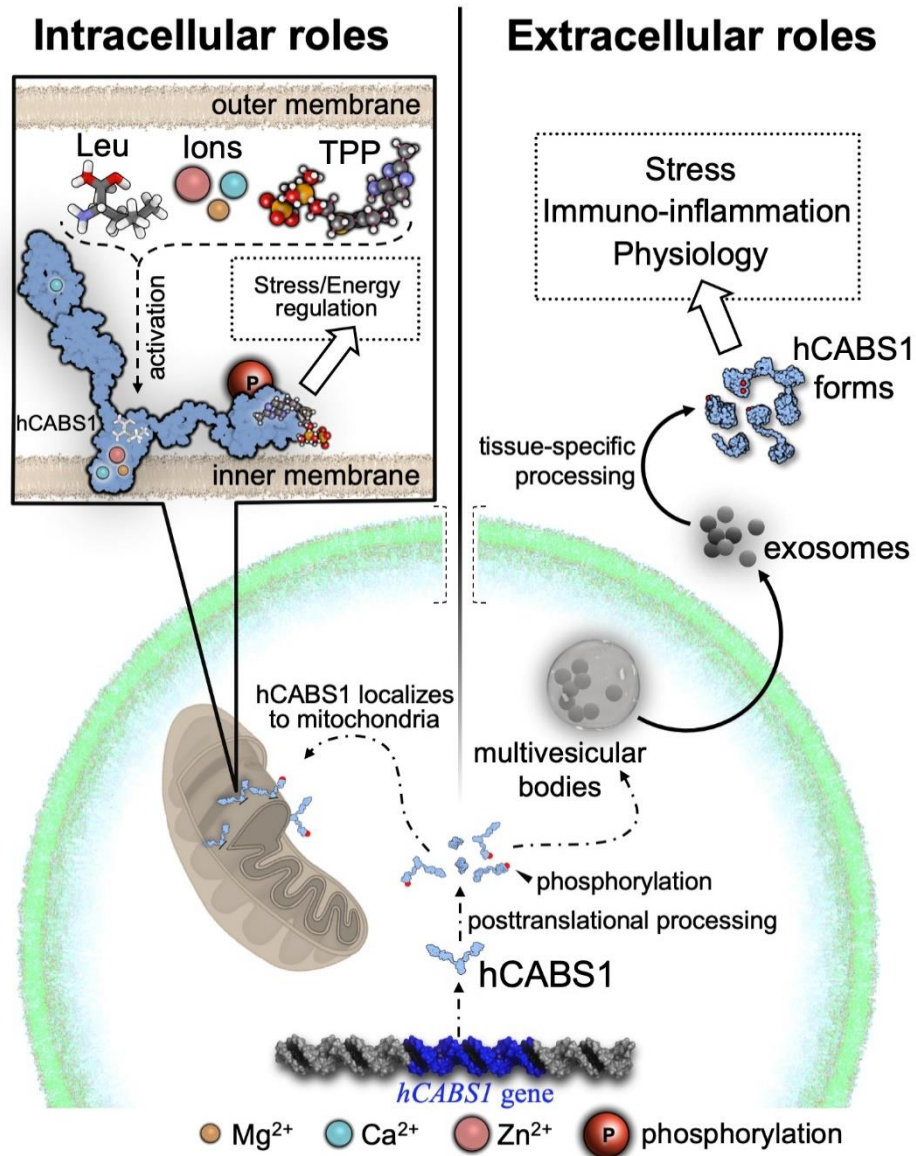
Figure 6-7. Conceptual model of hCABS1 biology.

The human CABS1 gene (hCABS1 gene, blue label) contains a single exon and generates a single gene product. The polypeptide translated from this transcript (hCABS1, black label) undergoes posttranslational intracellular modifications such as proteolytic processing and phosphorylation (red circles). We postulate that in a tissue-specific manner, various forms of hCABS1 can either localize to the mitochondria or be secreted via multivesicular bodies and exosomes. Mitochondrial hCABS1 is associated to the inner mitochondrial membrane and interacts with various cofactors including leucine (Leu), Mg²⁺ (yellow ion), Ca²⁺ (blue ion), Zn²⁺ (orange ion), and thiamine diphosphate (TPP). Interaction of cofactors with hCABS1 enhances its function in regulating energy metabolism and intracellular stress pathways. Secreted hCABS1 undergoes further tissue-specific processing. hCABS1 processing would vary according to the proteolytic enzyme environment. Various hCABS1 molecular forms (hCABS1 forms) are likely to have specific roles in stress, immuno-inflammation and physiology.

The stability of proteins in the extracellular environment impacts their function and mechanism of regulation. CABS1 lacks a stable tertiary structure and is therefore intrinsically disordered by nature. There is an "order-structure continuum"[206] for tertiary structures, with rigid and well-structured protein families at one end of the spectrum, and extremely flexible and dynamic proteins at the other. It has been estimated that more than 50% of all proteins in eukaryotes contain long disordered regions that may play important roles in their function[207]. In this study authors reviewed the role of several disordered domains proteins in the biomineralization of teeth including dentin sialophosphoprotein, osteopontin and dentin matrix protein-1. Others have reviewed the role of disordered domains and how this entropic ability allows, for example, spring-like function of titin and the bristle-like role of MAP2, to provide spacing in the cytoskeleton[208]. Disordered proteins may also function as inhibitors as is the case of calpastatin and its ability to inhibit calpain due to long disordered domains that facilitate positioning of the inhibitory domains. The disordered nature of hCABS1 may enable its increased proteolytic processing by enzymes such as neutrophil elastase (**Figure 6-5** B, C). It is not surprising that there is an obvious overlap between predicted intrinsically disorder regions (**Figure 6-1** C) and neutrophil elastase cleavage sites (**Figure 6-5** C).

Neutrophil elastase activity may produce bioactive fragments of hCABS1 and contribute toward tissue-specific processing events. Indeed, the location of hCABS1 anti-inflammatory domain (380-TDIFELL-386) appears to be strategically isolated near the C-terminal, adjacent to a region with the highest density of neutrophil elastase putative P1 residues (**Figure 6-5** C). We predict that neutrophil elastase cleaves salivary hCABS1 to produce active components such as TDIFELL-containing peptides, which may act locally or possibly disseminate systemically to exert physiological effects in other tissues. Interestingly, the anti-inflammatory peptide sequence in rat SMR1, TDIFEGG, has an adjacent elastase cleavage site (unpublished, observation) and we have previously identified TDIFEGG-containing immunoreactivity in a <3000 Da fraction of rat

saliva[53]. We aim to identify the role of neutrophil elastase and other proteases in the processing and function of molecular forms of hCABS1.

Due to the high abundance of acidic residues in hCABS1, the migration of hCABS1 is slowed during electrophoresis, resulting in a significant discrepancy between its predicted molecular mass (M_r) and its observed M_r in SDS-PAGE. This observation has been reported in human[18] (43 kDa calculated, 75 kDa observed), *Sus scrofa*[5] (42.8 kDa calculated, 75 kDa observed), mouse[4] (42.3 kDa calculated, 66 kDa observed) and rat[1] (42.3 kDa calculated, 80.0 kDa observed). Neutralization of acidic residues in CABS1 with carbodiimide/ethanolamine altered the migration profile of rat CABS1 close to its predicted M_r[1], supporting acidic residues as the reason for the M_r discrepancy. In agreement with this observation, we have shown that N- or O-glycanase treatment does not alter CABS1 M_r in SDS-PAGE, suggesting that glycosylation events do not explain the discrepancies in M_r of the protein[18].

Other posttranslational modifications like phosphorylation have been observed for CABS1 *in vivo*[1]. However, a single phosphorylation event only contributes 80 Da in M_r. Thus, this posttranslational modification does not account for the unexpected increase of ~30 kDa in observed M_r.

Though phosphorylation minimally adds to molecular weight, phosphorylation events typically have enhancing effects on protein function. Protein kinase CK2 is critical in rat spermiogenesis, and CK2 was shown to phosphorylate rat CABS1 *in vitro* and confirmed *in vivo*[1]. The phosphorylation of CABS1 by CK2 suggests that their interaction plays an important role in spermiogenesis. We suspect that hCABS1 phosphorylation may play various roles in regulating mitochondrial pathways in energy metabolism and stress (**Figure 6-7**). Conversely, CABS1 phosphorylation may be necessary for its secretion. Recently, Klement and Medzihradszky provided an in-depth review on the importance of extracellular protein phosphorylation[209]. They reported that in some cases, as high as 50% of all secreted proteins may be released via non-

classical ER/Golgi pathways. Phosphorylation of this group of secreted proteins may be a required modification for secretion. In this case, hCABS1 phosphorylation may be a prerequisite for its secretion from SMG. Extracellular phosphorylation of hCABS1 could be critical in regulating its functions in stress, immuno-inflammation and physiology, possibly by controlling proteolytic processing of hCABS1.

Interestingly, calcium plays a role in regulating proteolytic cleavage and is involved in cell signaling within the salivary glands[210]. Reinhardt *et al.* showed that proteolytic degradation of fibrillin-1 in the presence of $CaCl_2$ was significantly slower than in the presence of EDTA, demonstrating that calcium confers protection against proteolysis[211]. This calcium-dependent protection from proteolysis has been reported in other studies[212,213].

The possibility that hCABS1 binds calcium is inferred from studies in mice and pigs using ruthenium red and Stains-all[4], and in rats using $^{45}Ca^{2+}$-binding autoradiography assays[1]. Our *in-silico* analysis confirms this hypothesis and predicts the location of these sites at positions 42-43 and 248-252 (**Figure 6-5** A). Future studies can be conducted to confirm these Ca^{2+}-binding sites by scanning mutagenesis and other labeling methods.

Calcium maintains structural stability of proteins, including a highly abundant salivary protein, α-amylase[214]. In the presence of sympathetic stimulus, calcium may be involved in signaling pathways for hCABS1, by inducing structural modifications that regulate proteolytic cleavage of a hCABS1 precursor, forming smaller molecular forms that may have varying properties. Proteolytic degradation assays should therefore show increased degradation of hCABS1 in the absence of calcium, and will be reversed in the presence of $CaCl_2$, providing evidence that Ca^{2+}-binding promotes a more ordered secondary structure, regulating hCABS1 processing.

We were intrigued by the I-TASSER predictions for hCABS1 binding sites for cofactors thiamine diphosphate (TPP), Ca^{2+}, and Mg^{2+} (**Figure 6-6** A). In sperm, CABS1 localizes to the mitochondria, flagella and the acrosome suggesting a role in energy supply[1]. In humans, there are

12 enzymes that use TPP as a cofactor as reported in the Kyoto Encyclopedia of Genes and Genomes (KEGG), all of which play crucial roles in energy metabolism. Interestingly, all TPP-binding enzymes are intracellular proteins. If hCABS1 binds TPP, this would be indicative of novel intracellular roles likely in the regulation of energy metabolism. Based on metabolic pathways, TPP-binding enzymes can be divided into 6 groups, 3 groups that function as cytosolic enzymes and 3 other groups that function within mitochondria. The first group of cytosolic enzymes converts thiamine into TPP or into thiamine triphosphate; these enzymes are thiamine phosphate kinase (2.7.4.16), thiamine diphosphokinase (2.7.6.2), thiamine triphosphatase, (3.6.1.28) and thiamine diphosphate kinase (2.7.4.15). The second group of cytosolic enzymes are involved in ATP hydrolysis; these enzymes are adenylate kinase (2.7.4.3) and nucleoside-triphosphate phosphatase (3.6.1.15). The third group of cytosolic enzymes is transketolase (2.2.1.1), involved in the pentose phosphate pathway.

The 3 groups that are inside mitochondria are involved in the TCA cycle, pyruvate metabolism, and branched chain amino acid catabolism, respectively. These 3 groups of enzymes form closely related multienzyme complexes. Within the oxoglutarate dehydrogenase complex in the mitochondrial matrix, the enzyme oxoglutarate decarboxylase (1.2.4.2) of the TCA cycle requires TPP. Another mitochondrial matrix complex is the pyruvate dehydrogenase complex involved in the conversion of pyruvate to acetyl-CoA; within this complex, pyruvate dehydrogenase (1.2.4.1) also requires TPP. In the mitochondrial inner membrane, the branched-chain alpha-ketoacid dehydrogenase complex plays a role in the metabolism of branched-chain amino acids (leucine, isoleucine and valine); within this complex, the enzyme branched-chain alpha-ketoacid dehydrogenase (1.2.4.4) mediates the TPP-requiring step. For a more comprehensive list of TPP enzymes present in other organisms including bacteria, see review[215].

For TPP-binding enzymes, the combination of TPP with either Mg^{2+} or Ca^{2+} is necessary for enzyme activation[216,217]. The divalent cation location observed in X-ray crystallography studies for

pyruvate dehydrogenase[218] and branched-chain alpha-ketoacid dehydrogenase[219] show the ion in close proximity to TPP. In contrast, the hCABS1 structure shows Ca^{2+} and Mg^{2+} binding sites relatively far from the TPP site (**Figure 6-6** A). It is possible that the long random coil (res 268-315) of hCABS1 acts as a molecular switch to bring TPP close to either Ca^{2+} or Mg^{2+} ions. In this model, hCABS1 would have enzymatic activity when the TPP and divalent ion regions are in close proximity. Putative sites for neutrophil elastase cleavage exist between these cofactor domains of hCABS1, thus elastase-mediated cleavage could result in deactivation of hCABS1 enzymatic activity extracellularly.

The branched-chain alpha-ketoacid dehydrogenase complex is located in the inner mitochondrial membrane where it utilizes TPP in the first irreversible step in the catabolism of leucine (Leu)[220]. Leu is an essential amino acid that plays a role in protein structure and function. Leu also plays roles in numerous other protective pathways including wound healing, muscle repair and protects against stress-induced breakdown of muscle proteins. Given hCABS1 association with stress responses, it is possible that binding of Leu to hCABS1 could play a regulatory function by acting as an allosteric regulator. Indeed, Leu functions as an allosteric activator of the enzyme glutamate dehydrogenase[221].

To enable the analysis of genetic data, the Gene Ontology (GO) project developed the Phylogenic Annotation and Inference Tool (PAINT). One of the PAINT objectives was to assist annotators in assignment of protein function within a given protein family. This tool predicts that hCABS1 should have a subcellular location to the cytosol and the inner mitochondrial membrane[222]. Indeed, Calvel L, *et al*. reported that rat CABS1 is associated to mitochondria inner membranes of spermatids[1]. The mitochondria inner membrane is home to numerous metabolic pathways, key in energy metabolism. As described above, the branched-chain alpha-ketoacid dehydrogenase complex metabolizes Leu catabolism, requires TPP and Mg^{2+} and it is found in the inner

mitochondrial membrane, all features we have identified for hCABS1 in this manuscript. At this point, it is difficult to predict weather Leu acts as a substrate or as a regulator of hCABS1 activity.

We are also interested in the occurrence of CABS1 across species. Annotations of the protein only appear to occur in placental mammals. An additional segment at the amino terminus of at least 7 amino acids was observed in annotated felines, most pinnipeds, most bats, bovids, camelids, the grizzly bears, wild boars, and sea otters. Since we have shown that hCABS1 contains an anti-inflammatory domain, TDIFELL, near the C-terminus, we investigated the species distribution of this or similar motifs. Interestingly, the 14 species with TDIFELL were all primates (**Figure 6-3**). A domain in CABS1 with anti-inflammatory properties, is conserved only in parvorders Catarrhini (Old World monkeys, humans) and Platyrrhini (New World monkeys), which belong to the order Primates (**Figure 6-3**, highlighted red square)[223]. This domain is not present in *Philippine tarsier (*Carlito syrichta*),* which is also part of this order. Two primate species showed a point mutation in the anti-inflammatory motif, D→G. However, aspartic acid and glycine share the physicochemical property of being small[81]. Moreover, we have showed that FELL is sufficient to elicit an anti-inflammatory effect in rodents[18], so we speculate that this CABS1 domain has anti-inflammatory activity across primates.

NCBI's CDD (Conserved Protein Domain Family Database), reports hCABS1 as the only member of its superfamily. This analysis reflects the unique nature of the protein, a limitation that hampers our ability to make functional predictions using current repositories. Future research on hCABS1 regulation and function will garner insight on how hCABS1 contributes to the stress response and the relationship between its localization and its function. Beyond a biomarker of stress, this research may reveal other unrecognized roles of hCABS1, including possible enzymatic activities. This manuscript contributes to the growing body of knowledge on the regulation of this emerging protein with wide-ranging implications on our understanding of its biology.

Acknowledgements

Chapter 7 : Overall discussion

This chapter integrates the collective findings and contributions of the previous six chapters, addresses the limitations that our project faces, and ultimately leads to the final chapter that proposes strategies to continue research on hCABS1.

The objectives of this dissertation, outlined in Chapter I, were:

1. To characterize polyclonal and monoclonal antibodies of hCABS1 using immunoprobing techniques on complex human biological samples

2. To validate the presence of hCABS1 in human-derived samples by optimizing protein isolation protocols and facilitating mass spectrometry analysis

3. To validate the study of saliva-derived hCABS1 in acute stress

4. To contribute to the body of knowledge of hCABS1 by analyzing the protein sequence using *in silico* tools

Objective 1: I characterized the WB profiles given by pAbs and mAbs targeting hCABS1 in a transient overexpression cell lysate (OEL), its negative control (NCL), human submandibular gland (SMG), saliva supernatant, and blood serum.

Firstly, I described pAbs-based WB profiles of hCABS1 in serum and saliva before and after methodology re-evaluation and found discrepancies based on the amount of total protein evaluated and the amount of working antibody. These discrepancies led to question previous assertions about hCABS1 that our group had published[18,21,66] and contributed to the decision to create monoclonal antibodies (mAbs) targeting hCABS1.

The WB profiles we obtained with pAbs suggested several hCABS1 variants were present in all samples we evaluated, with some bands common in different tissue/fluid samples (see Chapter 2 - **Table 2-4**). After introducing a validation protocol involving a more rigorous titration of

antibody and sample amounts, I began questioning the pAbs and the way in which they were generated. An analysis of the entire hCABS1 sequence using the 'B cell epitope prediction tool' from the Immune epitope database and analysis resource[224–230] shows that the peptide sequence used to produce H2.n pAbs (hCABS1 a.a. 184-197) is predicted to elicit a B-cell mediated response, while only a part of the peptide sequence used to create H1.0 pAbs (hCABS1 a.a. 375-388) is predicted to elicit such a response (**Figure 7-1**); i.e., the anti-inflammatory domain of hCABS1 is not predicted to be a strong B-cell epitope (**Figure 7-1**, green plot enclosed in black rectangle).
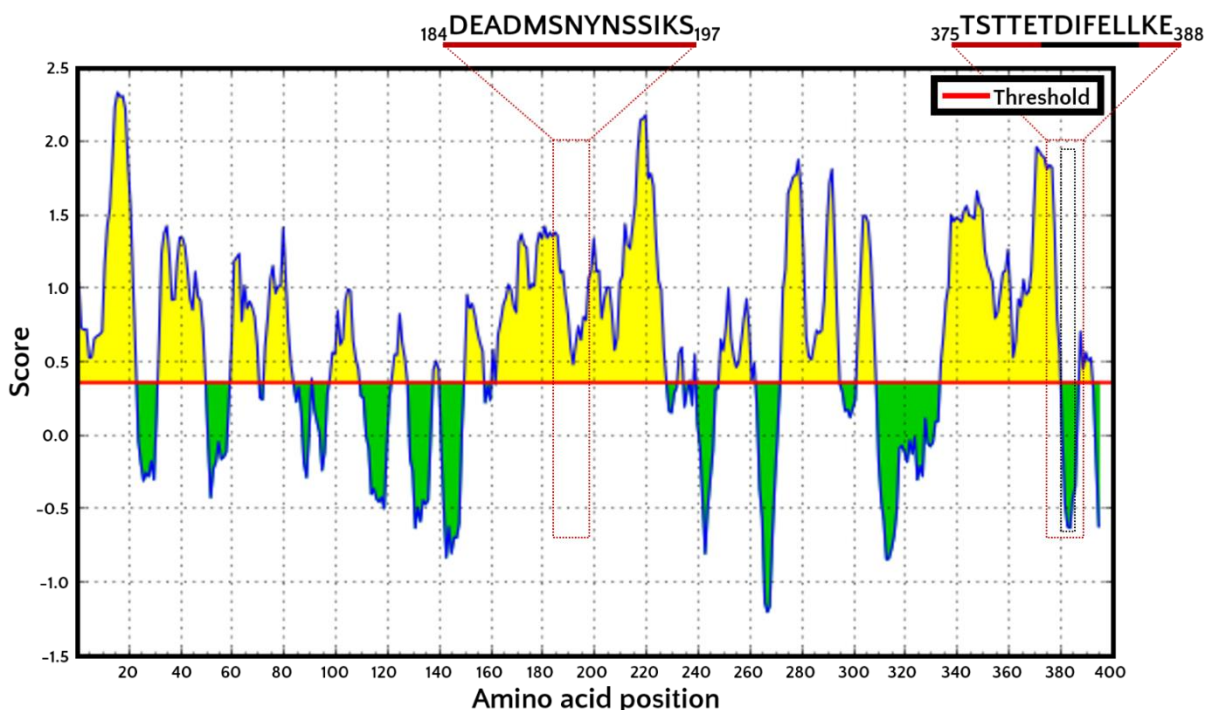
Figure 7-1. Predicted segments of hCABS1 likely to elicit an antibody response (yellow).

The representative linear amino acid residue position for hCABS1 is depicted on the horizontal axis, while the residue score (a.u.) is depicted on the vertical axis. Residues with scores above the default threshold value (~0.5) are predicted to be part of regions likely to elicit a B cell response. Enclosed in red rectangles are the domains used for creating pAbs H2 (hCABS1 a.a. 184-197) and H1 (hCABS1 a.a. 375-388, anti-inflammatory section underlined in black). *Plot generated using 'B cell epitope prediction tool' from the Immune epitope database and analysis resource.*

Were the New Zealand rabbits good hosts to produce our pAbs? Leenaars and Hendriksen list the critical steps on antibody production as (1) antigen preparation, (2) animal species selection, (3) adjuvant selection and preparation, (4) injection protocol, (5) post-injection follow-up, and (6) antibody collection[148]. The protocol used by GenScript to produce our pAbs was in agreement with industry standards. However, if we focus on Leenaars and Hendriksen critical step (2), they note

that selection of animal species is impacted by the species from which the antigen is taken[148]. While they recognize that rabbits are used most times to produce pAbs, they remark that the larger the phylogenetic distance between animal species (i.e., antigen source species and species to be host for pAb production), the superior the evoked immune response[148]. Alignment of our hCABS1 immunogens with the rabbit CABS1 sequence is detailed and discussed in (Chapter 2 - **Figure 2-24**). For pAbs production, Leenaars and Hendriksen suggest producing pAbs in chicken, whose phylogenetic distance to mammals could result in better pAbs batches[148]. But at the time our best research tool were rabbit-generated pAbs that had been affinity purified. pAbs-based WB resulted in complex profiles, endorsed the occurrence of hCABS1 in human saliva, serum, and SMG, and indicated that hCABS1 existed in those compartments as differently sized proteins.

The addition of purified mAbs to our research toolkit brought the potential to reduce the complexity of WB profiles. Careful validation of mAbs profiles in WB identified a limited number of immunoreactive bands in SMG and serum. Moreover, mAbs-based WB casted doubt on the presence of hCABS1 in saliva supernatant altogether (see Chapter 4 - **Table 4-5**). However, I recognize that evidence provided in this document is insufficient to discard the occurrence of hCABS1 in saliva. Recently, I began questioning the role our secondary antibody plays in recognizing molecules in saliva supernatant. I suspect that the secondary antibody may be reacting with proteins in WB membranes that do not reflect hCABS1 and instead reflect immunoglobulins present in saliva (see '*No primary antibody*' panel in **Figure 4-18** – *56 and 25 kDa*, **Figure 4-19** – *56 kDa*, **Figure 4-20** – *56 kDa*). In Chapter 8: Future directions, I propose a strategy to test this postulate. For now, we do not have unequivocal evidence that human saliva contains hCABS1. Altogether, WB profiles suggest that hCABS1 occurs in SMG and serum (aside from our transient overexpression control lysate) with bands detected at 70 kDa (pAbs)/63 kDa (mAbs) in both samples (**Table 5-1**). This poses the question of SMG being a source of circulating hCABS1, and of the role that it might play in other organs. To date, the American Type Culture Collection does not offer a validated human SMG-derived cell line[231]. When such a cell line is

available, it could be used as a model to assess hCABS1 transcript and protein levels under different conditions.

We studied the distribution of hCABS1 in SMG because our data supported the presence of the protein in this compartment. We did immunohistochemical studies using our pAbs, in collaboration with Dr Michiko Watanabe (Case Western Reserve University, Cleveland, USA). These results suggested that in SMG hCABS1 is present throughout the cytoplasm of duct cells and, potentially, has an abundant presence in the abluminal side of some duct cells (**Figure 2-15**). More recently, through a collaboration with Dr Lakshmi Puttagunta (University of Alberta, Edmonton, Canada), we obtained the first immunohistochemical data on hCABS1 distribution in human testicular tissue using mAb 15B11-1. Results on this compartment suggested that hCABS1 is present outside of seminiferous tubules in Leydig cells, and inside seminiferous tubules in precursor cells to primary spermatids (**Figure 4-26**).

Objective 2: I developed a 2D-e protocol to increase the resolution of protein separation, and recently collaborated in the first optimization steps of a magnetic beads-based immunoprecipitation protocol for hCABS1.

Experiments downstream of 2D-e included WB and MS-seq. WB helped us determine the gel location of putative hCABS1 spots detected by our pAbs. Once 2D-e-WB was optimized, we selected these spots for MS-seq analysis. hCABS1 was not detected using this technique just as it wasn't detected when using a 1D-e platform with human samples. Two hypotheses arose from this data: (a) it is possible that hCABS1 is present in saliva in low abundance and that MS-seq is not sensitive enough to detect it, (b) hCABS1 is not present in saliva. Our current evidence does not allow to distinguish between these hypotheses.

<u>Objective 3</u>: I optimized a capillary nano-immunoassay (CNIA) protocol to validate our observations on the association between psychosocial stress and hCABS1.

Our group reported that in WB, pAb H2.0 detected a band of 27 kDa that positively correlated to self-perceived stress, and bands <27 kDa that seemed to be indicators of resilience to stress[21]. The ability of CNIA to use minuscule amounts of saliva samples and stock antibodies allowed us to evaluate the same samples[21] with H2.0, for validation, and H1.0, an antibody detecting the putative anti-inflammatory sequence in hCABS1, TDIFELL[18]. Using CNIA, H2.0 detected a 35 kDa protein in saliva, while H1.0 detected a 60 kDa protein. Interestingly, the levels of the 35 kDa protein followed the same pattern with regards to distress as those from the H2.0 WB-detected 27 kDa band[66], validating that H2.0 detects a protein that positively correlates to self-perceived psychosocial stress. As mentioned, MS-seq evaluation of 27 kDa gel spots representative of H2.0-detected WB bands and, potentially, of the 35 kDa protein detected in CNIA, suggest that hCABS1 is not present at that location. However, analysis of the proteins at that location identified carbonic anhydrase 6 (CA6), a protein that contains a domain with similarities to the peptide used as an immunogen for creating H2.0 (see **Figure C-4** in "Appendix C – MS-seq detected proteins in transient overexpression cell lysates and human saliva"); thus, a potential candidate for reacting with H2.0. However, a WB of recombinant CA6 probed with pAb H2.0 suggested that our pAb was not interacting with the recombinant CA6 (see **Figure 2-21** in Chapter 2). CA6 in SDS-PAGE has been reported at 37 kDa[232], similar to the molecular weight H2.0 detects in CNIA. Conversely, the antibody database provided by ProteinSimple, the company that developed CNIA, lists the occurrence of CA6 in their CNIA platform at 56 kDa[130], contrasting the peak we detect in saliva when using H2.0 at 35 kDa. Presently, we can say that H2.0 detects a protein in WB at 27 kDa and in CNIA at 35 kDa that positively correlates with perceived psychosocial stress. Whether this protein is hCABS1 or not remains to be confirmed. Adding to the enigma, mAb-based WB do not resolve this open question.

<u>Objective 4</u>: Dr Marcet-Palacios and I collaborated to analyze the hCABS1 protein sequence using *in silico* tools and widen knowledge of hCABS1.

We showed that predicted disordered regions in hCABS1 are mostly located near the carboxyl terminus of the protein. Dr Marcet-Palacios generated three putative 3-dimensional (3D) structures for hCABS1, all suggesting the occurrence of disordered regions as random coils and, interestingly, of the anti-inflammatory domain $_{380}$TDIFELL$_{386}$ of hCABS1 located near the carboxyl terminus, as an α-helix. I presented evidence of the conservation of this anti-inflammatory domain only in primates of the infraorder Simiiformes, of which humans are members. Dr Marcet-Palacios showed evidence on predicted phosphorylation sites, possible cofactor interaction sites, and the lack of a signal peptide sequence in hCABS1, likely impacting the way in which the protein is secreted *in vivo*. Given our previous observations in saliva of several discrete bands indicating proteolytic processing of hCABS1, we generated the predicted neutrophil elastase (a protease present in the oral cavity) degradome of hCABS1. Unsurprisingly, hCABS1 is predicted to be readily cleaved by neutrophil elastase (48 cleavage sites) at locations that were predicted to have an unfolded secondary structure.

While this degradome information of hCABS1 partially supports our previous findings of different-sized variants of hCABS1[18,21], our recent work on WB methodology and novel CNIA analysis suggest that such findings require further analyses and validation. Past this limitation, our *in silico* work supports CABS1 findings from other groups. The set of predicted cofactors interacting with hCABS1 is typical of those associated to energy metabolism and mitochondrial enzymes. Moreover, rat CABS1 has been observed using TEM in the inner mitochondrial membrane of developing spermatozoa[1]. Whether hCABS1 plays a role in energy metabolism is an exciting postulate that remains to be tested.Conclusion

The main hypotheses of this dissertation were:

1. Calcium-binding protein, spermatid-associated 1 (hCABS1) is found in human SMG lysates, saliva supernatant, and blood serum and our antibodies confirm its expression in these samples

2. Antibodies raised against hCABS1 sequence $_{184}$DEADMSNYNSSIKS$_{197}$ detect a variant(s) of the protein in saliva supernatant that is/are a biomarker(s) of acute psychosocial distress

This dissertation provides evidence for the existence of three hCABS1 variants in SMG (**Figure 7-2**, 2), the larger of which seems to be also present in serum (**Figure 7-2**, 3). Whether the three variants present in SMG are a result of proteolytic processing or post-translational modifications remains to be elucidated. I cannot confidently conclude that in response to distress (**Figure 7-2**, 1), hCABS1 is released into saliva (**Figure 7-2**, 3). However, I now recognize two limitations in
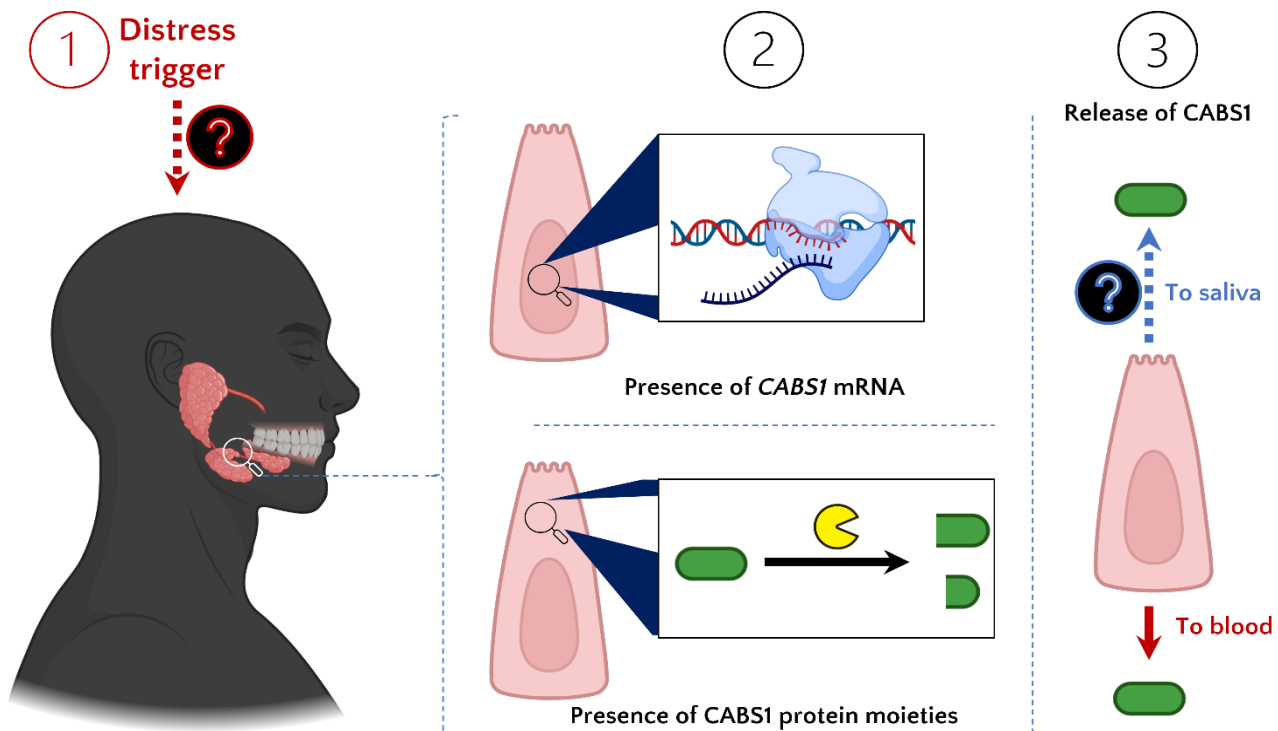
Figure 7-2. Revisited conceptual model.

Magnifying lenses represent zooming into the compartment where they are placed. Pink diagrams in panel (2) and (3) are representative of submandibular gland (SMG) cells. Careful optimization of monoclonal antibody (mAb)-based techniques warrants further studies to validate whether hCABS1 is associated to distress (1). (2) Our group has reported presence of CABS1 transcript in SMG lysates, and mAb-based Western blots suggest that 3 variants of varying size are present in SMG, potentially derivates of proteolytic degradation within that body compartment. (3) mAb-based WB are unable to confirm that hCABS1 is released into saliva; conversely, a variant of the same size is present in blood serum, suggesting its source could be SMG. *Figure made with Biorender.com*

my studies of saliva supernatant; (1) a potential cross-reactivity between the secondary antibody used in WB analyses, and (2) a lack of resolving power of the proteins present in this biofluid that may be addressed using 2D-e.

Important factors that contribute to my conclusions are:

(1) The similarities between rat SMR1 and human CABS1:

   a. The anti-inflammatory activity of heptamers TDIFEGG$_{SMR1}$ and TDIFELL$_{CABS1}$[18].

   b. The location of both genes in a cluster that seems to be conserved across both species in homologous chromosomes[18]

   c. Presence of both proteins in SMG and testes (of rats and humans)

(2) The evolutionary conservation of CABS1 anti-inflammatory domain TDIFELL in primate subgroup Simiiformes of which humans are part

(3) The presence of hCABS1 transcript in salivary glands, as reported by Shi et al.[16], Dela Cruz et al.[233] and our group[18]

(4) Our overall findings implying presence of hCABS1 in SMG and serum (the latter supported by Jin et al.[159]), and potential presence of hCABS1 in saliva being a result of following the International Working Group for Antibody Validation standards by:

   a. Using multiple antibodies to probe for the target protein and compare the profiles

   b. Using a tag-specific antibody to encounter a tag-including modified target protein

   c. Using two antibody-dependent methods (WB and CNIA) to cross-validate findings

   d. Optimizing antibody-dependent methods as a function of sample and context (WB, CNIA, immunohistochemistry and immunoprecipitation)

Thus, I conclude that (1) hCABS1 domain TDIFELL is analog to SMR1 domain TDIFEGG, (2) that evolutionary events may have relocated TDIFELL into *CABS1* of members of Simiiformes subgroup, and (3) that in humans hCABS1 is expressed in testes, SMG, and serum just as SMR1

is expressed in these compartments in rats. Further validation of saliva supernatant may show another biofluid where hCABS1 is expressed, just as SMR1 is found in rat saliva[53].

Chapter 8 : Future directions

We have suggested that hCABS1 is a candidate biomarker of stress in humans[21]. A biomarker may help in diagnosing a disease, assess severity or risk of an intervention, predict the effect(s) of a drug, or monitor the response of an intervention[234]. Proficient biomarkers should be significantly modified in diseased patients, when compared to controls, in turn aiding clinicians to make meaningful decisions that can improve a patient's quality of life[234]. Prior to biomarker discovery, a protocol that ensures reproducibility and specific targeting of the potential biomarker must be defined. Then, analysis of samples from a cohort using the streamlined protocol can validate if the putative marker is indicative of a biological difference when comparing the biomarker's profile between "case" and "control" groups[235]. Notably, the label "control" is subjective, and researchers must establish a rigorous set of characteristics that define "control" subjects. To validate the association between a candidate biomarker and disease, I consider there are two paramount checkpoints. Firstly, is proper sample collection and handling, and secondly, is ensuring that the analytical technique has specificity for the biomarker. Ideally, researchers could develop a diagnostic panel evaluating several biomarkers to better reflect the health of a patient.

With regards to the first checkpoint, I encourage collaborations with clinicians that follow rigorous patient recruitment and characterization techniques and who gather relevant data at each collection timepoint. Access to properly preserved and curated samples/data is necessary to study associations between any candidate biomarker and a malady.

Regarding the second checkpoint, the antibody-based techniques described in Chapter 2, Chapter 3 and Chapter 4 portray the evolution of methodologies and reagents used to target hCABS1. By translating a rigorous titration strategy across analytical platforms, I generated evidence that our antibodies detect hCABS1 in human testes, SMG, and serum. In SMG, WB profiles suggest that hCABS1 has at least 3 variants (**Table 5-1**, *mAbs detected: 63, 52, 42 kDa*), while a single form of the protein may be present in serum (**Table 5-1**, *mAbs detected: 63 kDa*). Moreover, the

occurrence of the 63 kDa band in both SMG and serum promotes the idea that this variant is released from SMG, an endocrine organ[178,179], into the bloodstream. We recognize that other endocrine organs could be a source of hCABS1. However, our research trail from rat to human suggests that SMG is an important source of this protein. Our initial evidence suggests that females and males express hCABS1 in SMG, but characterization of hCABS1 in serum was done from a male sample only. Future experiments of serum depleted of HSA and immunoglobulins from males and females could determine if there are sexually dimorphic variants of hCABS1 in this biofluid.

Despite my careful optimization of mAbs in WB, it is unclear if hCABS1 is present in saliva supernatant, mainly due to suspicion about interactions of our secondary antibodies in Western blot. Thus, I recommend removing secondary antibodies from our protocol by using an antibody labelling kits to tag our primary mAbs with a fluorescent molecule (suggestion: DyLight™ 800, Thermo Fisher Scientific – cat. # 53062). Comparison of secondary antibody and non-secondary antibody WB can validate if the bands we have observed in saliva supernatant reflect hCABS1. I also propose the use of our mAbs in the established 2D-e-WB system. The combination of labelled mAbs and 2D-e-WB could answer if hCABS1 is present in saliva supernatant and is being masked by abundant proteins with a similar molecular weight.

I encourage continuation of the magnetic beads-based immunoprecipitation (IP) platform using mAbs targeting hCABS1 to capture the protein from human-derived samples. Optimization can be assessed via Western blots of IP eluates (as shown in Chapter 4), and mass spectrometry sequencing of immunoprecipitated material. Once the IP protocol is optimized, pAb H2.0 should also be used to immunoprecipitate proteins from saliva supernatant. This could lead to determining the identities of the 27 kDa WB band that correlated with distress, and the <27 kDa bands that were linked to resilience to stress.

Provided hCABS1 can be sequenced from biofluids such as saliva supernatant and blood serum, the addition of an ELISA platform to analyze cohort samples can shed light on whether hCABS1 levels change in specific situations. Ideally, and provided it is technically and economically feasible, a panel of other candidate biomarkers should be analyzed in parallel, as more indicator molecules could better reflect the state of a patient.

Once our immunohistochemical analyses of hCABS1 in normal human tissues is complete, I recommend further immunohistochemical analyses to determine if distribution and abundance of hCABS1 changes in pathological states, such as Sjögren's syndrome, where other groups have shown downregulation of h*CABS1* transcript in females with this condition[16,17]. Collaborations with two groups (Case Western Reserve University, USA; University of Alberta, CA) with access to these tissues are in place and will facilitate the study on whether hCABS1 can be used as a biomarker of pathological states when evaluated via immunohistochemistry.

I further recommend synthesizing the anti-inflammatory domain of hCABS1 (hCABS1 a.a.: TDIFELL) and using it in assays to evaluate its anti-inflammatory effects on human cells. These assays could be performed using readily available cell lines in our group, the Alberta Respiratory Centre, such as Calu3, an epithelial cell line derived from lung adenocarcinoma, and LAD2, a mast cell (MC) line established from a MC sarcoma[236], as well as primary human neutrophils. An air-liquid interface culture system using primary human epithelial cells has already been established by members of the Alberta Respiratory Centre and this would be a good model to test the effects of hCABS1 and its anti-inflammatory domain on epithelial cell functions. Tests on the effects of TDIFELL in pro-inflammatory settings, such as during exposure to influenza, of which our group has strains A/WSN/1933 (H1N1) and A/Hong Kong/8/68 (H3N2), could shed light on whether TDIFELL has a therapeutic effect. If so, collaborations with the National Research Council of Canada Nanotechnology Research Centre, already in place, could lead to the development of a vector that effectively transports TDIFELL to target tissues, such as the lung, a location primarily

affected during flu infection. In parallel, these cell lines could be used to elucidate putative receptors for TDIFELL. This would continue a line of research published last in 2003, where TDIFEGG, a hCABS1 homolog anti-inflammatory peptide present in rat SMR1, showed binding and anti-inflammatory effects on rat neutrophils[24,43].

An ideal cell model to evaluate hCABS1 message and protein levels would be one derived from human SMG. Presently, the ATCC does not offer a human-derived SMG cell line[231]. When such a cell line becomes available, the hCABS1 transcript and protein profile should be characterized. The WB profiles using pAbs with this cell line would be ideal to validate if some of the bands reported[18,21] remain. Moreover, the localization of hCABS1 in this cell line could test if the protein exists inside mitochondria of SMG, as it has been reported in rat sperm[1]. Functional studies could help indicate what hCABS1 does in SMG. The use of knockout technology to ablate hCABS1 expression would prove beneficial. The effectiveness of hCABS1 knockout could be evaluated via RT-PCR and WB. Once two cell lines, hCABS1[(+)] and hCABS1[(-)], are established, both can be exposed to specific conditions depending on our group's research interests. Cell morphology and functional assays post-treatment could broaden the current understanding of hCABS1 function outside testicular tissue.

In silico analyses and the acquisition of data mining abilities would be important throughout these projects. Results from MS-seq-based analyses of diverse human-derived samples are freely available online, but processing the data is, to date, a skill that our group will need to develop further. There is a possibility that hCABS1 has been identified in large public domain proteomic studies, where there is no focus on any particular protein, potentially explaining why hCABS1 presence in tissues/fluids other-than-testes has not been explicitly reported. Of note, I have encountered reports of sequenced hCABS1 protein in Wang et al.[19] and Jin et al.[159] in tissues/fluids other-than-testes..

Collectively, these recommendations will help us elucidate if hCABS1 is truly present in SMG, blood serum, and saliva supernatant, if it is associated to stress and is an indicator of pathological state(s). Moreover, such approaches could help determine if the putative anti-inflammatory domain, TDIFELL, is associated with inflammation, and if hCABS1 has been annotated, but not reported, in other proteomic studies. Ultimately, we could write a treatise on the steps required to characterize a molecule and its functions, define challenges and their resolution, and contribute to scientific knowledge through a fascinating journey.

References

1. Calvel, P. *et al.* CLPH, a novel casein kinase 2-phosphorylated disordered protein, is specifically associated with postmeiotic germ cells in rat spermatogenesis. *J. Proteome Res.* **8**, 2953–2965 (2009).

2. Alves, V. S., Pimenta, D. C., Sattlegger, E. & Castilho, B. A. Biophysical characterization of Gir2, a highly acidic protein of Saccharomyces cerevisiae with anomalous electrophoretic behavior. *Biochem. Biophys. Res. Commun.* **314**, 229–234 (2004).

3. Graceffa, P., Jancsó, A. & Mabuchi, K. Modification of acidic residues normalizes sodium dodecyl sulfate-polyacrylamide gel electrophoresis of caldesmon and other proteins that migrate anomalously. *Arch. Biochem. Biophys.* (1992). doi:10.1016/0003-9861(92)90639-E

4. Kawashima, A. *et al.* CABS1 is a novel calcium-binding protein specifically expressed in elongate spermatids of mice. *Biol. Reprod.* **80**, 1293–1304 (2009).

5. Shawki, H. H. *et al.* Identification, localization, and functional analysis of the homologues of mouse CABS1 protein in porcine testis. *Exp. Anim.* **65**, 253–265 (2016).

6. MacLennan, D. H. & Wong, P. T. Isolation of a calcium-sequestering protein from sarcoplasmic reticulum. *Proc. Natl. Acad. Sci. U. S. A.* (1971). doi:10.1073/pnas.68.6.1231

7. Stevens, F. C. Calmodulin: an introduction. *Canadian journal of biochemistry and cell biology = Revue canadienne de biochimie et biologie cellulaire* (1983). doi:10.1139/o83-115

8. Opas, M., Dziak, E., Fliegel, L. & Michalak, M. Regulation of expression and intracellular distribution of calreticulin, a major calcium binding protein of nonmuscle cells. *J. Cell. Physiol.* (1991). doi:10.1002/jcp.1041490120

9. Nash, P. D., Opas, M. & Michalak, M. Calreticulin: not just another calcium-binding protein. *Mol. Cell. Biochem.* (1994). doi:10.1007/BF00925962

10. Huang, Q. *et al.* Integrated proteomics and metabolomics analysis of rat testis: Mechanism of arsenic-induced male reproductive toxicity. *Sci. Rep.* (2016). doi:10.1038/srep32518

11. Zhang, X. *et al.* Cabs1 Maintains Structural Integrity of Mouse Sperm Flagella during Epididymal Transit of Sperm. *Int. J. Mol. Sci.* **22**, (2021).

12. Omolaoye, T. S., Hachim, M. Y. & du Plessis, S. S. Using publicly available transcriptomic data to identify mechanistic and diagnostic biomarkers in azoospermia and overall male infertility. *Sci. Reports 2022 121* **12**, 1–17 (2022).

13. Calhoun, K. C. *et al.* Bisphenol A exposure alters developmental gene expression in the fetal rhesus macaque uterus. *PLoS One* **9**, e85894 (2014).

14. Cerny, K. L., Garrett, E., Walton, A. J., Anderson, L. H. & Bridges, P. J. A transcriptomal analysis of bovine oviductal epithelial cells collected during the follicular phase versus the luteal phase of the estrous cycle. *Reprod. Biol. Endocrinol.* **13**, (2015).

15. Krepischi, A. C. V. *et al.* Large germline copy number variations as predisposing factor in childhood neoplasms. *Futur. Oncol.* **10**, 1627–1633 (2014).

16. Shi, H. *et al.* Long non-coding RNA expression profile in minor salivary gland of primary Sjögren's syndrome. *Arthritis Res. Ther.* **18**, (2016).

17. De la Cruz, A. *et al.* Gene expression alterations in salivary gland epithelia of Sjögren's syndrome patients are associated with clinical and histopathological manifestations. *Sci. Rep.* **11**, 11154 (2021).

18. St. Laurent, C. D., St. Laurent, K. E., Mathison, R. D. & Befus, A. D. Calcium-binding protein, spermatid-specific 1 is expressed in human salivary glands and contains an anti-inflammatory motif. *Am. J. Physiol. - Regul. Integr. Comp. Physiol.* **308**, R569–R575 (2015).

19. Wang, D. *et al.* A deep proteome and transcriptome abundance atlas of 29 healthy human tissues. *Expression Atlas* **15**, (2019).

20. Ramaswamy, K. *et al.* Marked antiinflammatory effects of decentralization of the superior cervical ganglia. *J. Exp. Med.* **172**, 1819–1830 (1990).

21. Ritz, T. *et al.* A novel biomarker associated with distress in humans: calcium-binding protein, spermatid-specific 1 (CABS1). *Am. J. Physiol. - Regul. Integr. Comp. Physiol.* **312**, R1004–R1016 (2017).

22. Grisham, M. B., Everse, J. & Janssen, H. F. Endotoxemia and neutrophil activation in vivo. *Am. J. Physiol. - Hear. Circ. Physiol.* (1988). doi:10.1152/ajpheart.1988.254.5.h1017

23. Kindt, T. J., Goldsby, R. A. & Osborne, B. A. Kuby immunology, Sixth edition. in *Immunology* (2007).

24. Carter, L., Ferrari, J. K., Davison, J. S. & Befus, D. Inhibition of neutrophil chemotaxis and activation following decentralization of the superior cervical ganglia. *J. Leukoc. Biol.* (1992). doi:10.1002/jlb.51.6.597

25. Human Phenotype Ontology. Impaired oxidative burst. (2019). Available at: https://hpo.jax.org/app/browse/term/HP:0003203. (Accessed: 4th February 2020)

26. Mathison, R. *et al.* Role for the submandibular gland in modulating pulmonary inflammation following induction of systemic anaphylaxis. *Brain Behav. Immun.* (1992). doi:10.1016/0889-1591(92)90012-D

27. Miles, K., Chelmicka-Schorr, E., Atweh, S., Otten, G. & Arnason, B. G. Sympathetic ablation alters lymphocyte membrane properties. *J. Immunol.* (1985).

28. Bourne, H. R. *et al.* Modulation of inflammation and immunity by cyclic AMP. *Science* (1974). doi:10.1126/science.184.4132.19

29. Mathison, R., Befus, D. & Davison, J. S. Removal of the submandibular glands increases the acute hypotensive response to endotoxin. *Circ. Shock* (1993).

30. Parham, P. Over-reactions of the immune system. in *The Immune System* 364–400 (Garland Science, Taylor & Francis Group, LLC, 2009).

31. Bissonnette, E. Y., Mathison, R., Carter, L., Davison, J. S. & Befus, A. D. Decentralization of the superior cervical ganglia inhibits mast cell mediated TNFα-dependent cytotoxicity: 1 - Potential role of salivary glands. *Brain. Behav. Immun.* (1993). doi:10.1006/brbi.1993.1029

32. Mathison, R. *et al.* Temporal analysis of the anti-inflammatory effects of decentralization

of the rat superior cervical ganglia. *Am. J. Physiol. - Regul. Integr. Comp. Physiol.* (1994). doi:10.1152/ajpregu.1994.266.5.r1537

33. Mathison, R., Davison, J. S. & Dean Befus, A. Neuroendocrine regulation of inflammation and tissue repair by submandibular gland factors. *Immunol. Today* **15**, 527–532 (1994).

34. Perez, P., Rowzee, A. M., Zheng, C., Adriaansen, J. & Baum, B. J. Salivary epithelial cells: An unassuming target site for gene therapeutics. *International Journal of Biochemistry and Cell Biology* (2010). doi:10.1016/j.biocel.2010.02.012

35. Mathison, R. D., Befus, A. D. & Davison, J. S. A novel submandibular gland peptide protects against endotoxic and anaphylactic shock. *Am. J. Physiol. - Regul. Integr. Comp. Physiol.* (1997). doi:10.1152/ajpregu.1997.273.3.r1017

36. Rougeot, C. *et al.* Targets for SMR1-pentapeptide suggest a link between the circulating peptide and mineral transport. *Am. J. Physiol.* 1309–1320 (1997).

37. Mathison, R., Lo, P., Moore, G., Scott, B. & Davison, J. S. Attenuation of intestinal and cardiovascular anaphylaxis by the salivary gland tripeptide FEG and its D-isomeric analog feG. *Peptides* (1998). doi:10.1016/S0196-9781(98)00048-5

38. Liljeruhm, J. Exotic ribosomal enzymology. (Uppsala Universitet, 2019).

39. Mathison, R., Woodman, R. & Davison, J. S. Regulation of leukocyte adhesion to heart by the tripeptides feG and feG(NH2). *Can. J. Physiol. Pharmacol.* (2001). doi:10.1139/cjpp-79-9-785

40. Mathison, R., Lo, P., Tan, D., Scott, B. & Davison, J. S. The tripeptide feG reduces endotoxin-provoked perturbation of intestinal motility and inflammation. *Neurogastroenterol. Motil.* (2001). doi:10.1046/j.1365-2982.2001.00294.x

41. Metwally, E. *et al.* Submandibular gland tripeptide FEG (Phe-Glu-Gly) and analogues: Keys to structure determination. *Peptides* (2002). doi:10.1016/S0196-9781(01)00595-2

42. Shaji, J. & Patole, V. Protein and peptide drug delivery: Oral approaches. *Indian Journal of Pharmaceutical Sciences* (2008). doi:10.4103/0250-474X.42967

43. Mathison, R. D., Befus, A. D., Davison, J. S. & Woodman, R. C. Modulation of neutrophil function by the tripeptide feG. *BMC Immunol.* (2003). doi:10.1186/1471-2172-4-3

44. Dery, R. E. *et al.* Frontline: Inhibition of allergen-induced pulmonary inflammation by the tripeptide feG: A mimetic of a neuro-endocrine pathway. *Eur. J. Immunol.* (2004). doi:10.1002/eji.200425461

45. Mathison, R. D. & Davison, J. S. The tripeptide feG regulates the production of intracellular reactive oxygen species by neutrophils. *J. Inflamm.* (2006). doi:10.1186/1476-9255-3-9

46. User, H. M., Zelner, D. J., McKenna, K. E. & McVary, K. T. Microarray analysis and description of SMR1 gene in rat penis in a post-radical prostatectomy model of erectile dysfunction. *J. Urol.* (2003). doi:10.1097/01.ju.0000060882.75475.5a

47. Messaoudi, M., Desor, D., Nejdi, A. & Rougeot, C. The endogenous androgen-regulated sialorphin modulates male rat sexual behavior. *Horm. Behav.* (2004). doi:10.1016/j.yhbeh.2004.06.012

48. Davies, K. P., Tar, M., Rougeot, C. & Melman, A. Sialorphin (the mature peptide product of Vcsa1) relaxes corporal smooth muscle tissue and increases erectile function in the ageing

rat. *BJU Int.* (2007). doi:10.1111/j.1464-410X.2006.06577.x

49.   Wisner, A. *et al.* Human Opiorphin, a natural antinociceptive modulator of opioid-dependent pathways. *Proc. Natl. Acad. Sci. U. S. A.* (2006). doi:10.1073/pnas.0605865103

50.   Tong, Y. *et al.* hSMR3A as a marker for patients with erectile dysfunction. *J. Urol.* (2007). doi:10.1016/j.juro.2007.03.004

51.   Morris, K. *et al.* Vcsa1 gene peptides for the treatment of inflammatory and allergic reactions. *Recent Pat. Inflamm. Allergy Drug Discov.* **1**, 124–132 (2007).

52.   Rougeot, C., Rosinski-Chupin, I. & Rougeon, F. Novel genes and hormones in salivary glands: From the gene for the submandibular rat 1 protein (SMR1) precursor to receptor sites for SMR1 mature peptides. *Biomedical Reviews* (1998). doi:10.14748/bmr.v9.133

53.   Morris, K. E. *et al.* Autonomic nervous system regulates secretion of anti-inflammatory prohormone SMR1 from rat salivary glands. *AJP Cell Physiol.* **296**, C514–C524 (2008).

54.   Rougeot, C., Rosinski-Chupin, I., Njamkepo, E. & Rougeon, F. Selective processing of submandibular rat 1 protein at dibasic cleavage sites: Salivary and bloodstream secretion products. *Eur. J. Biochem.* (1994). doi:10.1111/j.1432-1033.1994.tb18556.x

55.   Stratakis, C. A. & Chrousos, G. P. Neuroendocrinology and Pathophysiology of the Stress System. *Ann. N. Y. Acad. Sci.* **771**, 1–18 (1995).

56.   Trueba, A. F., Mizrachi, D., Auchus, R. J., Vogel, P. D. & Ritz, T. Effects of psychosocial stress on the pattern of salivary protein release. *Physiol. Behav.* (2012). doi:10.1016/j.physbeh.2011.10.014

57.   Hellewell, S. C. & Cernak, I. Measuring resilience to operational stress in Canadian Armed Forces personnel. *J. Trauma. Stress* (2018). doi:10.1002/jts.22261

58.   Duric, V., Clayton, S., Leong, M. L. & Yuan, L. L. Comorbidity factors and brain mechanisms linking chronic stress and systemic illness. *Neural Plasticity* (2016). doi:10.1155/2016/5460732

59.   Dhabhar, F. S. Effects of stress on immune function: The good, the bad, and the beautiful. *Immunologic Research* (2014). doi:10.1007/s12026-014-8517-0

60.   Proctor, G. B. & Carpenter, G. H. Regulation of salivary gland function by autonomic nerves. *Autonomic Neuroscience: Basic and Clinical* (2007). doi:10.1016/j.autneu.2006.10.006

61.   Hu, S., Loo, J. A. & Wong, D. T. Human saliva proteome analysis and disease biomarker discovery. *Expert Review of Proteomics* (2007). doi:10.1586/14789450.4.4.531

62.   Pedersen, A. M. L., Sørensen, C. E., Proctor, G. B., Carpenter, G. H. & Ekström, J. Salivary secretion in health and disease. *Journal of Oral Rehabilitation* (2018). doi:10.1111/joor.12664

63.   Garrett, J. R. & Emmelin, N. Activities of salivary myoepithelial cells: A review. *Medical Biology* (1979).

64.   Lima, D. P., Diniz, D. G., Moimaz, S. A. S., Sumida, D. H. & Okamoto, A. C. Saliva: reflection of the body. *International Journal of Infectious Diseases* (2010). doi:10.1016/j.ijid.2009.04.022

65.   National Library of Medicine (US), N. C. for B. I. Protein [Internet]. *Calcium-binding and spermatid-specific protein 1 [Homo sapiens]* Available at: https://www.ncbi.nlm.nih.gov/protein/NP_149113.3?report=graph. (Accessed: 5th February 2020)

66.   Reyes-Serratos, E., Marcet-Palacios, M., Rosenfield, D., Ritz, T. & Befus, A. D. A method to study protein biomarkers in saliva using an automated capillary nano-immunoassay platform (Wes™). *J. Immunol. Methods* **479**, 112749 (2020).

67.   Foley, P. & Kirschbaum, C. Human hypothalamus-pituitary-adrenal axis responses to acute psychosocial stress in laboratory settings. *Neuroscience and Biobehavioral Reviews* **35**, 91–96 (2010).

68.   Atkinson, A. J. *et al.* Biomarkers and surrogate endpoints: Preferred definitions and conceptual framework. *Clinical Pharmacology and Therapeutics* (2001). doi:10.1067/mcp.2001.113989

69.   Guidance, T., Analysis, D. & Moore, B. C. Introduction to Western blotting. *MorphoSys UK Ltd* (2009).

70.   Forsström, B. *et al.* Proteome-wide epitope mapping of antibodies using ultra-dense peptide arrays. *Mol. Cell. Proteomics* (2014). doi:10.1074/mcp.M113.033308

71.   Taussig, M. J., Fonseca, C. & Trimmer, J. S. Antibody validation: a view from the mountains. *New Biotechnology* (2018). doi:10.1016/j.nbt.2018.08.002

72.   Signore, M. & Reeder, K. A. Antibody validation by western blotting. *Methods Mol. Biol.* (2012). doi:10.1007/978-1-60327-216-2_10

73.   Bajpai, R. & Terskikh, A. Genetic manipulation of human embryonic stem cells: Lentivirus vectors. in *Human Stem Cell Manual* (2007). doi:10.1016/B978-012370465-8/50024-7

74.   ProImmune Limited. *Protocols for the preparation of blood plasma and serum.* (2009).

75.   Salimetrics, L.L.C., SalivaBio, L. L. C. Saliva collection and handling advice. *Methods* (2011). doi:10.1016/s0927-7757(99)00503-8

76.   Deutsch, O. *et al.* An approach to remove alpha amylase for proteomic analysis of low abundance biomarkers in human saliva. *Electrophoresis* (2008). doi:10.1002/elps.200800207

77.   Bio-Rad Laboratories, I. TGX™ and TGX Stain-Free™ FastCast™ acrylamide kit and starter kit instruction manual.

78.   The UniProt Consortium. UniProt: a worldwide hub of protein knowledge The UniProt Consortium. *Nucleic Acids Res.* (2019). doi:10.1093/nar/gky1049

79.   Sievers, F. *et al.* Fast, scalable generation of high-quality protein multiple sequence alignments using Clustal Omega. *Mol. Syst. Biol.* (2011). doi:10.1038/msb.2011.75

80.   Brown, N. P., Leroy, C. & Sander, C. MView: A web-compatible database search or multiple alignment viewer. *Bioinformatics* (1998). doi:10.1093/bioinformatics/14.4.380

81.   Taylor, W. R. The classification of amino acid conservation. *J. Theor. Biol.* (1986). doi:10.1016/S0022-5193(86)80075-3

82.   Vitorino, R. *et al.* Identification of human whole saliva protein components using

proteomics. *Proteomics* (2004). doi:10.1002/pmic.200300638

83.	Jain, S., Ahmad, Y. & Bhargava, K. Salivary proteome patterns of individuals exposed to high altitude. *Arch. Oral Biol.* (2018). doi:10.1016/j.archoralbio.2018.09.002

84.	Sigma-Aldrich. *Normal serum, ascites, and cell supernatant typical immunoglobulin concentration ranges.*

85.	Gromov, P. *et al.* A single lysis solution for the analysis of tissue samples by different proteomic technologies. *Mol. Oncol.* (2008). doi:10.1016/j.molonc.2008.09.003

86.	Appleton, J. A., Bell, R. G., Homan, W. & Van Knapen, F. Consensus on Trichinella spiralis antigens and antibodies. in *Parasitology Today* (1991). doi:10.1016/0169-4758(91)90135-b

87.	Riegman, P. H. J., Morente, M. M., Betsou, F., de Blasio, P. & Geary, P. Biobanking for better healthcare. *Molecular Oncology* (2008). doi:10.1016/j.molonc.2008.07.004

88.	Ngoka, L. C. M. Sample prep for proteomics of breast cancer: Proteomics and gene ontology reveal dramatic differences in protein solubilization preferences of radioimmunoprecipitation assay and urea lysis buffers. *Proteome Sci.* (2008). doi:10.1186/1477-5956-6-30

89.	Sigma-Aldrich. Product information: Protease inhibitor cocktail for use with mammalian cell and tissue extracts. **Vol. 572**,

90.	Pringle, J. R. Chapter 9: Methods for avoiding proteolytic artifacts in studies of enzymes and other proteins from yeasts. *Methods Cell Biol.* (1975). doi:10.1016/S0091-679X(08)60956-5

91.	Kurien, B. T. & Scofield, R. H. Common artifacts and mistakes made in electrophoresis. *Methods Mol. Biol.* (2012). doi:10.1007/978-1-61779-821-4_58

92.	Burgess, R. R. Chapter 44: Important but little known (or forgotten) artifacts in protein biochemistry. in *Methods in Enzymology* (2009). doi:10.1016/S0076-6879(09)63044-5

93.	Rosinski-Chupin, I., Rougeot, C., Courty, Y. & Rougeon, F. Localization of mRNAs of two androgen-dependent proteins, SMR1 and SMR2, by in situ hybridization reveals sexual differences in acinar cells of rat submandibular gland. *J. Histochem. Cytochem.* (1993). doi:10.1177/41.11.8409372

94.	Howat, W. J. & Wilson, B. A. Tissue fixation and the effect of molecular fixatives on downstream staining procedures. *Methods* (2014). doi:10.1016/j.ymeth.2014.01.022

95.	O'Hurley, G. *et al.* Garbage in, garbage out: A critical evaluation of strategies used for validation of immunohistochemical biomarkers. *Molecular Oncology* (2014). doi:10.1016/j.molonc.2014.03.008

96.	Salamat, M. S. Robbins and Cotran: Pathologic basis of disease, 8th Edition. *J. Neuropathol. Exp. Neurol.* (2010). doi:10.1097/nen.0b013e3181cd8dbc

97.	Hawkes, R., Niday, E. & Gordon, J. A dot-immunobinding assay for monoclonal and other antibodies. *Anal. Biochem.* (1982). doi:10.1016/0003-2697(82)90677-7

98.	Shi, S. R., Key, M. E. & Kalra, K. L. Antigen retrieval in formalin-fixed, paraffin-embedded tissues: An enhancement method for immunohistochemical staining based on microwave oven heating of tissue sections. *J. Histochem. Cytochem.* (1991). doi:10.1177/39.6.1709656

99.	Stoeckelhuber, M. *et al.* The human submandibular gland: Immunohistochemical analysis of SNAREs and cytoskeletal proteins. *J. Histochem. Cytochem.* (2012). doi:10.1369/0022155411432785

100.	Ascoli, C. A. & Aggeler, B. Overlooked benefits of using polyclonal antibodies. *BioTechniques* (2018). doi:10.2144/btn-2018-0065

101.	Uhlen, M. Response to: Should we ignore western blots when selecting antibodies for other applications? *Nature Methods* (2017). doi:10.1038/nmeth.4194

102.	Bass, J. J. *et al.* An overview of technical considerations for Western blotting applications to physiological research. *Scandinavian Journal of Medicine and Science in Sports* (2017). doi:10.1111/sms.12702

103.	Cifù, A., Domenis, R., Pistis, C., Curcio, F. & Fabris, M. Anti-β2-glycoprotein I and anti-phosphatidylserine/prothrombin antibodies exert similar pro-thrombotic effects in peripheral blood monocytes and endothelial cells. *Autoimmun. Highlights* **10**, (2019).

104.	Chen, J., Chen, L., Xie, F. & Li, X. *Drug delivery applications of starch biopolymer derivatives. Drug Delivery Applications of Starch Biopolymer Derivatives* (2019). doi:10.1007/978-981-13-3657-7

105.	Jessie, K., Hashim, O. H. & Rahim, Z. H. A. Protein precipitation method for salivary proteins and rehydration buffer for two-dimensional electrophoresis. *Biotechnology* (2008). doi:10.3923/biotech.2008.686.693

106.	Ghafouri, B., Tagesson, C. & Lindahl, M. Mapping of proteins in human saliva using two-dimensional gel electrophoresis and peptide mass fingerprinting. in *Proteomics* (2003). doi:10.1002/pmic.200300426

107.	Hardt, M. *et al.* Toward defining the human parotid gland salivary proteome and peptidome: Identification and characterization using 2D SDS-PAGE, ultrafiltration, HPLC, and mass spectrometry. *Biochemistry* (2005). doi:10.1021/bi048176r

108.	Hu, S. *et al.* Large-scale identification of proteins in human salivary proteome by liquid chromatography/mass spectrometry and two-dimensional gel electrophoresis-mass spectrometry. *Proteomics* (2005). doi:10.1002/pmic.200401037

109.	Psychogios, N. *et al.* The human serum metabolome. *PLoS One* (2011). doi:10.1371/journal.pone.0016957

110.	Liotta, L. A., Ferrari, M. & Petricoin, E. Written in blood. *Nature* (2003). doi:10.1038/425905a

111.	Nustad, K., Gautvik, K. & Orstavik, T. Radioimmunoassay of rat submandibular gland kallikrein and the detection of immunoreactive antigen in blood. *Adv. Exp. Med. Biol.* (1979). doi:10.1007/978-1-4757-0926-1_23

112.	Berg, T., Johansen, L. & Nustad, K. Enzymatic activity of rat submandibular gland kallikrein released into blood. *Am. J. Physiol. - Hear. Circ. Physiol.* (1985). doi:10.1152/ajpheart.1985.249.6.h1134

113.	Aloe, L., Alleva, E., Böhm, A. & Levi-Montalcini, R. Aggressive behavior induces release of nerve growth factor from mouse salivary gland into the bloodstream. *Proc. Natl. Acad. Sci. U. S. A.* **83**, 6184–6187 (1986).

114.	Riondel, A. *et al.* Estimation of testosterone in human peripheral blood using S35-

thiosemicarbazide. *J. Clin. Endocrinol. Metab.* **23**, 620–628 (1963).

115. Stoléru, S. G., Ennaji, A., Cournot, A. & Spira, A. LH pulsatile secretion and testosterone blood levels are influenced by sexual arousal in human males. *Psychoneuroendocrinology* (1993). doi:10.1016/0306-4530(93)90005-6

116. Lee, D. C. *et al.* Monitoring plasma processing steps with a sensitive Western blot assay for the detection of the prion protein. *J. Virol. Methods* (2000). doi:10.1016/S0166-0934(99)00135-4

117. McNeilly, T. N. *et al.* Immunization of cattle with a combination of purified intimin-531, EspA and Tir significantly reduces shedding of Escherichia coli O157:H7 following oral challenge. *Vaccine* (2010). doi:10.1016/j.vaccine.2009.10.076

118. Gogolewski, R. P., Kania, S. A., Liggitt, H. D. & Corbeil, L. B. Protective ability of antibodies against 78- and 40-kilodalton outer membrane antigens of Haemophilus somnus. *Infect. Immun.* (1988). doi:10.1128/iai.56.9.2307-2316.1988

119. Levine, S., Kaliaber-Franco, R. & Paradiso, P. R. Demonstration that glycoprotein G is the attachment protein of respiratory syncytial virus. *J. Gen. Virol.* (1987). doi:10.1099/0022-1317-68-9-2521

120. Nataro, J. P. *et al.* Aggregative adherence fimbriae I of enteroaggregative Escherichia coli mediate adherence to HEp-2 cells and hemagglutination of human erythrocytes. *Infect. Immun.* (1992). doi:10.1128/iai.60.6.2297-2304.1992

121. Lutz, H. *et al.* Specificity assessment of feline T-lymphotropic Lentivirus serology. *J. Vet. Med. Ser. B* (1988). doi:10.1111/j.1439-0450.1988.tb00559.x

122. Altschul, S. F. *et al.* Gapped BLAST and PSI-BLAST: A new generation of protein database search programs. *Nucleic Acids Research* (1997). doi:10.1093/nar/25.17.3389

123. Burke, H. B. Predicting clinical outcomes using molecular biomarkers. *Biomark. Cancer* (2016). doi:10.4137/bic.s33380

124. Jimeno, A. Molecular biomarkers: their increasing role in the diagnosis, characterization, and therapy guidance in pancreatic cancer. *Mol. Cancer Ther.* (2006). doi:10.1158/1535-7163.mct-06-0005

125. Whitcomb, B. W. & Schisterman, E. F. Assays with lower detection limits: Implications for epidemiological investigations. *Paediatric and Perinatal Epidemiology* (2008). doi:10.1111/j.1365-3016.2008.00969.x

126. Rosa, N. *et al.* Protein quality assessment on saliva samples for biobanking purposes. *Biopreserv. Biobank.* (2016). doi:10.1089/bio.2015.0054

127. Xiao, H. & Wong, D. T. W. Method development for proteome stabilization in human saliva. *Anal. Chim. Acta* (2012). doi:10.1016/j.aca.2012.02.017

128. Kirschbaum, C., Pirke, K. M. & Hellhammer, D. H. The 'Trier Social Stress Test'--a tool for investigating psychobiological stress responses in a laboratory setting. *Neuropsychobiology* (1993). doi:10.1159/000119004

129. Chen, J. Q., Wakefield, L. M. & Goldstein, D. J. Capillary nano-immunoassays: Advancing quantitative proteomics analysis, biomarker assessment, and molecular diagnostics. *Journal of Translational Medicine* (2015). doi:10.1186/s12967-015-0537-6

130. ProteinSimple. Simple Western antibody database. (2020). Available at: https://www.proteinsimple.com/antibody/antibodies.html.

131. Onder, S. *et al.* Mass spectral detection of diethoxyphospho-tyrosine adducts on proteins from HEK293 cells using monoclonal antibody depY for enrichment. *Chem. Res. Toxicol.* (2018). doi:10.1021/acs.chemrestox.8b00083

132. ProteinSimple. *Molecular weight determination by electrophoresis of SDS-denatured proteins.* (2016).

133. Jasim, H., Carlsson, A., Hedenberg-Magnusson, B., Ghafouri, B. & Ernberg, M. Saliva as a medium to detect and measure biomarkers related to pain. *Sci. Rep.* (2018). doi:10.1038/s41598-018-21131-4

134. R&D Systems. *Human E-Cadherin Antibody (cat. # MAB1838)*. (R&D Systems).

135. Mathison, R. D., Befus, A. D. & Davison, J. S. A novel submandibular gland peptide protects against endotoxic and anaphylactic shock. *Am. J. Physiol. - Regul. Integr. Comp. Physiol.* **273**, R1017–R1023 (1997).

136. CTRNet Biobank Registration Program. Canadian Biosample Repository, Canada. Available at: https://biobanking.org/canreg/view/407. (Accessed: 27th January 2022)

137. Madden, K. S., Felten, S. Y., Felten, D. L., Sundaresan, P. R. & Livnat, S. Sympathetic neural modulation of the immune system. I. Depression of T cell immunity in vivo and in vitro following chemical sympathectomy. *Brain Behav. Immun.* **3**, 72–89 (1989).

138. Alito, A. E. *et al.* Autonomic nervous system regulation of murine immune responses as assessed by local surgical sympathetic and parasympathetic denervation. *Acta Physiol. Pharmacol. Latinoam.* **37**, 305–19 (1987).

139. Fujiwara, R. & Orita, K. The enhancement of the immune response by pain stimulation in mice. I. The enhancement effect on PFC production via sympathetic nervous system in vivo and in vitro. *J. Immunol.* **138**, 3699–3703 (1987).

140. Besedovsky, H. O., Rey, A. del, Sorkin, E., Da Prada, M. & Keller, H. H. Immunoregulation mediated by the sympathetic nervous system. *Cell. Immunol.* **48**, 346–355 (1979).

141. Mathison, R. *et al.* Temporal analysis of the anti-inflammatory effects of decentralization of the rat superior cervical ganglia. *Am. J. Physiol. - Regul. Integr. Comp. Physiol.* **266**, R1537–R1543 (1994).

142. Mathison, R. *et al.* Role for the submandibular gland in modulating pulmonary inflammation following induction of systemic anaphylaxis. *Brain Behav. Immun.* **6**, 117–129 (1992).

143. Mathison, R. D., Davison, J. S. & Befus, A. D. A peptide from the submandibular glands modulates inflammatory responses. *Int. Arch. Allergy Immunol.* **113**, 337–338 (1997).

144. Rougeot, C. *et al.* Sialorphin, a natural inhibitor of rat membrane-bound neutral endopeptidase that displays analgesic activity. *Proc. Natl. Acad. Sci. U. S. A.* **100**, 8549–8554 (2003).

145. Messaoudi, M., Desor, D., Nejdi, A. & Rougeot, C. The endogenous androgen-regulated sialorphin modulates male rat sexual behavior. *Horm. Behav.* **46**, 684–691 (2004).

146. Davies, K. P., Tar, M., Rougeot, C. & Melman, A. Sialorphin (the mature peptide product of

Vcsa1) relaxes corporal smooth muscle tissue and increases erectile function in the ageing rat. *BJU Int.* **99**, 431–435 (2007).

147. Marcet-Palacios, M. *et al.* Structural and posttranslational analysis of human calcium-binding protein, spermatid-associated 1. *J. Cell. Biochem.* **121**, 4945–4958 (2020).

148. Leenaars, M. & Hendriksen, C. F. M. Critical steps in the production of polyclonal and monoclonal antibodies: Evaluation and recommendations. *ILAR J.* (2005). doi:10.1093/ilar.46.3.269

149. TaKaRa Bio Inc. TaKaRa OCR human papillomavirus typing set (cat. #6603).

150. Gregory, R. I., Chendrimada, T. P. & Shiekhattar, R. MicroRNA Biogenesis 33 3 MicroRNA Biogenesis Isolation and Characterization of the Microprocessor Complex. *From Methods Mol. Biol.* **342**,

151. Thermo Fisher Scientific Inc. Pierce protein A/G magnetic beads (pub. no. MAN0015742). (2017).

152. Li-cor Biosciences. IRDye 800CW Goat Anti-Mouse IgG Pack Insert - doc. # 988-19845. (2021).

153. Jackson ImmunoResearch Inc. Western blotting after immunoprecipitation. Available at: https://www.jacksonimmuno.com/technical/products/applications/western-blot/anti-light-chain. (Accessed: 3rd February 2022)

154. Berglund, L., Andrade, J., Odeberg, J. & Uhlén, M. The epitope space of the human proteome. *Protein Sci.* **17**, 606 (2008).

155. Hebbes, T. R., Turner, C. H., Thorne, A. W. & Crane-Robinson, C. A 'minimal epitope' anti-protein antibody that recognises a single modified amino acid. *Mol. Immunol.* **26**, 865–873 (1989).

156. The Single Nucleotide Polymorphism Database (dbSNP) of Nucleotide Sequence Variation & The National Center for Biotechnology Information (NCBI). CABS1 - dbSNP - NCBI. Available at: https://www.ncbi.nlm.nih.gov/snp/?term=cabs1. (Accessed: 26th January 2022)

157. Hettegger, P. *et al.* High similarity of IgG antibody profiles in blood and saliva opens opportunities for saliva based serology. *PLoS One* **14**, (2019).

158. Blanchard, A. A. *et al.* Towards further defining the proteome of mouse saliva. *Proteome Sci.* **13**, 1–9 (2015).

159. Jin, W. H. *et al.* Human plasma proteome analysis by multidimensional chromatography prefractionation and linear ion trap mass spectrometry identification. *J. Proteome Res.* **4**, 613–619 (2005).

160. Rodriguez, J. M., Pozo, F., Di Domenico, T., Vazquez, J. & Tress, M. L. An analysis of tissue-specific alternative splicing at the protein level. *PLoS Comput. Biol.* **16**, (2020).

161. Ellis, J. D. *et al.* Tissue-specific alternative splicing remodels protein-protein interaction networks. *Mol. Cell* **46**, 884–892 (2012).

162. Buljan, M. *et al.* Tissue-specific splicing of disordered segments that embed binding motifs rewires protein interaction networks. *Mol. Cell* **46**, 871–883 (2012).

163. Holewinski, R. J., Jin, Z., Powell, M. J., Maust, M. D. & Van Eyk, J. E. A fast and reproducible method for albumin isolation and depletion from serum and cerebrospinal fluid. *Proteomics* **13**, 743 (2013).

164. Fu, Q., Garnham, C. P., Elliott, S. T., Bovenkamp, D. E. & Van Eyk, J. E. A robust, streamlined, and reproducible method for proteomic analysis of serum by delipidation, albumin and IgG depletion, and two-dimensional gel electrophoresis. *Proteomics* **5**, 2656–2664 (2005).

165. Xiang, Z., Wang, X., Gao, J., Morrow, K. J. & Nakashima, R. A. Identification of a higher molecular weight protein that shows apparent cross-reactivity with anti-p21ras monoclonal antibodies on Western blots. *J. Immunol. Methods* **168**, 275–282 (1994).

166. Abu-Shakra, M. & Shoenfeld, Y. Natural hidden autoantibodies. *Isr. Med. Assoc. J.* **9**, 748–749 (2007).

167. Coutinho, A., Kazatchkine, M. D. & Avrameas, S. Natural autoantibodies. *Curr. Opin. Immunol.* **7**, 812–818 (1995).

168. Ahmed, N. *et al.* An approach to remove albumin for the proteomic analysis of low abundance biomarkers in human serum. *Proteomics* **3**, 1980–1987 (2003).

169. Young, B., O'Dowd, G. & Woodford, P. Male reproductive system. in *Wheater's Functional Histology* 337–350 (Elsevier, 2014).

170. Damiani, E. & Margreth, A. Subcellular fractionation to junctional sarcoplasmic reticulum and biochemical characterization of 170 kDa Ca2+-and low-density-lipoprotein-binding protein in rabbit skeletal muscle. *Biochem. J.* **277**, 825 (1991).

171. Köhler, C. & Neuhaus, G. Characterisation of calmodulin binding to cyclic nucleotide-gated ion channels from Arabidopsis thaliana. *FEBS Lett.* **471**, 133–136 (2000).

172. García-Ortega, L. *et al.* Anomalous electrophoretic behavior of a very acidic protein: Ribonuclease U2. *Electrophoresis* **26**, 3407–3413 (2005).

173. Ziemer, M. A., Mason, A. & Carlson, D. M. Cell-free translations of proline-rich protein mRNAs. *J. Biol. Chem.* **257**, 11176–11180 (1982).

174. Castle, A. M., Stahl, L. E. & Castle, J. D. A 13-amino acid n-terminal domain of a basic proline-rich protein is necessary for storage in secretory granules and facilitates exit from the endoplasmic reticulum. *J. Biol. Chem.* **267**, 13093–13100 (1992).

175. Chapter 13 Sodium dodecyl sulphate polyacrylamide gel electrophoresis (SDS-PAGE). *J. Chromatogr. Libr.* **63**, 217–274 (2001).

176. Uhlen, M. *et al.* A proposal for validation of antibodies. *Nat. Methods* **13**, 823–827 (2016).

177. Leão, R., Neris, S., Kaur, A. & Gomes, A. V. Incorrect molecular weights due to inaccurate prestained protein molecular weight markers that are used for gel electrophoresis and Western blotting. *bioRxiv* 2020.04.03.023465 (2020). doi:10.1101/2020.04.03.023465

178. Noguchi, S., Ohba, Y. & Oka, T. Influence of epidermal growth factor on liver regeneration after partial hepatectomy in mice. *J. Endocrinol.* (1991). doi:10.1677/joe.0.1280425

179. Kurachi, H., Okamoto, S. & Oka, T. Evidence for the involvement of the submandibular gland epidermal growth factor in mouse mammary tumorigenesis (mammary tumor growth/sialodenectomy). *Proc. Natl. Acad. Sci. U. S. A.* (1985).

doi:10.1073/pnas.82.17.5940

180. Rosinski-Chupin, I., Tronik, D. & Rougeon, F. High level of accumulation of a mRNA coding for a precursor-like protein in the submaxillary gland of male rats. *Proc. Natl. Acad. Sci. U. S. A.* (1988). doi:10.1073/pnas.85.22.8553

181. Prilusky, J. *et al.* FoldIndex©: A simple tool to predict whether a given protein sequence is intrinsically unfolded. *Bioinformatics* (2005). doi:10.1093/bioinformatics/bti537

182. Iakoucheva, L. M. Identification of intrinsic order and disorder in the DNA repair protein XPA. *Protein Sci.* (2001). doi:10.1110/ps.29401

183. Yang, J. *et al.* The I-TASSER suite: Protein structure and function prediction. *Nature Methods* (2014). doi:10.1038/nmeth.3213

184. Hu, X., Dong, Q., Yang, J. & Zhang, Y. Recognizing metal and acid radical ion-binding sites by integrating ab initio modeling with template-based transferals. *Bioinformatics* (2016). doi:10.1093/bioinformatics/btw637

185. Ma, J., Wang, S., Zhao, F. & Xu, J. Protein threading using context-specific alignment potential. in *Bioinformatics* (2013). doi:10.1093/bioinformatics/btt210

186. Schrödinger, L. The PyMol molecular graphics system, Version 1.8. *Thomas Holder* (2015). doi:10.1007/s13398-014-0173-7.2

187. Wiederstein, M. & Sippl, M. J. ProSA-web: Interactive web service for the recognition of errors in three-dimensional structures of proteins. *Nucleic Acids Res.* (2007). doi:10.1093/nar/gkm290

188. Colovos, C. & Yeates, T. O. Verification of protein structures: Patterns of nonbonded atomic interactions. *Protein Sci.* (1993). doi:10.1002/pro.5560020916

189. Blom, N., Sicheritz-Pontén, T., Gupta, R., Gammeltoft, S. & Brunak, S. Prediction of post-translational glycosylation and phosphorylation of proteins from the amino acid sequence. *Proteomics* (2004). doi:10.1002/pmic.200300771

190. Xue, Y. *et al.* GPS 2.1: Enhanced prediction of kinase-specific phosphorylation sites with an algorithm of motif length selection. *Protein Eng. Des. Sel.* (2011). doi:10.1093/protein/gzq094

191. Nielsen, H. Predicting secretory proteins with signaIP. in *Methods in Molecular Biology* (2017). doi:10.1007/978-1-4939-7015-5_6

192. Madeira, F. *et al.* The EMBL-EBI search and sequence analysis tools APIs in 2019. *Nucleic Acids Res.* (2019). doi:10.1093/nar/gkz268

193. Sievers, F. & Higgins, D. G. Clustal omega, accurate alignment of very large numbers of sequences. *Methods Mol. Biol.* (2014). doi:10.1007/978-1-62703-646-7_6

194. Waterhouse, A. M., Procter, J. B., Martin, D. M. A., Clamp, M. & Barton, G. J. Jalview Version 2-A multiple sequence alignment editor and analysis workbench. *Bioinformatics* (2009). doi:10.1093/bioinformatics/btp033

195. Dereeper, A. *et al.* Phylogeny.fr: robust phylogenetic analysis for the non-specialist. *Nucleic Acids Res.* (2008). doi:10.1093/nar/gkn180

196. Edgar, R. C. MUSCLE: Multiple sequence alignment with high accuracy and high

throughput. *Nucleic Acids Res.* (2004). doi:10.1093/nar/gkh340

197. Castresana, J. Selection of conserved blocks from multiple alignments for their use in phylogenetic analysis. *Mol. Biol. Evol.* (2000). doi:10.1093/oxfordjournals.molbev.a026334

198. Anisimova, M. & Gascuel, O. Approximate likelihood-ratio test for branches: A fast, accurate, and powerful alternative. *Syst. Biol.* (2006). doi:10.1080/10635150600755453

199. Chevenet, F., Brun, C., Bañuls, A. L., Jacq, B. & Christen, R. TreeDyn: Towards dynamic graphics and annotations for analyses of trees. *BMC Bioinformatics* (2006). doi:10.1186/1471-2105-7-439

200. Garcia-Boronat, M., Diez-Rivero, C. M., Reinherz, E. L. & Reche, P. A. PVS: a web server for protein sequence variability analysis tuned to facilitate conserved epitope discovery. *Nucleic Acids Res.* (2008). doi:10.1093/nar/gkn211

201. Díez-Rivero, C. M. & Reche, P. Discovery of conserved epitopes through sequence variability analyses. in *Bioinformatics for Immunomics* (2009). doi:10.1007/978-1-4419-0540-6_8

202. Shytaj, I. L. & Savarino, A. Cell-mediated anti-Gag immunity in pharmacologically induced functional cure of simian AIDS: A 'bottleneck effect'? *J. Med. Primatol.* (2015). doi:10.1111/jmp.12176

203. Geraghty, P. *et al.* Neutrophil elastase up-regulates Cathepsin B and Matrix Metalloprotease-2 expression. *J. Immunol.* (2007). doi:10.4049/jimmunol.178.9.5871

204. Keremi, B. *et al.* Stress and salivary glands. *Curr. Pharm. Des.* (2017). doi:10.2174/1381612823666170215110648

205. Dawes, C. & Wong, D. T. W. Role of saliva and salivary diagnostics in the advancement of oral health. *J. Dent. Res.* (2019). doi:10.1177/0022034518816961

206. Burger, V. M., Nolasco, D. O. & Stultz, C. M. Expanding the range of protein function at the far end of the order-structure continuum. *Journal of Biological Chemistry* (2016). doi:10.1074/jbc.R115.692590

207. Kalmar, L., Homola, D., Varga, G. & Tompa, P. Structural disorder in proteins brings order to crystal growth in biomineralization. *Bone* (2012). doi:10.1016/j.bone.2012.05.009

208. Pauwels, K., Lebrun, P. & Tompa, P. To be disordered or not to be disordered: is that still a question for proteins in the cell? *Cellular and Molecular Life Sciences* (2017). doi:10.1007/s00018-017-2561-6

209. Klement, E. & Medzihradszky, K. F. Extracellular protein phosphorylation, the neglected side of the modification. *Molecular and Cellular Proteomics* (2017). doi:10.1074/mcp.O116.064188

210. Ambudkar, I. Calcium signaling defects underlying salivary gland dysfunction. *Biochimica et Biophysica Acta - Molecular Cell Research* (2018). doi:10.1016/j.bbamcr.2018.07.002

211. Reinhardt, D. P., Ono, R. N. & Sakai, L. Y. Calcium stabilizes fibrillin-1 against proteolytic degradation. *J. Biol. Chem.* (1997). doi:10.1074/jbc.272.2.1231

212. Sohar, I., Bird, J. W. C. & Moore, P. B. Calcium-dependent proteolysis of calcium-binding proteins. *Biochem. Biophys. Res. Commun.* (1986). doi:10.1016/0006-291X(86)90387-6

213. Whiteman, P. *et al.* A G1127S change in calcium-binding epidermal growth factor-like domain 13 of human fibrillin-1 causes short range conformational effects. *J. Biol. Chem.* (2001). doi:10.1074/jbc.M006547200

214. Ramasubbu, N., Paloth, V., Luo, Y., Brayer, G. D. & Levine, M. J. Structure of human salivary α-amylase at 1.6 Å resolution: Implications for its role in the oral cavity. *Acta Crystallogr. Sect. D Biol. Crystallogr.* (1996). doi:10.1107/S0907444995014119

215. Pohl, M., Sprenger, G. A. & Müller, M. A new perspective on thiamine catalysis. *Current Opinion in Biotechnology* (2004). doi:10.1016/j.copbio.2004.06.002

216. Jung, E. H., Takeuchi, T., Nishino, K. & Itokawa, Y. Studies on the nature of thiamine pyrophosphate binding and dependency on divalent cations of transketolase from human erythrocytes. *Int. J. Biochem.* (1988). doi:10.1016/0020-711X(88)90228-5

217. Maguire, D., Talwar, D., Shiels, P. G. & McMillan, D. The role of thiamine dependent enzymes in obesity and obesity related chronic disease states: A systematic review. *Clinical Nutrition ESPEN* (2018). doi:10.1016/j.clnesp.2018.02.007

218. Ciszak, E. M., Korotchkina, L. G., Dominiak, P. M., Sidhu, S. & Patel, M. S. Structural basis for flip-flop action of thiamin pyrophosphate-dependent enzymes revealed by human pyruvate dehydrogenase. *J. Biol. Chem.* (2003). doi:10.1074/jbc.M300339200

219. Ævarsson, A. *et al.* Crystal structure of human branched-chain α-ketoacid dehydrogenase and the molecular basis of multienzyme complex deficiency in maple syrup urine disease. *Structure* (2000). doi:10.1016/S0969-2126(00)00105-2

220. Johnson, M. T., Yang, H. S. & Patel, M. S. Targeting E3 component of α-keto acid dehydrogenase complexes. *Methods Enzymol.* (2000). doi:10.1016/s0076-6879(00)24254-7

221. Tomita, T., Kuzuyama, T. & Nishiyama, M. Structural basis for leucine-induced allosteric activation of glutamate dehydrogenase. *J. Biol. Chem.* (2011). doi:10.1074/jbc.M111.260265

222. Gaudet, P., Livstone, M. S., Lewis, S. E. & Thomas, P. D. Phylogenetic-based propagation of functional annotations within the Gene Ontology consortium. *Brief. Bioinform.* (2011). doi:10.1093/bib/bbr042

223. Perelman, P. *et al.* A molecular phylogeny of living primates. *PLoS Genet.* (2011). doi:10.1371/journal.pgen.1001342

224. Chou, P. Y. & Fasman, G. D. Prediction of the secondary structure of proteins from their amino acid sequence. in *Advances in Enzymology and Related Areas of Molecular Biology* (2006). doi:10.1002/9780470122921.ch2

225. Emini, E. A., Hughes, J. V, Perlow, D. S. & Boger, J. Induction of hepatitis A virus-neutralizing antibody by a virus-specific synthetic peptide. *J. Virol.* (1985). doi:10.1128/jvi.55.3.836-839.1985

226. Karplus, P. A. & Schulz, G. E. Prediction of chain flexibility in proteins - A tool for the selection of peptide antigens. *Naturwissenschaften* (1985). doi:10.1007/BF01195768

227. Kolaskar, A. S. & Tongaonkar, P. C. A semi-empirical method for prediction of antigenic determinants on protein antigens. *FEBS Lett.* (1990). doi:10.1016/0014-5793(90)80535-Q

228. Parker, J. M. R., Guo, D. & Hodges, R. S. New hydrophilicity scale derived from high-

performance liquid chromatography peptide retention data: Correlation of predicted surface residues with antigenicity and x-ray-derived accessible sites. *Biochemistry* (1986). doi:10.1021/bi00367a013

229. Larsen, J. E. P., Lund, O. & Nielsen, M. Improved method for predicting linear B-cell epitopes. *Immunome Res.* (2006). doi:10.1186/1745-7580-2-2

230. Jespersen, M. C., Peters, B., Nielsen, M. & Marcatili, P. BepiPred-2.0: Improving sequence-based B-cell epitope prediction using conformational epitopes. *Nucleic Acids Res.* (2017). doi:10.1093/nar/gkx346

231. American Type Culture Collection. Search | ATCC: human submandibular gland. Available at: https://www.atcc.org/search#q=submandibular gland&sort=relevancy&numberOfResults=24&f:Productcategory=[Human cells]. (Accessed: 29th March 2022)

232. Thatcher, B. J., Doherty, A. E., Orvisky, E., Martin, B. M. & Henkin, R. I. Gustin from human parotid saliva is carbonic anhydrase VI. *Biochem. Biophys. Res. Commun.* (1998). doi:10.1006/bbrc.1998.9356

233. Dela Cruz, A. *et al.* Gene expression alterations in salivary gland epithelia of Sjögren's syndrome patients are associated with clinical and histopathological manifestations. *Sci. Rep.* **11**, 11154 (2021).

234. Ray, P., Manach, Y. Le, Riou, B. & Houle, T. T. Statistical Evaluation of a Biomarker. *Anesthesiology* **112**, 1023–1040 (2010).

235. Loth, E. *et al.* The meaning of significant mean group differences for biomarker discovery. *PLOS Comput. Biol.* **17**, e1009477 (2021).

236. Kirshenbaum, A. S. *et al.* Characterization of novel stem cell factor responsive human mast cell lines LAD 1 and 2 established from a patient with mast cell sarcoma/leukemia; Activation following aggregation of FcεRI or FcγRI. *Leuk. Res.* (2003). doi:10.1016/S0145-2126(02)00343-0

237. Sigma-Aldrich. Stains-All. (2022). Available at: https://www.sigmaaldrich.com/CA/en/product/sial/e9379?gclid=CjwKCAjwuYWSBhBy EiwAKd_n_qg4s-f7JJcmpcYGCsmulDO9tZtG6VR4xGz26gpBZA4Lpv8S8ltwvBoCjxcQAvD_BwE.

Appendix A – A novel biomarker associated with distress in humans: calcium-binding protein, spermatid-specific 1 (CABS1)

To whom it may concern,

We have appended the article entitled A novel biomarker associated with distress in humans: calcium-binding protein, spermatid-specific 1 (CABS1) published in 2017 in the American journal of physiology, regulatory, integrative and comparative physiology volume 312, issue 6.

Eduardo contributed to this article by performing an SDS-PAGE separation of a human saliva supernatant sample, excising the section of the gel corresponding to 27 kDa, the same where pAb to CABS1 H2.0 detects a band that correlates to psychosocial stress, and submitting the gel sections for mass spectrometry sequencing (MS-seq) analysis. MS-seq results did not identify CABS1 in the sample. On this basis, the following sentence was added to the article:

> "As we experienced with salivary gland extracts and despite several attempts to immunoprecipitate and sequence CABS1 immunoreactive bands from saliva, it is a limitation of our work that we have been unable to confirm the identity of these immunoreactive bands with mass spectroscopy."

Respectfully yours,

Thomas Ritz
PhD, Professor of Psychology
Dedman College of Humanities & Sciences
Southern Methodist University

A. Dean Befus
Professor Emeritus
Alberta Respiratory Centre
University of Alberta

Eduardo Reyes Serratos
MSc Candidate
Alberta Respiratory Centre
University of Alberta

RESEARCH ARTICLE | *Neural Control*

A novel biomarker associated with distress in humans: calcium-binding protein, spermatid-specific 1 (CABS1)

Thomas Ritz,[1] David Rosenfield,[1] Chris D. St. Laurent,[2] Ana F. Trueba,[1,3] Chelsey A. Werchan,[1] Pia D. Vogel,[4] Richard J. Auchus,[5] Eduardo Reyes-Serratos,[2] and A. Dean Befus[2]

[1]*Department of Psychology, Southern Methodist University, Dallas, Texas;* [2]*Pulmonary Research Group, Department of Medicine, University of Alberta, Edmonton, Alberta, Canada;* [3]*Quito Brain and Behavior Laboratory, Universidad San Francisco de Quito, Quito, Ecuador;* [4]*Department of Biological Sciences, Southern Methodist University, Dallas, Texas; and* [5]*Department of Internal Medicine, University of Michigan Medical Center, Ann Arbor, Michigan*

Ritz T, Rosenfield D, St. Laurent CD, Trueba AF, Werchan CA, Vogel PD, Auchus RJ, Reyes-Serratos E, Befus AD. A novel biomarker associated with distress in humans: calcium-binding protein, spermatid-specific 1 (CABS1). *Am J Physiol Regul Integr Comp Physiol* 312: R1004–R1016, 2017. First published April 5, 2017; doi:10.1152/ajpregu.00393.2016.—Calcium-binding protein spermatid-specific 1 (CABS1) is expressed in the human submandibular gland and has an anti-inflammatory motif similar to that in submandibular rat 1 in rats. Here, we investigate CABS1 in human saliva and its association with psychological and physiological distress and inflammation in humans. Volunteers participated across three studies: *1*) weekly baseline measures; *2*) a psychosocial speech and mental arithmetic stressor under evaluative threat; and *3*) during academic exam stress. Salivary samples were analyzed for CABS1 and cortisol. Additional measures included questionnaires of perceived stress and negative affect; exhaled nitric oxide; respiration and cardiac activity; lung function; and salivary and nasal inflammatory markers. We identified a CABS1 immunoreactive band at 27 kDa in all participants and additional molecular mass forms in some participants. One week temporal stability of the 27-kDa band was satisfactory (test–retest reliability estimate = 0.62–0.86). Acute stress increased intensity of 18, 27, and 55 kDa bands; 27-kDa increases were associated with more negative affect and lower heart rate, sympathetic activity, respiration rate, and minute ventilation. In both acute and academic stress, changes in 27 kDa were positively associated with salivary cortisol. The 27-kDa band was also positively associated with VEGF and salivary leukotriene B4 levels. Participants with low molecular weight CABS1 bands showed reduced habitual stress and negative affect in response to acute stress. CABS1 is readily detected in human saliva and is associated with psychological and physiological indicators of stress. The role of CABS1 in inflammatory processes, stress, and stress resilience requires careful study.

calcium-binding protein, spermatid-specific 1; saliva; acute and chronic stress; negative affect; cortisol; submandibular rat 1; anti-inflammatory activity

SALIVA HAS BEEN used successfully to analyze changes in hormonal, immune, and enzymatic activity related to stress in humans (5a, 46, 47). Most frequently, salivary free cortisol has been analyzed, and increases have been demonstrated in paradigms of laboratory speech and mental-challenge tasks (24,

30). Other studies have identified a range of markers involved in the innate mucosal immune response, such as IgA, mucins, lactoferrin, and cystatin S, which respond to acute laboratory (7, 54, 75) or real-life (6, 28, 40, 48) stress. Markers of adaptive immune activity, such as ILs or chemokines, have also been found secreted in saliva and altered by stressors in the laboratory (27, 53) or real life (2, 76). Exploration of stress-sensitive protein markers in saliva continues to evolve (10, 34, 46, 70, 75), and discovery of new markers and their function in organisms' adaptation to challenge and adverse life conditions holds promise for improved understanding of the stress response and the development of novel interventions.

One such marker may be calcium-binding protein, spermatid-specific 1 (CABS1), previously also known as casein-like phosphoprotein, chromosome 4, open-reading frame 35, and testis development protein NYD-SP26, identified in spermatids in selected phases of spermatogenesis and originally thought to be testis specific (11, 29). However, recently, we detected CABS1 expression in human submandibular and parotid glands and lungs and described multiple molecular weight forms of CABS1, the profile that appears to be tissue specific (71). Moreover, we discovered that human CABS1 contains an amino acid sequence (TDIFELL) with anti-inflammatory activities and with close homology to an anti-inflammatory sequence (TDIFEGG) identified in a related salivary gland protein, submandibular rat 1 (SMR1) (38).

Interestingly, SMR1 is a prohormone with peptide fragments that have a diversity of biological activities, ranging from inhibition of inflammatory responses (18, 33, 37, 41) to effects on erectile function (41, 72, 79), analgesic activity (60), and modulation of mineral balance in tissues (61). SMR1 is under neuroendocrine regulation (39, 45, 59), and it has been postulated that its fragments and their functions are differentially regulated by autonomic and endocrine pathways.

Given that CABS1 may be an ortholog of SMR1, with similar tissue distribution and multiple molecular weight forms, we postulated that CABS1 might be influenced by neuroendocrine pathways as is SMR1. To test this hypothesis, we investigated whether CABS1 might be found in human saliva and whether its levels might be influenced by acute or prolonged stress, perhaps in a manner similar to the effects of stress on cortisol levels in saliva. Specifically, we examined susceptibility of CABS1 to an acute psychosocial stressor in

Address for reprint requests and other correspondence: A. D. Befus, Pulmonary Research Group, Dept. of Medicine, Univ. of Alberta, HMRC, Rm. 557, Edmonton, AB, Canada, T6G 2S2 (e-mail: dean.befus@ualberta.ca).

the laboratory with a free speech and mental arithmetic challenge under evaluative threat. This design also allowed us to study the association of CABS1 with typically well-documented, short-term cortisol elevations following stress (24), as well as cardiorespiratory responses to the stress protocol. CABS1 was also measured in college students during a final exam stress period and compared with a low-stress period during their academic term. This protocol allowed for the examination of stress levels sustained over multiple days and also the association of CABS1 with slower developing inflammatory processes. In addition, we sought to examine the temporal stability of CABS1 levels across multiple weeks. All three studies also provided us with the opportunity to study the association of CABS1 with basic demographics, asthmatic vs. nonasthmatic status, and measures of negative affect, including perceived stress, anxiety, and depression.

METHODS

Overview of Studies

Saliva samples were collected from participants in three studies. *Study 1* included a multiple baseline study with five weekly assessments to study the temporal stability of CABS1 and baseline associations with questionnaire measures of negative affect. In *study 2*, participants were administered a psychosocial laboratory stress-induction tool with a speech and mental arithmetic stressor under evaluative threat, which allowed us to study the response of CABS1 to an acute psychosocial stressor under controlled conditions. *Study 3* was an observational protocol of academic final examination stress, allowing us to examine the response of CABS1 to conditions of more sustained real-life stress. Participants in the two stress protocols participated in larger data collections, focused on stress and airway inflammation in health and asthma (57, 74a, 77), and the protocols included salivary cortisol measures and exhaled nitric oxide as a marker of airway inflammation. VEGF and leukotriene B4 (LTB4)—markers of inflammatory processes—were collected from the upper airways in one of these protocols.

Participants

For the laboratory stress study, participants were recruited mostly from the undergraduate psychology research volunteer pool at a university in the Southwestern US and additionally, from the community. Students received extra course credit points for participation. Those not interested in credit and community participants were reimbursed with $35 (in *studies 2* and *3*) for their time. Participants had to be free of known respiratory diseases, except for asthma in *studies 2* and *3*. Exclusion criteria also included self-reported current smoking and any severe heart conditions, such as angina, myocardial infarction, congestive heart failure, transient ischemic attacks, or cerebrovascular accidents. Those with asthma required a physician diagnosis of their condition and no administration of oral or injected corticosteroids in the previous 6 wk (or 3 mo in *study 2*). Asthma control was rated according to the Global Initiative for Asthma (20a). Studies were approved by the local Institutional Review Board in accordance with the Code of Ethics of the World Medical Association (Declaration of Helsinki), and all participants provided written, informed consent.

Collection of Saliva

Saliva samples were collected with cotton swabs (Salivettes; Sarstedt, Newton, NC), which participants placed in their mouth for 2 min. Once completed, participants placed them into individual plastic capsules. Samples were frozen at −80°C until they were analyzed. For analyses, cotton swabs were centrifuged, and collected saliva volumes were recorded to account for changes in salivary flow, which may affect protein concentrations across assessments.

Salivary samples were shipped to the University of Alberta (Edmonton, AB, Canada) on dry ice and then stored at −20°C until analyses. As described previously for Western blot analyses (71), saliva samples were boiled in 1% SDS with 20 mM 1,4-DTT for 5 min, and then proteins were separated on 12% polyacrylamide gels (25 μg salivary protein solution was loaded for each sample) and transferred to nitrocellulose membranes (Bio-Rad Laboratories, Mississauga, ON, Canada). Prestained protein standards (Bio-Rad Laboratories) were run on each gel with rabbit anti-CABS1 (immunogen was amino acids 184–197; DEADMSNYNSSIKS) primary antibody that was affinity purified with the immunogen (previously identified as H2 antibody AB_2571742) (71) at a final concentration of 3 μg/ml. Preimmune serum from rabbit H2 was used as an isotype control, and as a blocking control, the immunizing peptide was incubated in 10× amounts (30 μg/ml) with H2 (3 μg/ml) for 18 h before applying to the membrane. Omission of the primary antibody was also used as a negative control. The secondary antibody was IRDye 800CW goat anti-rabbit (1:10,000; AB_621843; Mandel, Guelph, ON, Canada). Mouse anti-human β-actin (AB_1119529) was used to assess protein loading (1:5,000; Santa Cruz Biotechnology, Dallas, TX) with the secondary antibody, goat anti-mouse IRDye 680 (AB_10956588; Mandel). Blots were visualized with an Odyssey imager (Li-Cor Biosciences, Lincoln, NE) by scanning simultaneously at 700 and 800 nm. Odyssey software was used for molecular weight determination and quantitation of band intensity on Western blots.

To standardize quantitation of bands, an internal control was established using a human submandibular gland extract that we previously described (71). This standard sample was run on each Western blot, and all immunoreactive bands detected in saliva were normalized to the 27-kDa band from this human submandibular gland extract and reported as relative fluorescent units. All saliva samples were run in duplicate on different days, and their normalized values were averaged.

Detection of Salivary Cortisol

Salivary cortisol concentrations were determined using a commercially available kit, Coat-A-Count cortisol kit (cat. no. TKCO2; Siemens Medical Solutions Diagnostics, Los Angeles, CA), which had a detection limit of 0.03 pg/ml with serial dilution of the lowest calibrator standard.

Additional Physiological Measures

Fractional exhaled nitric oxide (FE_NO) was measured with a hand-held electrochemical analyzer (Niox Mino; Aerocrine, Solna, Sweden) in accordance with current guidelines (1, 68). Major sources of measurable airway nitric oxide are epithelial cells in healthy individuals and a variety of immune cells, including macrophages, mast cells, and eosinophils, in individuals with allergic asthma (19, 20, 33, 52). One exhalation was performed against a stable resistance of 50 ml for a duration of 10 s. Participants were instructed not to eat and only to drink water, 2 h before assessments, to avoid the influences by nitrate-rich foods. Exercise or heavier physical activity was also discouraged for at least 1 h before the session. Spirometric lung function was measured in *study 3* with a hand-held electronic spirometer (AM2; Jaeger/Toennies, Würzburg, Germany) as the best of three blows.

As parameters reflecting upper airway inflammatory activity, VEGF was measured in nasal fluid and LTB4 in nasal fluid and saliva. Collection of saliva followed the same protocol as outline above. Nasal fluid was sampled by 3 ml saline solution (0.9% sodium chloride; Addipak Unit Dose Solutions, model HUD20039; Teleflex Medical, Morrisville, NC), instilled into each nostril with an Intranasal Mucosal Atomization Device (LMA MAD Nasal syringe; Teleflex

Medical). The liquid was collected in a kidney dish and transferred into small storage tubes (58, 74a).

The samples were stored immediately at −80°C. For analysis, samples were concentrated twofold using an Eppendorf Vacufuge and a Fisher Scientific MaximaDry vacuum pump. With the use of enzyme immunoassay kits (Enzo Life Science, Plymouth Meeting, PA), the amounts of LTB4 and VEGF were determined, as described in Trueba et al. (74a). The detection limits of the kits were 5.6 pg/ml for LTB4 and 14.0 pg/ml for VEGF. Controls were performed that showed that the increased salt concentration, resulting from the vacuum concentration of the samples, did not affect the sensitivity of the kits.

In *study 2*, the electrocardiogram and respiration were measured by respiratory inductance plethysmography (LifeShirt; VivoMetrics, Ventura, CA) with two inductance bands for the thorax and abdomen, with Ag/AgCl electrodes placed on the sternum, left costal arch of the 10th rib, and left clavicle. Signals were amplified and analog-to-digital converted with a sampling rate of 200 Hz. Bands were calibrated using a fixed volume bag (800 ml), followed by offline qualitative diagnostic calibration (62) and fixed volume calibration. A dedicated biosignal analysis program (Vivologic; VivoMetrics) was then used to eliminate artifacts (e.g., ectopic beats, movement artifacts) and extract relevant parameters. For respiratory parameters, tidal volume (V_T) and total respiratory cycle time (T_{TOT}) were extracted and also used to calculate minute ventilation ($\dot{V}_E$). Heart rate (HR) was calculated from the distance between adjacent R-waves. The cardiac T-wave amplitude (TWA; in millivolts) was extracted using the ECG boundary location function (32), embedded in the Acq*Knowledge* biosignal analysis software package (version 4.1; Biopac Systems, Goleta, CA). The TWA has been used as a surrogate measure of cardiac sympathetic activity because of its sensitivity to isoproterenol and β-adrenergic blockade (15, 31, 43, 51). In adults, stressful laboratory challenges typically attenuate the TWA (25, 31, 64). Although measures from impedance cardiography are more common for noninvasive estimation of cardiac sympathetic activity (50, 67), the implementation of this technique was not possible in this study because of the potential for interference with the respiratory inductance plethysmography measurements. As a noninvasive estimate of cardiac vagal activity, respiratory sinus arrhythmia (RSA) was extracted from fluctuations of the interbeat interval in the time domain by the peak-valley method (21) using the customized RSA Toolbox software (65). RSA was log transformed to improve distributional characteristics. Because RSA is strongly influenced by the respiratory pattern (5, 9, 21, 22, 26), with both longer and deeper breaths increasing RSA—potentially independent of cardiac vagal activity changes—an additional within-individual correction of RSA was used (56). Raw RSA was normalized by V_T (RSA/V_T); then coefficients from a within-individual regression equation, based on the pace-breathing measurements, were used to determine the predicted RSA/V_T for any given T_{TOT} during the experiment; and the deviation of observed from predicted RSA/V_T was then calculated. This strategy has been shown to improve the estimation of cardiac vagal activity (21, 55, 63). The grand mean of unadjusted RSA/V_T was added to obtain the respiration-corrected RSA, and the resulting values were log transformed. Results are also reported for respiration-uncorrected logRSA, to allow comparison with existing literature that does not control for respiration.

Questionnaire Measures

The Hospital Anxiety and Depression Scale (HADS) (16, 85) was used to assess depressive mood and anxious mood in the past week. Current-state negative affect was assessed with the negative affect subscale of the Positive Affect Negative Affect Schedule (PANAS-NA) (82). An additional ad hoc rating scale (0 = "not at all"; 10 = "extremely") was used to measure how much stress participants felt in the moment in *study 1*. Perceived stress was assessed with the Perceived Stress Scale (PSS) (13, 14), which measures feelings of being overwhelmed and unable to cope with challenges in the past 4

wk. The 10-item version was used at the beginning of all studies, except for approximately one-half of the participants of *study 1* ($n = 30$), who were administered the abbreviated four-item version to reduce the overall burden of the assessments in the second wave. Symptoms of acute upper respiratory infections (common cold) were measured with the Wisconsin Upper Respiratory Symptom Survey (WURSS)-21 (3). Symptom severity was captured with 10 items on an 8-point scale, ranging from 0 ("do not have this symptom at all") to 7 ("severe"). The scale has good change sensitivity and a positive association with biological infection markers (3, 4).

Procedures

Study 1. For multiple baseline assessments, participants were invited for five weekly assessments over a period of 4 wk. Day of the week was kept constant for individual participants, as was time of day (between 8 AM and 6 PM) to control for diurnal effects. In each session, participants provided saliva samples and performed measurements of FeNO. Afterwards, participants completed a questionnaire battery at a computer terminal. Upon completion of the fifth visit, participants were debriefed about the purpose of the study.

Study 2. Participants attending sessions in this study were administered the Trier Social Stress Test (30). Sessions were scheduled in the early afternoon, beginning between 12 and 3 PM. Initially, participants completed a questionnaire battery, including trait measures of stress, anxiety, and depression. After the baseline assessments, the participants were told that they will be asked to give a presentation, which should make a particularly good case for them as candidates for the chief executive officer position of a major US retailer. Two "experts on presentation skills" (one male and one female confederate of the experimenter), who would evaluate the performance regarding intelligence, creativity, and body language, were then introduced briefly to the participants. Each participant was then given 5 min alone to prepare the speech. Afterwards, the experts returned, and the participant was expected to give a 5-min speech standing in a conference room with a video camera turned on. Then, the participants were unexpectedly asked to perform a mental arithmetic task that consisted of subtracting the number 13 from the number 6,233 and to keep subtracting the remainder aloud as accurately and as quickly as possible. The duration of the mental arithmetic task was 5 min. Throughout, the confederates were required to maintain neutral facial expression and offer no encouragement. Only simple instructions were provided to continue with the speech or to start again from the beginning when the arithmetic task contained a mistake. Saliva samples were scheduled at 15 and 0 min prestress and at 0, 15, 30, and 45 min poststress. Participants also completed a questionnaire on momentary negative affect at these time points. Quiet sitting measures of cardiac and respiratory activity were initiated 3 min before saliva sampling and FE$_{NO}$ measurement at 18 and 3 min prestress and at 12, 27, and 42 min poststress. Additional measures during the 10 min of stress task performance were extracted in 2.5-min increments, of which the last 2.5-min increment of the mental arithmetic task was used as a measure preceding the first 0-min poststress saliva sample. For poststress assessments, participants returned to sitting posture and were then fully debriefed, and the experimenter explored any signs of residual distress. Before the session, participants with asthma were asked to discontinue short-acting bronchodilators for 6 h, long-acting beta-adenergic agonists for 12 h, and leukotriene modifiers for 3 days.

Study 3. Participants provided data at three assessment points: one at a low-stress period during the middle of the term when participants had no exams or major projects and two during the 10 days of final academic exams at the end of the term. The low-stress assessment was scheduled 2–6 wk before the first final exam assessment. During the exam period, an early and a late final exam assessment were spaced 5 to 7 days apart. Assessments thus captured sustained academic pressures associated with a final exam period rather than acute stress of an

Table 1. *Characteristics of participants in the 3 studies of CABS1 in saliva*

	Study 1, n = 64	Study 2, n = 16	Study 3, n = 19
Gender, women, n (%)	51 (79.7)	6 (37.5)	18 (94.7)
Age, mean (SD)	20.2 (4.3)	33.6 (15.0)	19.8 (1.0)
Race, white, n (%)	39 (61.9)	14 (87.5)	16 (84.2)
Ethnicity, Hispanic, n (%)	10 (15.9)	1 (6.3)	2 (10.5)
Asthma, n (%)	3 (4.7)	10 (62.5)	6 (31.6)
Asthma, n (%) women	3 (100.0)	4 (40.0)	6 (100.0)
Asthma well controlled, n (%)*	3 (100.0)	8 (80.0)	5 (83.3)
Age of asthma onset, yr, mean (SD)	Not available	6.3 (6.1)	7.8 (4.8)
Maintenance medication, n (%)	0 (0.00)	6 (60.0)	3 (50.0)

*Rated according to Global Initiative for Asthma (2013) (20a).

examination (6). To control for diurnal effects, each participant was scheduled at the same time of day for all assessments. At each assessment, participants completed a questionnaire package, followed by saliva collection and FE_{NO} assessments. After the third session, participants were thanked and debriefed about the purpose of the study. For participants with asthma, the same instructions for discontinuation of medication were used as in *study 2*.

Data Reduction and Analyses

In *study 1*, data were obtained from a total of 64 participants (51 women). Three of the participants had asthma and were excluded from the group statistics to reduce potential variability. From the remaining participants, 60 provided samples in the first and second assessment, 48 in the third assessment, 50 in the fourth assessment, and 47 in the fifth assessment. Pearson correlations were calculated to study the stability of the levels of the 27-kDa band across assessments. *Studies 2* and *3* involved 16 (11 women) and 19 participants (18 women), respectively (Table 1).

Mixed effects models (MEMs) were used to analyze the data, since these models are intent-to-treat analyses that include all subjects, regardless of missing data. Two sets of analyses were conducted for each study. First, we examined the longitudinal associations between the 27-kDa band and possible related predictors, including demographics, mood, lung function, and physiological measures. Because recent research indicates that to assess accurately the longitudinal relations between variables, one must disaggregate the between-subjects effects from the within-subjects effects (81), we first calculated the average level of each predictor for each individual across the assessments. This average level provided the score for the between-subjects differences in the predictor. Then, for each predictor, we calculated the deviations from the average level for each individual at each assessment. These deviation scores provided the within-subjects measures of changes in the predictor over time. Both the deviation scores and the average scores were included as predictors of the 27-kDa band in the MEMs. We also included asthma status (yes/no), age, body mass index (BMI), and time as control variables in all analyses.

The second set of analyses examined the change in our variables over time. These analyses were performed as repeated-measures

ANOVAs, using MEMs to calculate the ANOVAs (which therefore retain all participants regardless of dropout or missing data). We modeled the covariance matrix of the errors of the repeated measures as "unstructured" in all MEMs.

RESULTS

Abundance of Bands Immunoreactive to CABS1

Western blot analyses of the saliva identified a 27-kDa band of CABS1 in each of the 99 participants of the 3 studies (for basic description of participants, see Table 1). In 13 participants across the three studies, low-abundance CABS1 immunoreactive bands below 27 kDa were also detected at 20, 18, 15, and/or 12 kDa (Table 2 and Fig. 1). The extra bands were seen in relatively greater proportions in men (20.8%) than women (10.6%). They also tended to co-occur; thus three women and one man showed both 18 and 12 kDa bands, one man showed bands at 18, 15, and 12 kDa, and two women showed all four bands at 20, 18, 15, and 12 kDa. The 12-kDa band was found alone in two women and the 18-kDa band alone in three men and one woman. Participants with extra bands below 27 kDa self-identified as white, except for one with a 12-kDa band who was African-American and had asthma, and one with an-18 kDa band who was Hispanic and had no asthma. One of the women with all four additional bands identified as white and had asthma.

An additional 10 participants also showed bands with a higher molecular mass between 33 and 90 kDa (Fig. 1); 6 of these were asthmatic. Proportionally, extra bands above 27 kDa were seen more in men (16.6%) than women (8%). A band at 55 kDa was most frequently seen, and it co-occurred with the 90-kDa band in five cases (2 of these were men). One man showed all three bands at 33, 55, and 90 kDa. All participants with extra bands in this range self-identified as white, except for one African-American woman with bands at 55 and 90 kDa.

Table 2. *Abundance of immunoreactive bands of CABS1 in 3 studies for total sample and for subsamples of women*

	90 kDa	55 kDa	33 kDa	27 kDa	12 kDa	15 kDa	18 kDa	20 kDa	Total 12–20 kDa	Total 33–90 kDa
Study 1, n = 64, n (%)	0 (0.0)	0 (0.0)	0 (0.0)	64 (100.0)	5 (7.8)	0 (0.0)	4 (6.3)	0 (0.0)	6 (9.4)	0 (0.0)
Women, n = 51, n (%)	0 (0.0)	0 (0.0)	0 (0.0)	51 (100.0)	5 (9.8)	0 (0.0)	4 (7.8)	0 (0.0)	6 (11.8)	0 (0.0)
Study 2, n = 16, n (%)	5 (31.3)	7 (43.8)	1 (6.3)	16 (100.0)	2 (12.5)	1 (6.3)	5 (31.3)	0 (0.0)	5 (31.3)	7 (43.8)
Women, n = 6, n (%)	3 (18.1)	3 (36.4)	0 (9.1)	6 (100.0)	0 (0.0)	0 (0.0)	0 (0.0)	0 (0.0)	0 (0.0)	3 (36.4)
Study 3, n = 19, n (%)	0 (0.0)	3 (15.8)	0 (0.0)	19 (100.0)	2 (10.5)	2 (10.5)	2 (10.5)	2 (10.5)	2 (10.5)	3 (15.8)
Women, n = 18, n (%)	0 (0.0)	3 (16.7)	0 (0.0)	18 (100.0)	2 (11.1)	2 (11.1)	2 (11.1)	2 (10.5)	2 (11.1)	3 (16.7)
Total, n = 99, n (%)	5 (0.5)	10 (10.1)	1 (0.0)	99 (100.0)	9 (9.1)	3 (3.0)	11 (11.1)	2 (2.0)	13 (13.1)	10 (10.1)
Women, n = 75, n (%)	3 (4.0)	6 (8.0)	0 (0.0)	75 (100.0)	7 (9.3)	2 (2.6)	6 (8.0)	2 (2.6)	8 (10.6)	6 (8.0)

Fig. 1. CABS1 is detected in saliva at varying molecular weights among different individuals and stress conditions. A representative Western blot showing CABS1 detected in saliva from 3 different individuals across 3 studies. *Lane 1* contains human submandibular gland (SMG) as a normalization control. *Lanes 2–5* contain saliva samples collected weekly over 4 wk from 1 participant in *study 1* (multiple baseline assessment). *Lanes 6–11* contain saliva samples collected at 6 time points (−15 and −0 m are prestress; +0, +15, +30, and +45 m are poststress) from 1 participant during *study 2* (acute laboratory stress). *Lanes 12–14* contain saliva samples collected at 3 time points (pre is before exams begin; early and late are during exams) from 1 participant in *study 3* (final exam stress). All lanes were loaded with 25 μg protein, and all immunoreactive band intensity values were normalized to the 27-kDa band in SMG.
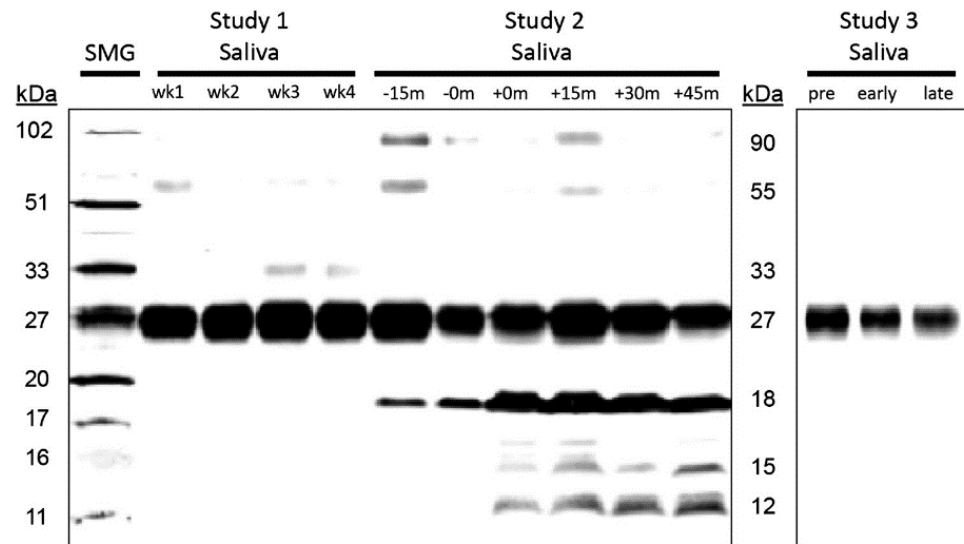
Multiple Baseline Assessments: Study 1

Temporal consistency of CABS1 27-kDa band intensity levels in saliva. The consistency of the 27-kDa band intensity (relative fluorescent units normalized to the standard) in 25 μg salivary protein between individuals was very good to fair in the range of test–retest reliability estimate = 0.51–0.86 (Table 3; lower correlation matrix) across all weeks. This was comparable with the consistency of FE_{NO} levels (Table 3; upper correlation matrix). Consistency of the levels did not decline for the 27-kDa band as a function of time, whereas such a decline was the case for FE_{NO}. Intensity of the 27-kDa band across weeks did not change significantly for the sample overall, although there was some fluctuation of individual intensity levels (Fig. 2). Saliva volume did not change significantly across time points ($P = 0.537$).

Association of the CABS1 27-kDa band with demographics and negative affect. No significant associations were found for the quantitative assessment of the 27-kDa band with age, gender, race, or ethnicity. The quantity of the 27-kDa band was positively associated with BMI ($P < 0.05$). Participants with overall higher ratings of current stress had higher amounts of the 27-kDa band ($P < 0.001$), as had those with a higher depressive mood in the past week (HADS depressive mood; $P < 0.05$), as well as those with a higher anxious mood in the past week (HADS anxious mood; $P < 0.10$), after controlling for age, gender, BMI, and assessment wave.

Association of the CABS1 27-kDa band with airway nitric oxide. FE_{NO} changes from week to week were positively associated with 27 kDa band changes ($P < 0.01$), after controlling for age, gender, BMI, and assessment wave.

Acute Laboratory Stress: Study 2

Effects of acute stress on the CABS1 band at 27 kDa in saliva. MEM analysis indicated that the 27-kDa band changed significantly over pre- and poststress assessments ($P < 0.01$), with visible and significant increases from 0 min prestress to 0 min poststress ($P < 0.01$) and a drop at 45 min poststress ($P < 0.05$; Fig. 3). Saliva volume varied significantly across time [$F(5,13) = 3.66$, $P = 0.028$], which was probably due to higher values for the initial 15-min prestress measurement relative to subsequent measurements, but none of the individual time point comparisons was significant ($P > 0.112$).

Association of the CABS1 band at 27 kDa with demographics and negative affect. No significant associations were observed between the levels of the 27-kDa band and age, gender, or race/ethnicity. Changes in PANAS-NA were positively associated with changes in the levels of the 27-kDa band ($P < 0.01$) (Table 4).

Table 3. *Comparison of the stability of CABS1 (27 kDa; lower half of matrix) in saliva and of fractional exhaled nitric oxide (upper half of matrix) in study 1 (5 weekly baseline assessments)*

	Week 1	Week 2	Week 3	Week 4	Week 5
Week 1	1	0.68 (57)	0.66 (49)	0.66 (50)	0.54 (43)
Week 2	0.62 (55)	1	0.84 (49)	0.77 (49)	0.70 (43)
Week 3	0.70 (43)	0.62 (44)	1	0.81 (42)	0.77 (37)
Week 4	0.51 (44)	0.63 (45)	0.86 (37)	1	0.78 (38)
Week 5	0.72 (43)	0.67 (43)	0.81 (35)	0.66 (36)	1

All $P < 0.001$. Pearson correlations (r) are shown; sample n in parentheses.

Fig. 2. CABS1 band of 27 kDa for individual participants across 5 weekly baseline assessments.

27 kDa Band of CABS1 Pre-and Post-Stress Testing
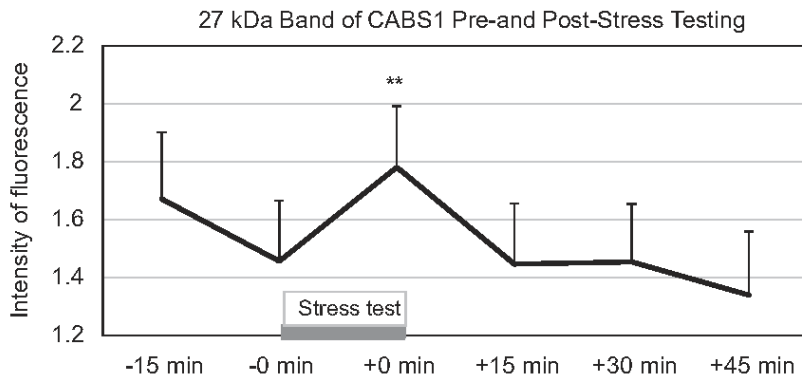
Fig. 3. CABS1 band of 27 kDa during the laboratory stress assessment protocol with the Trier Social Stress Test. **$P <$ 0.01 relative to measurement at 0 min before stress (-0 min).

Association of the CABS1 band at 27 kDa with salivary cortisol, FE$_{NO}$, and cardiorespiratory activity. MEM analyses, controlling for age, gender, BMI, and time, showed a higher overall 27-kDa band intensity for participants with lower HR ($P < 0.001$). Within subjects, greater increases in the 27-kDa band were related to weaker HR increases ($P < 0.001$), less reduction in TWA ($P < 0.05$), slower breathing (longer T$_{TOT}$; $P < 0.01$), and greater cortisol increases ($P < 0.05$; Table 4).

Academic Exam Stress: Study 3

Effects of final exam stress on CABS1 in saliva. MEM analysis with the three time points did not show any significant change in the 27-kDa band over time. Including the between-subject group variable asthma (yes/no) did not change the findings. No group differences or interactions of time with the

group variable were found. The 27-kDa band showed a marked variability in the direction of change from low to high stress periods (Fig. 4). Saliva volume remained stable across measurements ($P = 0.775$). To examine whether date of sample testing impacted the 27-kDa band, we performed a cross-classified MEM, with baseline date, early exam date, and late exam date as a cross-classified grouping variable for the 27-kDa band level. We found no effect of any cross-classified groupings (baseline data, early exam date, or late exam date) on the level of the 27-kDa band ($P > 0.238$).

Association of the CABS1 27-kDa band with demographics, negative affect, and asthma. The 27-kDa band was not substantially associated with age, gender, or asthma status but showed a marginal positive association with BMI ($P < 0.10$). Variables of negative affect were not significantly associated with the band in this sample (Table 5).

Association of the CABS1 27-kDa band with salivary cortisol and FEV$_1$. The levels of the 27-kDa band were positively and significantly associated with levels of cortisol, both between ($P < 0.01$) and within ($P < 0.05$) subjects, after controlling for group, age, BMI, and time (Table 5). Thus participants with higher overall levels of cortisol had higher 27 kDa band values, and changes in cortisol from low to high stress exam periods were also positively associated with changes in the 27-kDa band. No association was found between CABS1 in saliva and forced expiratory volume in the first second (FEV$_1$).

Table 4. *Between- and within-subject associations of the CABS1 27-kDa band with other physiological parameters and the negative-affect rating and time effects of parameters across the Trier Social Stress Test (study 2)*

	Time[a]	Between[b]	Within[b]
HR	28.7‡	−0.08‡	−0.03‡
TWA	−0.13‡	3.70	1.37*
logRSA	−10.5*	0.00	0.00
logRSA$_c$	−8.23	0.01	0.00
T$_{TOT}$	0.06	0.15	0.13‡
V$_T$	−0.03	−0.19	−0.15
V̇$_E$	0.81	−0.01	−0.03*
FE$_{NO}$	0.11	0.00	−0.15
Salivary cortisol	1.05	−0.06	0.02*
PANAS-NA	0.49†	−1.06	0.34†
PSS		−0.26	
27 kDa band	0.32†		

Results are from mixed effects models (MEMs) analyses of individual parameters as a single-time varying covariate of the 27-kDa band. Time effects show contrast of 0 min prestress vs. final 2.5 min of the math stressor for cardiac and respiratory indices, 0 min prestress vs. 0 min poststress for Fe$_{NO}$, and 0 min prestress vs. the mean of 0, 15, 30, and 45 min poststress for cortisol. For Time effects, positive coefficients indicate increases over 0 min prestress and negative coefficients indicate decreases. HR, heart rate; TWA, T-wave amplitude; logRSA, logarithm of respiratory sinus arrhythmia; logRSA$_c$, logarithm of respiratory sinus arrhythmia corrected for tidal volume (V$_T$) and residualized by total respiratory cycle time (T$_{TOT}$); V̇$_E$, minute ventilation; FE$_{NO}$, fractional exhaled nitric oxide; PANAS-NA, Positive Affect Negative Affect Schedule subscale negative affect; PSS, Perceived Stress Scale. *$P < 0.05$. †$P < 0.01$. ‡$P < 0.001$. [a]Controlling for age and gender. [b]Controlling for age, gender, and time.

27 kDa Band Of CABS1 in Final Exam Stress
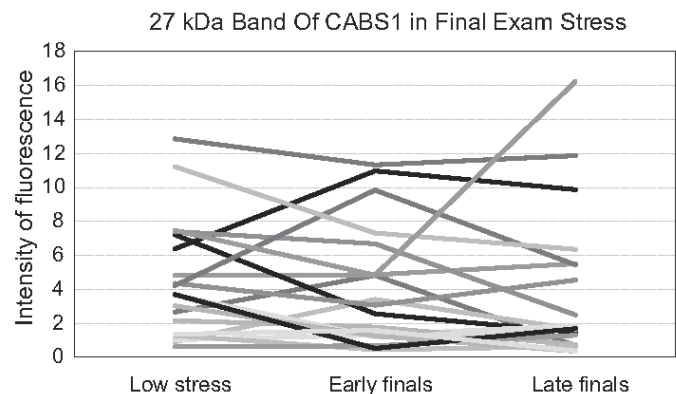
Fig. 4. CABS1 band of 27 kDa for individual participants during low stress and final exam stress periods.

Table 5. *Between- and within-subject associations of the CABS1 27-kDa band with other physiological parameters and the negative-affect rating and time effects of parameters across low stress (during term) and high stress (early and late in finals) periods*

	Time[a]	Between[b]	Within[b]
Salivary cortisol	0.01	12.1†	3.74*
FE$_{NO}$	−0.06§	0.09	1.77
FEV$_1$	−6.08‡	−0.03	−0.00
Nasal VEGF	33.0*	0.04*	0.00
Nasal LTB4	−0.63*	0.75	0.27
Salivary LTB4	−18.25	0.008*	0.00
PANAS-NA	1.61‡	−0.20	−0.04
PSS		−0.15	
WURSS-21	0.15	−0.02	−0.02
27 kDa band	−0.32		

Results are from MEM analyses of individual parameters as a single-time varying covariate of the quantity of the 27-kDa band. Time effects are linear trends from baseline to early-to-late final period, except for FE$_{NO}$, which is contrasted with baseline vs. early and late final period. Negative coefficients indicate decreases, and positive coefficients indicate increases of the respective parameter during final periods relative to baseline. FEV$_1$, forced expiratory volume in the first second; LTB4, leukotriene B4; WURSS-21, Wisconsin Upper Respiratory Symptom Scale 21 (see Table 4 legend for other abbreviations). *$P < 0.05$. †$P < 0.01$. ‡$P < 0.001$. §$P < 0.10$. [a]Controlling for group, age, and BMI. [b]Controlling for group, age, BMI, and time.

Association of the CABS1 27-kDa band with inflammatory markers. FE$_{NO}$ increases within subjects were associated positively and in concordance ($P < 0.10$) with the 27-kDa band, but the addition of time as a covariate eliminated the effect. Between subjects, higher levels of salivary LTB4 and nasal VEGF across assessments were associated with higher levels of the 27-kDa band ($P < 0.05$; Table 5).

Exploratory Analyses of Additional Immunoreactive Bands in the Three Studies

Because few participants showed additional bands immunoreactive to CABS1 beyond the 27-kDa band, analysis of these bands was highly exploratory. The 18-kDa band in five participants of *study 2* showed a substantial increase following the stress test (Fig. 5), with a significant time effect in the MEM analysis [$F(5,19) = 7.31, P < 0.001$] and significant elevations in levels from 0 min prestress to 0 min poststress ($P < 0.001$) and 30 min poststress ($P = 0.029$). These participants showed no change in PANAS-NA from 0 min prestress to 0 min poststress compared with the remaining 11 participants who showed increases in PANAS-NA but lacked the additional bands (Mann-Whitney $U = 0.00, P < 0.001$; in Fig. 6A, note that U was 0 because there was no overlap in ranks between both groups). Significant increases following the laboratory stressor were also observed in seven participants who showed a 55-kDa band [$F(5,28) = 3.37, P = 0.017$], with significant elevations from 0 min prestress to 0 min poststress ($P < 0.001$). However, participants with this band did not differ in their PANAS-NA response from those without the band. Elevations after stress were also observed in the 90-kDa band ($n = 5$ participants), but no significant time effect emerged ($P = 0.333$).

In *study 3*, although only two participants showed additional CABS1 bands, the abundance of the 20-, 18-, 15-, and 12-kDa molecular forms was elevated at the late exam stress time (5- to 60-fold) compared with the baseline or early exam stress period.

Participants with additional bands at molecular mass 12–18 kDa showed significantly lower values in the PSS in *study 2* [$U = 7.0, P = 0.018$ ($n_1 = 5$, median = 5; $n_2 = 11$, median = 16)] and a trend toward lower values in the second wave of *study 1* [$U = 36.5, P = 0.065$ ($n_1 = 6$, median = 7.5; $n_2 = 24$, median = 11)] (Fig. 6, B and C). No participants of those receiving the 10-item version of the PSS in *study 1* showed additional bands. Participants with additional bands at molecular mass 33–90 kDa did not show significantly lower values in PSS than those without these bands.

DISCUSSION

Our studies provide the first description of CABS1 and its multiple forms in human saliva and the association with psychological stress and inflammation. The predominant molecular form of CABS1 was detected at 27 kDa, and additional immunoreactive bands were also identified between 12 and 20
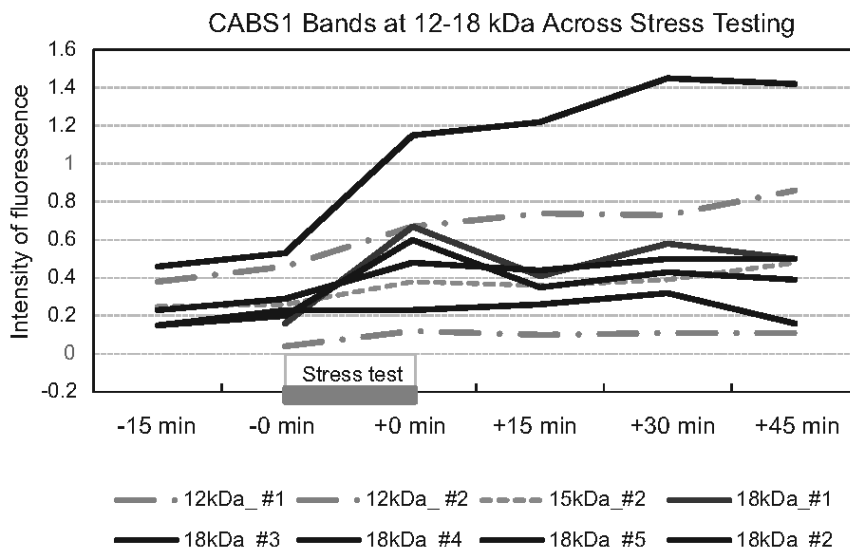
Fig. 5. Effects of the Trier Social Stress Test on levels of CABS1 bands of 18, 15, and 12 kDa for 5 individual participants.

A Study 2: Negative Affect Change After Stress

B Study 1: Perceived Stress Scale

C Study 2: Perceived Stress Scale
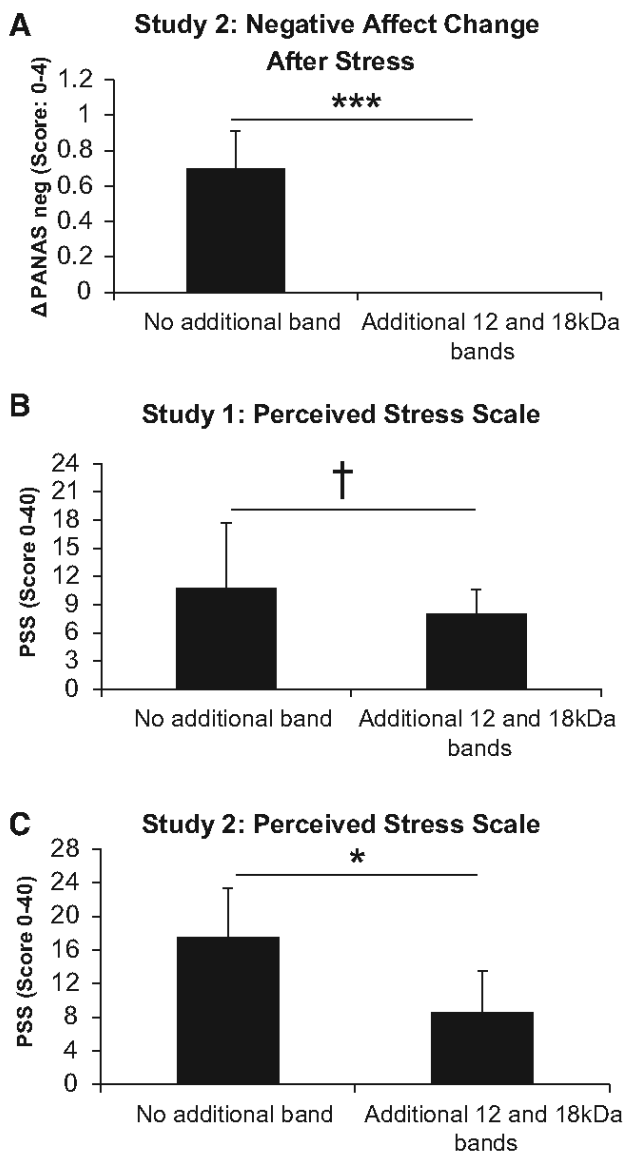
Fig. 6. A: changes in negative affect [PANAS negative-affect subscale (ΔPANAS neg)] in response to the Trier Social Stress Test in those with ($n = 5$) and without ($n = 11$) additional CABS1 bands at 18, 15, and/or 12 kDa. ***$P < 0.001$. B: perceived Stress Scale (PSS) scores in those with ($n = 6$) and without ($n = 24$) additional CABS1 bands at 18 and/or 12 kDa in *study 1*. †$P < 0.10$. C: PSS scores in those with ($n = 5$) and without ($n = 11$) additional CABS1 bands at 18, 15, and/or 12 kDa in *study 2*. *$P < 0.05$.

kDa and between 33 and 90 kDa in a small (13/99 and 10/99, respectively) number of participants.

We originally identified CABS1 in human salivary gland extracts (71) during our search for a human protein with a sequence similarity to the anti-inflammatory peptide sequence near the carboxy terminus of the rat prohormone, SMR1 (36, 44). The *Smr1* gene we studied in rats is not present in humans, and although sequence similarity for other peptides derived from *Smr1* with analgesic or erectile function activities had been identified in human *PROL1* and *SMR3A* and *SMR3B* genes (73, 74, 79), the human gene with a sequence similar to the anti-inflammatory sequence from *Smr1* was unknown. Interestingly, just as SMR1 has many molecular forms that

vary in size and isoelectric point (45), with the use of Western blot analyses and five different anti-CABS1 antibodies, we identified several molecular forms of CABS1 in salivary gland extracts, lungs, and testes, with evidence for organ-specific differences in the forms. With the use of mass spectrometry, we confirmed the presence of CABS1 sequences in bands at 75, 51, 33, 27, 20, and 16 kDa from a CABS1 overexpression lysate but could not confirm or refute that an 11-kDa form was CABS1 (71). The predicted molecular size of human CABS1 is 43 kDa, a size inconsistent with any of the bands that we identified. Given our mass spectrometry data, we suggested that both the 75- and 51-kDa forms represent full-length CABS1 (good sequence coverage 69–73%) but could provide no explanation for the two molecular mass forms. Interestingly, others have similar observations with CABS1 from rat testes at 79 kDa (11), from mouse testes at 66 kDa (29), and from porcine testes at 70 and 75 kDa (66). CABS1 immunoreactive bands below 51 kDa presumably represent fragments of full-length CABS1 (proteolysis).

There are several potential explanations for detecting proteins at various estimated molecular weights relative to that predicted by their amino acid sequence, including the following: glycosylation, aggregation, proteolysis, and anomalous SDS binding due to amino acid content. Calvel et al. (11) provided evidence that CABS1 is an intrinsically disordered protein with a low isoelectric point (3.4), lacking a fixed or ordered structure and with unusual behavior in electrophoretic separation. Moreover, these authors showed that CABS1 is hypersensitive to trypsin digestion, suggesting structural flexibility and susceptibility to digestion with various proteases. This is consistent with our observations of multiple immunoreactive bands in salivary gland extracts, testes, and lung (71) and in saliva and tissue-specific distinctions in the band profiles, presumably determined, at least in part, by the protease cocktails in each tissue or fluid.

As we experienced with salivary gland extracts and despite several attempts to immunoprecipitate and sequence CABS1 immunoreactive bands from saliva, it is a limitation of our work that we have been unable to confirm the identity of these immunoreactive bands with mass spectroscopy. Our current hypothesis is that CABS1 is in relatively low abundance (we can detect by Western blot but are unable to see corresponding bands using silver staining or Coomassie brilliant blue), in part, because it is an intrinsically disordered protein that is highly susceptible to proteolytic cleavage, further lessening the abundance of any particular molecular form.

The 27-kDa form of CABS1 was present in the saliva from all participants and aligns well with 27 kDa in extracts of human salivary glands, lung, and testes (71). Although in some salivary gland extracts, the 27 kDa appeared to be a doublet (71), we could not clearly establish a doublet in saliva, perhaps because the band in saliva was relatively disperse, suggesting multiple forms. Whether the bands detected in saliva at 20, 18, 15, and 12 kDa are the same as CABS1 bands detected at 20 kDa and below in salivary gland extracts (20, 17, 16, and 11 kDa) remains to be determined. Nevertheless, given our work with several anti-CABS1 antibodies, mass spectroscopy sequencing of CABS1 molecular mass forms from overexpression lysates, and with several tissues, it is likely that all of these molecular forms in saliva have CABS1 sequences, i.e., are fragments of CABS1.

Interestingly, the molecular mass forms of CABS1 at 20 kDa and below were seen only in 13% of participants and relatively more in men (20.8 vs. 10.6%). Similarly, CABS1 forms at 33 kDa and above were seen more often in men (16.6%) versus women (8.0%). Sex differences in the prevalence of CABS1 forms would be consistent with the evidence of sexual dimorphism in SMR1 expression in rats (61). Larger samples with more equal ratios of men and women would be needed to consolidate these findings. It is tempting to speculate that the different molecular forms of CABS1 will have overlapping but potentially also distinct functions, including anti-inflammatory activities associated with the TDIFELL motif and with putative differences in their three-dimensional structures and potential receptor systems, as previously explored in studies of SMR1 and its molecular forms (37, 42, 60).

In part, because rat SMR1 is a marker of stress (61), we analyzed the levels of the CABS1 bands in saliva in response to standardized psychological stress induction, and their association with real-life stress, as well as common questionnaire measures of distress, and generated some intriguing findings. In general, findings suggest a sensitivity of CABS1 to acute stress and an association with self-reporting of perceived stress and depressive mood. Intensity of the 27-kDa band significantly increased following the laboratory psychosocial stress paradigm. On the other hand, no systematic changes were observed across periods of longer-lasting stress in our observational paradigm of academic finals stress. However, the variability of the 27-kDa band in the latter paradigm was considerable, with some individuals showing pronounced increases, others decrease, and others little change. It is possible that in longer real-life observational periods, additional moderator variables become more relevant that were not captured by our assessment protocols, such as individual coping resources or factors of changing environmental demand. Interestingly, greater increases in 27 kDa band intensity were associated with greater increases in cortisol in both the laboratory acute stress and chronic academic final examination protocols, suggesting an association with hypothalamus-pituitary adrenal axis functioning across different types of psychological stress (note that this association was found despite significant average changes of CABS1 and cortisol in the academic finals stress study). The observed between-subject association of salivary cortisol levels across assessments of academic finals stress further supports a link with hypothalamus-pituitary adrenal axis function. Whether these correlational findings represent any correspondence in the underlying physiological process remains to be explored. Recent research has shown that cortisol is not equally responsive to all types of stress; rather, it is particularly elevated in psychosocial stress and situations that constitute a threat to social self-esteem of the individuals and elicit social emotions, such as shame (23, 69). Thus our picture of hormonal adaptations to stress is far from complete. We do not view the purpose of our research in the identification of one, or the best, stress marker, but in the identification of the variety of possible organ and tissue responses to the variety of stress situations and styles of coping with stress. The present findings suggest that CABS1 protein secretion by the salivary glands is one of the hormonal pathways responding to stress, but whether it is activated in a more global fashion or more specific to particular stress challenges still has to be elucidated. Our initial finding of a diverging response to acute vs. chronic stress challenges is more suggestive of specificity.

Interestingly, the pattern of associations with autonomic and respiratory function across the acute stress protocol suggested an involvement in system deactivation rather than activation. Increases in 27-kDa band intensity were linked to slower breathing with reduced $\dot{V}_E$, reduced HR, and larger TWAs, the latter being suggestive of a reduced cardiac sympathetic activation. At the same time, no association was observed with RSA as an index of cardiac parasympathetic function. It therefore appears that CABS1 is related to an attenuated cardiorespiratory response to acute stress through dampening of sympathetic excitation. Because rat SMR1 secretion is regulated by both branches of the autonomic nervous system (45), with larger quantities of protein secreted in sympathetic stimulation, it is possible that the observed associations with human CABS1 may more closely reflect the effective outcome of CABS1 secretion on the autonomic and respiratory systems than the coordination of its initial secretion in response to stress. One function of CABS1 may be the dampening of acute stress responses, consistent with the interpretation that regulation of SMR1, the rat analog of CABS, may serve as a pathway in the organism's protective responses, including anti-inflammatory activities following a variety of insults (45). Protocols with more frequent collection of saliva samples throughout stress periods or direct manipulation of the CABS1 pathway will be needed to determine the exact temporal trajectories of CABS1 secretion relative to changes in autonomic excitation.

Another interesting finding with the 27-kDa band of CABS1 was its systematic association with self-reported distress. Positive associations were found with changes in momentary affect across the acute stress protocol, with momentary stress-level ratings across multiple baseline assessments, and with questionnaires of perceived stress and depression in the past week(s). These findings are compatible with CABS1 upregulation during acute stress but complicate the interpretation of CABS1 associations with autonomic and respiratory parameters in acute stress. Thus whereas it appears that distress experience increases the CABS1 27-kDa band with some consistency, physiological concomitants are only partly compatible with such stress-induced increases. At this point, it is unclear whether this could be a reflection of other recent findings of reduced cardiac stress reactivity in depressed individuals (12, 35). Larger studies involving clinical groups and more extensive stress protocols will be needed to shed more light on these findings. Perhaps distinct functions of the multiple molecular forms of CABS1 will also help explain some of the complexities (see below).

The observational protocol of academic finals stress also enabled us to study CABS1 relative to slower developing inflammatory processes. Consistent with a role of SMR1 in inflammation, demonstrated in previous studies in animal models (39, 45), we expected to find positive associations of CABS1 with indicators of inflammation in nasal and lower-airway passages, as suggested by the positive association with FE_{NO} changes across multiple baselines and nasal VEGF in the academic stress study (*study 3*). Similarly, salivary LTB4 levels also showed a positive association with the 27-kDa band, and a tendency toward higher intensities in this band was also found for participants with asthma in one study. Both LTB4 and VEGF are mediators involved in inflammation and

airway infection, orchestrating leukocyte traffic to infected sites and enhancing vessel growth to support increased perfusion. FE_{NO} levels could indicate inflammation of the airways, because a number of immune cells, such as macrophages and mast cells, secrete nitric oxide under this condition (19, 20, 52). However, given that FE_{NO} was observed in healthy participants across multiple weeks, it is more likely that FE_{NO} levels were indicative of a constitutional secretion of nitric oxide by epithelial cells, a major source of this gas in the absence of allergic processes (33). Under these conditions, nitric oxide supports innate immune functions by providing an early line of defense against pathogens (49, 80). For the CABS1 27-kDa band, the positive association with FE_{NO} changes may therefore indicate a role in infection, which would be consistent with the role of the anti-inflammatory sequence in reducing concomitants of LPS-induced lung inflammation in an animal model (71). However, associations with the WURSS, a questionnaire measure of perceived cold symptoms (3), were nonsignificant. It should also be noted that both positive and negative associations of CABS1 with inflammatory parameters and symptoms could be interpreted as a role of CABS1 in counteracting infection (negative associations could indicate that a lack of CABS1 facilitates inflammation; positive associations could mean that inflammation leads to a protective or restorative mobilization of CABS1). Thus a more definite interpretation of the significance of fluctuations of CABS1 levels in saliva or of CABS1 in lung tissues (71) during airway inflammation must come from future mechanistic and longitudinal studies. Taken together, fluctuations in both longitudinal airway nitric oxide levels and individual differences in nasal and oral mediators of inflammation are positively associated with the levels of the 27-kDa band of CABS1 in saliva.

The additional immunoreactive bands of CABS1 at molecular mass 12–20 kDa also showed evidence for responsivity to stress, with 18 kDa, in particular, showing strong elevations following the acute laboratory stressor. However, different from the associations uncovered for the ubiquitous 27-kDa band, the presence of this band was associated with psychological unresponsiveness to acute stress, since no change in negative affect from before to after the stressor was observed in participants with this band. Additionally, in *studies 1* and *2*, values of the PSS, a measure capturing perceived stress levels retrospectively over the past weeks, were lower in those with the 18- and 12-kDa bands than in those without additional bands. The differences were particularly pronounced in *study 2*, which used a longer version of the PSS, in that scores of participants with the additional bands were less than one-half of those of the other participants. It is therefore possible that additional bands provide a marker of stress resilience. The interpretation is compatible with the pattern of cardiorespiratory deactivation associated with the 27-kDa band observed in the acute stress protocol, but it is at odds with the significant positive associations observed for this band with self-reported measures of distress. It is possible that different molecular forms of CABS1 yield functionally diverging effects. Unfortunately, these observations were limited by the small number of individuals who showed the additional bands and must await replication in larger studies.

Our exploration of CABS1 in human saliva and its association with distress were limited by small sample sizes in individual studies and an overall unequal gender distribution with relatively fewer male participants. Thus further replication of our findings is needed. Our study population was also mostly composed of young undergraduate student volunteers, thus limiting the generalizability of our findings to the general population. Despite these limitations, our findings provide first evidence for the importance of psychological distress in the regulation of CABS1 and its various molecular weight forms in saliva. Although associations with endocrine, autonomic, and immune function were observed, they were modest in size and could indicate an independent role of salivary CABS1 in adaptation of the organism to a stressful environment.

Perspectives and Significance

Our results with CABS1 in humans suggest that as in rats, there is exquisite autonomic control of biologically important molecules produced by the salivary glands. CABS1 in humans and SMR1 rats are both responsive to stressful stimuli and are both processed into several molecular forms, at least some of which contain an anti-inflammatory peptide motif. Interestingly, only human—but not rat, mouse, bovine, or porcine—CABS1 contains the sequence TDIFELL (66, 71), similar to the anti-inflammatory sequence TDIFEGG, in rat SMR1. Given that in humans, not only CABS1 but also SMR3A, SMR3B, and proline-rich lacrimal 1, have homologies with the rat prohormone SMR1 (73, 74, 83), it will be intriguing to determine if these genes and their proteins are also associated with stressful stimuli. Furthermore, this raises crucial questions about the potential roles of these proteins and their processed forms in the responses to distress or potential to eustress, the locations in the body where they act, and their mechanisms of action. Presumably, the actions of CABS1 or some of these other proteins support or modulate the stress response, and whether some have a functional role in an evolutionary sense (e.g., facilitate mobilization of the organism to challenges or strengthen its defenses or resilience), have pathological significance or consequences (e.g., are indicative of pathophysiological processes or facilitate them), or might be of therapeutic value (e.g., as agents that dampen stress responses, pain processes, or inflammation) is a direction for future research.

DISCLOSURES

T. Ritz, C. D. St. Laurent, and A. D. Befus have a new international Patent Application Serial No. PCT/CA2017/050331 on the use of CABS1 as a biomarker of stress. The sponsors had no role in study design, data collection, analysis, or interpretation or in the preparation of the manuscript.

AUTHOR CONTRIBUTIONS

T.R. and A.D.B. conceived and designed research; A.F.T., C.A.W., P.D.V., and E.R-S. performed experiments; T.R., D.R., C.D.S.L., A.F.T., C.A.W., P.D.V., E.R-S., and A.D.B. analyzed data; T.R. and A.D.B. interpreted results

of experiments; T.R. C.D.S.L. and A.D.B. prepared figures; T.R., D.R., and A.D.B. drafted manuscript; T.R., D.R., C.D.S.L., P.D.V., R.J.A., E.R-S., and A.D.B. edited and revised manuscript; T.R., D.R., C.D.S.L., A.F.T., C.A.W., P.D.V., R.J.A., E.R-S., and A.D.B. approved final version of manuscript.

REFERENCES

REFERENCES

1. **American Thoracic Society; European Respiratory Society.** ATS/ERS recommendations for standardized procedures for the online and offline measurement of exhaled lower respiratory nitric oxide and nasal nitric oxide, 2005. *Am J Respir Crit Care Med* 171: 912–930, 2005. doi:10.1164/rccm.200406-710ST.

2. **An K, Salyer J, Kao HF.** Psychological strains, salivary biomarkers, and risks for coronary heart disease among hurricane survivors. *Biol Res Nurs* 17: 311–320, 2015. doi:10.1177/1099800414551164.

3. **Barrett B, Brown R, Mundt M, Safdar N, Dye L, Maberry R, Alt J.** The Wisconsin Upper Respiratory Symptom Survey is responsive, reliable, and valid. *J Clin Epidemiol* 58: 609–617, 2005. doi:10.1016/j.jclinepi.2004.11.019.

4. **Barrett B, Brown R, Voland R, Maberry R, Turner R.** Relations among questionnaire and laboratory measures of rhinovirus infection. *Eur Respir J* 28: 358–363, 2006. doi:10.1183/09031936.06.00002606.

5. **Bernardi L, Wdowczyk-Szulc J, Valenti C, Castoldi S, Passino C, Spadacini G, Sleight P.** Effects of controlled breathing, mental activity and mental stress with or without verbalization on heart rate variability. *J Am Coll Cardiol* 35: 1462–1469, 2000. doi:10.1016/S0735-1097(00)00595-7.

5a.**Bosch JA.** The use of saliva markers in psychobiology: mechanisms and methods. *Monogr Oral Sci* 24: 99–108, 2014. doi:10.1159/000358864.

6. **Bosch JA, de Geus EE, Ring C, Nieuw Amerongen AV, Stowell JR.** Academic examinations and immunity: academic stress or examination stress? *Psychosom Med* 66: 625–626, 2004.

7. **Bosch JA, de Geus EJ, Veerman EC, Hoogstraten J, Nieuw Amerongen AV.** Innate secretory immunity in response to laboratory stressors that evoke distinct patterns of cardiac autonomic activity. *Psychosom Med* 65: 245–258, 2003. doi:10.1097/01.PSY.0000058376.50240.2D.

9. **Brown TE, Beightol LA, Koh J, Eckberg DL.** Important influence of respiration on human R-R interval power spectra is largely ignored. *J Appl Physiol (1985)* 75: 2310–2317, 1993.

10. **Byrne ML, O'Brien-Simpson NM, Reynolds EC, Walsh KA, Laughton K, Waloszek JM, Woods MJ, Trinder J, Allen NB.** Acute phase protein and cytokine levels in serum and saliva: a comparison of detectable levels and correlations in a depressed and healthy adolescent sample. *Brain Behav Immun* 34: 164–175, 2013. doi:10.1016/j.bbi.2013.08.010.

11. **Calvel P, Kervarrec C, Lavigne R, Vallet-Erdtmann V, Guerrois M, Rolland AD, Chalmel F, Jégou B, Pineau C.** CLPH, a novel casein kinase 2-phosphorylated disordered protein, is specifically associated with postmeiotic germ cells in rat spermatogenesis. *J Proteome Res* 8: 2953–2965, 2009. doi:10.1021/pr900082m.

12. **Carroll D, Phillips AC, Hunt K, Der G.** Symptoms of depression and cardiovascular reactions to acute psychological stress: evidence from a population study. *Biol Psychol* 75: 68–74, 2007. doi:10.1016/j.biopsycho.2006.12.002.

13. **Cohen S, Williamson GM.** Perceived stress in a probability sample of the United States. In: *The Social Psychology of Health*, edited by Spacapan S and Oskamp S. Newbury Park, CA: Sage, 1988, p. 31–67.

14. **Cohen S, Kamarck T, Mermelstein R.** A global measure of perceived stress. *J Health Soc Behav* 24: 385–396, 1983. doi:10.2307/2136404.

15. **Contrada RJ, Krantz DS, Durel LA, Levy L, LaRiccia PJ, Anderson JR, Weiss T.** Effects of beta-adrenergic activity on T-wave amplitude. *Psychophysiology* 26: 488–492, 1989. doi:10.1111/j.1469-8986.1989.tb01957.x.

16. **Crawford JR, Henry JD, Crombie C, Taylor EP.** Normative data for the HADS from a large non-clinical sample. *Br J Clin Psychol* 40: 429–434, 2001. doi:10.1348/014466501163904.

17. **Dery RE, Ulanova M, Puttagunta L, Stenton GR, James D, Merani S, Mathison R, Davison J, Befus AD.** Frontline: Inhibition of allergen-induced pulmonary inflammation by the tripeptide feG: a mimetic of a neuro-endocrine pathway. *Eur J Immunol* 34: 3315–3325, 2004. doi:10.1002/eji.200425461.

19. **Forsythe P, Gilchrist M, Kulka M, Befus AD.** Mast cells and nitric oxide: control of production, mechanisms of response. *Int Immunopharmacol* 1: 1525–1541, 2001. doi:10.1016/S1567-5769(01)00096-0.

20. **Gilchrist M, McCauley SD, Befus AD.** Expression, localization, and regulation of NOS in human mast cell lines: effects on leukotriene production. *Blood* 104: 462–469, 2004. doi:10.1182/blood-2003-08-2990.

20a.**Global Initiative for Asthma.** GINA Report, Global Strategy for Asthma Management and Prevention (2013 version) (Online). http://www.ginasthma.org/.

21. **Grossman P, Karemaker J, Wieling W.** Prediction of tonic parasympathetic cardiac control using respiratory sinus arrhythmia: the need for respiratory control. *Psychophysiology* 28: 201–216, 1991. doi:10.1111/j.1469-8986.1991.tb00412.x.

22. **Grossman P, Taylor EW.** Toward understanding respiratory sinus arrhythmia: relations to cardiac vagal tone, evolution and biobehavioral functions. *Biol Psychol* 74: 263–285, 2007. doi:10.1016/j.biopsycho.2005.11.014.

23. **Gruenewald TL, Kemeny ME, Aziz N, Fahey JL.** Acute threat to the social self: shame, social self-esteem, and cortisol activity. *Psychosom Med* 66: 915–924, 2004. doi:10.1097/01.psy.0000143639.61693.ef.

24. **Hellhammer DH, Wüst S, Kudielka BM.** Salivary cortisol as a biomarker in stress research. *Psychoneuroendocrinology* 34: 163–171, 2009. doi:10.1016/j.psyneuen.2008.10.026.

25. **Heslegrave RJ, Furedy JJ.** Sensitivities of HR and T-wave amplitude for detecting cognitive and anticipatory stress. *Physiol Behav* 22: 17–23, 1979. doi:10.1016/0031-9384(79)90397-4.

26. **Hirsch JA, Bishop B.** Respiratory sinus arrhythmia in humans: how breathing pattern modulates heart rate. *Am J Physiol Heart Circ Physiol* 241: H620–H629, 1981.

27. **Izawa S, Sugaya N, Kimura K, Ogawa N, Yamada KC, Shirotsuki K, Mikami I, Hirata K, Nagano Y, Nomura S.** An increase in salivary interleukin-6 level following acute psychosocial stress and its biological correlates in healthy young adults. *Biol Psychol* 94: 249–254, 2013. doi:10.1016/j.biopsycho.2013.06.006.

28. **Jemmott JB III, Magloire K.** Academic stress, social support, and secretory immunoglobulin A. *J Pers Soc Psychol* 55: 803–810, 1988. doi:10.1037/0022-3514.55.5.803.

29. **Kawashima A, Osman BA, Takashima M, Kikuchi A, Kohchi S, Satoh E, Tamba M, Matsuda M, Okamura N.** CABS1 is a novel calcium-binding protein specifically expressed in elongate spermatids of mice. *Biol Reprod* 80: 1293–1304, 2009. doi:10.1095/biolreprod.108.073866.

30. **Kirschbaum C, Pirke KM, Hellhammer DH.** The 'Trier Social Stress Test'—a tool for investigating psychobiological stress responses in a laboratory setting. *Neuropsychobiology* 28: 76–81, 1993. doi:10.1159/000119004.

31. **Kline KP, Ginsburg GP, Johnston JR.** T-wave amplitude: relationships to phasic RSA and heart period changes. *Int J Psychophysiol* 29: 291–301, 1998. doi:10.1016/S0167-8760(98)00021-X.

32. **Laguna P, Jané R, Caminal P.** Automatic detection of wave boundaries in multilead ECG signals: validation with the CSE database. *Comput Biomed Res* 27: 45–60, 1994. doi:10.1006/cbmr.1994.1006.

33. **Lane C, Knight D, Burgess S, Franklin P, Horak F, Legg J, Moeller A, Stick S.** Epithelial inducible nitric oxide synthase activity is the major determinant of nitric oxide concentration in exhaled breath. *Thorax* 59: 757–760, 2004. doi:10.1136/thx.2003.014894.

34. **Laudenslager ML, Calderone J, Philips S, Natvig C, Carlson NE.** Diurnal patterns of salivary cortisol and DHEA using a novel collection device: electronic monitoring confirms accurate recording of collection time using this device. *Psychoneuroendocrinology* 38: 1596–1606, 2013. doi:10.1016/j.psyneuen.2013.01.006.

35. **Lovallo WR.** Do low levels of stress reactivity signal poor states of health? *Biol Psychol* 86: 121–128, 2011. doi:10.1016/j.biopsycho.2010.01.006.

36. **Mathison RD, Befus AD, Davison JS.** A novel submandibular gland peptide protects against endotoxic and anaphylactic shock. *Am J Physiol Regul Integr Comp Physiol* 273: R1017–R1023, 1997.

37. **Mathison RD, Davison JS, Befus AD, Gingerich DA.** Salivary gland derived peptides as a new class of anti-inflammatory agents: review of preclinical pharmacology of C-terminal peptides of SMR1 protein. *J Inflamm (Lond)* 7: 49–60, 2010. doi:10.1186/1476-9255-7-49.

38. **Mathison RD, Davison JS, Metwally E.** Identification of a binding site for the anti-inflammatory tripeptide feG. *Peptides* 24: 1221–1230, 2003. doi:10.1016/j.peptides.2003.07.011.

238

39. **Mathison RD, Davison JS, St. Laurent CD, Befus AD.** Autonomic regulation of anti-inflammatory activities from salivary glands. *Chem Immunol Allergy* 98: 176–195, 2012. doi:10.1159/000336513.

40. **McClelland DC, Ross G, Patel V.** The effect of an academic examination on salivary norepinephrine and immunoglobulin levels. *J Human Stress* 11: 52–59, 1985. doi:10.1080/0097840X.1985.9936739.

41. **Messaoudi M, Desor D, Nejdi A, Rougeot C.** The endogenous androgen-regulated sialorphin modulates male rat sexual behavior. *Horm Behav* 46: 684–691, 2004. doi:10.1016/j.yhbeh.2004.06.012.

42. **Metwally E, Befus AD, Davison JS, Mathison R.** Probing for submandibular gland peptide-T receptors on leukocytes with biotinylated-Lys-[Gly](6)-SGP-T. *Biochim Biophys Acta* 1593: 37–44, 2002. doi:10.1016/S0167-4889(02)00329-4.

43. **Montoya P, Brody S, Beck K, Veit R, Rau H.** Differential β- and α-adrenergic activation during psychological stress. *Eur J Appl Physiol Occup Physiol* 75: 256–262, 1997. doi:10.1007/s004210050157.

44. **Morris K, Kuo B, Wilkinson MD, Davison JS, Befus AD, Mathison RD.** Vcsa1 gene peptides for the treatment of inflammatory and allergic reactions. *Recent Pat Inflamm Allergy Drug Discov* 1: 124–132, 2007. doi:10.2174/187221307780979892.

45. **Morris KE, St. Laurent CD, Hoeve RS, Forsythe P, Suresh MR, Mathison RD, Befus AD.** Autonomic nervous system regulates secretion of anti-inflammatory prohormone SMR1 from rat salivary glands. *Am J Physiol Cell Physiol* 296: C514–C524, 2009. doi:10.1152/ajpcell.00214.2008.

46. **Nater UM, Rohleder N.** Salivary alpha-amylase as a non-invasive biomarker for the sympathetic nervous system: current state of research. *Psychoneuroendocrinology* 34: 486–496, 2009. doi:10.1016/j.psyneuen.2009.01.014.

47. **Oskis A, Clow A, Thorn L, Loveday C, Hucklebridge F.** Differences between diurnal patterns of salivary cortisol and dehydroepiandrosterone in healthy female adolescents. *Stress* 15: 110–114, 2012. doi:10.3109/10253890.2011.582529.

48. **Phillips AC, Carroll D, Evans P, Bosch JA, Clow A, Hucklebridge F, Der G.** Stressful life events are associated with low secretion rates of immunoglobulin A in saliva in the middle aged and elderly. *Brain Behav Immun* 20: 191–197, 2006. doi:10.1016/j.bbi.2005.06.006.

49. **Proud D.** Nitric oxide and the common cold. *Curr Opin Allergy Clin Immunol* 5: 37–42, 2005. doi:10.1097/00130832-200502000-00008.

50. **Quigley KS, Stifter CA.** A comparative validation of sympathetic reactivity in children and adults. *Psychophysiology* 43: 357–365, 2006. doi:10.1111/j.1469-8986.2006.00405.x.

51. **Rau H.** Responses of the T-wave amplitude as a function of active and passive tasks and beta-adrenergic blockade. *Psychophysiology* 28: 231–239, 1991. doi:10.1111/j.1469-8986.1991.tb00415.x.

52. **Ricciardolo FL, Sterk PJ, Gaston B, Folkerts G.** Nitric oxide in health and disease of the respiratory system. *Physiol Rev* 84: 731–765, 2004. doi:10.1152/physrev.00034.2003.

53. **Riis JL, Granger DA, DiPietro JA, Bandeen-Roche K, Johnson SB.** Salivary cytokines as a minimally-invasive measure of immune functioning in young children: correlates of individual differences and sensitivity to laboratory stress. *Dev Psychobiol* 57: 153–167, 2015. doi:10.1002/dev.21271.

54. **Ring C, Harrison LK, Winzer A, Carroll D, Drayson M, Kendall M.** Secretory immunoglobulin A and cardiovascular reactions to mental arithmetic, cold pressor, and exercise: effects of alpha-adrenergic blockade. *Psychophysiology* 37: 634–643, 2000. doi:10.1111/1469-8986.3750634.

55. **Ritz T.** Studying noninvasive indices of vagal control: the need for respiratory control and the problem of target specificity. *Biol Psychol* 80: 158–168, 2009. doi:10.1016/j.biopsycho.2008.08.003.

56. **Ritz T, Dahme B.** Implementation and interpretation of respiratory sinus arrhythmia measures in psychosomatic medicine: practice against better evidence? *Psychosom Med* 68: 617–627, 2006. doi:10.1097/01.psy.0000228010.96408.ed.

57. **Ritz T, Trueba AF, Simon E, Auchus RJ.** Increases in exhaled nitric oxide after acute stress: association with measures of negative affect and depressive mood. *Psychosom Med* 76: 716–725, 2014. doi:10.1097/PSY.0000000000000118.

58. **Roponen M, Seuri M, Nevalainen A, Randell J, Hirvonen MR.** Nasal lavage method in the monitoring of upper airway inflammation: seasonal and individual variation. *Inhal Toxicol* 15: 649–661, 2003. doi:10.1080/08958370390197290.

59. **Rosinski-Chupin I, Rougeon F.** A new member of the glutamine-rich protein gene family is characterized by the absence of internal repeats and

60. **Rougeot C, Messaoudi M, Hermitte V, Rigault AG, Blisnick T, Dugave C, Desor D, Rougeon F.** Sialorphin, a natural inhibitor of rat membrane-bound neutral endopeptidase that displays analgesic activity. *Proc Natl Acad Sci USA* 100: 8549–8554, 2003. doi:10.1073/pnas.1431850100.

61. **Rougeot C, Vienet R, Cardona A, Le Doledec L, Grognet JM, Rougeon F.** Targets for SMR1-pentapeptide suggest a link between the circulating peptide and mineral transport. *Am J Physiol Regul Integr Comp Physiol* 273: R1309–R1320, 1997.

62. **Sackner MA, Watson H, Belsito AS, Feinerman D, Suarez M, Gonzalez G, Bizousky F, Krieger B.** Calibration of respiratory inductive plethysmograph during natural breathing. *J Appl Physiol (1985)* 66: 410–420, 1989.

63. **Saul JP, Berger RD, Chen MH, Cohen RJ.** Transfer function analysis of autonomic regulation. II. Respiratory sinus arrhythmia. *Am J Physiol Heart Circ Physiol* 256: H153–H161, 1989.

64. **Scher H, Furedy JJ, Heslegrave RJ.** Phasic T-wave amplitude and heart rate changes as indices of mental effort and task incentive. *Psychophysiology* 21: 326–333, 1984. doi:10.1111/j.1469-8986.1984.tb02942.x.

65. **Schulz SM, Ayala E, Dahme B, Ritz T.** A MATLAB toolbox for correcting within-individual effects of respiration rate and tidal volume on respiratory sinus arrhythmia during variable breathing. *Behav Res Methods* 41: 1121–1126, 2009. doi:10.3758/BRM.41.4.1121.

66. **Shawki HH, Kigoshi T, Katoh Y, Matsuda M, Ugboma CM, Takahashi S, Oishi H, Kawashima A.** Identification, localization, and functional analysis of the homologues of mouse CABS1 protein in porcine testis. *Exp Anim* 65: 253–265, 2016. doi:10.1538/expanim.15-0104.

67. **Sherwood A, Allen MT, Fahrenberg J, Kelsey RM, Lovallo WR, van Doornen LJ.** Methodological guidelines for impedance cardiography. *Psychophysiology* 27: 1–23, 1990. doi:10.1111/j.1469-8986.1990.tb02171.x.

68. **Silkoff PE, Erzurum SC, Lundberg JO, George SC, Marczin N, Hunt JF, Effros R, Horvath I; American Thoracic Society; HOC Subcommittee of the Assembly on Allergy, Immunology, and Inflammation.** ATS workshop proceedings: exhaled nitric oxide and nitric oxide oxidative metabolism in exhaled breath condensate. *Proc Am Thorac Soc* 3: 131–145, 2006. doi:10.1513/pats.200406-710ST.

69. **Skoluda N, Strahler J, Schlotz W, Niederberger L, Marques S, Fischer S, Thoma MV, Spoerri C, Ehlert U, Nater UM.** Intra-individual psychological and physiological responses to acute laboratory stressors of different intensity. *Psychoneuroendocrinology* 51: 227–236, 2015. doi:10.1016/j.psyneuen.2014.10.002.

70. **Slavish DC, Graham-Engeland JE, Smyth JM, Engeland CG.** Salivary markers of inflammation in response to acute stress. *Brain Behav Immun* 44: 253–269, 2015. doi:10.1016/j.bbi.2014.08.008.

71. **St. Laurent CD, St Laurent KE, Mathison RD, Befus AD.** Calcium-binding protein, spermatid-specific 1 is expressed in human salivary glands and contains an anti-inflammatory motif. *Am J Physiol Regul Integr Comp Physiol* 308: R569–R575, 2015. doi:10.1152/ajpregu.00153.2014.

72. **Tong Y, Tar M, Davelman F, Christ G, Melman A, Davies KP.** Variable coding sequence protein A1 as a marker for erectile dysfunction. *BJU Int* 98: 396–401, 2006. doi:10.1111/j.1464-410X.2006.06247.x.

73. **Tong Y, Tar M, Melman A, Davies K.** The opiorphin gene (ProL1) and its homologues function in erectile physiology. *BJU Int* 102: 736–740, 2008. doi:10.1111/j.1464-410X.2008.07631.x.

74. **Tong Y, Tar M, Monrose V, DiSanto M, Melman A, Davies KP.** hSMR3A as a marker for patients with erectile dysfunction. *J Urol* 178: 338–343, 2007. doi:10.1016/j.juro.2007.03.004.

74a. **Trueba A, Ryan MW, Vogel PD, Ritz T.** Effects of academic exam stress on nasal leukotriene B4 and vascular endothelial growth factor in asthma and health. *Biol Psychol* 118: 44–51, 2016. doi:10.1016/j.biopsycho.2016.04.009.

75. **Trueba AF, Mizrachi D, Auchus RJ, Vogel PD, Ritz T.** Effects of psychosocial stress on the pattern of salivary protein release. *Physiol Behav* 105: 841–849, 2012. doi:10.1016/j.physbeh.2011.10.014.

76. **Trueba AF, Rosenfield D, Oberdörster E, Vogel PD, Ritz T.** The effect of academic exam stress on mucosal and cellular airway immune markers among healthy and allergic individuals. *Psychophysiology* 50: 5–14, 2013. doi:10.1111/j.1469-8986.2012.01487.x.

77. **Trueba AF, Smith NB, Auchus RJ, Ritz T.** Academic exam stress and depressive mood are associated with reductions in exhaled nitric oxide in healthy individuals. *Biol Psychol* 93: 206–212, 2013. doi:10.1016/j.biopsycho.2013.01.017.

79. **User HM, Zelner DJ, McKenna KE, McVary KT.** Microarray analysis and description of SMR1 gene in rat penis in a post-radical prostatectomy model of erectile dysfunction. *J Urol* 170: 298–301, 2003. doi:10.1097/01.ju.0000060882.75475.5a.

80. **Vareille M, Kieninger E, Edwards MR, Regamey N.** The airway epithelium: soldier in the fight against respiratory viruses. *Clin Microbiol Rev* 24: 210–229, 2011. doi:10.1128/CMR.00014-10.

81. **Wang LP, Maxwell SE.** On disaggregating between-person and within-person effects with longitudinal data using multilevel models. *Psychol Methods* 20: 63–83, 2015. doi:10.1037/met0000030.

82. **Watson D, Clark LA, Tellegen A.** Development and validation of brief measures of positive and negative affect: the PANAS scales. *J Pers Soc Psychol* 54: 1063–1070, 1988. doi:10.1037/0022-3514.54.6.1063.

83. **Wisner A, Dufour E, Messaoudi M, Nejdi A, Marcel A, Ungeheuer MN, Rougeot C.** Human Opiorphin, a natural antinociceptive modulator of opioid-dependent pathways. *Proc Natl Acad Sci USA* 103: 17979–17984, 2006. doi:10.1073/pnas.0605865103.

85. **Zigmond AS, Snaith RP.** The hospital anxiety and depression scale. *Acta Psychiatr Scand* 67: 361–370, 1983. doi:10.1111/j.1600-0447.1983.tb09716.x.
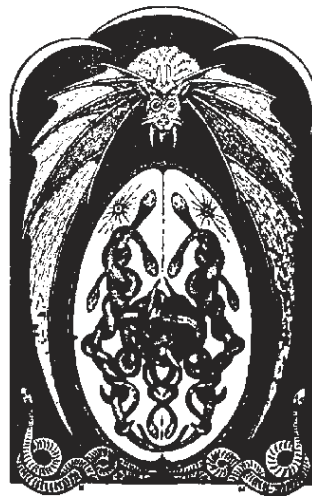
Appendix B – 2D-e protocol for MS-seq analysis

Acetone precipitation of saliva supernatant (preparation for 2D SDS-PAGE)

<u>Material</u>

- 1.5mL microfuge tube
- Cold acetone (pre-stored at -20°C)
- -20°C freezer
- Biosafety cabinet
- Fume hood
- Vortex
- Microcentrifuge
- Waste beaker
- Micropipettes (P200, P1000)
- Micropipette tips (P200, P1000)

1. In a 1.5 mL microfuge tube place 200μL of saliva supernatant and add 800μL of cold acetone
2. Vortex and incubate at -20°C for t=30 min
3. Centrifuge at 16,100*g at T_{room} for t=10 min
4. In a waste beaker inside a fume hood, pour off supernatant (a protein pellet may be visible, or not)
5. Inside a biosafety cabinet allow acetone to evaporate (T_{room}) for t=30 min
6. To perform downstream 2D SDS-PAGE, resuspend pellet in the recommended volume Rehydration buffer (Bio-Rad, Mississauga, ON, CA) (see **Table B-1**).

Table B-1. Volume of rehydration buffer is a function of IPG strip length.

When a sample has been precipitated into a pellet, Bio-Rad suggests that the pellet is resuspended in its proprietary rehydration solution.

	IPG strip length (cm)				
	7	11	17	18	24
Rehydration solution (µL)	125	200	300	315	450

Two-dimensional electrophoresis protocol

DAY 0: Preparation of solutions

Equilibration buffers

See Bio-Rad protocol below to prepare Equilibration buffer $_{stock}$

Once done, prepare 10mL aliquots and store at -20°C

Reagents

Tris-HCl buffer (25 ml)
1.5 M Tris-HCl (pH 8.8)

Dissolve 4.55 g of Tris base in ~20 ml of deionized or distilled H_2O. Adjust the pH of the solution with diluted HCl and adjust the volume to 25 ml with distilled or deionized H_2O.

Equilibration stock buffer (500 ml)
6 M urea, 30% (w/v) glycerol, 2% (w/v) SDS in 0.05 M Tris-HCl buffer, (pH 8.8). Pre-prepared equilibration buffers can also be purchased.

Combine 180 g of urea, 150 g of glycerol, 10 g of SDS, and 16.7 ml of Tris-HCl buffer. Dissolve in deionized distilled H_2O and adjust the volume to 500 ml. Store frozen.

Equilibration buffer 1 (10 ml)
Add 100 mg of DTT to 10 ml of equilibration stock buffer.

Equilibration buffer 2 (10 ml)
Add 400 mg of iodoacetamide to 10 ml of equilibration stock buffer.

Source: Bio-Rad

Prepare enough equilibration buffers 1 and 2. Store at -20°C

Table 10.1. Recommended equilibration volumes.					
IPG Strip Length	7 cm	11 cm	17 cm	18 cm	24 cm
Equilibration buffer 1	2.5 ml	4 ml	6 ml	6 ml	8 ml
Equilibration buffer 2	2.5 ml	4 ml	6 ml	6 ml	8 ml

Source: Bio-Rad

SDS-PAGE running buffer 10X stock (1 L)

Tris base: 30.3 g

Glycine: 144.0 g

SDS: 10.0 g

Add $H_2O_{sterile}$ to a total volume of 1,000 L

"Blue silver" Coomassie Staining Solution (adapted from Dr Richard Fahlman's protocols) (1 L)

To a 1 L volumetric flask add 100 mL of water $_{double\ distilled}$

Add 100 g of ammonium sulfate

Add 1.2 g of Coomassie blue G-250

Add 200 mL of 100% methanol

BTV 1 L with water $_{double\ distilled}$

Fixing solution (500 mL)

To a 500 mL volumetric flask add 100 mL of water $_{double\ distilled}$

Add 250 mL of ethanol $_{100\%}$

Add 10 mL of phosphoric acid

BTV 500 mL with water $_{double\ distilled}$

DAY 1: IPG strip rehydration

<u>Materials and reagents to have inside the biosafety cabinet</u>

- Micropipettes and sterile tips
- P10
- P200
- Rehydration/equilibration tray and lid
- Mineral Oil
- Bio-Rad forceps (2)

- 1.5 mL microfuge Eppendorf tubes

- Items that must be in fridge/freezer and retrieved just before using:

- Rehydration solution (4°C fridge)

- IPG strip (-20°C freezer)

Steps 1 to 9 must be done inside a Biosafety Cabinet

1. Select Immobilized pH Gradient (IPG) strip length to use for the experiment

See Table 2.1 for volumes of rehydration solution and mineral oil to be used based on (1) but **don't pour anything yet**!

Table 2.1. Rehydration volumes, sample loads, and mineral oil volumes. The values listed are recommendations. Optimum sample load depends on sample type. See Appendix A, Reagent and Sample Preparation, for more details.

	IPG Strip Length				
	7 cm	11 cm	17 cm	18 cm	24 cm
Rehydration Solution	125 µl	200 µl	300 µl	315 µl	450 µl
Protein Load					
Coomassie (Brilliant) Blue	50–100 µg	100–200 µg	200–400 µg	200–400 µg	400–800 µg
Fluorescent stains	5–100 µg	20–200 µg	50–400 µg	50–400 µg	80–800 µg
Silver stains	5–20 µg	20–50 µg	50–80 µg	50–80 µg	80–150 µg
Mineral Oil	4 ml	5 ml	7 ml	7 ml	9 ml

Source: Bio-Rad

2. Most likely, you will use a 7cm IPG strip. Rehydrate the saliva pellet that you precipitated with acetone in 125 µL $_{\text{Rehydration solution}}$

3. With a micropipette (avoiding the formation of bubbles) slowly pipet resuspended sample along the length of one lane of the rehydration/equilibration tray

4. Retrieve IPG strip from the -20°C freezer and bring it into the biosafety cabinet

5. Using Bio-Rad forceps, remove the cover sheet from IPG strip

6. Place strip <u>facing down</u> onto the resuspended sample in the lane of the rehydration/equilibration tray (**<u>gently</u> move the strip back and forth and avoid the formation of bubbles**)

7. Cover rehydration/equilibration tray with lid and allow IPG strip to rehydrate with resuspended sample for **<u>1 hour</u>**

8. After 1 hour of rehydration, add recommended V $_{\text{mineral oil}}$ (see Table 2.1). **Apply on both ends of the channel so that oil flows towards the middle**

9. Cover the tray and leave it overnight (12 to 18 hours) for complete rehydration

DAY 2: IEF, the first dimension

Steps 10 to 15 must be done inside a Biosafety Cabinet

10. Place i12 focusing tray inside the biosafety cabinet, along with electrode assemblies, IPG strip retainers, gel-side down wicks, and ultrapure water (see image below)
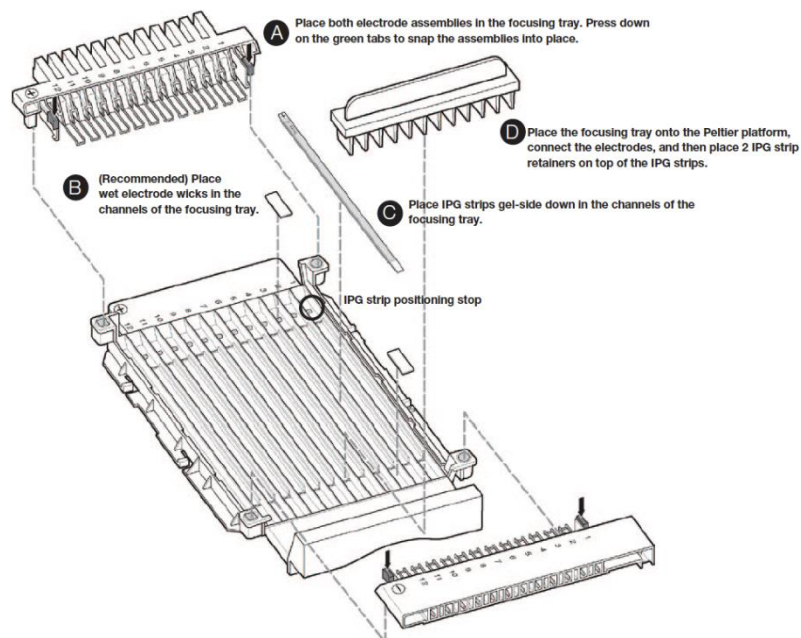
Source: Bio-Rad

11. Position electrode assemblies in place on the i12 focusing tray and press down until secured (you will feel a gentle snap)

12. Using Bio-Rad forceps, place a gel-side down wick on each electrode (+ and -)

13. Using a micropipette, pour ~150µL of ultrapure water on each wick to moist them (**without pouring excess water**)

14. Using Bio-Rad forceps, remove IPG from rehydration/equilibration tray and remove the excess mineral oil by lifting strip and letting the oil drip into the channel

15. Place IPG strip **gel-side down** in a channel on the focusing tray. Make sure that the gel is touching the moist wicks, as the electrical current will travel through them (**keep track of which channel you placed your strip on**)

16. Take i12 focusing tray to IEF instrument and secure tray on the Peltier platform (carefully connect electrodes to the instrument)

17. Overlay IPG strip(s) with recommended V $_{mineral oil}$ (see Table 2.1)

18. Gently place IPG strip retainers **without moving IPG strip**, as this can damage the gel and risk the integrity of the experiment

19. Select the running protocol and start the run (**leave overnight**)

Wash your rehydration/equilibration tray with dish soap and Bio-rad cleaning brushes. Rehydration/equilibration trays will be used on DAY 3

DAY 3: IPG strip equilibration → SDS-PAGE, the second dimension

Materials and reagents to have inside the biosafety cabinet

- Micropipette and sterile tips

- P1000

- Rehydration/equilibration tray and lid

- SDS-PAGE Running buffer **1X** (prepare from stock)

- Beaker for liquid waste

- Bio-Rad forceps (2)

- Items that must be in the freezer and retrieved before using (they delay ~10 min in thawing):

- Equilibration buffer 1

- Equilibration buffer 2

- Warm agarose (stored at 4°C)

- Microwave for 15 sec until it melts (if it is still solid/semi-solid, microwave in intervals of 5 sec until it is entirely liquid)

IPG strip equilibration

20. Select: 'End Run' at IEF instrument

21. Remove IPG strip retainers

22. Retrieve i12 focusing tray from IEF instrument and bring it into the biosafety cabinet

23. Using forceps, retrieve IPG strips and place it gel-side up at a channel in the rehydration/equilibration tray

24. Fill the channel with recommended $V_{equilibration\ buffer\ 1}$ (see Table 10.1 on p. 1) and place lid on the tray

25. Take rehydration/equilibration tray to the orbital shaker (set to 60 rpm) and incubate for 10 min

26. Once done, bring the tray back to biosafety cabinet and decant Equilibration buffer 1 on the waste beaker.

27. Fill with recommended $V_{equilibration\ buffer\ 2}$

28. Take rehydration/equilibration tray to the orbital shaker (set to 60 rpm) and incubate for 10 min

29. Decant Equilibration buffer 2

SDS-PAGE

Steps 30 to 35 must be done inside a Biosafety Cabinet

30. Position SDS-PAGE gel leaning slightly backward

31. Using Bio-Rad forceps, place equilibrated IPG strip (plastic side against the long plate and + side on the left)

32. Using Bio-Rad forceps (ensuring that plastic backing remains in contact with long plate) slide IPG strip until both gels (IPG strip gel and SDS-PAGE gel) are in contact with each other (**avoid the formation of bubbles**)

33. Using a P1000, pour warm agarose into well to secure the strip in place (**if bubbles form, tap back of the long plate to dislodge them**)

34. Stand gel upright, secure in sandwich clamp assembly, and allow agarose to set for 10 min

35. Place sandwich clamp assembly inside SDS-PAGE electrophoresis chamber, pour SDS-PAGE running buffer 1X and put its lid on

36. Take SDS-PAGE chamber onto lab bench and connect it to the power supply

37. Run SDS-PAGE at 125 V (track the Bromophenol blue dye (which came with the rehydration buffer) and turn off power supply when it reaches the bottom of the gel)

Blue-Silver staining of 2-Dimensional electrophoresis gel

1. Transfer gel to a glass container with Fixing solution and place it in a rocker (room temperature) for t=30 min.

2. Discard Fixing solution in a glass container. Be careful not to discard gel

3. Pour water double distilled on the glass container with the gel. Place it in a rocker (T_{room}) for t=20 min.

4. Discard water on sink being careful not to discard the gel

5. Repeat steps 3 and 4 again

6. Add staining solution

7. Leave gel staining in a rocker overnight

8. Discard Coomassie blue dye in an appropriate glass container

9. Rinse gel with water $_{double\ distilled}$ several times aiming to get rid of blue precipitates

10. Read gel in Li-cor Odyssey by carefully placing gel on reading glass and placing a previously cleaned glass on top of gel (to avoid gel from curling)

Appendix C – MS-seq detected proteins in transient overexpression cell lysates and human saliva

The following tables are intended to be used as hypotheses generators. In them we list the accession numbers of each protein, as these are unlikely to be modified in the foreseeable future. These accession numbers are compatible with the UniProt Knowledgebase. In **Table *C-1*** and **Table *C-2*** we list the area under the curve (arbitrary units, a.u.) obtained when analysing each sample by mass spectrometry sequencing (MS-seq) after being separated via one-dimensional SDS-PAGE.

In **Table *C-1*** we compiled the list of proteins present in both a human calcium-binding protein, spermatid-associated 1 (hCABS1) transient overexpression cell lysate (OEL) and its negative control cell lysate (NCL), 387 in total. In **Table *C-2*** we compared the proteins present in OEL, NCL, and human saliva supernatant. Since we are listing the common proteins in both samples, hCABS1 (accession number: Q96KC9) is not present. These tables compare the presence of proteins across samples and represent n=1.

Of note, the area under the curve reported in **Table *C-1*** and **Table *C-2*** can't be used to compare across samples. Thus, we recommend that these MS-seq experiments are repeated at least twice to reach n=3. Once done, we suggest normalization of this area values by selecting a housekeeping protein found in all three, OEL, NCL and saliva supernatant. The area value of each MS-seq detected protein, then, should be divided by the area of the housekeeping protein within the sample. Once done, we could compare the expression of proteins across samples.

In **Table *C-3*** we list the proteins found on selected spots (see **Figure C-1**) doing MS-seq of a human saliva supernatant sample separated via 2D SDS-PAGE. Spots were selected based on the locations that gave a signal on Western blot assays using polyclonal antibodies (pAbs) to hCABS1. hCABS1 was not detected on these locations, but we speculate that the proteins found there could be interacting with our pAbs to hCABS1. The data presented from **Figure C-2** - **Figure C-10** is a sequence alignment between the immunogen we used to create pAb H2.0 (hCABS1 a.a. $_{184}$DEADMSNYNSSIKS$_{197}$) and proteins found in spots F, G, H, I (see **Figure C-1**), where we speculated a form of hCABS1 associated with stress[21] could be located. In **Figure C-2** - **Figure C-10**, consensus patterns ('***consensus***/*100%*') are based on equivalence classes, sets of residues that share some predefined property[81]. MView[80], the software used to align sequences, uses a consensus mechanism that chooses the most specific class that summarizes a given column at the desired percent identity ('*consensus/**100%***').

Table C-1. List of proteins present in OEL and NCL and detected by MS-seq analysis.

Proteins are represented by their UniProt accession number. The area (a.u.) is indicative of the abundance of each protein in the sample indicated between parentheses.

Proteins present in OEL and NCL		
Accession	**Area (NCL)**	**Area (OEL)**
Q9Y617	1.631E7	6.636E6
Q9Y5L4	6.588E5	1.500E5
Q9Y5B9	2.021E6	1.391E6
Q9Y490	3.405E6	2.049E6
Q9Y295	2.729E6	2.474E6
Q9Y277	1.218E7	1.635E6
Q9Y266	1.632E7	7.766E6
Q9Y265	1.347E7	3.741E6
Q9Y230	7.771E6	2.370E6
Q9UQE7	1.097E6	1.370E6
Q9UQ80	4.952E7	1.054E7
Q9UNM6	6.624E6	2.521E6
Q9UKK9	9.817E6	2.142E6
Q9UBB4	4.552E6	3.995E5
Q9P2J5	2.562E6	9.465E5
Q9NZI8	6.401E6	5.107E6
Q9NTK5	1.552E7	1.032E7
Q9NSB4	1.705E7	9.392E5
Q9NR45	4.966E6	5.841E6
Q9NR31	7.255E6	3.764E6
Q9NR30	1.475E6	4.376E5
Q9HB71	7.821E6	3.295E6
Q9BXW7	9.406E6	1.464E6
Q9BVC6	7.404E6	9.742E5

Q9BVA1	1.950E8	6.879E7
Q9BT78	2.237E6	2.342E6
Q9BQE3	1.830E8	4.515E7
Q99832	1.446E7	2.266E6
Q99714	6.463E6	3.408E6
Q99456	2.246E7	8.282E5
Q96CX2	1.935E6	1.193E6
Q96AG4	1.591E7	1.682E6
Q92973	1.300E6	2.766E6
Q92928	1.353E6	1.085E7
Q92841	2.053E7	2.955E6
Q92598	3.877E6	3.580E6
Q8WVC2	1.107E6	1.054E6
Q8NC51	1.352E7	8.687E5
Q8NBS9	4.602E6	1.397E6
Q7Z794	1.794E8	4.612E7
Q7L2H7	1.965E6	4.988E5
Q7L1Q6	6.912E6	1.007E6
Q7KZF4	1.864E6	3.022E6
Q6EEV6	6.348E6	8.782E5
Q6AWB1	1.126E6	3.716E5
Q5T8U3	4.141E6	5.837E6
Q5T7C4	2.326E7	6.341E6
Q5QNZ2	3.034E6	2.396E6
Q5JR95	9.722E6	1.219E6
Q5HY54	4.046E6	2.091E6
Q5D862	1.659E6	6.977E5
Q32Q12	4.785E7	6.699E6
Q16543	9.535E6	3.906E6
Q15717	5.275E6	1.029E6

Q15393	1.419E6	2.164E6
Q15365	2.700E7	1.547E7
Q15233	9.141E6	2.913E6
Q15185	5.343E6	9.907E5
Q15102	5.072E6	2.064E6
Q15084	1.702E7	6.071E6
Q15029	3.678E6	1.600E7
Q14974	9.224E6	6.675E6
Q14152	6.792E6	6.917E5
Q13885	1.950E8	6.879E7
Q13283	6.298E6	3.276E6
Q13263	8.642E6	3.108E6
Q13200	8.402E5	6.719E5
Q13185	2.629E6	9.275E5
Q13162	9.595E6	5.193E6
Q12931	7.242E7	5.460E7
Q12906	7.828E6	8.192E5
Q09028	2.174E7	1.068E7
Q08211	2.331E6	5.515E5
Q06830	5.435E7	5.678E7
Q04917	2.097E7	7.061E6
Q04760	3.871E6	8.835E6
Q02878	5.713E6	2.395E6
Q02790	1.389E7	3.842E6
Q01082	1.510E6	7.113E5
Q00839	4.568E6	1.954E6
Q00688	8.144E6	1.430E6
Q00610	3.586E6	3.087E6
P78371	2.440E7	5.031E6
P68371	2.332E8	6.549E7

P68363	1.830E8	4.515E7
P68104	4.638E7	3.545E7
P68032	3.304E8	1.118E8
P67936	1.214E7	2.101E6
P67809	2.396E7	5.517E6
P63244	2.096E7	6.624E6
P63104	3.897E7	9.873E6
P62937	4.595E7	2.426E7
P62913	1.316E7	5.275E6
P62857	4.098E6	6.097E5
P62851	3.609E7	2.681E6
P62829	1.946E6	8.470E4
P62826	3.819E7	3.116E7
P62805	9.778E6	4.023E6
P62701	7.508E6	7.128E6
P62333	3.977E6	1.229E5
P62318	1.128E7	3.962E6
P62316	3.354E6	1.626E6
P62304	1.228E6	7.085E6
P62277	1.326E7	1.800E6
P62269	2.690E7	3.254E6
P62263	1.718E7	5.288E6
P62258	1.957E7	1.510E7
P62249	8.850E6	4.489E5
P62081	1.945E6	9.152E4
P61981	2.327E7	7.667E6
P61978	2.557E7	5.108E6
P61586	1.379E6	2.259E6
P61204	1.162E7	1.602E6
P61160	5.564E6	1.850E6

P61088	6.367E6	3.420E5
P60891	7.646E6	2.729E6
P60866	9.478E6	3.348E6
P60842	2.241E7	1.163E7
P60709	7.605E8	2.271E8
P60174	5.295E7	5.502E7
P56192	2.550E6	1.781E6
P55072	1.219E7	1.426E7
P55060	5.058E6	1.446E6
P54886	2.504E6	2.850E6
P54577	2.236E7	8.466E6
P53999	4.857E6	9.327E5
P52597	3.187E6	1.189E6
P52292	1.375E7	1.190E6
P52272	1.503E7	1.778E5
P51991	8.934E6	3.851E6
P51665	6.701E6	2.878E6
P51572	6.285E6	4.999E6
P51571	1.456E6	1.183E5
P51148	4.529E6	2.537E6
P50991	2.872E7	1.427E6
P50990	4.487E7	1.161E7
P49721	1.854E6	2.360E6
P49588	1.790E6	2.360E6
P49368	3.558E7	6.369E6
P49321	6.517E6	3.420E6
P49006	4.210E6	7.791E5
P48668	7.655E7	7.837E6
P48047	2.777E6	8.616E5
P43487	1.839E7	3.880E6

P42704	6.203E6	6.424E5
P40926	5.394E7	6.512E6
P40925	2.522E7	8.703E6
P40227	2.346E7	2.349E6
P38646	5.704E7	1.473E7
P37802	7.018E6	3.197E6
P37108	1.810E6	1.028E6
P36578	2.598E7	1.559E6
P35998	4.294E6	1.254E6
P35908	1.843E8	4.970E7
P35527	4.908E6	8.452E6
P34932	6.507E6	1.223E7
P34931	2.862E8	2.175E7
P34897	1.205E7	2.011E6
P32119	2.895E7	4.445E7
P31948	2.560E7	8.610E6
P31946	2.446E7	8.089E6
P31939	9.464E6	5.839E6
P31153	8.491E6	4.799E6
P30101	2.252E7	7.787E6
P30086	7.727E6	3.302E5
P30048	1.010E7	7.252E6
P30044	3.514E6	8.343E5
P30041	1.792E7	1.227E7
P30040	1.033E7	2.264E6
P28838	9.090E6	2.338E6
P28074	1.074E6	3.433E6
P28072	1.632E6	7.332E6
P27824	1.292E7	1.368E7
P27348	2.474E7	1.015E7

P26641	2.564E7	8.886E6
P26583	3.679E6	2.553E6
P26373	1.014E7	1.421E5
P25705	3.964E7	5.491E6
P25398	5.312E6	1.851E5
P24752	1.435E7	6.159E6
P24666	3.996E6	7.393E5
P24534	5.305E7	1.054E6
P23526	8.748E6	2.537E6
P23396	1.850E7	2.193E6
P23284	1.262E7	3.836E6
P22626	9.818E6	4.745E5
P22314	2.273E7	1.858E7
P22061	5.539E6	7.587E6
P21796	2.637E7	4.440E6
P20340	1.928E6	1.122E7
P19623	9.574E6	1.355E6
P19338	2.009E7	1.479E7
P19013	4.506E7	1.948E7
P18669	1.656E7	1.136E7
P18206	5.533E6	3.672E6
P17612	1.988E8	1.051E8
P17174	4.787E5	6.861E5
P16949	1.278E7	7.432E6
P16403	4.327E7	4.545E6
P16152	6.605E6	1.149E6
P15531	4.186E7	6.038E6
P14625	2.958E7	4.056E7
P14618	1.913E7	9.700E6
P14406	2.827E7	3.610E6

P13667	2.337E7	3.097E6
P13647	7.235E7	2.349E6
P13646	3.334E7	6.389E6
P13645	1.520E8	3.945E7
P13639	2.830E7	4.682E7
P13010	5.834E6	5.736E6
P12956	2.096E7	3.883E6
P12532	1.009E7	7.913E6
P12277	2.021E8	3.377E7
P12004	1.445E7	4.572E6
P11586	1.345E7	5.629E6
P11177	4.077E6	4.722E6
P11142	3.318E8	4.001E7
P11021	1.477E8	8.558E6
P10809	1.905E8	1.589E7
P10599	8.746E6	5.596E6
P0DMV8	3.092E8	5.276E7
P09960	4.720E6	1.707E5
P09936	9.364E6	7.322E6
P09874	1.475E7	1.616E7
P08758	1.037E7	6.190E6
P08727	3.685E7	8.282E5
P08708	8.548E6	2.820E6
P08670	1.928E7	7.754E6
P08559	7.355E6	1.454E6
P08238	1.786E8	9.311E7
P07900	1.786E8	8.060E7
P07814	7.603E6	1.990E6
P07737	2.447E7	5.762E6
P07437	2.375E8	8.379E7

P07355	5.196E6	4.249E6
P07195	1.692E8	3.688E7
P06748	1.755E7	1.480E7
P06733	2.656E8	7.839E7
P06576	5.494E7	2.569E7
P05787	6.759E6	5.872E5
P05455	2.109E7	1.158E7
P05388	4.851E7	2.050E7
P05387	6.565E6	4.473E6
P05141	2.114E6	3.079E6
P05023	2.999E6	1.323E6
P04406	2.734E8	9.161E7
P04264	2.098E8	5.915E7
P04181	1.794E7	3.881E6
P04080	2.997E6	1.589E6
P04075	1.026E8	6.721E7
P02786	4.108E5	3.191E5
P02538	7.655E7	7.837E6
P02533	2.891E7	1.423E6
P00918	1.543E7	6.683E6
P00558	7.269E7	2.134E7
P00505	2.777E7	9.020E6
P00492	7.287E6	7.560E6
P00491	2.316E6	1.206E6
P00441	2.468E7	1.017E6
P00387	3.487E6	4.743E6
P00367	9.785E6	5.744E6
P00338	1.207E8	3.106E7
O95373	3.081E6	2.676E6
O95347	1.881E6	1.134E6

O75937	6.587E6	8.688E6
O75396	1.524E6	2.296E6
O75369	1.844E6	2.224E6
O60814	1.445E7	4.364E5
O43809	3.609E6	3.844E6
O43707	5.540E6	9.868E6
O43399	3.100E6	6.990E5
O43175	4.688E7	1.471E7
O15067	2.669E6	2.533E6
O14737	3.924E5	5.461E5
O00410	7.797E6	1.175E6
O00303	8.991E6	1.439E6
O00264	1.863E6	2.133E5
O00231	8.087E6	1.676E6
M0R080	1.172E6	1.806E6
M0QZN2	5.973E6	7.974E5
K7ER90	4.872E6	3.234E6
K7EQ48	2.526E7	6.912E6
K7ELW0	3.822E6	7.355E5
K7EJT5	1.391E7	6.905E6
J3QT28	7.488E6	2.700E6
J3QR09	1.027E7	4.578E6
J3QQM1	3.027E6	2.097E6
J3QL05	4.298E6	1.345E6
J3KTF8	7.876E6	2.622E6
J3KTA4	2.181E7	2.955E6
J3KR24	2.582E6	5.117E6
J3KPG2	5.731E6	6.704E6
I3L3P7	1.004E7	6.729E6
I3L397	8.364E6	3.016E5

I3L1L3	5.600E5	2.314E5
H7C4H2	2.588E6	4.412E6
H7C3I1	3.999E7	1.412E7
H7C2W9	1.655E7	4.809E5
H7BZJ3	1.988E7	6.696E6
H3BRU6	4.087E7	1.114E7
H3BRG4	4.189E6	1.840E6
H3BR27	4.467E6	1.317E6
H3BMH2	3.315E6	1.737E5
H0YNX5	1.634E6	6.406E5
H0YNW5	9.483E5	2.417E5
H0YN26	1.441E7	1.400E7
H0YMZ1	4.300E6	3.209E5
H0YMA0	1.674E6	4.597E6
H0YL12	4.336E6	2.780E5
H0YHC3	1.864E7	3.798E6
H0Y8E6	3.452E6	9.486E5
H0Y4R1	2.378E7	1.101E7
G3V576	1.639E7	1.029E6
G3V3U4	8.637E6	1.327E6
G3V2K7	4.376E6	1.006E6
G3V203	4.282E6	3.152E6
F8W6I7	2.104E7	5.435E6
F8W1A4	8.465E6	2.789E6
F8VZJ2	2.650E7	4.244E6
F8VPF3	3.509E6	5.180E6
F6WIT2	5.466E6	1.782E6
F5H6X6	5.688E6	3.387E6
F5H6P7	1.383E6	5.093E5
F5H3C5	2.426E6	2.627E6

F5H282	4.386E6	2.543E6
F5H265	7.235E6	3.382E6
F5GZS6	1.449E6	4.991E5
F5GY37	2.066E7	5.736E6
F2Z393	1.892E7	9.731E6
E9PQD7	1.797E7	1.840E6
E9PN17	3.038E6	1.704E6
E9PLK3	2.696E6	2.079E6
E9PKD5	4.416E6	2.346E6
E9PK01	8.584E6	1.630E6
E9PJD9	2.060E7	5.972E5
E9PFN5	1.914E6	1.887E6
E9PFD4	8.897E6	1.278E6
E9PEX6	3.029E6	8.913E5
E9PES6	5.820E6	3.420E6
E9PCY7	2.447E7	4.285E6
E9PC52	2.344E7	8.283E6
E7EX73	2.037E6	4.426E5
E7EU96	2.644E6	1.777E5
E7ETK0	5.089E6	2.214E6
E7EPB3	8.286E6	1.571E6
E7ENZ3	1.265E7	2.714E6
E5RIF1	1.252E7	1.978E6
E5RI99	7.531E6	1.567E6
D6RJ96	3.056E6	2.920E6
D6RAF8	2.554E7	1.349E7
D6R9P3	2.881E7	1.368E7
D6R9B6	4.033E6	9.618E5
C9K0U8	7.116E6	8.260E5
C9JZ20	3.704E6	3.143E6

C9JXB8	1.632E7	2.617E6
C9JRH2	9.119E6	2.494E6
C9JQD4	1.349E6	3.108E5
C9JPM4	8.783E6	5.057E6
C9J9K3	9.687E7	3.070E7
C9J592	2.683E6	6.747E5
C9J1Z8	1.326E7	2.258E6
C9J1E7	6.118E5	3.563E5
B9A067	6.016E6	1.205E6
B8ZZQ6	2.489E6	2.245E5
B8ZZL8	5.664E6	2.879E6
B5MCT8	1.068E7	3.853E6
B4DY09	2.547E7	8.982E6
B4DWR3	4.987E6	4.534E6
B4DT28	5.756E6	5.131E6
B3KQV6	3.915E6	2.305E6
A8MUD9	1.477E7	1.909E6
A6NLN1	1.039E7	3.444E6
A0A1B0GTJ7	8.717E6	2.791E6
A0A0G2JJZ9	1.164E7	6.823E6
A0A0D9SFB3	7.363E6	1.880E6
A0A0D9SF54	3.373E6	3.184E6
A0A0C4DGH5	2.154E6	1.475E6
A0A0C4DGB6	1.444E7	5.905E8
A0A0A0MSQ0	1.687E7	3.837E6
A0A087X2D0	4.714E6	1.495E6
A0A087WY81	6.236E6	3.967E6
A0A087WX29	4.869E6	2.401E6
A0A087WWU8	9.438E6	2.020E6
A0A087WUV8	7.419E6	2.512E6

A0A087WTT1	1.745E7	2.514E6
A0A087WTP3	2.225E7	4.390E6
A0A087WTB8	1.183E6	1.727E6

Table C-2. List of proteins detected in OEL, NCL and saliva supernatant.

Proteins are represented by their UniProt accession number. The area (a.u.) is indicative of the abundance of each protein in the sample indicated between parentheses.

Protein accession	Area (OEL)	Area (NCL)	Area (Saliva)
Q92928	1.085E7	1.353E6	1.133E7
Q13162	5.193E6	9.595E6	2.828E7
P68032	1.118E8	3.304E8	1.407E9
P63104	9.873E6	3.897E7	5.244E7
P62937	2.426E7	4.595E7	3.638E8
P60709	2.271E8	7.605E8	1.551E9
P60174	5.502E7	5.295E7	1.251E8
P40925	8.703E6	2.522E7	2.901E7
P35908	4.970E7	1.843E8	1.755E8
P35527	8.452E6	4.908E6	1.834E8
P32119	4.445E7	2.895E7	1.899E7
P31946	8.089E6	2.446E7	5.171E7
P30086	3.302E5	7.727E6	5.001E7
P30044	8.343E5	3.514E6	7.583E7
P30041	1.227E7	1.792E7	3.492E7
P23284	3.836E6	1.262E7	3.049E8
P22314	1.858E7	2.273E7	2.258E6
P19013	1.948E7	4.506E7	6.827E7
P18669	1.136E7	1.656E7	3.880E7
P18206	3.672E6	5.533E6	7.537E6
P17174	6.861E5	4.787E5	5.068E6

|			
P16403	4.545E6	4.327E7	2.899E7
P13647	2.349E6	7.235E7	7.649E7
P13645	3.945E7	1.520E8	2.940E8
P11142	4.001E7	3.318E8	7.448E7
P11021	8.558E6	1.477E8	3.426E7
P10599	5.596E6	8.746E6	4.150E8
P0DMV8	5.276E7	3.092E8	7.575E7
P07737	5.762E6	2.447E7	2.680E8
P07195	3.688E7	1.692E8	4.291E7
P06733	7.839E7	2.656E8	2.574E8
P04406	9.161E7	2.734E8	1.574E8
P04264	5.915E7	2.098E8	2.708E8
P04080	1.589E6	2.997E6	2.074E9
P04075	6.721E7	1.026E8	1.147E8
P02538	7.837E6	7.655E7	1.029E8
P02533	1.423E6	2.891E7	1.413E8
P00918	6.683E6	1.543E7	3.831E6
P00558	2.134E7	7.269E7	1.076E8
P00338	3.106E7	1.207E8	9.530E7
O60814	4.364E5	1.445E7	2.561E7
K7ELW0	7.355E5	3.822E6	1.302E7
I3L1L3	2.314E5	5.600E5	2.714E8
H3BMH2	1.737E5	3.315E6	3.109E7
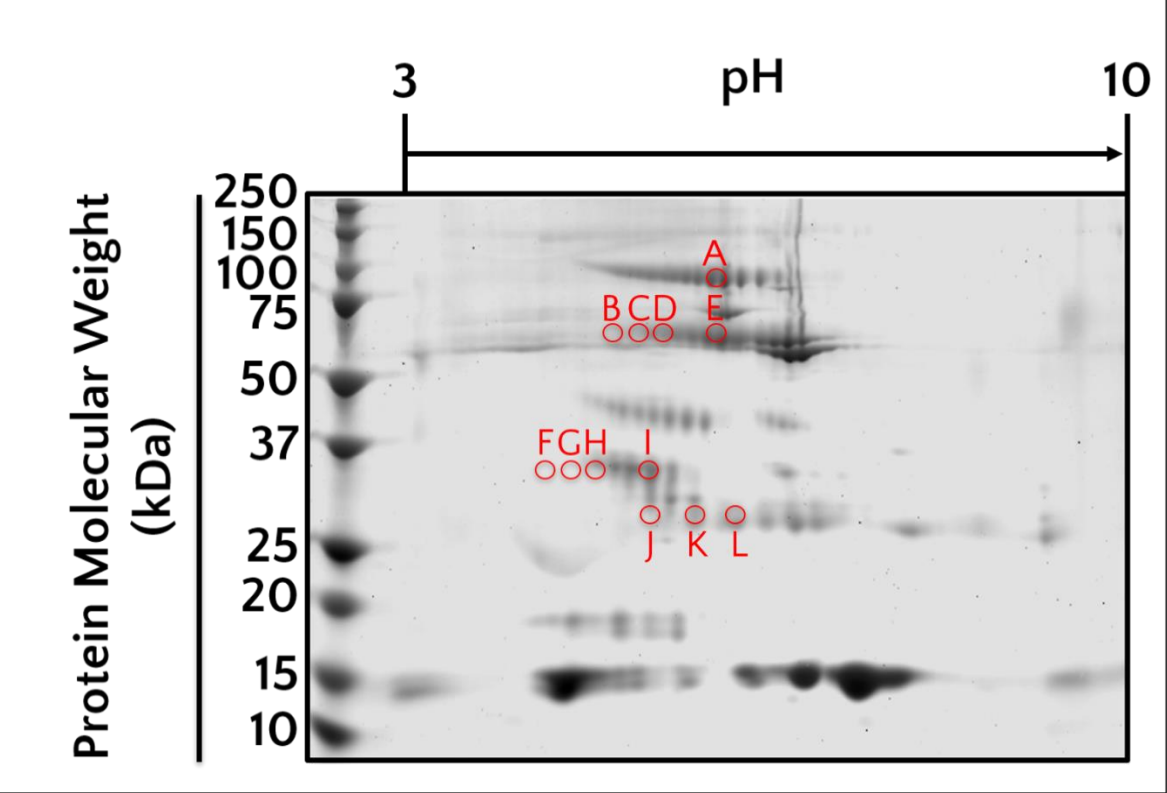
Figure C-1. Blue silver stained gel of human saliva supernatant separated by 2D-e.

 Red circles indicate the spots that were excised to be analysed by MS-seq. 85-98 kDa: A (pH 6.0-6.1); 68-64 kDa: B (pH 4.9-5.1), C (pH 5.2-5.3), D (pH 5.5-5.6), E (pH 6.0-6.1); 33-29 kDa: F (pH 4.3-4.4), G (pH 4.5-4.7), H (pH 4.8-4.9), I (pH 5.3-5.4); 25-24 kDa: J (pH 5.3-5.5), K (pH 5.7-5.9), L (pH 6.1-6.3).

Table C-3. List of proteins found in human saliva supernatant separated by 2D-e.

The UniProt accession number is listed on the first column. The spot where it was detected indicated in the second column (see **Figure C-1** as reference), and the predicted molecular weight (kDa) on the third column. Cells shaded in yellow correspond to possible interactors with pAb H2.0.

| Protein accession	Spot(s) where it was detected	Predicted Molecular weight (kDa)
BPIFA2	J, K F, G, H, I C	27

265

ZG16B	J, K F, G, H, I E	20
AMY1A	L G, I B, C, D, E A	58
IGKV2-40	L	11
TPI1	L	12
ALB	L I B, C, D, E A	69
HRNR	F, I D	282
DSP	F	332
CA6	F, G, H, I E	35
AZGP1	F, G, H, I	34
CLU	F, G, H, I	24
CST1	F, G, H, I	16
PRSS1	F, G, I	27
AMY1B	F	26
LEG1	F, G, H, I	38
DSG1	F, I	114
JUP	F A	82
ACTA2	G	42
MYH2	G	223
MYH1	G	223
MYH7	G	223
PIP	G, H, I	17
GAPDH	G A	28
APOE	H, I	36

AMY2A	H	24
PRSS8	I	36
PRSS3	I	19
CRISP3	I	28
PIGR	I B, C, E A	83
GLOD4	I	35
S100A8	I	11
FCGBP	B	445
IGHV3-72	C, E	11
NUCB1	C	54
HPX	E	52
TPP1	E	61
A0A0J9YY99	E	13
PRSS1	E	27
IGHV3OR 16-13	E	13
IGHV3-43	E	13
IGHV4-28	E	13
IGHV3-15	E	13
A1BG	E	54
UBA6	E	118
DSP	A	2871
LTF	A	696
FLG	A	4061
HSPB1	A	205
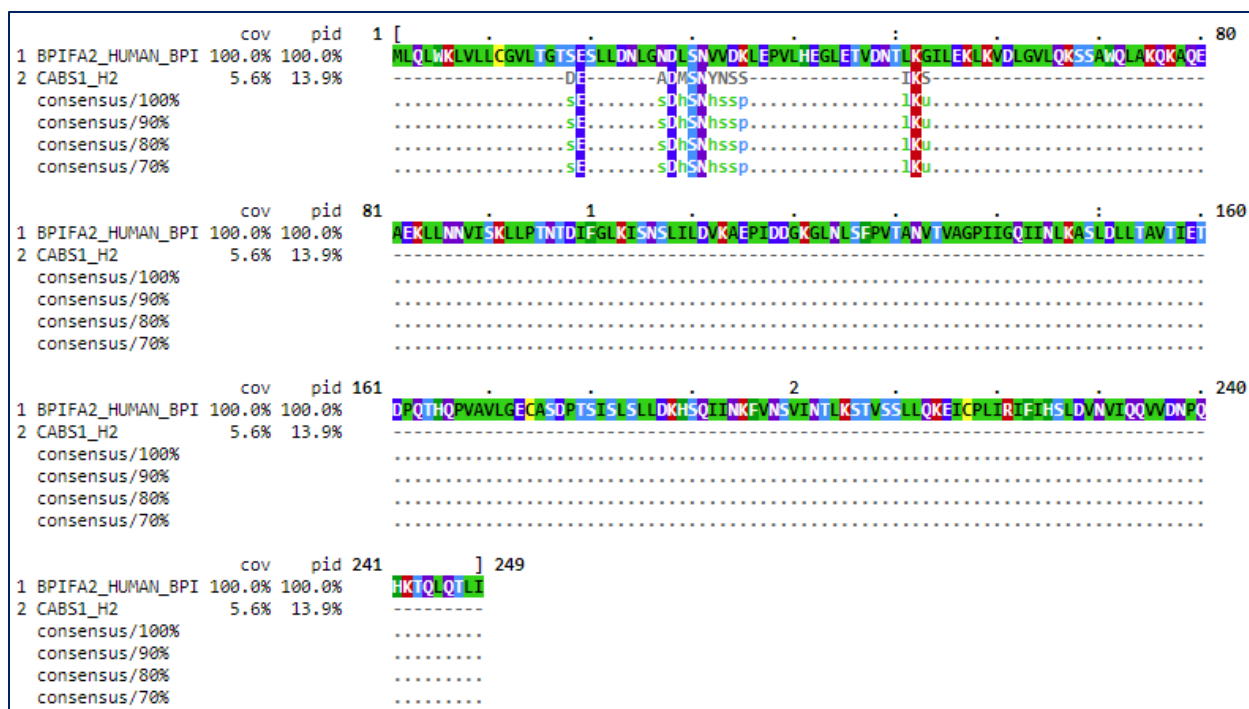
Figure C-2. Comparison of sequences between BPI fold-containing family A member 2 (BPIFA2) and the domain used to create H2.n pAbs to hCABS1 (CABS1_H2).

Consensus patterns (%) are based on sets of residues that share a predefined property based on the classification by W.R. Taylor. s: small, h: hydrophobic, p: polar.
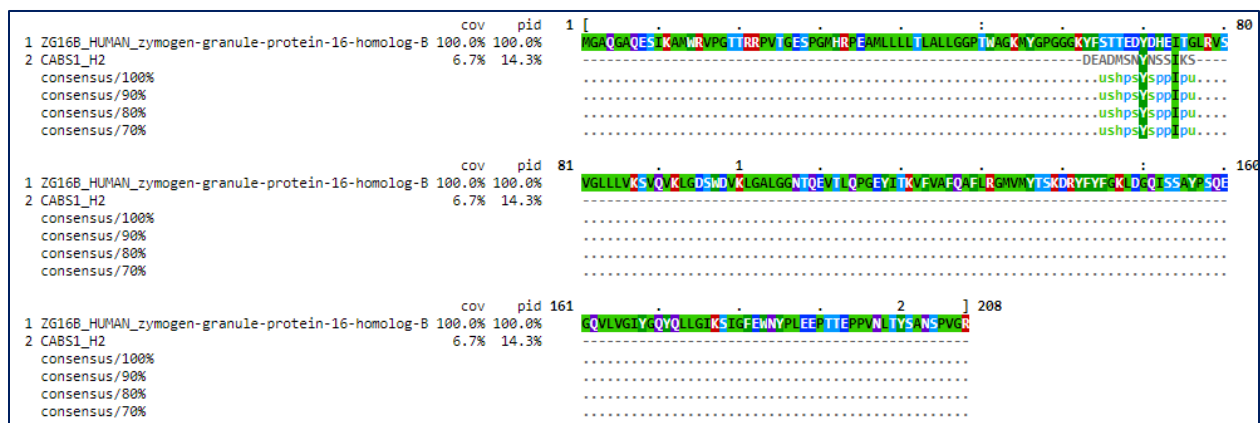
Figure C-3. Comparison of sequences between zymogen granule protein 16, homolog B (ZG16B) and the domain used to create H2.n pAbs to hCABS1 (CABS1_H2).
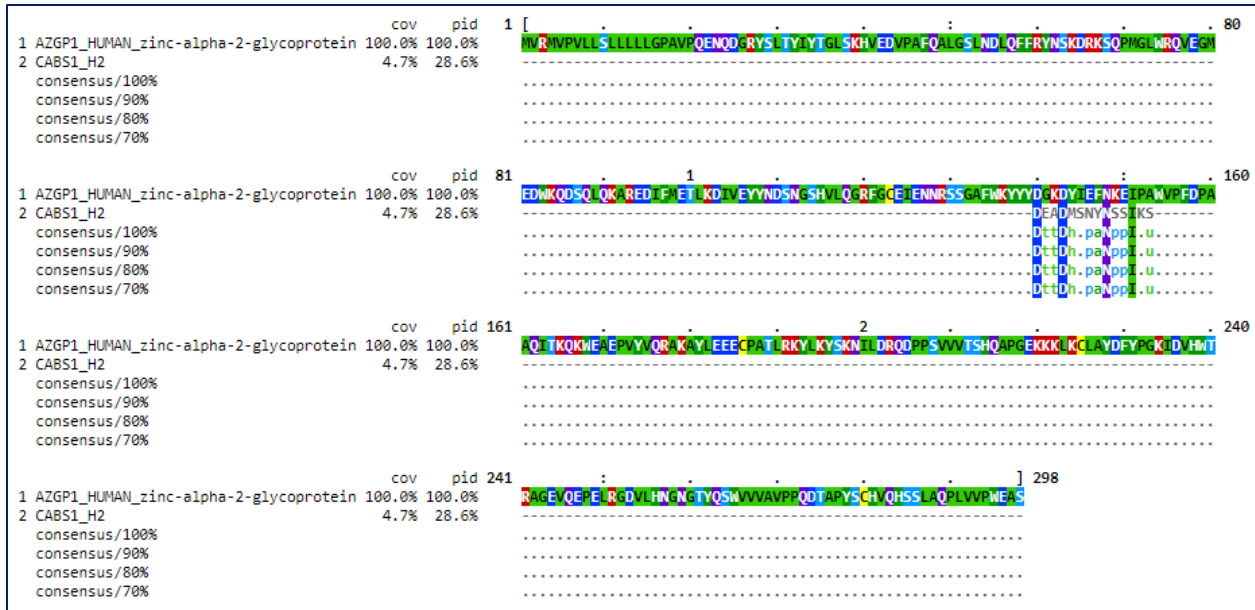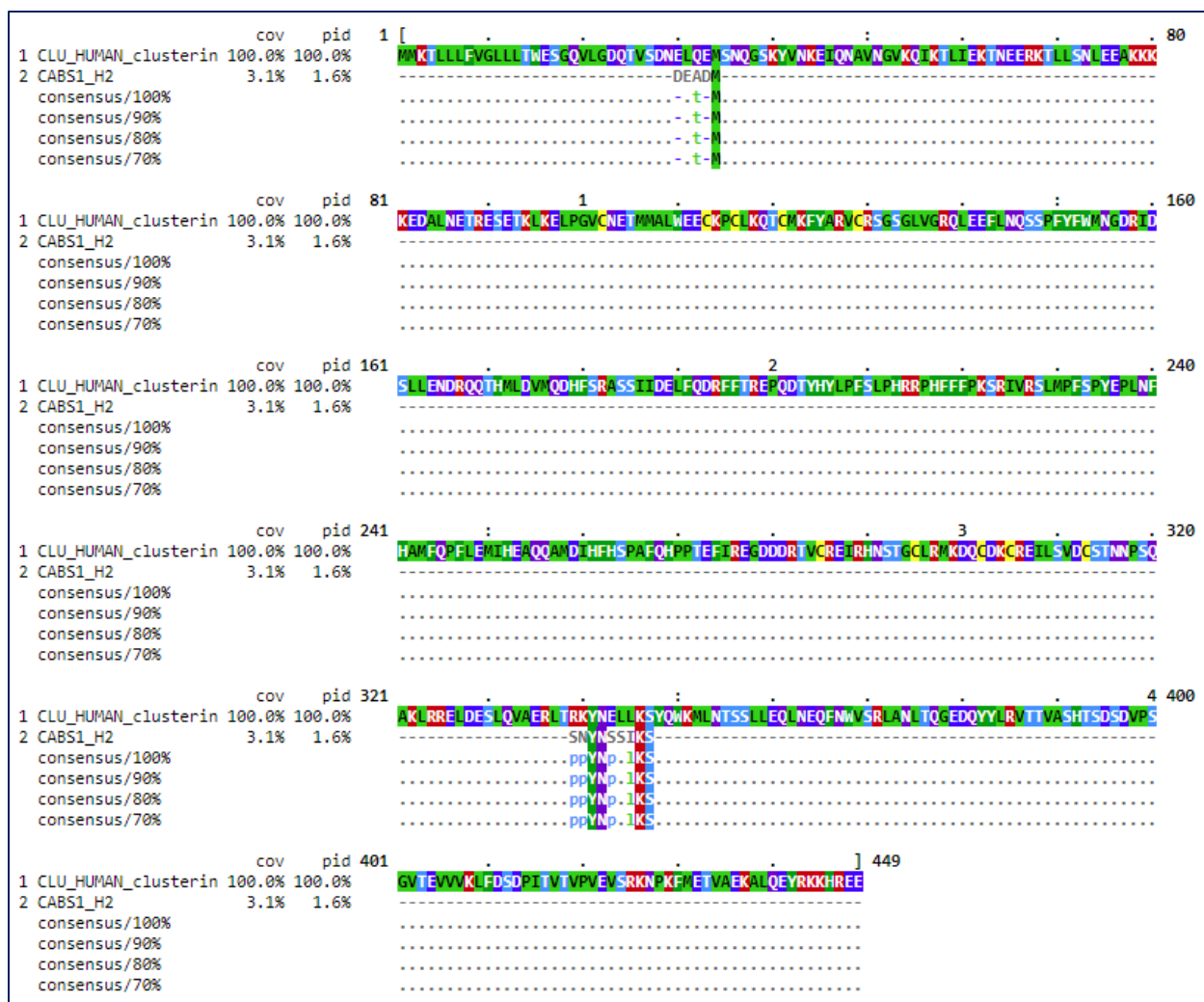
Consensus patterns (%) are based on sets of residues that share a predefined property based on the classification by W.R. Taylor. u: tiny, s: small, h: hydrophobic, p: polar
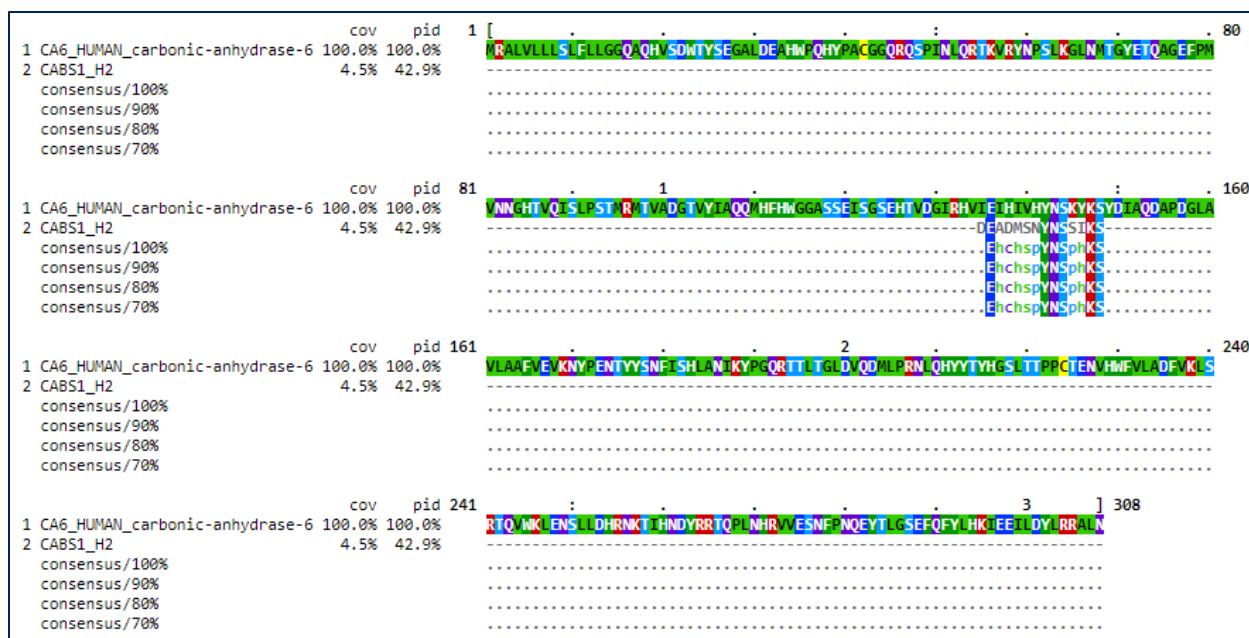
Figure C-4. Comparison of sequences between carbonic anhydrase 6 (CA6) and the domain used to create H2.n pAbs to hCABS1 (CABS1_H2).

Consensus patterns (%) are based on sets of residues that share a predefined property based on the classification by W.R. Taylor. h: hydrophobic, c: charged, s: small, p: polar
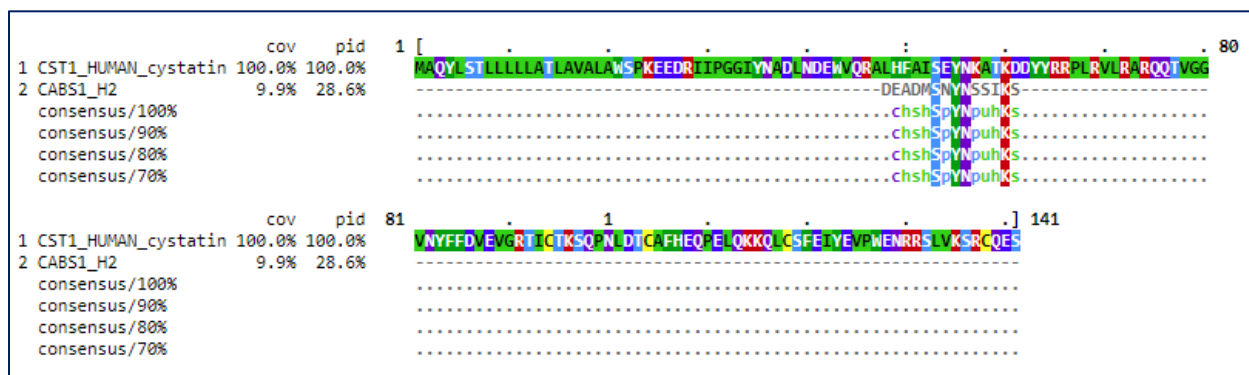
Figure C-5. Comparison of sequences between zinc alpha 2 glycoprotein (AZGP1) and the domain used to create H2.n pAbs to hCABS1 (CABS1_H2).

Consensus patterns (%) are based on sets of residues that share a predefined property based on the classification by W.R. Taylor. t: turnlike, h: hydrophobic, p: polar, a: aromatic, u: tiny
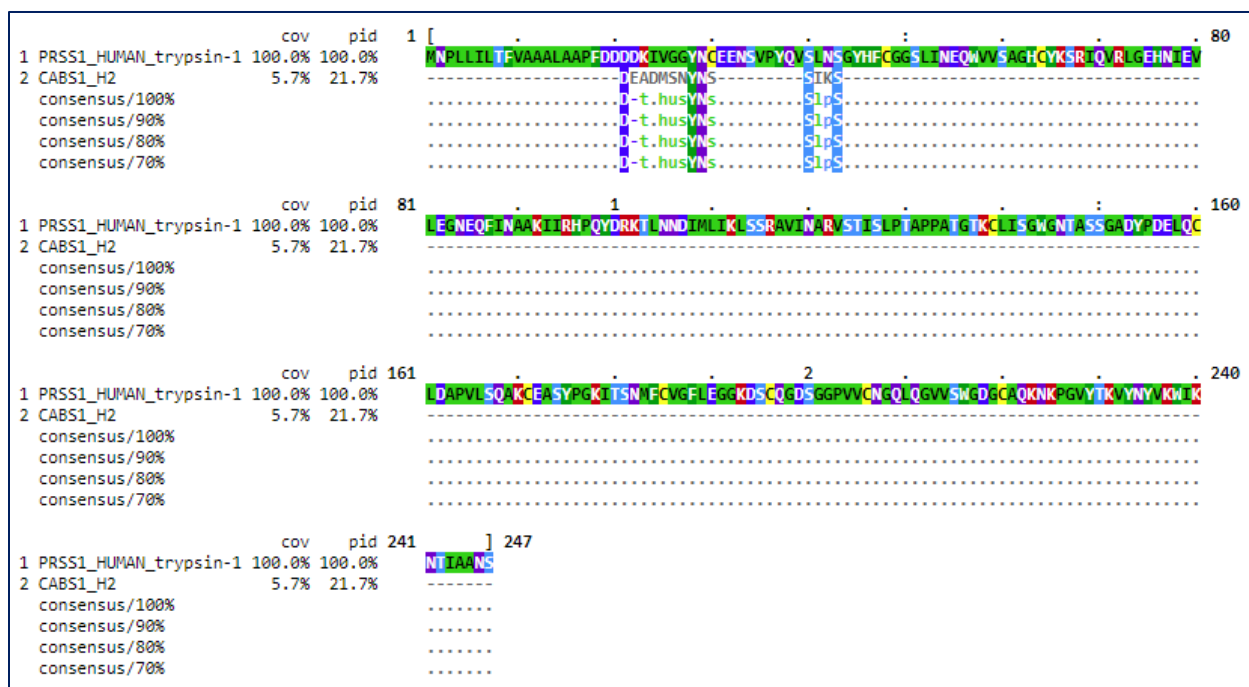
Figure C-6. Comparison of sequences between clusterin (CLU) and the domain used to create H2.n pAbs to hCABS1 (CABS1_H2).

Consensus patterns (%) are based on sets of residues that share a predefined property based on the classification by W.R. Taylor. t: turnlike, p: polar, l: aliphatic
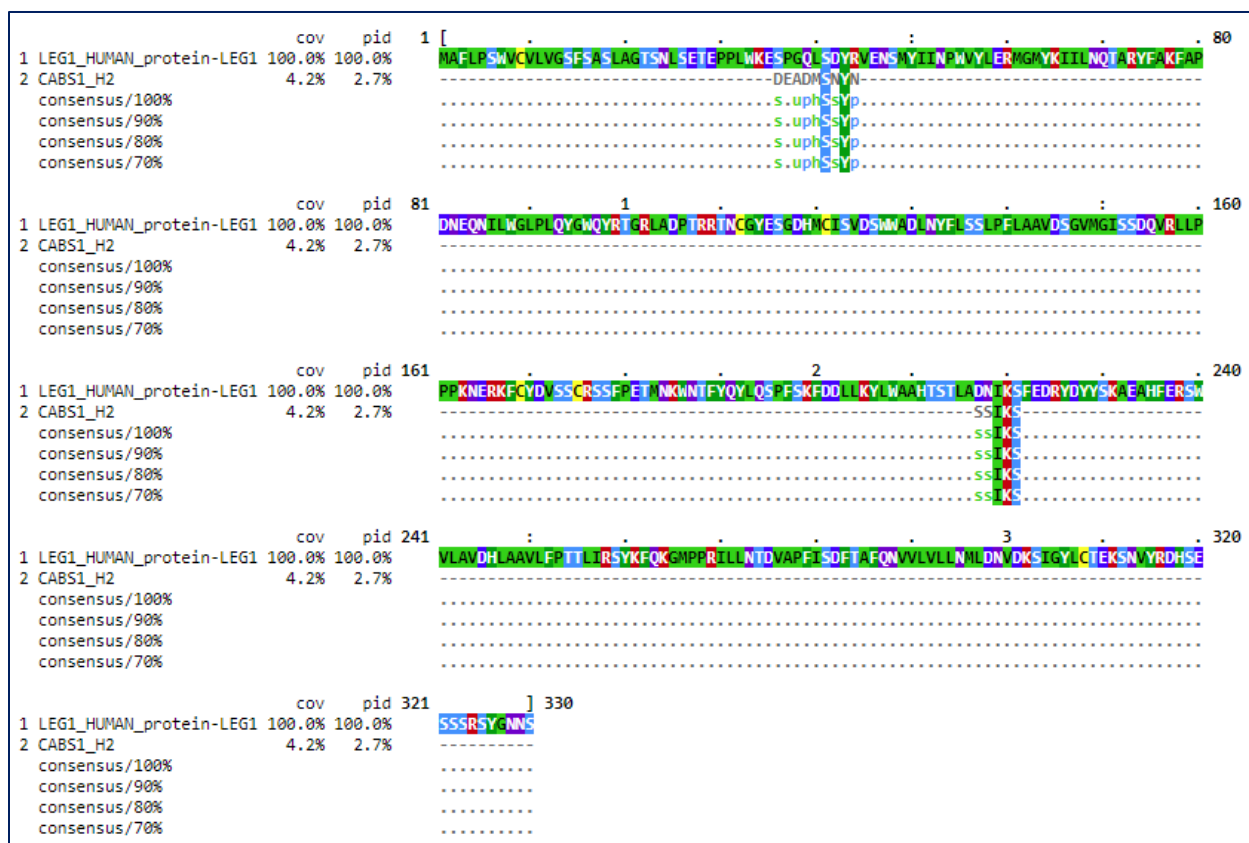
Figure C-7. Comparison of sequences between cystatin (CST1) and the domain used to create H2.n pAbs to hCABS1 (CABS1_H2).

Consensus patterns (%) are based on sets of residues that share a predefined property based on the classification by W.R. Taylor. c: charged, h: hydrophobic, s: small, p: polar, u: tiny
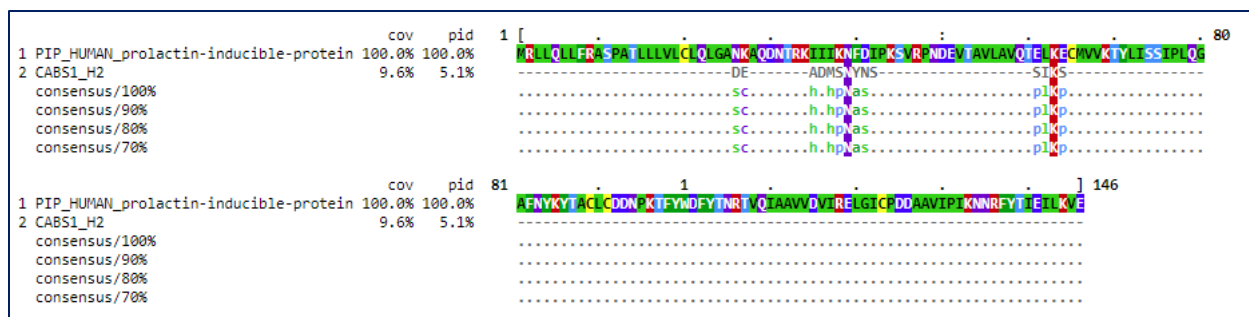
Figure C-8. Comparison of sequences between trypsin 1 (PRSS1) and the domain used to create H2.n pAbs to hCABS1 (CABS1_H2).

Consensus patterns (%) are based on sets of residues that share a predefined property based on the classification by W.R. Taylor. t: turnlike, h: hydrophobic, u: tiny, s: small, l: aliphatic, p: polar

Figure C-9. Comparison of sequences between human protein LEG1 (LEG1) and the domain used to create H2.n pAbs to hCABS1 (CABS1_H2).

Consensus patterns (%) are based on sets of residues that share a predefined property based on the classification by W.R. Taylor. s: small, u: tiny, p: polar, h: hydrophobic


Figure C-10. Comparison of sequences between human prolactin inducible protein (PIP) and the domain used to create H2.n pAbs to hCABS1 (CABS1_H2).

Consensus patterns (%) are based on sets of residues that share a predefined property based on the classification by W.R. Taylor. s: small, c: charged, h: hydrophobic, p: polar, a: aromatic, l: aliphatic

Appendix D - Immunohistochemical analyses of submandibular gland and testicular tissue with monoclonal antibody 15B11-1 (target: hCABS1)

In late 2021/early 2022 a collaboration with Dr Lakshmi Puttagunta and Ms. Sarah Canil resulted in immunohistochemical images depicting presumed localization of hCABS1 in human submandibular gland and testis. These images show preliminary data and have been left out from the main body of this dissertation because the protocol may require further refinement.

In SMG, hCABS1 seems to localize throughout the cytoplasm of duct cells (**Figure D-1** B, C). In testis, hCABS1 localizes in Leydig cells outside seminiferous tubules and in primary spermatogonia in seminiferous tubules (**Figure D-2** B, C).
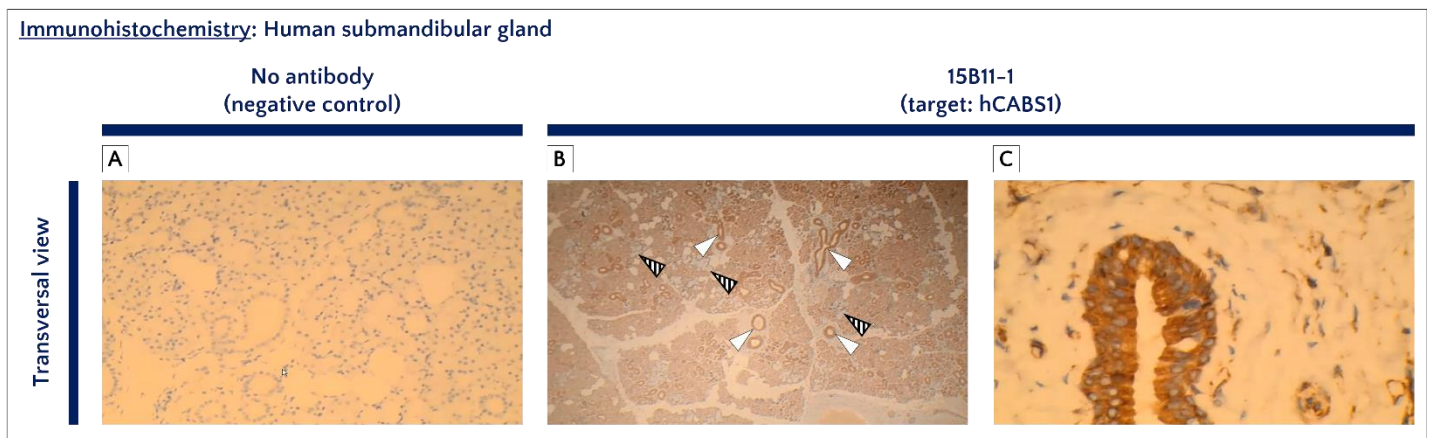
Figure D-1. Immunohistochemical analysis of human submandibular gland. (add serous and mucinous cells in B – change panel C for the one used in the PPT)

(A) Background signal observed when analyzing without antibody targeting hCABS1, 200 X. (B) Strong staining is present in duct cells (white arrows). In comparison, serous cells show less intense staining and mucinous cells show no signal (striped arrows, light purple cells), 40 X. (C) Staining is present throughout the cytoplasm of duct cells, 630 X.

Immunohistochemistry: Human testicular tissue

No antibody
(negative control)

15B11–1
(target: hCABS1)

Transversal view

A

B

C
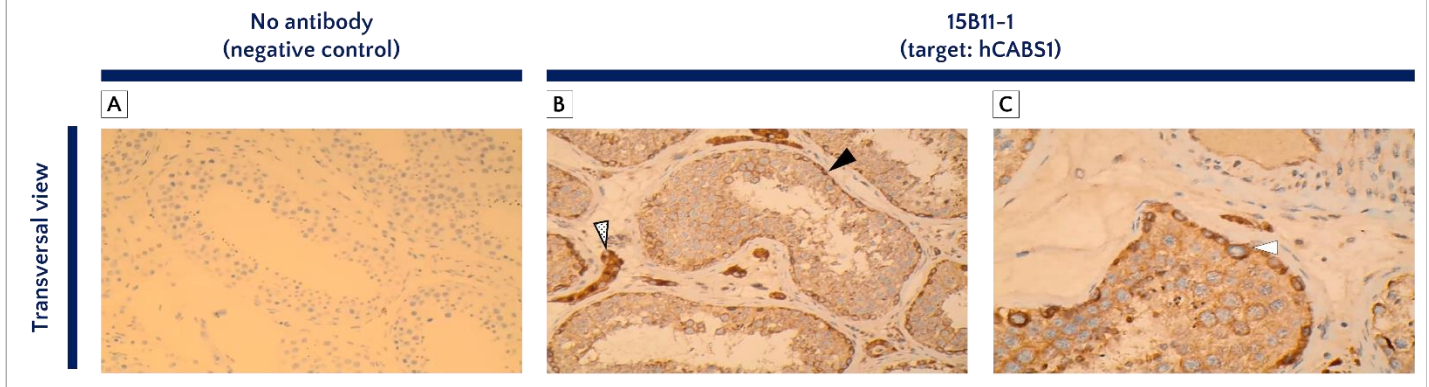
Figure D-2. Immunohistochemical analysis of human testicular tissue suggest CABS1 localizes in Leydig cells and primary spermatocytes.

(A) Background signal observed when analyzing without antibody targeting hCABS1, 200 X. (B) Strong signal indicates that CABS1 is present in Leydig cells in the interstitial space between seminiferous tubules (dotted arrow). Inside seminiferous tubules, strong staining is present in primary spermatogonia adjacent to the abluminal side, and staining seems to decrease as sperm mature and relocate towards the luminal side (black arrow), 200 X. (C) Strong staining is present in primary spermatogonia (white arrow), 400 X.